



THE HONG KONG
POLYTECHNIC UNIVERSITY

香港理工大學

Pao Yue-kong Library

包玉剛圖書館

Copyright Undertaking

This thesis is protected by copyright, with all rights reserved.

By reading and using the thesis, the reader understands and agrees to the following terms:

1. The reader will abide by the rules and legal ordinances governing copyright regarding the use of the thesis.
2. The reader will use the thesis for the purpose of research or private study only and not for distribution or further reproduction or any other purpose.
3. The reader agrees to indemnify and hold the University harmless from and against any loss, damage, cost, liability or expenses arising from copyright infringement or unauthorized usage.

IMPORTANT

If you have reasons to believe that any materials in this thesis are deemed not suitable to be distributed in this form, or a copyright owner having difficulty with the material being included in our database, please contact lbsys@polyu.edu.hk providing details. The Library will look into your claim and consider taking remedial action upon receipt of the written requests.

DETECTING AND ASSESSING OLDER ADULTS' STRESSFUL INTERACTIONS
WITH THE BUILT ENVIRONMENT: AN ELDERLY-CENTRIC AND WEARABLE
SENSING-BASED APPROACH

ALEX TORKU

PhD

The Hong Kong Polytechnic University

2022

The Hong Kong Polytechnic University

Department of Building and Real Estate

Detecting and Assessing Older Adults' Stressful Interactions with the Built Environment: An
Elderly-Centric and Wearable Sensing-Based Approach

Alex Torku

A thesis submitted in partial fulfilment of the requirements
for the degree of Doctor of Philosophy

JUNE 2021

CERTIFICATE OF ORIGINALITY

I hereby declare that this thesis is my own work and that, to the best of my knowledge and belief, it reproduces no material previously published or written, nor material that has been accepted for the award of any other degree or diploma, except where due acknowledgment has been made in the text.

_____ (Signed)

Alex Torku _____ (Name of Student)

DEDICATION

To my family

ABSTRACT

Globally, one in six people is expected to age 65 years by 2050. Not only is the global population ageing, but also the built environment infrastructure in many cities and communities are approaching their design life. This phenomenon is referred to as “double ageing”. Ageing built environment infrastructure with defects are likely to result in environmental barriers with excessive demands; humans experience stress and/or their mobility is limited when the environmental demands exceed their functional capability. Given that human’s functional capability declines with ageing, there is more likelihood for older adults to experience stressful environmental interactions that could limit their mobility than the average person. Current approaches to detect environmental barriers are inefficient, time-consuming, and costly, which may limit the frequency and scope of the built environment assessment. In order to promote active ageing in cities and communities, urban planners and municipal decision-makers need a more efficient approach to assess and detect excessively demanding environmental conditions. The aim of this research is to promote older adults’ mobility by reducing environmental demands. The overall goal of this research is in two folds: (1) to enable practitioners to detect stressful older adults-environment interactions in near real-time and (2) to bring to the limelight the influence of urban environment configurations on older adults’ stress response. To achieve this goal, this research harnessed the current advances in wearable sensing technologies to collect older adults’ bodily responses (i.e., physiological, behavioural, and cognitive responses) to their interaction with the environment as a means of assessing and detecting environmental barriers.

Specifically, a methodological framework was developed for researchers and practitioners to determine the relevance and informativeness of people’s bodily responses in the context of their study. Based on this framework, it was identified that older adults’ physiological response

is more informative than the cognitive and behavioural responses. The informativeness of the cognitive response was affected by the walking activity, and the gait abnormality among older adults affected their behavioural responses. A statistical, spatial and space-time pattern mining was conducted to understand the relationships in older adults' physiological responses to the built environment. The results demonstrate that the relationships between older adults' physiological response and the environmental condition are less apparent at the individual level. However, using collective sensing (i.e., aggregating multiple participants' physiological responses) can accommodate the individual variability and capture any normality in the data, which is indicative of an environment's condition. An optimised environmental stress hot spot detection framework was developed using an Ensemble bagged tree algorithm that achieved 98% accuracy. A simulation-based approach was used to examine areas within the study area that are sufficiently powered to detect stress hot spots that pose high risk to older adults. The results demonstrate that urban planners and municipal decision-makers can use this approach to detect and alleviate stressful environmental conditions more efficiently; as a result, improving older adult's mobility in the built environment. An integrated methodology based on machine learning and an evolutionary rule-based system was developed to further understand the influence of visuospatial configurations (specifically, isovist indicators) of urban space on older adults' physiological stress. The results demonstrate that isovist minimum visibility, occlusivity and isovist area are the most influential determinants of older adults' physiological stress and non-stress response. Older adults prefer urban configurations where they can be seen. The generated visuospatial configurations can be used to inform urban design and planning.

LIST OF PUBLICATIONS

Journal Papers (Published or Accepted)

Torku, A., Chan, A.P.C., Yung, E.H.K., Seo, J. (2021). The influence of urban visuospatial configuration on older adults' stress: A wearable physiological-perceived stress sensing and data mining based-approach, *Building and Environment*, 108298. <https://doi.org/10.1016/j.buildenv.2021.108298>

Torku, A., Chan, A.P.C., and Yung, E.H.K. (2021). Implementation of age-friendly initiatives in smart cities: Probing the barriers through a systematic review, *Built Environment Project and Asset Management*, 11(3), 412-426. <https://doi.org/10.1108/BEPAM-01-2020-0008>

Torku, A., Chan, A.P.C., and Yung, E.H.K. (2021). Age-friendly cities and communities: A critical review and future directions, *Ageing & Society*, 41(1), 2242-2279. <https://doi.org/10.1017/S0144686X20000239>

Journal Papers (Under Review)

Torku, A., Chan, A.P.C., Yung, E.H.K., Seo, J. (2021). Wearable sensing and mining of the informativeness of older adults' bodily responses to detect demanding environmental conditions, *Environment and Behavior*. (Under Review). E&B-20-0532.R2

Torku, A., Chan, A.P.C., Yung, E.H.K., Seo, J. (2021). Learning to detect older adults' environmental stress hotspots to improve neighbourhood mobility: A multimodal physiological sensing, machine learning and risk hotspot analysis-based approach, *Cities* (Under Review). JCIT-D-21-01443

Conference Papers (Published or Presented)

Torku, A., Chan, A.P.C., Yung, E.H.K., Seo, J., Yang, Y. (2021). Neural signatures of older adults as indicators of the age-friendliness of the built environment, *American Real Estate Society (ARES) 2021*, 17-20 March 2020, Las Vegas, USA (Virtual conference).

Torku, A. (2021). An elderly-centric sensing approach to assessing and detecting built environment barriers to improve the age-friendliness of cities and communities. Presented at the *2021 doctoral program sponsored by the James R. Webb American Real Estate Society (ARES) Foundation*, 17-20 March 2020, Las Vegas, USA (Virtual conference).

Torku, A., Chan, A.P.C., and Yung, E.H.K. (2019). The status of age-friendly community research. In *The International Council for Research and Innovation in Building and Construction (CIB) World Building Congress 2019 – Constructing Smart Cities*, 189-197. 17-21 June 2019, Hong Kong. (Invited to the special issue of the Emerald Journal of Built Environment Project and Asset Management).

Honours and Awards

Recognition of Research Performance (April 28, 2021), Grant Amount: HK\$ 20,000 Awarded by the University Grant Council (UGC) of Hong Kong, under the Hong Kong PhD Fellowship Scheme (HKPFS).

Best Presentation Award (April 9, 2021), Workshop on Sustainable Urban Systems, Department of Building and Real Estate, The Hong Kong Polytechnic University. Presentation Title: Detecting Built Environment Barriers to Promote Older Adults' Mobility: A Wearable Sensing Approach.

James Webb American Real Estate Society (ARES) Foundation Award (January 19, 2021). Funding to support doctoral students to attend the 2021 American Real Estate Society (ARES) Annual Meeting in Las Vegas.

Best Presentation Award (1st Place) (May 18, 2019), 18 Academic Conference for Post-Graduate Student in Construction Management and Real Estate, Department of Building and Real Estate, organised by The HK PolyU Student Chapter of CIB, The Hong Kong Polytechnic University. Presentation Title: Ageing in Cities and Communities: Active or Vulnerable?

ACKNOWLEDGEMENTS

I acknowledge that God alone deserves the glory for this work. I express my profound gratitude to my Chief supervisor, Ir. Professor Albert P. C. Chan for his continuous support, guidance, encouragement, and insightful advice over the years. I am forever humbled by your kindness. My appreciation also goes to my Co-supervisor, Dr. Esther H. K. Yung for all her directions. Thank you for encouraging me to understand the theoretical foundation of any work I present to you. I especially want to thank Dr. JoonOh Seo and Dr. Changbum R. Ahn for their support and contribution to this study. Their directions have immensely influenced my approach to research. Thank you, Dr. JoonOh Seo for shaping my thinking and research philosophy, especially how to approach problems and communicate ideas.

I am thankful to the Research Grant Council of Hong Kong for awarding me with the Hong Kong Ph.D. Fellowship Scheme and the Department of Building and Real Estate, The Hong Kong Polytechnic University for providing further financial support to complete this work. I could not be more grateful for the funding. The funding allowed me to focus on my research.

I would like to acknowledge the Institute of Active Ageing, particularly Prof. Daniel W. L. Lai and Mr. Jeffrey Chan for their support in participant recruitment. I would like to especially thank Dr. Jackie Yang for helping me during the participant recruitment, screening, scheduling appointments, data collection, and even translating some of the instruments. This work would not have been completed without you. Thank you very much. Many thanks to Dr. Maxwell Fordjour Antwi-Afari and Dr. Adabre Michael Atafo for taking the time out of your busy schedules to help me during my data collection. God richly bless you. To all the older adults that participated in the study, thank you for your time and efforts in making our cities and communities more age-friendly. I have also been fortunate to be part of a great research team; thank you to each of you!

Finally, I would like to thank all my family members for their love, support and understanding. To my parents (Frank and Veronica), thank you for making me who I am today. To my siblings (Freedom, Fortune, Justice and Delphine), you are the best! You have been there with me since the beginning. Also, many thanks to Mrs. Philomena Hevi Anderson and Mr. Alfred Agbosu for your constant love and support. I am especially thankful to Eugenia. Thank you for your love and encouragement.

CONTENTS

DEDICATION.....	III
ABSTRACT.....	IV
ACKNOWLEDGEMENTS	VIII
CONTENTS.....	IX
LIST OF FIGURES	XVI
LIST OF TABLES	XIX
LIST OF ABBREVIATIONS AND ACRONYMS	XXI
PART I: INTRODUCTION AND LITERATURE REVIEW	1
CHAPTER 1:INTRODUCTION.....	2
1.1 Background.....	2
1.2 The Problem: Current Approaches to Assess and Detect Environmental Barriers	4
1.3 The Proposal and Research Aim: An Elderly-Centric and Wearable Sensing Approach	6
1.4 Research Aim and Objectives.....	7
1.5 Research Design and Approach	8
1.6 Research Significance	11
1.7 Organisation of the Thesis	11
CHAPTER 2:LITERATURE REVIEW	13
2.1 Introduction.....	13
2.2 Age-friendly Cities and Communities	14
2.3 Why the Outdoor Environment.....	18
2.4 Built Environment Determinant of Walking.....	19

2.5 Assessing the Built Environment to Promote Mobility	21
2.6 Sensing of Bodily Responses to the Environment	23
2.7 Bodily Response for Assessing Environmental Features	25
2.7.1 Electrodermal Activity (EDA).....	25
2.7.2 Electrocardiogram (ECG or EKG) and Blood Volume Pulse (BVP).....	27
2.7.3 Gait.....	29
2.7.4 Eye Movement	29
2.7.5 Electroencephalogram (EEG)	30
2.8 Summary and Research Gaps	38
2.8.1 Research Gap One: Informativeness of Bodily Response	38
2.8.2 Research Gap Two: Relationships in Older Adult’s Bodily Responses Resulting from their Interaction with the Environment	40
2.8.3 Research Gap Three: Optimised Environmental Stress Detection	40
2.8.4 Research Gap Four: Influence of Visuospatial Configuration of Urban Space on Older Adults’ Stress Response.....	41
PART II: TOWARDS ELDERLY-CENTRIC AND WEARABLE SENSING.....	42
CHAPTER 3:RESEARCH METHODOLOGY	43
3.1 Introduction.....	43
3.1.1 Methodological Underpinning: Ecological Validity.....	44
3.2 Experiment Design.....	45
3.2.1 Enrolment.....	45
3.2.2 Screening: Eligibility Criteria	47
<i>Age</i>	47
<i>Walking Ability</i>	47
<i>Cognitive Status</i>	47
3.2.3 Eligible Participants	49
3.2.4 Practice Session	50
3.2.5 Path for Environmental Walk	50
3.3 Field Data Collection: Observers’ Audit of Path Condition.....	53
3.4 Field Data Collection: Bodily Response and Perceived Response Collection	62
3.4.1 Collected Bodily Responses and Environmental Data	63
3.4.2 Older Adults’ Perceived Stress During Environmental Walk	64

3.5 Wearable Sensors for Collecting Bodily Response and Environmental Data	65
3.5.1 Physiological Response Sensors	65
3.5.2 Cognitive Response Sensors	66
3.5.3 Behavioural (Gait and Motion) Response Sensors	67
3.5.4 Environmental Data Sensors	68
3.6 Ethics Statement.....	69
3.7 Data Analysis	69
3.7.1 Pre-Processing of Bodily Response Data	69
<i>HRV Detection and Signal Pre-processing</i>	69
<i>EDA Signal Pre-processing</i>	70
<i>EEG Signal Pre-processing</i>	70
<i>Plantar Pressure and Acceleration Signal Pre-processing</i>	70
3.7.2 Baseline Normalisation.....	71
3.7.3 Methods.....	71
3.8 Chapter Summary	71

PART III: DETECTING STRESSFUL OLDER ADULTS-ENVIRONMENT INTERACTIONS.....73

CHAPTER 4:ASSESSMENT OF THE INFORMATIVENESS OF OLDER ADULTS' BODILY RESPONSE.....74

4.1 Introduction.....	74
4.2 Methodological Framework: Assessing Informativeness of Bodily Response	75
4.2.1 Feature Extraction.....	75
4.2.2 AI-based Information Mining	80
4.2.3 Validation.....	84
4.3 Results and Discussion	85
4.3.1 Physiological Response	85
4.3.2 Cognitive Response	89
4.3.3 Behavioural Response.....	93
4.4 Chapter Summary	97

CHAPTER 5:INTERACTION OF OLDER ADULTS’ PHYSIOLOGICAL RESPONSE WITH THE BUILT ENVIRONMENT: STATISTICAL, SPATIAL AND TEMPORAL RELATIONSHIPS.....99

5.1 Introduction.....99

5.2 Methods..... 100

5.2.1 Physiological Reflectors of Human-Environment Stressful Interactions 100

5.2.2 Statistical Analysis..... 102

5.2.3 Spatial Analysis 103

5.2.4 Spatiotemporal Analysis 104

5.3 Results..... 106

5.3.1 Physiological Reflectors of Human-Environment Stressful Interactions 106

5.3.2 Statistical Analysis..... 108

5.3.3 Spatial Analysis 111

5.3.4 Spatiotemporal Analysis 114

5.4 Discussion..... 116

5.4.1 A Comparison of Older Adults’ Physiological-Environmental Interactions, Older Adults’ Perceived Stress Assessments, and Observers’ Path Audit 116

5.4.2 Collective Sensing can Address Individual Variability 120

5.5 Chapter Summary 120

CHAPTER 6:AN OPTIMISED ENVIRONMENTAL STRESS DETECTION FRAMEWORK BASED ON MACHINE LEARNING INTELLIGENCE122

6.1 Introduction..... 122

6.2 Optimised Stress Detection Framework 124

6.2.1 The Optimum Set of Informative Features 124

6.2.2 Multimodal Sensing and Fusion 124

6.2.3 Machine Learning Algorithms..... 125

6.2.4 Validation..... 127

6.2.5 Visualisation of Detected Stress Samples..... 128

6.2.6 Identifying Spatial Clusters of Risk Stress Hot spot..... 128

6.3 Results..... 130

6.3.1 The Optimum Set of Informative Features 130

6.3.2 Performance of the Machine Learning Algorithms 130

6.3.3 Visualisation of Detected Stress Samples.....	132
6.3.4 Spatial Relative Risk Stress Hot spot.....	133
6.3.5 Examination of Spatial Clusters of Risk Stress Hot spot.....	137
6.4 Discussion.....	141
6.5 Chapter Summary	142

PART IV: THE INFLUENCE OF URBAN ENVIRONMENT CONFIGURATIONS ON OLDER ADULTS’ STRESS RESPONSE.....144

CHAPTER 7:INFLUENCE OF VISUOSPATIAL CONFIGURATION OF THE URBAN ENVIRONMENT ON OLDER ADULTS’ PHYSIOLOGICAL STRESS145

7.1 Introduction.....	145
7.2 Visuospatial Perception	146
7.3 Methods.....	149
7.3.1 Detecting Stress and Non-stress Responses.....	149
7.3.2 Measuring Visuospatial Perception: Isovist Analysis.....	150
7.3.3 Influence of Visuospatial Perception on Physiological Response: Self-Organising Map	154
7.3.4 Identifying the Most Influential Isovist Indicators of Physiological Response	156
7.3.5 Design by Evolutionary Algorithmic Rule: Generative Design	157
7.3.6 Multi-Objective Evolutionary Fuzzy Systems.....	158
7.3.7 Validation.....	160
7.4 Results.....	161
7.4.1 Detected Stress and Non-stress Responses	161
7.4.2 Influence of Visuospatial Perception on Stress and Non-stress Response	163
7.4.3 The Learning Process.....	165
7.4.4 Visualisation of the SOM.....	167
7.4.5 Most Influential Isovist Indicators of Physiological Response.....	169
7.4.6 Multi-objective Evolutionary Fuzzy Systems: Generated Visuospatial Configurations with Physiological Effect	170
7.5 Discussion.....	170
7.5.1 Comparison with Similar Studies	176
7.6 Chapter Summary	179

PART V: RESEARCH CONCLUSION	180
CHAPTER 8: CONCLUSIONS AND RECOMMENDATIONS.....	181
8.1 Summary of Research	181
8.1.1 Objective 1: To Assess the Informative of People’s Bodily Responses	182
8.1.2 Objective 2: To Examine the Relationships in Older Adult’s Bodily Responses Resulting from their Interaction with the Environment.....	183
8.1.3 Objective 3: To Detect Older Adults’ Stressful Environmental Interactions in Near-Real Time.....	184
8.1.4 Objective 4: To Examine the Influence of Visuospatial Configuration of Urban Space on Older Adults’ Stress Response	185
8.2 Contribution to Knowledge, Practice and Impact.....	185
8.2.1 Contributions to Academia	185
8.2.2 Incorporating the Elderly-centric Wearable Sensing-based Approach into Urban Planning	186
8.2.3 Research Impact.....	190
<i>Older Adults</i>	190
<i>Society and Community</i>	190
<i>Urban Planners and Policymakers</i>	190
<i>The Economy</i>	191
8.3 Limitations and Future Research	191
APPENDIX A	193
TINETTI ASSESSMENT TOOL.....	193
Tinetti Assessment Tool: Balance	194
Tinetti Assessment Tool: Gait	195
APPENDIX B	196
THE MINI-MENTAL STATE EXAMINATION.....	196
The Original Version of the Mini-Mental State Examination	196
The Cantonese Version of the Mini-Mental State Examination.....	197
APPENDIX C	198

INTEGRATED VERSION OF THE EAST-HK WITH SWEAT-R ASSESSMENT TOOL.....	198
REFERENCES.....	206

LIST OF FIGURES

Figure 1.1: Flowchart of research design, approach and the interrelations between the objectives.	10
Figure 2.1: Bodily response sensors.	24
Figure 3.1: Flowchart of experiment procedure.	46
Figure 3.2: Field experiment overview. (a) Predefined path for environmental walk. (b) Older adult equipped with wearable sensors.	51
Figure 3.3: Photo description of path segment A to D.	52
Figure 3.4: Photo description of path segment E to H.	53
Figure 3.5: The commonly perceived stress among the participants. The path label is the perception of at least four participants out of ten.	64
Figure 3.6: The physiological sensor used in the experiment.	66
Figure 3.7: The cognitive sensor used in the experiment. (a) 14 channel mobile EEG headset. (b) The position of the 14 channels corresponds to the international 10-20 position system.	67
Figure 3.8: The behavioural (gait and motion) sensor used in the experiment. (a) Positions of pressure sensors and inertial measurement unit (IMU) in the insole sensor. (b) Top view and bottom view of insole sensor. (c) Thickness of insole sensor.	68
Figure 3.9: The GPS sensor used in the experiment.	69
Figure 4.1: Methodological framework for assessing informativeness of bodily responses.	75
Figure 4.2: Distribution of the EEG channels across the scalp.	91
Figure 4.3: Plantar pressure sensors and IMU sensor positions.	97
Figure 5.1: Overview of the study.	99
Figure 5.2: Methodological flow chart.	100
Figure 5.3: A continuous decomposition of EDA into tonic component and phasic component.	102

Figure 5.4: Aggregating participants’ physiological responses into space-time bins with GPS coordinates (adapted from Esri, 2020a).....	106
Figure 5.5: The <i>LFHF</i> measure of two participants during the environmental walk on the path.	107
Figure 5.6: The PhasicMax measure of two participants during the environmental walk on the path.	107
Figure 5.7: Spatial clusters of collective physiological responses based on <i>LFHF</i> measure.	113
Figure 5.8: Spatial clusters of collective physiological responses based on PhasicMax measure.....	114
Figure 5.9: Spatiotemporal clusters of collective physiological responses based on <i>LFHF</i> measure.....	115
Figure 5.10: Comparison of perceived stress, observers’ path audit, and detected hot and cold spots on the path.	119
Figure 6.1: Optimised environmental stress detection framework.....	123
Figure 6.2: Confusion matrix of the best performance Ensemble bagged tree algorithm for (a) detecting non-stress and stress samples; (b) detecting low and high-stress samples.	132
Figure 6.3: (a) Detected stress hot spot locations. (b) Detected high-stress hot spot locations. (c) Perceived stress and non-stress assessment by participants. (d) Path audit by observers. The environmental condition was rated as poor, moderate or good. F = Rating for functionality; S = Rating for safety; A = Rating for aesthetics; O = Overall rating of path segment.	134
Figure 6.4: First iteration of simulated randomly generated point-level physiological data assuming complete spatial randomness.....	135
Figure 6.5: Clusters of SRR high-stress hot spot within study area (i.e., path segment A to H). (a) Proportion of simulation significant SRR high-stress hot spot clusters for the simulated 10,000 iterations. (b) Areas within the study area that are sufficiently powered to detect spatial clustering of a high-stress hot spot.	136
Figure 6.6: Environmental barriers at locations of risk stress hot spot. Base map and data copyrighted 2020 Esri, OpenStreetMap contributors and the GIS user community.	139
Figure 6.7: Pictures of environmental barriers at locations of risk stress hot spot.	140

Figure 7.1: Research overview and methodological framework.	146
Figure 7.2: Generated spatial layout with isovist from an observation point.	153
Figure 7.3: Path with perceiver’s view in the forward direction, starting from A to L.	154
Figure 7.4: Detected spatial significant stress and non-stress locations.	162
Figure 7.5: PCA biplot of spatially significant matched samples of isovist indicators and physiological responses.	164
Figure 7.6: SOM architecture.	166
Figure 7.7: Influence of isovist indicators on participants’ physiological stress.	168
Figure 7.8: Hierarchy of influential isovist indicator (s) subsets with corresponding performance when tested on machine learning algorithms with 10-fold cross- validation.	169

LIST OF TABLES

Table 2.1: AFCC concepts	16
Table 2.2: Built environment factors that may influence walking.....	20
Table 2.3: Bodily response for assessing environmental features	31
Table 3.1: Demographic information of participants.....	50
Table 3.2: Observers' path audit.....	56
Table 3.3: Sample of collected bodily response and location data during environmental walk	63
Table 3.4: Perceived stress distribution on path	64
Table 4.1: Features extracted from HRV signal	77
Table 4.2: Features extracted from EDA signal.....	78
Table 4.3: Features extracted from EEG signal	79
Table 4.4: Features extracted from plantar pressure signal	81
Table 4.5: Features extracted from acceleration signal.....	83
Table 4.6: Most informative HRV features	87
Table 4.7: Most informative EDA features.....	89
Table 4.8: Most informative EEG features	90
Table 4.9: Most informative plantar pressure features	94
Table 4.10: Most informative acceleration features.....	96
Table 5.1: A comparison of <i>LFHF</i> measure in environmental conditions perceived as non- stress and environmental conditions perceived as stress	109
Table 5.2: A comparison of PhasicMax measure in environmental conditions perceived as non- stress and environmental conditions perceived as stress	110
Table 6.1: Optimum set of informative features for stress detection.....	131
Table 6.2: Performance of the machine learning algorithms	131

Table 6.3: Classification of participant’s interaction with the environment into (1) non-stress and stress; and (2) low-stress and high-stress samples based on Ensemble bagged tree algorithm	133
Table 7.1: Isovist indicators and corresponding experiential properties	148
Table 7.2: Parameters used to run multi-objective evolutionary fuzzy rule-based system...	160
Table 7.3: Optimal hyperparameters settings for SOM and SOM validation result.....	165
Table 7.4: Dominant pattern in the SOM.....	170
Table 7.5: Visuospatial configurations with physiological effect.....	171
Table 7.6: Summary of previous studies.....	177

LIST OF ABBREVIATIONS AND ACRONYMS

AFCC	Age-friendly city and community
AI	Artificial intelligence
ANS	Autonomic nervous system
AUROC	Area under the receiver operating characteristic
BMU	Best matching unit
BVP	Blood volume pulse
CMMSE	Cantonese version of the Mini-Mental State Examination
DBN	Deep belief network
DT	Decision tree
EAST-HK	Environment in Asia Scan Tool—Hong Kong version
ECG	Electrocardiogram
EDA	Electrodermal activity
EEG	Electroencephalography
EMG	Electromyography
GIS	Geographic Information System
GPS	Global Positioning System
GSR	Galvanic skin response
HR	Heart rate
HRV	Heart rate variability
HSESC	Human Subjects Ethics Sub-committee
IBI	Interbeat interval
IMU	Inertial measurement unit
KDE	Kernel density estimation
kNN	k-Nearest Neighbour
LR	Logistic regression
MMSE	Mini-Mental State Examination
NB	Naïve Bayes

PCA	Principal component analysis
PPG	Photoplethysmography
RF	Random Forest
SCL	Skin conductance level
SCR	Skin conductance response
SOM	Self-organising map
SRR	Spatial relative risk
STC	Space-time cube
SU	Symmetrical uncertainty
SVM	Support Vector Machine
SWEAT-R	Older adults Senior Walking Environmental Assessment Tool—Revised
WHO	World Health Organisation

PART I: INTRODUCTION AND LITERATURE REVIEW

CHAPTER 1

INTRODUCTION¹

1.1 Background

Ageing is not new to humans, but longevity is. The global population is ageing with increasing life expectancy. The proportion of the global population aged 65 years or over (referred to as older adults in this study) has increased substantially over the years. The people in the global population aged 65 and over are projected to increase from 9.3% in 2020 to 16.0% in 2050 (United Nations, 2020). Globally, one in six people is expected to age 65 years by 2050 (United Nations, 2020). With the changing age structure of the projected population, many countries are confronted with unprecedented challenges. An effective local approach for responding to population ageing is by creating environments that are inclusive and accessible to promote active ageing (WHO, 2007). Active ageing is a concept developed by the World Health

¹ This chapter is based on studies that are currently under consideration for publication.

Torku, A., Chan, A.P.C., Yung, E.H.K., Seo, J. (2021). The influence of urban visuospatial configuration on older adults' stress: A wearable physiological-perceived stress sensing and data mining based-approach, *Building and Environment*, 108298. <https://doi.org/10.1016/j.buildenv.2021.108298>

Torku, A., Chan, A.P.C., Yung, E.H.K., Seo, J. (2021). Wearable sensing and mining of the informativeness of older adults' bodily responses to detect demanding environmental conditions, *Environment and Behavior*. (Under Review). E&B-20-0532.R2

Torku, A., Chan, A.P.C., Yung, E.H.K., Seo, J. (2021). Learning to detect older adults' environmental stress hotspots to improve neighbourhood mobility: A multimodal physiological sensing, machine learning and risk hotspot analysis-based approach, *Cities* (Under Review). JCIT-D-21-01443

Organisation (WHO), which emphasises creating an enabling environment for older adults to continue participating in social, economic, civic engagement and physical activity in order to enhance their quality of life as they age (WHO, 2018; Torku et al., 2021). Since the launch of the Global Network for Age-friendly Cities and Communities in 2010, an increasing number of cities, communities and organisations are committed to listening to the needs of their ageing population, assessing, and monitoring their age-friendliness and working collaboratively with older people and across sectors to create age-friendly physical and social environments (WHO, 2020). For instance, there are currently 1000 cities and communities in 41 countries, covering over 240 million people worldwide committed to becoming more age-friendly (WHO, 2020). The older adult's mobility—their ability to achieve access to their desired places (physical environment) and people (social environment)—is critical for such an enabling environment (referred to as age-friendly cities and communities) to adequately function. Mobility is essential to accessing commodities, using neighbourhood facilities, engaging in social, cultural, and physical activity; thus, fundamental to active ageing (Rantanen, 2013). Although mobility restrictions are more common in older adults, they are not typically the result of the individual's conditions but arise from interactions between individual factors and environmental demand (Webber et al., 2010; Verbrugge, 2020; WHO, 2001). The two main interventions to promote mobility is either by increasing capability or reducing demand (Verbrugge and Jette, 1994; Verbrugge, 2020). This study focuses on the modification of the built environment to reduce environmental demand. Environmental demand is the collective influence of elements constituting the environment to produce expectations for certain human actions and reactions (Hagedorn, 2001; Lee et al., 2020). When environmental demand meets a person's capability, the person can achieve successful mobility. On the other hand, the person experience stress and/or their mobility is limited when the environmental demand exceeds his

or her capability (Mair et al., 2011; Yang and Matthews, 2010; Lawton, 1982; Webber et al., 2010).

Stress is a type of relationship between person and environment which occurs when demands tax or exceed the person capability (Lazarus, 1990). Given that an individual's functional capability increases in childhood, peaks in early adulthood, and eventually decline (WHO, 2007; Kalache and Kickbusch, 1997), it is more likely for older adults to experience stress in the urban environment than other age groups. In fact, recent studies have reported that the desire to reduce encounter with environmental barriers (an environmental barrier is an environmental condition or physical feature that can impede older adult's mobility [Rantanen, 2013]) has led to a significant reduction in mobility of older adults in the built environment (van Heezik et al., 2020; Portegijs et al., 2017). As a result, there has been a rapid decline in mobility indices, including trip frequency, trip distance, and unmet travel demands among older adults (Shumway-Cook et al., 2003; Portegijs et al., 2017). Therefore, detecting environmental barriers with excessive demand for older adults is an important step to alleviate stressful interactions with the urban environment; as a result, promoting mobility and the effectiveness of age-friendly cities and communities.

1.2 The Problem: Current Approaches to Assess and Detect Environmental Barriers

It is important to mention that previous approaches have been developed and deployed to detect environmental conditions that inhibit older adult's mobility. A common approach for detecting such conditions is the Older Adults Senior Walking Environmental Assessment Tool (Michael et al., 2009; Cunningham et al., 2005). This tool consists of four attributes: (1) functionality, (2) safety, (3) aesthetics, and (4) destination. This type of assessment is often completed by trained observers or older adults. Participatory assessment method such as interviews, visual

inspection and photovoice are among the commonly used methods to assess people's perception of environmental condition (Aghaabbasi et al., 2018; Moura et al., 2017; Cerin et al., 2011). Although these methods have improved the detection of environmental barriers, thereby increasing older adult's mobility in neighbourhood environments, several issues limit its practicability in age-friendly cities. For instance, assessment tools with several attributes are time-consuming to complete and are not user-friendly for older adults and people without expert knowledge or skill (Michael et al., 2009). Visual inspections and photovoice are often influenced by the inspector or older adult's attachment with the environment, recent experiences, and momentary emotions. These assessment methods are also costly and labour intensive (e.g., trained inspectors and staff), which may limit the frequency and scope of the built environment assessment (Yameqani and Alesheikh, 2019). For a city or community to remain age-friendly, it needs to be continuously assessed (Van Hoof et al., 2018) and relying on these assessment methods will severely interfere and obstruct older people's daily lives.

Another emerging approach is the use of passively generated urban data such as infrastructure data, global positioning system (GPS) and street view imagery to audit neighbourhood environments (Yin, 2017; Wan et al., 2018; Knöll et al., 2018; Zhou et al., 2019). Although passively generated urban data are less obstructive and can increase the frequency and scope of the built environment assessment, they cannot adequately capture older adult's stressful interaction with the environment. The dynamic nature of human-environment interactions significantly impacts what an individual will perceive as a stressful environmental feature with excessive demand (Kim et al., 2016). In this regard, passively generated data may be misleading since it depends on a specific objective criterion and cannot distinguish between an environmental feature that is stressful for one person and non-stressful for another person. Therefore, there is a need for a more human-centred assessment approach that takes into

consideration the individual older adult's interaction with the environment while facilitating a continuous assessment of the environment without obstructing older people's daily lives.

1.3 The Proposal and Research Aim: An Elderly-Centric and Wearable Sensing Approach

Presently, sensing technologies offer great potential to improve continuous monitoring, real-time measurement, and assessment of the built environment. The advancement in wearable sensing technology provides the opportunity to objectively study and collect continuous unbiased data on humans' bodily responses to their interactions with the environment (Birenboim et al., 2019; Twardzik et al., 2019; Kim et al., 2019; Neale et al., 2017). This concept is termed "human-centric sensing", which sought to transform human users' into sensors (Kim et al., 2016). However, the term "elderly-centric sensing" adapted from "human-centric sensing" is used in this study because the focus is on older adults. This concept is motivated by the fact that involving older adults is very important in evaluating the age-friendliness of the environment (WHO, 2007).

The human experience in the environment is the human state of being affected by the surrounding environments (Kaplan, 1988). Signals for inferring changes in demanding environmental conditions are regulated by the autonomic nervous system (ANS) (van den Berg et al., 2015; Ulrich et al., 1991). The ANS consist of the sympathetic and parasympathetic nervous systems that usually act involuntarily to regulate human response to stress (Birenboim et al., 2019; van den Berg et al., 2015). When the body is stressed, the ANS provoke responses in humans which are reflected in the physiological, behavioural, and cognitive signals (Ulrich et al., 1991; Alberdi et al., 2016). The physiological signals are involuntary actions or responses that are almost impossible to notice by external observation because they relate to how a living

organism or bodily part functions. Behavioural signals are somewhat voluntary actions that can be externally observed. The cognitive signals relate to the activities of the brain or mental state (Alberdi et al., 2016).

This research harnesses the current advances in wearable sensing technologies to collect older adults' bodily responses to their interaction with the environment as a means of assessing and detecting environmental barriers. The bodily responses (i.e., physiological, behavioural, and cognitive responses) that the older adults naturally and unconsciously portray while interacting with different environmental conditions may offer vital information about the environment's condition. Given the rate of population ageing coupled with the ageing of built environment infrastructures, a phenomenon now referred to as "double ageing" (Ling and Lee, 2019), there is more likelihood of older adults encountering excessive environmental demands during their daily trips. Adopting an elderly-centric sensing approach is essential to efficiently and timely understand older adults-environment interactions to inform urban planning and design.

1.4 Research Aim and Objectives

This study aims to promote older adults' mobility by reducing environmental demands. Given the above proposal, the overall goal of this research is in two folds: (1) to enable practitioners to detect stressful older adults-environment interactions in near real-time and (2) to bring to limelight the influence of urban environment configurations on older adults' stress response. The specific objectives of this research are as follows.

- 1. To assess the informative of people's bodily responses (i.e., physiological, behavioural, and cognitive responses) to different environmental conditions:**
Deploying wearable sensors in an ambulatory, real-world environment poses several challenges that can diminish the signals' informativeness. An approach to determine

the informative bodily responses is essential for the effectiveness of elderly-centric sensing.

2. **To examine the relationships in older adult's bodily responses resulting from their interaction with the environment:** Human responses to environmental conditions are complicated and are inherently subject to greater variability. Therefore, it is important to understand the variability in older adults' bodily responses to different environmental conditions before adopting elderly-centric sensing.
3. **To detect older adults' stressful environmental interactions in near-real time:** Current approaches are costly and time-consuming when deployed on a large scale because they are manually planned. A smart and more efficient approach that enables a near real-time assessment is needed.
4. **To examine the influence of visuospatial configuration of urban space on older adults' stress response:** The affordance for older adults' involvement in the environment differs from the average person. In order to guide universal designs and the creation of age-friendly cities and communities, it is important to further our understanding of the relationship between the visuospatial configuration of urban space and older adults' stress.

1.5 Research Design and Approach

An interdisciplinary design and approach were used to achieve the research objectives. The flowchart depicting the research design, approach and the interrelations between the objectives is depicted in Figure 1.1. First, a field experiment was designed to collect three different types of data. The first data was from two observers who audited the conditions of the experimental path using an integrated version of the Environment in Asia Scan Tool—Hong Kong version and Older adults Senior Walking Environmental Assessment Tool—Revised developed in this

study (Appendix C). The second data were older adults' bodily response and location data collected using non-intrusive wearable sensors. The bodily responses included physiological response (heart rate, heart rate variability, and electrodermal activity), cognitive response (electroencephalography), behavioural response (foot plantar pressure distribution and contact forces, and 3-axis acceleration data), and location and environmental data (GPS coordinates, temperature, humidity, time-of-day, and recorded video). The third data type was older adults' perceived assessment of the conditions of the experimental path. Prior to the field data collection, older adults were recruited and screened to meet the eligibility criteria. Only ten eligible older adults participated in the research.

The collected bodily responses were pre-processed to remove artefacts and baseline normalised to reduce inter-individual variance. The first analytical approach in this research was based on information entropy. In information theory, the concept of entropy was introduced to quantify the amount of uncertainty involved in the value of a random variable or the outcome of a random process (Wehrl, 1978). This concept enabled the assessment of the relevance of the information in older adults' bodily response signals (Research Objective 1). Statistically analysis (Wilcoxon signed-rank test), spatial clustering analysis (Getis-Ord General G statistic and Getis-Ord G_i^* statistics) and space-time pattern mining were used to infer the relationships in older adults' bodily responses to the environment (Research Objective 2). Several machine learning algorithms, including Gaussian Support Vector Machine, Ensemble bagged tree, and deep belief network were trained and tested to detect older adult's stressful interactions. The Ensemble bagged tree achieved the best performance. Kernel density estimation was used to estimate the density of the detected older adult's stressful interactions. A simulation-based approach was used to examine areas within the study area that are sufficiently powered to detect stress hot spots that pose higher risk to older adults (Research Objective 3). Finally, self-

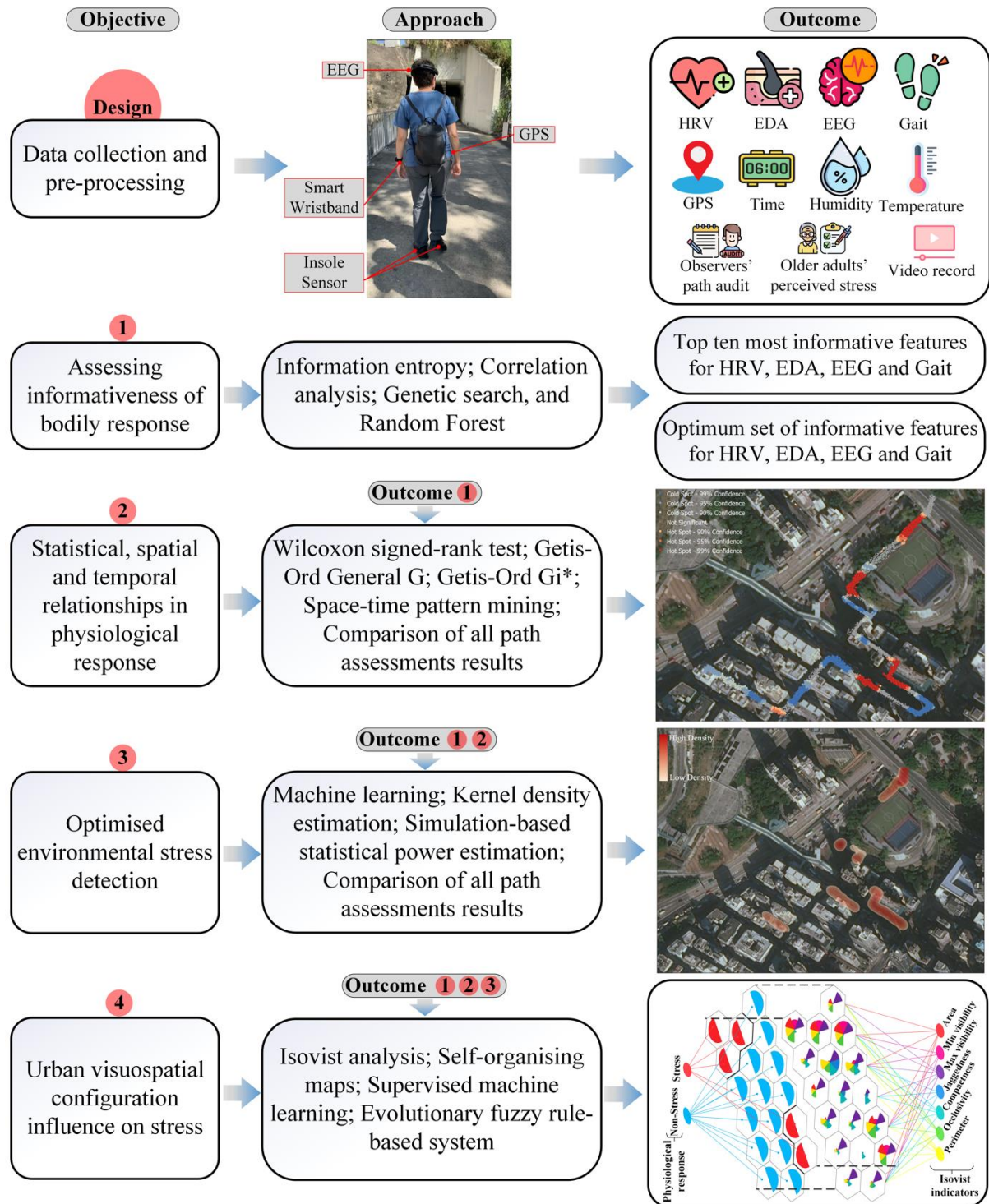


Figure 1.1: Flowchart of research design, approach and the interrelations between the objectives.

Note. HRV = heart rate variability; EDA = electrodermal activity; EEG = electroencephalography; GPS = Global Positioning System.

organising maps, supervised machine learning and evolutionary fuzzy rule-based system were integrated to examine the influence of visuospatial configuration of urban space on older adults' stress response. The perceived visual elements of the urban environment were extracted using isovist analysis (Research Objective 4).

1.6 Research Significance

Overall, this research will enable urban planners and municipal decision-makers to detect and alleviate stressful environmental conditions more effectively, particularly in cities and communities whose built environment infrastructures are approaching their design life (e.g., old districts which require urban renewal). As a result, older adults will be more likely to achieve successful mobility within their neighbourhoods, thereby promoting active ageing.

1.7 Organisation of the Thesis

The rest of the thesis consists of five parts and eight chapters. The rest of PART I is a literature review on the conceptualisation of age-friendly cities and communities, and the current built environment assessment approaches. PART II describes the research methodology, which covers Chapter 3. The experiment design, field data collection of bodily responses, perceived response, and observers' audit, are presented in this chapter. The pre-processing and analysis of bodily responses are discussed in this chapter. PART III describes the detection of stressful older adults-environment interactions, where Chapter 4 presents an assessment of the informativeness of the bodily response, Chapter 5 focuses on understanding the relationships in older adults' physiological response resulting from their interaction with the environment, Chapter 6 introduces a machine learning approach for representing human-environment interaction using an optimum set of informative physiological features and for detecting older adults' stressful environmental hot spot. Part IV, which includes Chapter 7, aims to further our

understanding of the relationship between the visuospatial configuration of urban space and older adults' physiological stress response using current advances in machine learning and evolutionary computing. Finally, PART V, which includes Chapter 8, summarises the conclusions and recommendation drawn from the research. The future works that could overcome the limitations of this study are provided in this chapter.

CHAPTER 2

LITERATURE REVIEW²

2.1 Introduction

This chapter review existing studies on the conceptualisation of age-friendly cities and communities and the current built environment assessment approaches. The sensors and bodily responses that have been used to represent human-environment interactions are presented in the chapter. Finally, research and methodological gaps are revealed.

² This chapter is based on studies that are published or currently under consideration for publication.

Torku, A., Chan, A.P.C., Yung, E.H.K., Seo, J. (2021). The influence of urban visuospatial configuration on older adults' stress: A wearable physiological-perceived stress sensing and data mining based-approach, *Building and Environment*, 108298. <https://doi.org/10.1016/j.buildenv.2021.108298>

Torku, A., Chan, A.P.C., and Yung, E.H.K. (2021). Implementation of age-friendly initiatives in smart cities: Probing the barriers through a systematic review, *Built Environment Project and Asset Management*, 11(3), 412-426. <https://doi.org/10.1108/BEPAM-01-2020-0008>

Torku, A., Chan, A.P.C., and Yung, E.H.K. (2021). Age-friendly cities and communities: A critical review and future directions, *Ageing & Society*, 41(1), 2242-2279. <https://doi.org/10.1017/S0144686X20000239>

Torku, A., Chan, A.P.C., Yung, E.H.K., Seo, J. (2021). Wearable sensing and mining of the informativeness of older adults' bodily responses to detect demanding environmental conditions, *Environment and Behavior*. (Under Review). E&B-20-0532.R2

Torku, A., Chan, A.P.C., Yung, E.H.K., Seo, J. (2021). Learning to detect older adults' environmental stress hotspots to improve neighbourhood mobility: A multimodal physiological sensing, machine learning and risk hotspot analysis-based approach, *Cities* (Under Review). JCIT-D-21-01443

2.2 Age-friendly Cities and Communities

One of the fundamental questions posed by the change in demographics is how cities and communities will remain age-friendly. The WHO defined an age-friendly city and community (AFCC) as a city or community with

“policies, services, settings and structures support and enable people to age actively by: recognizing the wide range of capacities and resources among older people; anticipating and responding flexibly to ageing-related needs and preferences; respecting their decisions and lifestyle choices; protecting those who are most vulnerable; and promoting their inclusion in and contribution to all areas of community life” (WHO, 2007, p.5).

The term elder-friendly community was also used by Feldman and Oberlink (2003), Hanson and Emlet (2006) and Alley et al. (2007). An elder-friendly community is “a place where older people are actively involved, valued, and supported with infrastructure and services that effectively accommodate their needs” (Alley et al., 2007, p. 4). It is important to draw the attention of researchers and practitioners to the fact that different studies have adopted different terminologies to describe the concept WHO (2007) referred to as age-friendly cities. Other terminologies identified in the literature include elder-friendly community, age-friendly communities, liveable community and lifetime neighbourhood (Lui et al., 2009; Feldman and Oberlink, 2003; Kihl et al., 2005; Hanson and Emlet, 2006; Alley et al., 2007). The term age-friendly community was mainly used in Canada, liveable community was mainly used in the United States of America (USA), and lifetime neighbourhood was mainly used in the United Kingdom (UK) (Lui et al., 2009). Despite the differences in the terminologies, they all share a common theme with the WHO (2007) definition of age-friendly cities.

The sense of urgency to create AFCC was heightened by the statistical data of most of the developed countries. Responding to the demands of the ageing population led to the development of AFCC models highlighting the features, domains, or elements of AFCC. The Visiting Nurse Service of New York's AdvantAge Initiative identified four main domains of an elder-friendly community. The domains are presented in Table 2.1 (Feldman and Oberlink, 2003). AARP introduced eight elements of a liveable community that is friendly to older adults (Kihl et al., 2005). These elements shown in Table 2.1 were identified through focus groups with older residents and caregivers in 13 cities in five areas of the USA (Kihl et al., 2005). Furthermore, Alley et al. (2007) identified 15 characteristics of an elder-friendly community based on the perception of practitioners. These characteristics are presented in Table 2.1.

Also, the WHO (2007) identified eight features of an age-friendly city and community (Table 2.1). The WHO (2007) further added a checklist of features of age-friendly cities and communities based on the Vancouver Protocol to serve as a guide for self-assessment and comparison of findings. The features were derived by working with older adults in 33 cities and communities worldwide (WHO, 2007). Building on the WHO (2007) framework, Menec et al. (2011) applied ecological theory to the concept of age-friendly cities proposed by WHO (2007). Menec et al. (2011) framework was based on the premise that the conditions of the environment are interrelated, and a fit between the person and the environment is crucial to promoting social connectivity. As a result, Menec et al. (2011) proposed seven AFCC domains; these are presented in Table 2.1.

Table 2.1: AFCC concepts

Author (s)	Concept	Characteristics
Elder-friendly community (University of Calgary, Canada)	<ul style="list-style-type: none"> • A place to call home • Building community • Making ends meet • Being valued and respected • Staying active 	This concept focused on the assessment of the assets, capacities and needs of older adults. However, this concept is not statistically generalisable to other locations.
Austin et al. (2001)	<ul style="list-style-type: none"> • Getting what you need • Getting around • Feeling safe 	
Elder-friendly community (AdvantAge Initiative)	<ul style="list-style-type: none"> • Maximises independence for frail and disabled • Addresses basic needs • Promotes social and civic engagement • Optimises physical and mental health and well-being 	This concept solely focused on older adults and included both physical and social elements that sustain active participation, independence and engagement. This concept is unique in that it includes items such as the “percentage of people age 65+ who would like to be working for pay” and “percentage of people age 65+ who had problems paying for medical care”. This concept provides quantified results of lacking needs, and it is easier to identify and prioritise ageing issues that need immediate attention.
Feldman and Oberlink (2003, p. 269)		
Liveable community (American Association of Retired Persons)	<ul style="list-style-type: none"> • Transportation • Walking • Housing • Shopping • Safety and security • Recreation and culture 	This concept emphasised more on the availability, suitability and affordability of the physical environment and the supportive community services for facilitating independence and social engagement for dependent (frail) and independent older adults and the general population. It includes items such as “Are the sidewalks adequately lighted at night?” and “Does your community have an information hotline or a directory of services for older persons?”. Unlike Feldman and Oberlink (2003, p. 269)’s concept, this concept only identifies the presence or absence of physical and social environmental needs.
Kihl et al. (2005)	<ul style="list-style-type: none"> • Health services • Caring and mutual support 	
Elder-friendly community	<ul style="list-style-type: none"> • Accessible and affordable transportation • Housing • Safety • Health care • Community involvement opportunities 	This concept stressed on important characteristics of becoming age-prepared. This concept is in alignment with Feldman and Oberlink (2003, p. 269) and Kihl et al. (2005) concepts. Although this concept captured a wide variety of physical and social environmental factors, it may be limited in that it only included the most important characteristics which may limit its adoption in different settings. The other concepts presented various physical and social environmental age-friendly features for communities to identify issues that its members consider as important.
Alley et al. (2007, p. 7)		

Author (s)	Concept	Characteristics
Age-friendly city and community WHO (2007)	<ul style="list-style-type: none"> • Outdoor spaces and buildings • Transportation • Housing • Social participation • Respect and inclusion • Civic participation and employment • Communication and information • Community supports and health services 	<p>This concept includes physical settings and structures, social policies, and services for active ageing. This concept consists of eight domains (physical and social environment) with several items within each domain. Unlike Feldman and Oberlink (2003, p. 269), Kihl et al. (2005) and Alley et al. (2007, p. 7)'s concepts, this concept is very flexible, can be used to generate qualitative and quantitative results of lacking needs depending on the users' preference. As a result, it captures essential information that can be rigorously analysed for developing age-friendly interventions and policies.</p>
Lifetime neighbourhood (Department for Communities & Local Government, UK) Harding (2007)	<ul style="list-style-type: none"> • Built environment • Housing • Social inclusion • Social cohesion and sense of place • Innovation and cross-sectoral planning • Services and amenities 	<p>The concept is underpinned by the principle of inclusive design, sustainability and participation. Similar to the lifetime home concept and the WHO (2007)'s concept, this concept focus on the neighbourhood with a number of key features to plan a sustainable community.</p>
Positive ageing framework New Zealand Ministry of Social Development (2007)	<ul style="list-style-type: none"> • Housing • Transport • Access to facilities and services • Income • Employment • Opportunities • Health • Living in the community • Cultural identity • Attitudes 	<p>This concept is underpinned by the principle that the years of old age are viewed and experienced positively. The concept embraces ten domains with unique desired outcomes. However, the indicators are generally limited to aspects of older adult's lives at a particular time.</p>
Menec et al. (2011, p. 484)	<ul style="list-style-type: none"> • Physical environment • Housing • Transportation options • Communication and information • Social environment • Opportunities for participation • Informal and formal community supports and health services 	<p>Menec et al. (2011, p. 484)'s concept is consistent with the WHO (2007)'s concept. However, this concept focused on the interaction between older adults and the environmental conditions (social connectivity) to advance age-friendly policy decisions. This concept argued that some of these domains proposed in previous concepts such as respect and inclusion (WHO, 2011) and safety (Alley et al. 2007, p. 7; Kihl et al., 2005) do not fit as an aspect of the environment but rather the outcome of implementing age-friendly interventions.</p>

All the models share a central theme which is to develop cities and communities that support active ageing, reduce isolation, sustain independence, improve accessibility and affordability for the older adults and general population. The AFCC features broadly span from the physical environment to social environment. However, this study focuses on the outdoor environment, which is one of the elements of the physical environment in AFCC.

2.3 Why the Outdoor Environment

The AFCC concept was proposed in pursuit of developing communities and cities that support active ageing (WHO, 2002). Physical activity and independent mobility are critical determinants of active ageing, healthy longevity, and maintenance of the quality of life in older adults (Holliday et al., 2017; WHO, 2009; US Department of Health and Human Services, 2008). Findings of the WHO (2009) affirmed that a lack of physical activity is the fourth globally ranked risk factor for mortality and burden of disease attributable. For this reason, advocates of physical activity promotion, including public health researchers and practitioners, recommend environmental interventions that support and encourage people to engage in physical activity (Sallis et al., 1998; Brownson et al., 2008; Kelly et al., 2013). The outdoor environment is one of the key features of the city and community's physical environment that strongly influence personal mobility, safety from injury, security from crime, health behaviour and social participation (WHO, 2007). Therefore, the outdoor environment has the potential to facilitate physical activity and independent mobility, thus promoting active ageing among older adults (Van Cauwenberg et al., 2011; Timmermans et al., 2016; Inclusive Design for Getting Outdoors, 2013).

The outdoor environment generally works well for healthy and able-bodied people. An individual's functional capacity increases in childhood, peaks in early adulthood and eventually

decline (WHO, 2007; Kalache and Kickbusch, 1997). People with declined functional capacity, such as older adults, must contend with many physical environmental barriers that may hinder older adults' participation in outdoor activities. Evidence indicates that the frequency and time older adults spend outdoors depends on the age-friendliness of the outdoor environment features (Inclusive Design for Getting Outdoors, 2013). Research has shown that older adults residing in areas with environmental barriers, such as poor sidewalk conditions, are at greater risk of reporting mobility limitations (Twardzik et al., 2019). An age-friendly environment has a crucial influence on older adults' activity levels, general health and overall satisfaction with life (Inclusive Design for Getting Outdoors, 2010; WHO, 2007). An age-friendly living environment can influence and may reverse the speed of decline in the functional capacity of older adults (WHO, 2007; Kalache and Kickbusch, 1997).

In this research, the outdoor environment, built environment, and physical environment are used interchangeably. The outdoor environment, built environment, or physical environment is the physical form of cities and communities (Brownson et al., 2009).

2.4 Built Environment Determinant of Walking

The main evidence-based framework of physical environmental factors that may influence walking in the local neighbourhood was developed by Pikora et al. (2003). Based on published evidence and policy literature, interviews with experts and a Delphi study, Pikora et al. (2003) identified four built environmental domains: functionality, safety, aesthetics, and destination. Functionality relates to the physical attributes of the street and path that reflects the condition of the structural elements of the built environment (Pikora et al., 2003; Cunningham et al., 2005; Michael et al., 2009).

Table 2.2: Built environment factors that may influence walking

Domain	Element
Functionality	<ul style="list-style-type: none"> • Path condition (wet and slippery streets) • Path slope • Path obstruction • Major barriers (roadwork, steep staircases) • Minor barriers (cracks, holes, bumps, parking meters) • Street crowd • Motor vehicles parked on footpath • Hawkers and shops on streets • Path width • Path material • Curb cut features
Safety	<ul style="list-style-type: none"> • Permeability • Pedestrian crossing • Traffic load • Traffic calming devices • Streetlight • Directional sign • Presence of people • Signs of crime/disorder • Stray dogs /other animals
Aesthetics	<ul style="list-style-type: none"> • Views • Building attractiveness • Attractive natural sights • Streetscape • Litter • Graffiti • Pollution • Greenery
Destination	<ul style="list-style-type: none"> • Transport-related • Public open space • Recreational • Government/public services • Public facilities • Commercial destinations

Source: Pikora et al., (2003); Cunningham et al. (2005); Michael et al. (2009); Cerin et al. (2011).

Safety reflects elements of the environment that strengthen the feeling of safeness and increase the degree of comfort of the older pedestrians (Pikora et al., 2003; Rebecchi et al., 2019; Michael et al., 2009). Aesthetics reflects elements of the environment relating to the human scale, are visually interesting, appealing, and increase the attractiveness of the environment

(Pikora et al., 2003; Rebecchi et al., 2019; Michael et al., 2009). The destination domain relates to the availability of community and commercial facilities in the neighbourhood (Pikora et al., 2003). The built environmental domains and factors that contribute to each of these domains are presented in Table 2.2.

2.5 Assessing the Built Environment to Promote Mobility

Since the 1980s, urban planners and travel behaviour researchers have studied how the built environment affects people's outdoor physical activities, recreational behaviours, and quality of life (Sallis, 2009; Handy et al., 2002; Papas et al., 2007; Brownson et al., 2009). In recognition of the importance of physical activity, planners have developed conceptualisations of community design such as walkability, that is, the extent to which the built environment supports and encourages mobility by walking (Forsyth, 2015). Mobility is defined as the ability to achieve access to the desired place (Rantanen, 2013). Conceptual models on the built environment and mobility postulate that mobility is affected by different built environment attributes (Pikora et al., 2003; Ramirez et al., 2006). To understand the effect of the built environment on mobility, it is of paramount importance to develop a high-quality assessment approach (Brownson et al., 2009). Of central concern among the active living researcher is developing accurate and efficient built environment assessment approaches (Sallis, 2009; Brownson et al., 2009). Four categories of built environment assessment approaches are being used: perceived environment assessment approach, systematic observational assessment approach, Geographical information systems (GIS)-based assessment approach, and bodily response-based assessment approach.

The perceived (also known as self-report) environment assessment approach often requires untrained raters to judge the extent to which the built environment promotes or hinders their

mobility (Sallis, 2009). The perceived environment assessment approach is mainly collected using interview or self-administered questionnaires (Brownson et al., 2009; Hoehner et al., 2005). The systematic observational assessment approach, also known as environmental audit, often requires trained observers to quantify the attributes of the built environment. Trained observers use pre-defined protocols or tools to assess the built environment attributes as it is directly observed (in-person observation) (Sallis and Saelens, 2000; Brownson et al., 2009; Cerin et al., 2011). These audit tools have enabled a systematic and objective assessment of the built environment. The GIS-based assessment often relies on archived (existing) data that have spatial reference to assess the built environment (Li et al., 2021). Data such as infrastructure-based data (e.g., air quality and sound level), user-generated data (e.g., GPS) and street view imagery (e.g., Google Street View, Google Earth, and Bing Map) are often used to audit built environment (Gullón et al., 2015; Yin, 2017; Knöll et al., 2018; Zhou et al., 2019; Kelly et al., 2013). GIS-based assessment enables an objective assessment of built environment dispersed across a large area (Brownson et al., 2009). The fourth category of assessment approach involves data collected from users' direct bodily responses to assess the built environment objectively and continuously (Kim et al., 2016; Birenboim et al., 2021; Birenboim et al., 2019). The bodily responses (i.e., physiological, behavioural, or cognitive responses) collected using sensing technologies are spatially matched with GPS data to assess the built environment.

Each of the built environment assessment approaches has its own advantage and disadvantage, which could affect its effectiveness. Because the perceived environment assessment involves interview or self-administered questionnaires, its main drawback is declining response rates (Brownson et al., 2009). Also, interviewing or administering questionnaires to older adults might obstruct their daily lives; especially in large scale neighbourhood assessment that takes

a longer period to complete. The subjectivity of individual reported perception can influence built environment assessment (Aghaabbasi et al., 2018). Although the observational assessment approach is objective, it involves in-person observation, which is time-consuming and costly (Brownson et al., 2009). Observational assessment demands investment in staff, training of observers, transportation to the assessment site, among others. Because this approach is time-consuming, labour intensive and costly, it may limit the scope and frequency of conducting neighbourhood assessment. Although the GIS-based assessment can provide an objective, less obstructive, less labour intensive, less time consuming, and large-scale assessment of the built environment (Chiang et al., 2017), it is inefficient in detecting older adults' environmental barriers. By definition, an environmental barrier is a relative concept; dependent on the interaction between an individual's capability and environmental demand (Mair et al., 2011; Yang and Matthews, 2010; Lawton, 1982; Webber et al., 2010). Therefore, an environment may be a barrier for one person and not a barrier for another person. Sensing people's direct bodily responses to the environment can detect such environmental barriers that could not be detected using the GIS-based or observational assessment approach (Kim et al., 2016; Birenboim et al., 2019; Twardzik et al., 2019; Kim et al., 2019; Neale et al., 2017). The bodily response-based assessment provides a continuous assessment of the built environment and less obstructive depending on the sensing technology adopted. The bodily response-based approach is the main focus of this study because of its potential to detect older adults' environmental barriers more efficiently.

2.6 Sensing of Bodily Responses to the Environment

Researchers have been using various sensors for monitoring bodily responses to represent human-environment interaction. Signals identified from the literature are illustrated in Figure 2.1. Many of the signals fall into one of two categories. The first category of sensors is

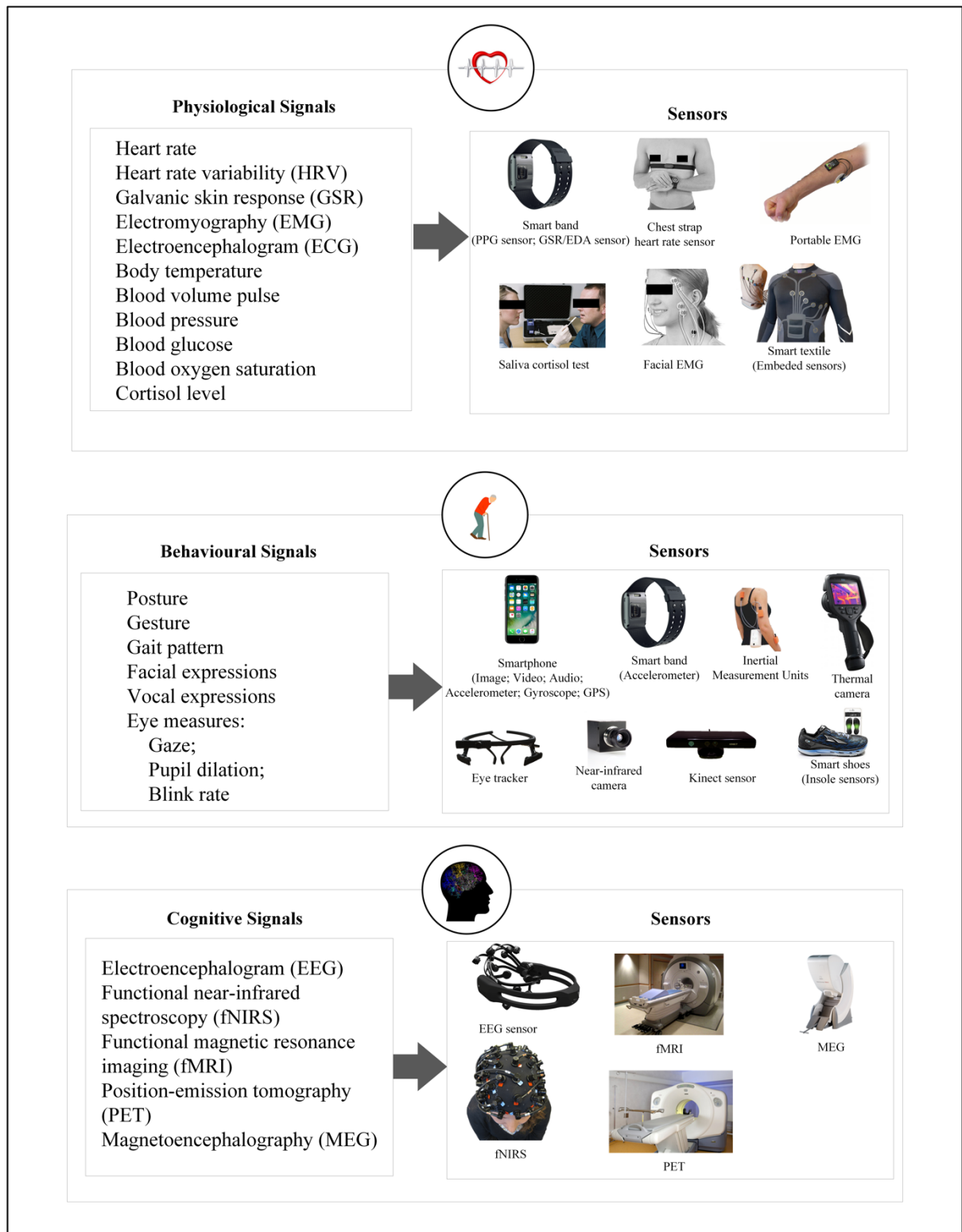


Figure 2.1: Bodily response sensors.

laboratory sensors, and the second category is wearable sensors (Ragot et al., 2017). Laboratory sensors are stationary and deployed in a controlled environment with restrictions on human

movements (e.g., subjects are connected to multiple electrodes and wires, usually in the laboratory). In contrast, wearable sensors are mobile, wireless and can be deployed in a naturalistic environment (Milstein and Gordon, 2020). Utilising wearable sensors to monitor bodily responses rather than laboratory sensors are more desirable for elderly-centric sensing because they provide more realistic insights into natural human reactions to the environment (van Beers et al., 2020). These wearable sensing devices have enabled elderly-centric sensing to be less interruptive because individuals can go about their daily routines while their bodily responses are monitored and collected. As a result, researchers have been deploying wearable sensors to collect a continuous stream of bodily responses linked to spatiotemporal information, such as GPS data, to detect demanding environmental conditions.

2.7 Bodily Response for Assessing Environmental Features

The specific bodily responses and features that have been studied in relation to the environmental features are presented in Table 2.3. However, only a few of these signals have been proven to have a statistically significant correlation or association with the built environment features. This section reviews signals that have shown a statistically significant relationship with the built environment features, that can be continuously acquired using commercially available non-intrusive wearable sensors in ambulatory settings and the results can be analysed in real-time or semi-real time.

2.7.1 Electrodermal Activity (EDA)

EDA is also known as Galvanic skin response (GSR) or Skin Conductance. EDA measures the activation of the sympathetic nervous system non-invasively and is one of the most frequently employed signals for detecting physiological arousal (Kleckner et al., 2018; Boucsein, 2012). The sympathetic nervous system can be stimulated physically and emotionally, which intends

trigger variation in the eccrine sweat gland activity which is controlled by the sympathetic nervous system (Melander, et al., 2018; Chittaro and Sioni, 2014; Boucsein, 2012). An increase in the eccrine sweat gland activity is observed (emotional sweating) when the sympathetic nervous system is stimulated with a high-level arousal stimulus, thus changing the conductivity of the skin (Zhang et al., 2018; Kleckner et al., 2018). An increase in sweating results in a sharp increase in the conductivity of the skin (Chittaro and Sioni, 2014). High levels of EDA correlate with stress, and lower levels of EDA correlate with the relaxed state (Birenboim et al., 2019). Statistically significant positive associations were found between participant EDA in favourable features—such as greenery and attractive natural sights—of the environment (Chrisinger and King, 2018; Ojha et al., 2019; Saitis and Kalimeri, 2018). Statistically significant negative associations were found between participant EDA in stressful features—such as stressful crossing—of the environment (Chrisinger and King, 2018; Birenboim et al., 2019; Saitis and Kalimeri, 2018).

EDA is statistically analysed using mean and standard deviation of the amplitude, minimum and maximum values (Chrisinger and King, 2018; Osborne and Jones, 2017). The raw EDA signal decomposes into two components: the tonic component or skin conductance level (SCL) and the phasic component or the skin conductance response (SCR) (Ojha et al., 2019; Birenboim et al., 2019; Chen et al., 2018). The tonic component reflects the baseline level of skin conductivity and changes slowly over time –it correlates to the basic physiological state. The tonic component is not related to emotional responses or emotion-inducing stimuli (Chen et al., 2018; Birenboim et al., 2019). The phasic component increases in the amplitude of skin conductive, which reflects human reactions to discrete environmental stimuli (Birenboim et al., 2019; Chen et al., 2018). The common parameters used to analyse the phasic component are Number of significant phasic SCRs (nSCRs), Sum of SCR-amplitudes of significant SCRs

(AmpSum), Maximum value of phasic activity (PhasicMax), Mean skin conductivity value (GlobalMean) and Maximum level of skin conductivity (MaxDeflection). nSCRs, AmpSum and PhasicMax are more useful indicators of momentary changes in the outdoor environment because it considers the magnitude of local deflection (Birenboim et al., 2019; Ojha et al., 2019). However, GlobalMean and MaxDeflection consider the absolute values of EDA levels. Both GlobalMean and MaxDeflection may be useful in a controlled environment such as the laboratory. But, less useful in an uncontrolled environment such as an outdoor environment because absolute EDA can change rapidly to basic physiological state such as sweating due to increased heat regardless of a person's cognitive state (Birenboim et al., 2019).

2.7.2 Electrocardiogram (ECG or EKG) and Blood Volume Pulse (BVP)

Electrocardiogram (ECG) measures present digital wave patterns of the morphological and temporal parameters of the rhythm and electrical activity generated by the heart (Zhang et al., 2018; Walford et al., 2017). The raw ECG signal has not been used in built environment research. However, information about Heart Rate (HR) and Heart Rate Variability (HRV) has been extracted from the ECG data.

Photoplethysmography (PPG) is also used to measure the blood volume pulse, and it indicates the quantity of blood flowing into the peripheral vessel. The blood volume pulse is determined from the difference in light absorption that illuminates the skin from a pulse oximeter. The amount of light that returns to the PPG sensor is proportional to the volume of blood in the tissue (Peper et al., 2017). An increase in BVP amplitude indicates decreased sympathetic arousal and greater blood flow to peripheral vessels (Chang et al., 2008). The amplitude of the raw BVP has been used to study the restorative value of natural environments (Chang et al.,

2008). Also, HR and HRV parameters have been extracted from the raw BVP to assess environmental features (Kim et al. 2019).

HR measures the number of heart beats per minute and is commonly used to distinguish between positive and negative emotions (Zhang et al., 2018). Several researchers have studied the relationship between HR and different environmental features. However, the findings from these studies are inconsistent. For example, South et al. (2015) identified a significant relationship between the HR level and different walking segments (greening site and no greening site). Also, studies showed that HR was significantly lower when participants walked in a green environment than when they walked in the urban environment (Song et al., 2015a; Song et al., 2015c; Song et al., 2014; Song et al., 2013). A more recent study proved that no significant difference was detected in the HR level between different walking environment, including stressful and less stressful walking segments (Birenboim et al., 2019). The most effective HR parameters are the average heart rate and heart rate reserve (Walford et al., 2017; Kim et al., 2016).

HRV is the variation between the heart's inter-beat intervals (Birenboim et al., 2019; Li and Sullivan, 2016). A stimulated sympathetic system is associated with a decrease in HRV. In a relaxed state, the parasympathetic activity increases which are associated with an increase in HRV (Birenboim et al., 2019; Gladwell et al., 2016). The time-domain parameters, frequency domain parameters and non-linear HRV analysis methods were used to calculate various HRV indices associated with the environment. A statistically significant correlation has been established between HRV—specifically the frequency domain parameters—in detecting the difference between stressful environmental conditions and neutral conditions (Birenboim et al., 2019; Song et al., 2015a; Song et al., 2015c).

2.7.3 Gait

Gait is an individual movement pattern that can reflect the individual's emotional state, cognition, intent, personality, attitude, and health (Sun et al., 2017; Agmon and Armon, 2016). The gait pattern of individuals has been continuously monitored to detect the disturbance caused by environmental features, and studies have proved that the mobility of an individual is directly a function of the environment under the individual's feet (Twardzik et al., 2019; Duchowny et al., 2019). Human gait activities to environmental features have been monitored using camera-based systems and wearable motion sensors in real-time (Twardzik et al., 2019; Pedersen and Johansson, 2018). The gait features extracted from camera-based systems in relation to environmental features include walking speed, spacing behaviour, path change behaviour, step frequency, step length, platoon, rolling behaviour. The motion sensors measure the linear and angular motion of the body. The gait features extracted from the sensors in relation to the environmental features include gait speed, cadence, stride length, gait stability, gait acceleration. The gait features are most effective in predicting the presence of a built environment feature or the physical condition of a walking path. Gait speed, cadence, stride length, gait stability and gait acceleration are significantly associated with the conditions of a walking path such as slope, width, presence of holes, grooves, bumps, and curb cut (Twardzik et al., 2019; Kim et al., 2016).

2.7.4 Eye Movement

Eye movements are the visual perception that can be tracked to measure the allocation of visual attention over a visual stimulus (Cottet et al., 2018). Eye movements are normally recorded during cognitive processing tasks such as scene perception, reading, visual search tasks and recognition tasks (Berto et al., 2008). The widely used eye-related measures to acquire visual information about the environment include fixation, fixation count, fixation duration, saccade

amplitude, blink count, blink duration and scanpath length (Stevenson et al., 2019; Hollander et al., 2019; Crosby and Hermens, 2018). A fixation happens when the eyes are relatively stationary for visual perception of information, and saccades is the eye movements between fixations (Dupont et al., 2017; Miyasike-daSilva et al., 2011). The scanpath is the length of oculomotor event when perceiving a stimulus within a timespan (Dupont et al., 2017). The sequences of fixations and saccades are indicators of a person's internal state, such as cognitive load (Hollander et al., 2019; Elsadek et al., 2019) and emotional state (Matsuda et al., 2018; Crosby and Hermens, 2018), and external state such as the salience and organisation of a stimulus (Dupont et al., 2017; Valtchanov and Ellard, 2015). The effect of the natural and built environment was most predicted by the number of fixations per minute (Stevenson et al., 2019). Eye movement indicators is an effective substitute for visual aesthetic quality and tranquillity rating evaluation (Liu et al., 2019).

2.7.5 Electroencephalogram (EEG)

EEG refers to the measurement of voltage changes in the brain's electrical field produced by the flow of ions in the neurons of the brain (Seo et al., 2019; Subramanian et al., 2018). Recent studies have proven that different environmental features are associated with distinctive patterns of brain activity or brain wave production, which means humans interact differently with varying environments (Kim et al., 2019b; Bailey et al., 2018; Tilley et al., 2017; Chen et al., 2016). EEG spectral analysis is the common method to quantify brain activity when exposed to environmental features. The spectral analysis involves decomposing the raw EEG signal into oscillations of the different frequency band (Grassini et al., 2019).

The widely used frequency bands for assessing environmental features are the Delta (0.5–3 Hz), Theta (4–7 Hz), Alpha (8–15 Hz), Beta (16–31 Hz) and Gamma (32–100 Hz)

Table 2.3: Bodily response for assessing environmental features

Environmental features	Reference (s)	Bodily response	Feature	Parameter (s)
Physiological				
Outdoor walking route (urban busy, urban green, pedestrian traffic, length, gradient, noise, planted trees, gardens)	Birenboim et al. (2019), Kim et al. (2019), Gidlow et al. (2016b), South et al. (2015), Song et al. (2015a); Song et al. (2015c); Song et al. (2014); Song et al. (2013)	HR		Mean, Standard deviation, Minimum and maximum values of HR, Heart rate reserve
	Birenboim et al. (2019), Gladwell et al. (2016), Song et al. (2015a), Song et al. (2015c); Song et al. (2014); Song et al. (2013)	HRV		RR or NN interval, SDNN, RMSSD, pNN50, LF, HF, LF/HF, CCV-LF, CCV-HF, CCV-LF/HF, SD1
	Walford et al. (2017), Chen et al. (2018)	ECG	HR HRV	Average HR RR or NN interval, SDNN, RMSSD, QT variability index (QTVI)
	Birenboim et al. (2019), Chrisinger and King (2018), Chen et al. (2018), Osborne and Jones (2017)	EDA/GSR		nSCR; AmpSum; PhasicMax; Global Mean; Max Deflection
	Chen et al. (2018), Osborne and Jones (2017)	ST		Mean, Minimum and maximum values, Standard deviation
	Osborne and Jones (2017)	BVP		Amplitude, IBI, HR, HRV
	Gidlow et al. (2016b)	Salivary cortisol		Salivary cortisol concentrations
	Song et al. (2015b)	BP		SBP and DBP
	Chen et al. (2018)	EMG	Facial muscles	EMG amplitude
	Behaviour			
Twardzik et al. (2019); Kim et al. (2019), Dixon et al. (2018), Matsuda et al. (2018); Kim et al. (2016), Ottosson et al. (2015)	Gait	Gait speed Cadence Stride length Gait stability	Mean gait speed Mean left foot cadence Left foot stride length Maximum Lyapunov exponent (Max LE)	

Environmental features	Reference (s)	Bodily response	Feature	Parameter (s)
			Acceleration	Signal vector magnitude (SVM)
			Turning gait	
	Stevenson et al. (2019), Matsuda et al. (2018)	Eye movement		Fixations per minute, Fixation duration, Intensity of eye movement
	Matsuda et al. (2018)	Facial expressions	AUs	FACS
	Matsuda et al. (2018)	Head movement	Head tilt (Looking up/down, right/left)	Head tilt per second, average and standard deviation of the time interval looking at each direction
			Cognitive	
	Bailey et al. (2018), Tilley et al. (2017), Neale et al. (2017), Hollander and Foster (2016), Chen et al. (2016), Chen et al. (2018)	EEG		Delta (0.5–3 Hz), Theta (4–7 Hz), Alpha (8–15 Hz), Beta (16–31 Hz), Gamma (32–100 Hz)
				Levels of excitement, engagement, and frustration (as interpreted by Emotiv Affectiv Suite proprietary EEG software)
				Levels of meditation/relaxation (as interpreted by NeuroSky proprietary EEG software)
			Physiological	
Landscape – Natural (Water bodies, Green vegetation, mountain, forest) and Urban (Built environment)	Chang et al. (2008), Ulrich et al. (1991)	EMG	Facial muscles	EMG amplitude
	Chang et al. (2008)	BVP		BVP amplitude

Environmental features	Reference (s)	Bodily response	Feature	Parameter (s)
	Lacuesta et al. (2017), Sahlin et al. (2016), Greenwood and Gatersleben (2016), Valtchanov et al. (2010), Laumann et al. (2003), Triguero-Mas et al. (2017), Yu et al. (2018),	HR		Mean, Standard deviation, Minimum and maximum values of HR
	Elsadek et al. (2019), Yu et al. (2018), Song et al. (2018), Triguero-Mas et al. (2017), Lacuesta et al. (2017), Li and Sullivan (2016), Kobayashi et al. (2015), Lee et al. (2015)	HRV		LF, HF, LF/HF, CCV-LF, CCV-HF, CCV-LF/HF
	Valtchanov et al. (2010), Li and Sullivan (2016), Ulrich et al. (1991)	Skin-conductance level		
	Hunter (2019), Triguero-Mas et al. (2017), Kobayashi et al. (2017), Lee et al. (2015), Tyrväinen et al. (2014), Markevych et al. (2014), Jiang et al. (2014), Roe et al. (2013), Beil and Hanes (2013), Thompson et al. (2012), Lee et al. (2009)	Salivary cortisol		Salivary cortisol level
	Gidlow et al. (2016a)	Hair cortisol		Hair cortisol concentration
	Hunter (2019), Yu et al. (2018), Beil and Hanes (2013)	Alpha-amylase		Salivary amylase levels
	Yang et al. (2019), Yu et al. (2018), Triguero-Mas et al. (2017), Stigsdotter et al. (2017), Sahlin et al. (2016), Greenwood and Gatersleben (2016), Lee et al. (2015), Tsunetsugu et al. (2013), Beil and Hanes (2013), Lee et al. (2009)	BP		SBP and DBP
	Song et al. (2018)	oxyhemoglobin (oxy-Hb)		oxy-Hb concentration in the right and left prefrontal cortex

Environmental features	Reference (s)	Bodily response	Feature	Parameter (s)
	Song et al. (2017), Qin et al. (2013), Gladwell et al. (2012), Ulrich et al. (1991), Ulrich (1981)	ECG	HR HRV	Mean, Standard deviation, Minimum and maximum values of HR RR or NN interval, SDNN, RMSSD, LF, HF, LF/HF
	Laumann et al. (2003) van den Berg et al. (2015)	IBI ECG	RSA	Peak-valley RSA
	Li and Sullivan (2016) Lee et al. (2015), Lee et al. (2009)	ICG BT Pulse rate	PEP	
		Behaviour		
	Hollander et al. (2019), Elsadek et al. (2019), Crosby and Hermens (2018), Franěk et al. (2018a), Cottet et al. (2018), Dupont et al. (2017), Valtchanov and Ellard (2015), Berto et al. (2008) Korpela et al. (2002)	Eye movement		Fixations, Fixation Durations, Saccade amplitude, Blink counts, and Scanpath lengths
		Vocal expressions of joy, anger, and emotional neutrality		Reaction times to vocal expressions
	Franěk and Režný (2017) Hietanen et al. (2007), Svoray et al. (2018) Willis et al. (2004)	Gait Facial expressions		Walking speed
		Video-based observational/ Video camera recorded captured behaviour	Microscopic movement patterns	Walking behaviour (walking speed and spacing behaviour)

Environmental features	Reference (s)	Bodily response	Feature	Parameter (s)
			Cognitive	
	Kim et al. (2019b), Grassini et al. (2019), Qin et al. (2013), Yang et al. (2011), Chang et al. (2008), Ulrich (1981)	EEG		Delta (0.5–4 Hz), Theta (4–8 Hz), low Alpha (8–11 Hz), high Alpha (11–13 Hz), Beta (13–30 Hz), and low Gamma (30–45 Hz)
				Levels of excitement, engagement, and frustration (as interpreted by Emotiv Affectiv Suite proprietary EEG software)
	Tang et al. (2017), Kim et al. (2014), Martínez-Soto et al. (2013), Kim et al. (2010a), Kim et al. (2010b)	fMRI		Brain activation (frontal lobe, temporal lobe, parietal lobe and occipital lobe)
Soundscape - Nature sound (bird song)			Physiological	
Noise (traffic noise)	Dai and Lian (2018), Irwin et al. (2011)	ECG	HR	
	Hedblom et al. (2019), Alvarsson et al. (2010)	Skin conductance		Skin conductance levels
	Lu et al. (2018)	BP		SBP and DBP
			Behaviour	
	Franěk et al. (2018b)	Gait		Walking speed
			Cognitive	
	Dai and Lian (2018), Irwin et al. (2011)	fMRI		Cerebellum posterior activity; Parahippocampal gyrus activity; Cingulate gyrus activity; Precuneus activity
Landmark and Navigation			Behaviour	
	Wenczel et al. (2017), Aspinall et al. (2014)	Eye movement		Visual acuity, fixation count, fixation duration and pupil diameter
	Gaire et al. (2017)	Gait		Walking speed pattern

Environmental features	Reference (s)	Bodily response	Feature	Parameter (s)
			Cognitive	
	Slone et al. (2016)	fMRI		Brain (precuneus, retrosplenial cortex, and hippocampus) activity
Graffiti and Sculptures			Behaviour	
	James and O'Boyle (2019), Mitschke et al. (2017)	Eye movement		Fixation duration
			Cognitive	
	James and O'Boyle (2019)	fMRI		Parahippocampal gyrus (PH) activation level, Fusiform gyrus (FF) activation level
Outdoor/ Pedestrian lighting			Physiological	
	Castro-Toledo et al. (2017)	HR		Mean, Standard deviation
			Behaviour	
	Rahm and Johansson (2018); Pedersen and Johansson (2018)	Gait		Walking speed
				Ability to perform visual tasks
Stair walking			Behaviour	
	Miyasike-daSilva et al. (2011); Zietz and Hollands (2009)	Eye movement		number of fixations, fixation time, fixation duration
	Fujiyama and Tyler (2010)	Gait		Walking speed
Crosswalk			Behaviour	
	Tageldin and Sayed (2019), Kadali and Vedagiri (2016), Havard and Willis (2012)	Pedestrian behaviour recorded on camera		Step frequency, step length, platoon, rolling behaviour, speed and path change condition of pedestrian
Plant			Cognitive	
	Oh et al. (2019)	EEG		Frequency band: Alpha wave (8–13 Hz); Theta wave (4–8 Hz)
Floral scent			Physiological	

Environmental features	Reference (s)	Bodily response	Feature	Parameter (s)
	Jo et al. (2013)	HRV		
	Jo et al. (2013)	Pulse rate		
	Jo et al. (2013)	BP		
			Cognitive	
Plant colour	Jo et al. (2013)	NIRS		Cerebral activity
			Cognitive	
	Sadek et al. (2013)	NIRS		Brain activity in the frontal, temporal, parietal and occipital lobes.
Air pollution			Physiological	
	Shields et al. (2013)	HRV		SDNN, LF, HF, LF/HF
			Cognitive	
	Pujol et al. (2016)	fMRI		Brain activation

Note. HR = heart rate; HRV = heart rate variability; ECG or EKG = electrocardiogram; EDA = electrodermal activity; GSR = galvanic skin response; ST = skin temperature; BVP = blood volume pulse; BP = blood pressure; EMG = electromyography; SDNN = standard deviation of the NN interval; RMSSD = square root of the mean of the sum of difference of successive NN intervals; SDSD = standard deviation of difference between adjacent NN intervals; pNN50 = percentage of NN pairs that differ by 50 milliseconds in the entire recording, TINN = HRV triangular index (TI) and triangular interpolation of RR interval histogram; TP = total spectral power (0–0.4 Hz); VLF = spectral power in very low range frequencies (0.003–0.04 Hz); LF = spectral power in low range frequencies (0.04–0.15 Hz); HF = spectral power in high range frequencies (0.15 Hz); LF/HF = ratio between LF and HF power; CCV-LF = coefficient component variance of LF; CCV-HF = coefficient component variance of HF; CCV-LF/HF = coefficient component variance of LF/HF; AU = action units; FACS = facial action coding system; SBP = systolic blood pressure; DBP = diastolic blood pressure; ICG = impedance cardiogram; PEP = cardiac pre-ejection period; RSA = respiratory sinus arrhythmia; fMRI = functional magnetic resonance imaging; NIRS = near-infrared spectroscopy.

frequency bands. The lower frequency bands (Delta and Theta) correlate with less intense brain functions such as sleep, meditation, and daydreaming (Bailey et al., 2018). Precisely, the Delta band features slow and loud brainwaves and is generated in deepest meditation, and dreamless sleep and the Theta band occurs most often in light sleep or extreme relaxation (Kim et al., 2019b). Alpha frequency band correlates with a relaxed brain and is generated during quietly flowing thoughts and in some meditative states (Kim et al., 2019b; Bailey et al., 2018). The higher frequency bands: Beta band dominates our normal waking state of consciousness when attention, is directed towards cognitive tasks and is generated when anxious or stressed (Kim et al., 2019b) and Gamma band correlates with heavier mental loads such as concentration and stress (Bailey et al., 2018).

2.8 Summary and Research Gaps

This finding indicates that momentary stressful situations and abnormalities within the environment can evoke physiological (HR and HRV), behaviour (gait, eye movement) and cognitive (EEG) responses that could potentially be detected through wearable sensors. However, given the inconsistency in the previous findings, several necessary research and methodological gaps need to be addressed before adopting bodily response-based assessment for older adults.

2.8.1 Research Gap One: Informativeness of Bodily Response

Deploying wearable sensors in an ambulatory, real-world environment poses several challenges that can diminish the signals' informativeness. For instance, a recent study reported that their EDA data collected with a wearable sensor in an ambulatory, urban environment did not show any variation due to the low sampling rate (Birenboim et al., 2019). Another study using a wearable EEG sensor also reported stability issues (Saitis and Kalimeri, 2018). Even

stable wearable sensors with sufficient sampling rates usually have fluctuations in their raw signals caused by physiological factors, human variability, sensor variability, environmental condition, and physical effort resulting from walking (Kyriakou et al., 2019). Although the raw signal can be filtered to remove external interferences, it is still ambiguous what bodily responses contain relevant information about human-environment interaction in an ambulatory, real-world environment.

Prior studies adopting human-centric sensing used a modality (e.g., EEG, HRV, EDA, or gait) or a feature extracted from a modality (e.g., mean EDA, arousal, HR, or signal vector magnitude) to represent people's interaction and experience in the environment (Kim et al., 2020; Birenboim et al., 2019; Chrisinger and King, 2018; Triguero-Mas et al., 2017; Kim et al., 2016). Generally, all these modalities and features contain relevant information. However, the relevance of the information is determined by the task to be performed, the environmental stimuli, and the prevailing conditions (Hall, 1999; Muzammal et al., 2020; Mursalin et al., 2017). For example, Birenboim et al. (2019) used EDA, HR, and HRV to represent people's interaction with the environment. Their findings revealed that only EDA and HRV were consistent in detecting stressful environmental situations. This implies that although each feature or modality contains information about people's interactions, some of the features or modalities could be more informative than others. As a result, human-centric sensing can become ineffective and unreliable when people's interaction and experience with the environment is represented with an uninformative modality or feature. Therefore, the first objective of this research is to present an approach to assess the relevance and informativeness of people's bodily responses.

2.8.2 Research Gap Two: Relationships in Older Adult's Bodily Responses Resulting from their Interaction with the Environment

Older adults usually achieve mobility in outdoor neighbourhood environments either by walking on foot or with mobility aids. The common mobility aids include walking stick, walking frame and wheelchair (Grimmer et al., 2019). Most of the existing studies that use wearable sensing technologies focus only on humans or the interaction between humans. A few of these studies that focus on human-environment interaction often attach the sensors to the mobility aid to assess the environmental condition (Mascetti et al., 2020; Barbosa et al., 2018; Mourcou et al., 2013). An example is a recent study that attached inertial sensors to the users' wheelchair to detect urban features like curb ramps, steps, or other obstacles along a path (Mascetti et al., 2020). Although these works prove the feasibility of using sensor data collected during human movement (mobility) to assess an environmental condition, they might not be a good representation of human-environment interaction. Human responses to environmental conditions are more complicated than mobility aid usage; thus, sensors attached to humans are inherently subject to greater variability (than sensors attached to mobility aids), which could affect built environment assessment. Therefore, it is essential to understand the variability in older adults' responses to different environmental conditions before adopting elderly-centric sensing. Therefore, the second objective of this study is to examine the relationships in older adult's bodily responses resulting from their interaction with the environment.

2.8.3 Research Gap Three: Optimised Environmental Stress Detection

Although the older adults' perceived stress assessment and observers' audit provide a good assessment of an environmental condition, they will be less efficient, costly, and time-consuming when deployed on a large scale because they are manually planned. Given the rate

of population ageing and the likelihood of older adults encountering excessive environmental demands during their daily trips, such optimisation is important to efficiently and timely understand their relationship with the environment to inform urban planning and design. Therefore, the third objective of this study is to detect older adults' stressful environmental interactions in near-real time.

2.8.4 Research Gap Four: Influence of Visuospatial Configuration of Urban Space on Older Adults' Stress Response

There has been a rapid decline in mobility indices, including trip frequency, trip distance, and unmet travel demands among older adults (Shumway-Cook et al., 2003; Portegijs et al., 2017). In a sense, this may indicate that the affordance (i.e., what a perceived element or scene has to offer the perceiver [Gibson, 1977]) for older adults' involvement in the environment might be different from that of the average person. However, there is little to no research into understanding how the perceived elements (specifically, the visuospatial configuration) of the environment influence older adults' involvement—most studies focused on younger adults. A few studies have been conducted to understand the relationship between the visuospatial configuration of urban space and human physiological response (Li et al., 2016; Hijazi et al., 2016; Knöll et al., 2018; Ojha et al., 2019; Xiang et al., 2020). All of these studies focused on younger adults with an average age of about 25 years. Drawing on these findings to guide urban planning and design may discriminate against older adults even though they are more susceptible to stressful urban environment encounters. This could further hinder current efforts in creating universal designs and age-friendly cities and communities. Therefore, the fourth objective of this research is to examine the influence of visuospatial configuration of urban space on older adults' stress response.

**PART II: TOWARDS ELDERLY-CENTRIC AND WEARABLE
SENSING**

CHAPTER 3

RESEARCH METHODOLOGY³

3.1 Introduction

The research methodology to achieve the goal of this study is presented in this chapter. Older adults aged 65 and above were recruited to participate in an outdoor environmental walk on a predefined path while equipped with non-intrusive wearable sensors. The conditions of the path were assessed using older adults' perceived rating and observers' audit. Details of the experiment design, field data collection, summary of the collected data, wearable sensors, data pre-processing and methods are presented in this chapter.

³ This chapter is based on studies that are published or currently under consideration for publication.

Torku, A., Chan, A.P.C., Yung, E.H.K., Seo, J. (2021). The influence of urban visuospatial configuration on older adults' stress: A wearable physiological-perceived stress sensing and data mining based-approach, *Building and Environment*, 108298. <https://doi.org/10.1016/j.buildenv.2021.108298>

Torku, A., Chan, A.P.C., Yung, E.H.K., Seo, J. (2021). Wearable sensing and mining of the informativeness of older adults' bodily responses to detect demanding environmental conditions, *Environment and Behavior*. (Under Review). E&B-20-0532.R2

Torku, A., Chan, A.P.C., Yung, E.H.K., Seo, J. (2021). Learning to detect older adults' environmental stress hotspots to improve neighbourhood mobility: A multimodal physiological sensing, machine learning and risk hotspot analysis-based approach, *Cities* (Under Review). JCIT-D-21-01443

3.1.1 Methodological Underpinning: Ecological Validity

Understanding human behaviour and cognition in the ‘real-world’ setting has been a long-sought-after goal in psychological science. However, most of the existing studies in this field were conducted in the laboratory—they often employed stationary sensors (see literature review in Chapter 2). The experiment design used in laboratory or controlled settings to assess human reaction to the environment lack sufficient realism to produce adequately meaningful findings of a person’s interaction with the environment in real life. This study aims to approximate the real world as much as possible and ensure ecological validity, hence the reason for designing the experiment in a natural setting and using wearable sensors.

Ecological validity refers to the extent to which a situation or task within a study can be generalised beyond the present situation (Schmuckler, 2001; Adolph, 2020). A prominent definition of ecological validity within the environment context was provided by Bronfenbrenner (1977). According to Bronfenbrenner (1977), “ecological validity refers to the extent to which the environment experienced by the subjects in a scientific investigation has the properties it is supposed or assumed to have by the experimenter” (Bronfenbrenner, 1977, p. 516). The nature of the stimuli is another component of ensuring ecological validity (Schmuckler, 2001). For instance, Neisser (1976) stated that ecologically valid stimuli consist of spatially, temporally and multimodal information.

Using an environment that is natural or normal to the participant has higher ecological validity. It is more likely to obtain a result representing everyday life; in that way, results are more generalisable to the target population and other environment settings (Holleman et al., 2020; Adolph, 2020; Schmuckler, 2001). However, if a study is set up in laboratory settings or where there is high control, it is not in the participants’ natural settings. It, therefore, does not reflect

everyday life, so the ecological validity is low (Holleman et al., 2020; Adolph, 2020; Schmuckler, 2001). Also, conducting this type of research in laboratory settings or controlled setting is arguably reductionist since the situation is very controlled and only looks at one factor; it simplifies complex human behaviour by isolating the independent variable and does not look at the combination of factors (Adolph, 2020). It is also usually more complicated for the researcher to generalise and apply the results with low ecological validity; this is because there are likely to be demand characteristics or social desirability bias where the participants change their behaviour to what they think the researcher wants to see (Schmuckler, 2001).

In many ways, this work is firmly ecologically valid, examining naturalistic behaviour in natural settings and employing spatially and temporally rich stimuli that extend multimodally as well.

3.2 Experiment Design

The experiment design and procedures are in three main phases: (1) enrolment phase; (2) practice phase; and (3) experimental phase. The flowchart depicting the three phases is presented in Figure 3.1. A detailed explanation of each phase is presented in the following sections.

3.2.1 Enrolment

The enrolment phase and experimental phase were conducted between September and November 2019. Participant recruitment and data collection took place in Hong Kong (Hung Hom and Ho Man Tin). Recruitment posters and emails were distributed to potential participants in the networks of the Institute of Active Ageing, The Hong Kong Polytechnic

University. The Institute of Active Ageing is an interdisciplinary research and academic centre for the advancement of knowledge and practice to facilitate active ageing.

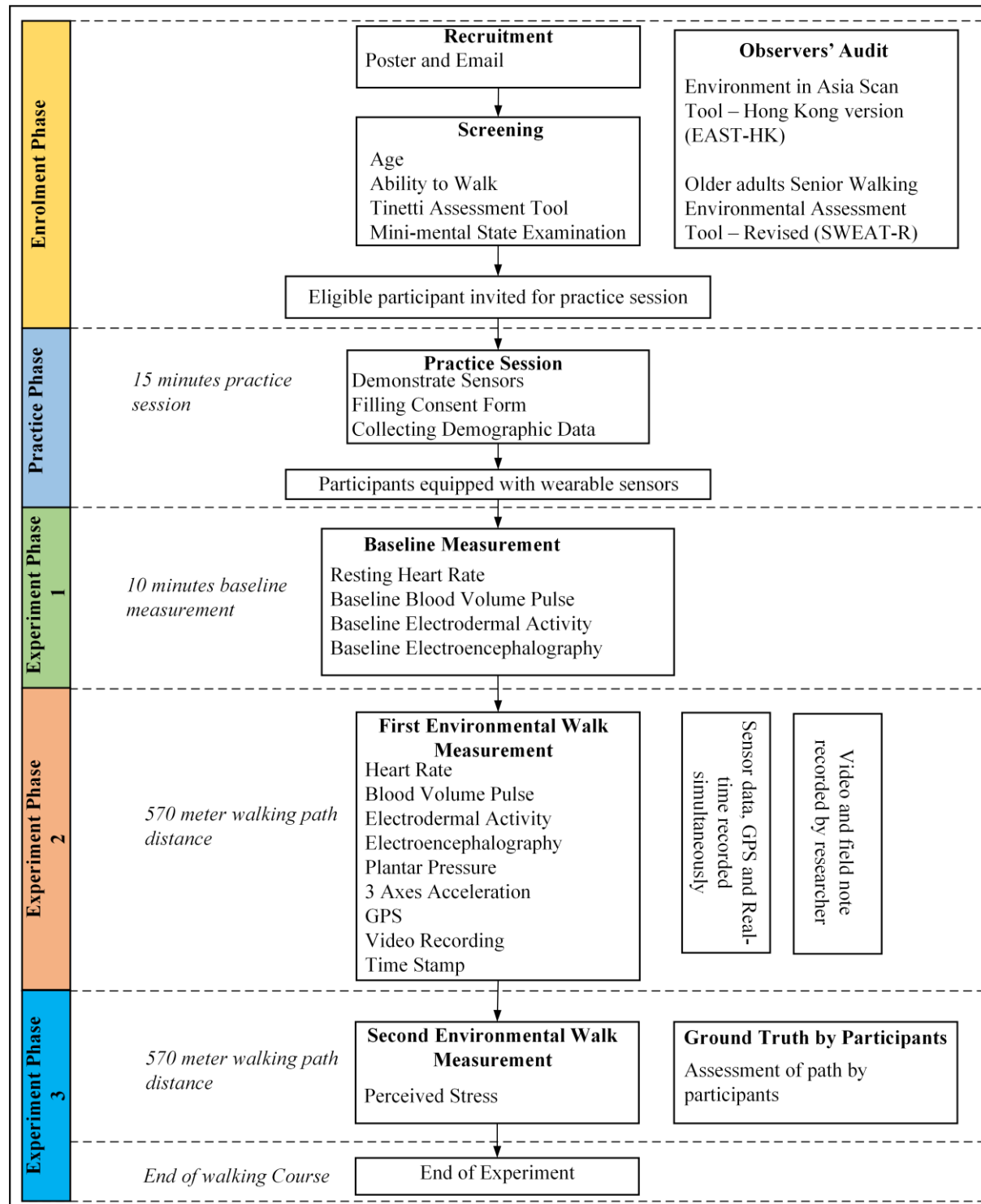


Figure 3.1: Flowchart of experiment procedure.

3.2.2 Screening: Eligibility Criteria

The eligibility criteria were set to ensure that all participants share a common characteristic. The following eligibility criteria were used to screen the participants: age, walking ability, and cognitive state. All participants must meet these criteria to be eligible to participate in this study. A detailed explanation of these criteria is provided in the following.

Age

In Hong Kong and many other countries, older adults are characterised as people aged 65 years or over (Elderly Commission, 2020; United Nations, 2020). Therefore, only people aged 65 years or over were eligible to participate in the study.

Walking Ability

This experiment involves walking on a predefine path for about 15 min walking distance. Hence, the physical ability to walk the path was assessed based on the participant's ability to walk unassisted by another person for at least 15 min. Furthermore, the Tinetti Assessment Tool (Tinetti, 1986) was used to assess the older adults' functional gait and balance. The Tinetti Assessment Tool is a valid, reliable, simple, easily administered task-performance test that measures older adults' gait and balance and requires 10 to 15 min to complete (Tinetti, 1986; Lewis, 1993; Wong, 2019). The Tinetti Assessment Tool is shown in Appendix A.

Cognitive Status

This experiment involves older adults self-reporting their experience (i.e., perceived assessment of the path). The prevalence of subjective cognitive decline among older adults could affect their assessment (Elderly Health Service, 2016; CDC, 2019). Therefore, the participants had to meet the recommended cut-off score for The Mini-Mental State

Examination (MMSE) to be eligible to participate in this study. The Mini-Mental State Examination (MMSE) (Folstein et al., 1975) was used to assess the cognitive mental status of older adults. The MMSE is quick, easy to use, acceptable, valid, reliable and widely used screening instruments for assessing cognitive functions both in clinical and research settings (Folstein et al., 1975; Bilgel et al., 2019; Pagliai, et al., 2019). The MMSE comprises eleven questions and requires only 5 to 10 min to administer. The MMSE consists of two main parts. Part one examines the participants' oral responses focusing on orientation, memory, and attention of the participants. Part two examines the participants' ability to name objects, follow verbal and written commands, write a sentence, and copy a complex polygon similar to a Bender-Gestalt Figure. The maximum score for part one is 21, the maximum score for part two is nine, and the maximum total score is 30. A cut-off score of 23/24 distinguishes between cognitive impairment and normal participants. The original version (Folstein et al., 1975) is shown in Appendix B.

The Cantonese version of the MMSE (CMMSE) (Chiu et al., 1994) was used to screen the older adults in Hong Kong. The CMMSE is readily comprehensible to the older adults in Hong Kong. The scale has been proven to have good reliability and validity to detect cognitive impairment among Hong Kong elderly (Chiu et al., 1994; Lao et al., 2019). A cut-off score of 19/20 is recommended as an indication of cognitive impairment among Hong Kong older adults. According to Chiu et al. (1994) the educational level of the participants has a significant effect on the MMSE scores. In order to factor in this difference, three different cut-off scores were recommended: cut-off score ≥ 18 points for the illiterate elders, cut-off score ≥ 20 points with 1–2 years of education; and cut-off score ≥ 22 points with more than 2 years of education (Chiu et al., 1998; Lao et al., 2019). The CMMSE is shown in Appendix B.

3.2.3 Eligible Participants

A total of 136 people responded to the invitation to participate in the experiment. Only 61 participants met the age requirement for this experiment (i.e., 65 years or over). These participants were scheduled for further screening, the practice phase and the experiment phase based on their availability. Two participants were scheduled for each working day (Monday to Friday) in November and October 2019. During the first week in November, a total of ten people aged 65 years or over were screened for their walking ability and cognitive status. They all met the eligibility criteria; hence they proceeded to the practice and experimental phase of the study. Details of their screening are provided in the following.

Unfortunately, there was political unrest in Hong Kong, and the University had to suspend all Teaching and Research activities (the University closure started from the second week in November). The university closure lasted for several months-this significantly affected this experiment. The COVID-19 restrictions in Hong Kong also affected the resumption of the experiment – especially because the participants in this study were among the COVID-19 vulnerable population.

Due to all these unforeseen and uncontrollable events and the completion time for this study, this study proceeded to analyse the data collected from only ten participants. All ten participants were able to walk unassisted by another person for at least 15 min. Nine participants achieved a total score between 25-28 points on the Tinetti Assessment Tool, indicating low fall risk. Only one participant (participant seven) achieved 19-24 points on the Tinetti Assessment Tool, indicating medium fall risk. Participant seven used a walking stick for mobility during the environment walk. All ten participants achieved a score ≥ 22 points on the CMMSE. A cut-off score of 19/20 is recommended to indicate cognitive impairment among

Hong Kong older adults (Chiu et al., 1998; Lao et al., 2019). The demographic information of the participants is presented in Table 3.1. Despite the small number, each participant provided rich multimodal data; the multimodal data was harnessed to enhance the generalisation of the study. More details about using multimodal data to improve generalisation are provided in Chapter 6.

Table 3.1: Demographic information of participants

Participant	Gender	Age (years)	Height (cm)	Weight (kg)	Body mass index (kg/m ²)
1	Female	65	162.0	57.0	21.7
2	Female	65	158.0	62.0	24.8
3	Male	66	160.0	71.0	27.7
4	Female	75	161.1	67.5	26.0
5	Male	68	173.0	83.0	27.7
6	Female	72	157.5	54.4	21.9
7	Female	71	152.4	60.5	26.0
8	Female	66	157.5	59.0	23.8
9	Female	66	154.9	60.0	25.0
10	Male	66	175.0	77.7	25.4

3.2.4 Practice Session

The practice session served as an opportunity to demonstrate the wearable sensors and familiarise the participants with the experiment procedures. The participants completed and signed an informed consent form after obtaining written and spoken information about the experiment procedures. The demographic information of the participants (Table 3.1) was collected during the practice session.

3.2.5 Path for Environmental Walk

An approximate 570 m path was carefully selected in the neighbourhood of Hung Hom, Kowloon, Hong Kong, to capture a range of environmental conditions. The path consists of

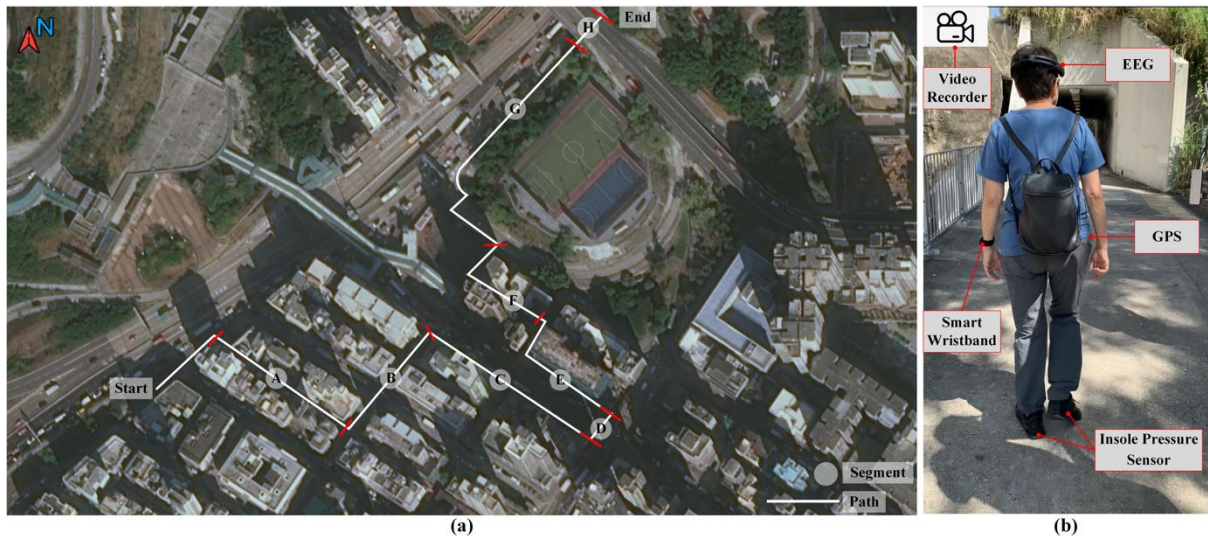


Figure 3.2: Field experiment overview. (a) Predefined path for environmental walk. (b) Older adult equipped with wearable sensors.

Note. Basemap data copyrighted Esri, DigitalGlobe, GeoEye, Earthstar Geographics, CNES/Air bus DS, USDA, USGS, AeroGRID, IGN, and the GIS User Community. Photographs by author.

spacious and narrow streets, green and high-density building areas, playgrounds, a gas station, a car wash, a car fitting shop, crosswalks (with and without traffic or pedestrian signal), sidewalks with even and uneven slopes, different street materials, among other features as shown in Figure 3.2, Figure 3.3, and Figure 3.4. Previous research efforts on human-environment interaction have proven that these environmental conditions stimulate unique human experiences (Birenboim et al., 2019; Duchowny et al., 2019; Triguero-Mas et al., 2017; Kim et al., 2016).



Figure 3.3: Photo description of path segment A to D.
Note. Photographs by author.



Figure 3.4: Photo description of path segment E to H.
Note. Photographs by author.

3.3 Field Data Collection: Observers' Audit of Path Condition

The environmental condition on the path was documented by two trained observers using the Environment in Asia Scan Tool—Hong Kong version (EAST-HK) (Cerin et al., 2011). The EAST-HK is a 91-item validated audit tool for assessing the walkability of neighbourhoods in Hong Kong. It was developed and validated in Hong Kong by researchers from The University of Hong Kong (Cerin et al., 2011). Other researchers have used the EAST-HK tool to assess

neighbourhood environments in Hong Kong (Barnett et al., 2015; Zhang et al., 2019). The EAST-HK tool was supplemented with the Older adults Senior Walking Environmental Assessment Tool—Revised (SWEAT-R) (Michael et al., 2009). The SWEAT-R is a 162-item validated tool for auditing the presence and quality of built environment features that are significant for older adult mobility (Michael et al., 2009; Cunningham et al., 2005). The SWEAT-R was validated in Portland, Oregon, by researchers from Oregon Health and Science University, The Center for Health Research, Kaiser Permanente, Portland, Oregon, Simon Fraser University- Harbour Centre, University of California – Irvine, and Oregon State University. Recent researchers that adopted the SWEAT-R tool for neighbourhood assessment include Moniruzzaman and Páez (2016) and Duchowny et al. (2019). Both tools are organised into four built-environment multidimensional domains: functionality; safety; aesthetics; and destination as shown in Appendix C (Cerin et al., 2011; Michael et al., 2009).

The EAST-HK was chosen because it contains walking-related environmental attributes common to East Asian ultra-dense cities, particularly relevant to Hong Kong. Additionally, SWEAT-R contains walking-related environmental attributes common to most urban environment, designed to be specific to older adults needs, but lacks most of the attributes in East Asian ultra-dense cities. Therefore, integrating the EAST-HK with SWEAT-R (Appendix C) is necessary for assessing the conditions of the path for older adults in Hong Kong. The integrated audit tool and the location of the path was presented to the observers before the path audit. Both observers have an MSc in urban planning. One of the observers works in The Hong Kong Polytechnic School of Design and the other in the Department of Building and Real Estate, The Hong Kong Polytechnic University. The observers assessed the path at the same time but worked independently. The average assessment time was 1 hr 13 min. The observers

compared their assessment and any differences in their assessment were discussed to reach a consensus.

The path was divided into 24 sections grouped in eight distinct environment scenarios—segment A to segment H—as shown in Figure 3.2. The length of each section is about 23.75 m. The segments were defined to cluster sections with a similar environmental condition expected to stimulate similar human experiences. For instance, the participants had to walk through an alley (segment A), walk along a busy street with bus stops (segment C), use a crosswalk with high traffic (segment D), pass through a green space (segment G), and walk through a subway with graffiti (segment H). Following previous research (Duchowny et al., 2019; Michael et al., 2009), each 23.75 m section was classified according to the level of built environmental demand (high or low) for older adults' mobility based on the integrated EAST-HK and SWEAT-R tool. Sections of the path that were assessed as high demand totalled 372.57 m (65%). The high-demand sections consist of existing built environment features such as path obstructions (32%), unattractive buildings and sights (49%), cracked, uneven and inconsistent path surfaces (4%), parked and moving vehicles (5%), crosswalk (4%), graffiti (4%). The overall conditions of the path in high-demand sections were rated as poor/moderate, while low-demand sections were rated as moderate/good. The path audit is presented in Table 3.2.

Table 3.2: Observers' path audit

Environmental feature	Segment A	Segment B	Segment C	Segment D
	Functionality			
Buildings				
Building type	6-12 floors apartment blocks	6-12 floors apartment blocks	6-20 floors apartment blocks	6-20 floors apartment blocks
Walking surface				
Type of path	Footpath	Footpath	Footpath	Crosswalk
Path condition	Poor condition, wet and slippery	Well-maintained	Well-maintained	Well-maintained
Path slope	Flat	Flat	Flat	Flat
Path obstructions	Bin, household items, bamboo scaffold, cracked path surface	Inconsistent path surface quality, cracked surface, and pothole, motor vehicles parked on footpath, shops on street	Bus stops, traffic cones, bollard barricade, shops on street	None
Path material	Concrete	Concrete	Brick	Concrete
Curb cut features	-	Yes, no colour and material contrast with ground surface	Yes, colour and material contrast with ground surface	Yes, colour and material contrast with ground surface
Permeability				
Street connectivity	Two connecting streets	Five connecting streets	Three connecting streets	Three connecting streets
Rating for functionality	Poor	Moderate	Moderate	Good
		Safety		
Personal				
Street lighting	Inadequate	Good	Good	Good

Environmental feature	Segment A	Segment B	Segment C	Segment D
Stray dogs /other animals	Stray dogs	None	None	None
Presence of people	Yes	Yes	Yes, crowded	Yes, crowded
Signs of crime/disorder	None	None	None	None
Traffic				
Traffic load	-	-	-	Crossing aids
Pedestrian safety	-	Parked vehicles make it difficult to see incoming traffic	Vehicles moving to and fro gas station and car wash	Traffic calming devices
Rating for safety	Poor	Moderate	Moderate	Good
Aesthetics				
Views				
Attractive buildings	None	Few	Few	Few
Abandoned/vacant buildings	None	None	None	None
Attractive natural sights	None	None	None	None
Streetscape				
Litter	Yes, dominant feature	Yes, but not dominant feature	None	None
Broken bottles and cans	Yes, dominant feature	None	None	None
Dog/animal fouling	Yes, but not dominant feature	None	None	None
Graffiti	None	None	None	None
Noise pollution	None	Low	Moderate	Moderate
Air pollution	None	None	Low	Low
Presence of trees	None	None	None	None

Environmental feature	Segment A	Segment B	Segment C	Segment D
Rating for aesthetics	Poor	Moderate	Moderate	Moderate
		Destinations		
Transport-related	-	Bus stop	Bus stop	Bus stop
Public open space	-	-	-	-
Recreational	-	-	Gym/fitness facility	Gym/fitness facility
Government/public services	-	-	Community/elderly centre, Health services	Community/elderly centre, Health services, Religious places
Public facilities	-	Benches/places for sitting	-	-
Commercial destinations	Convenience store, Chained fast food, Chinese coffee/tea, Chinese non-fast food, office buildings	Convenience store, Clothing, Pharmacy, Chained fast food, Chinese coffee/tea, Chinese non-fast food, Office buildings, Laundry	Convenience store, Supermarket, Fresh food, Clothing, Pharmacy, Chained fast food, Chinese coffee/tea, Chinese non-fast food, Bakery, Banks, Hotel, Office buildings, Salon/barber	Convenience store, Supermarket, Fresh food, Clothing, Pharmacy, Chained fast food, Chinese coffee/tea, Chinese non-fast food, Bakery, Banks, Laundry, Salon/barber
Overall rating for segment	Poor	Moderate	Moderate	Good

Table 3.2: Observers' path audit (continued)

Environmental feature	Segment E	Segment F	Segment G	Segment H
	Functionality			
Buildings				
Building type	6-20 floors apartment blocks	7-12 floors apartment blocks	None	None
Walking surface				
Type of path	Footpath	Footpath	Footpath and crosswalk	Subway
Path condition	On-going construction	Poor condition, wet and slippery	Well-maintained	Well-maintained
Path slope	Flat	Flat	Moderate	Moderate
Path obstructions	Inconsistent path surface material and quality, cracked surface and pothole	Stair, inconsistent path surface quality, cracked surface, and pothole	None	None
Path material	Brick and Steel	Concrete	Concrete	Concrete
Curb cut features	Yes, colour and material contrast with ground surface	None	Yes, no colour and material contrast with ground surface	None
Permeability				
Street connectivity	Two connecting streets	Two connecting streets	Two connecting streets	One connecting street
Rating for functionality	Poor	Poor	Good	Good
	Safety			
Personal				
Street lighting	Good	Inadequate	Good	Good
Stray dogs /other animals	None	None	None	None

Environmental feature	Segment E	Segment F	Segment G	Segment H
Presence of people	Yes, crowded	Yes	Yes	Yes
Signs of crime/disorder	None	None	None	None
Traffic				
Traffic load	-	-	No crossing aids	-
Pedestrian safety	Vehicles moving to and fro construction site	-	Incoming traffic is abrupt	-
Rating for safety	Poor	Poor	Moderate	Good
Aesthetics				
Views				
Attractive buildings	Few	None	Some	None
Abandoned/vacant buildings	None	None	None	None
Attractive natural sights	None	None	Some	None
Streetscape				
Litter	Yes, dominant feature	Yes, dominant feature	None	None
Broken bottles and cans	None	None	None	None
Dog/animal fouling	None	None	None	None
Graffiti	None	None	None	Yes, dominant feature
Noise pollution	Moderate	Low	Moderate	Moderate
Air pollution	Moderate	None	None	Low
Presence of trees	None	None	Yes	None
Rating for aesthetics	Poor	Poor	Good	Poor
Destinations				
Transport-related	Bus stop	-	Bus stop	Bus stop
Public open space	-	Parks, Playground	Parks, Playground	Parks, Playground

Environmental feature	Segment E	Segment F	Segment G	Segment H
Recreational Government/public services	- Community/elderly centre, Religious places	Outdoor sport fields -	Outdoor sport fields -	- -
Public facilities	-	-	Benches/places for sitting	Benches/places for sitting
Commercial destinations	Convenience store, Supermarket, Fresh food, Clothing, Pharmacy, Chained fast food, Chinese coffee/tea, Chinese non-fast food, Banks, Hotel, Office buildings	-	-	-
Overall rating for segment	Poor	Poor	Good	Moderate

3.4 Field Data Collection: Bodily Response and Perceived Response Collection

A field experiment was designed for older adults to participate in an environmental walk. Older adults' bodily responses and perceived stress assessment were collected during the environmental walk to achieve the aim of this study. The environment walk was conducted between 10 a.m. and 4 p.m. on dry days free from high winds or rain. The baseline measurements of the participants' bodily responses were recorded during a 10 min rest period. After the baseline measurement, the participants walked the predefined path at a self-directed pace (comfortable pace) to optimise their experience on the path. The self-pacing enabled ecological validity and ensured that the walking activity was of mostly light intensity. The participants were instructed to behave how they usually would on a walking path. Two researchers accompanied the participants. One of the researchers was responsible for providing direction if needed, troubleshoot any technical malfunction with the wearable sensors and also present for safety and health purposes. The other researcher recorded a video of the environmental walk and took notice of any abnormal activity or event (ground truth provided by researcher). The accompanied researchers remained half a stride behind the participants to allow the participants to determine the pace. The researchers did not talk or walk along with the participant unless the participant called for assistant.

After completing the first walk, the participants were asked to walk the same route again without wearing the sensors. Instead, the participants were asked to identify locations where they experienced stressful interactions with the environment (ground truth provided by participants). The participants also stated the intensity of their perceived stress (low or high intensity). A researcher accompanied and assisted the participants to document their responses. This approach was adopted to ensure that older adults accurately recall their experience. A shopping voucher of HK\$100 was offered as compensation for participation.

3.4.1 Collected Bodily Responses and Environmental Data

Only non-intrusive wearable sensing technologies were adopted in this study in order not to inhibit the older adults' daily activity. For example, older adults may find it more comfortable walking with a smart band on their wrist and an insole sensor in their shoes than an inertial measurement unit (IMU) sensor attached to their ankle, or an electromyography (EMG) sensor attached to their arm. These smart non-intrusive wearable devices were used to collect physiological, behavioural, and cognitive data without any significant obstruction and discomfort to the older adults. The total sample of the collected data is shown Table 3.3. The walking activity affected the stability and functioning of the electroencephalography (EEG) sensor for five participants. Participant seven did not have valid data for further analysis.

Table 3.3: Sample of collected bodily response and location data during environmental walk

Partici pant	Time to walk path (MM: SS)	Physiological data		Cognitive data	Behavioural data		GPS (ϕ, λ)
		HR (b/min)	EDA (μS)	EEG (μV)	Pressure (N/cm^2)	Acceleration (g)	
		1 Hz	4 Hz	128 Hz	50 Hz	50 Hz	1 Hz
1	11: 31	700	2801	76741	35019	35019	700
2	8: 47	527	2108	-	26300	26300	527
3	9: 59	599	2397	-	29899	29899	599
4	8: 55	535	2140	60745	26750	26750	535
5	13: 47	827	3309	93023	41498	41498	827
6	9: 56	596	2384	73592	29750	29750	596
7	15: 01	-	-	-	-	-	-
8	10: 57	657	2628	58423	32850	32850	657
9	8: 57	537	2148	-	26850	26850	537
10	9: 00	540	2160	-	27001	27001	540

Note. Ten min baseline measurements were recorded for each participant. HR = instantaneous heart rate computed from the inter-beat interval obtained from a PPG signal; b/min = beats per minute; μS = Microsiemens; μV = Microvolts; N/cm^2 = Newton per square metre; g = Acceleration of gravity; equivalent to $9.806 m/s^2$; (ϕ, λ) = (Latitude, Longitude) in degree; $n Hz$ = n data points per second.

3.4.2 Older Adults' Perceived Stress During Environmental Walk

All participants reported their perceived stress. The path was labelled using the commonly perceived stress reported by the participants (Figure 3.5).

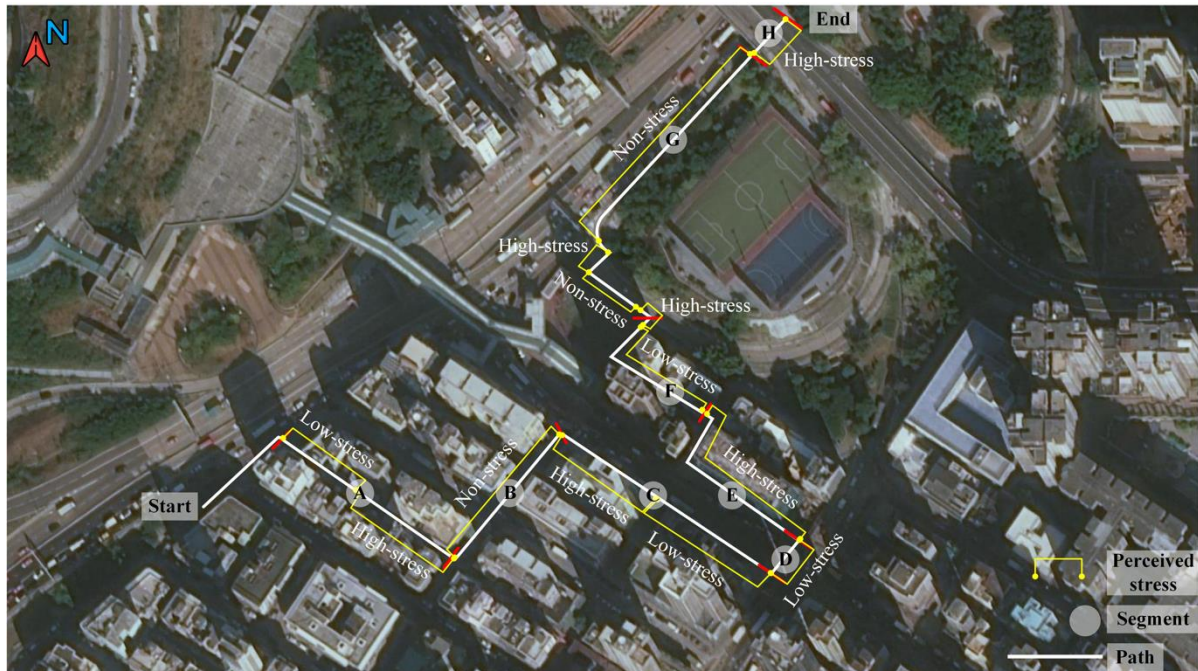


Figure 3.5: The commonly perceived stress among the participants. The path label is the perception of at least four participants out of ten.

Note. Basemap data copyrighted Esri, DigitalGlobe, GeoEye, Earthstar Geographics, CNES/Air bus DS, USDA, USGS, AeroGRID, IGN, and the GIS User Community.

Table 3.4: Perceived stress distribution on path

Segment	Total distance (m)	Non-stress (m)	Stress (m)	Low stress (m)	High stress (m)
A	85.65	0	85.65	43.01	42.64
B	72.60	72.60	0	0	0
C	100.77	0	100.77	49.76	51.01
D	15.45	0	15.45	15.45	0
E	68.47	0	68.47	0	68.47
F	78.48	0	78.48	57.98	20.50
G	127.87	111	16.87	0	16.87
H	19.88	0	19.88	0	19.88
Total	569.17	32.26%*	67.74%*	29.20%*	38.54%*

Note. * = Percentage of the total path; m = metre.

The path label is the perception of at least four participants (out of ten). This indicates that there is somewhat commonality in older adults' perception of the path, and that each segment influenced their reaction. The proportion of the perceived stress along the path is presented in Table 3.4. The participants perceived 32.26% of the path as non-stress, 67.74% of the path as stress, 29.20% of the path as low stress, and 38.54% of the path as high stress.

3.5 Wearable Sensors for Collecting Bodily Response and Environmental Data

3.5.1 Physiological Response Sensors

Heart rate (HR) measures, heart rate variability (HRV) measures and electrodermal activity (EDA) were recorded using a wristband-type sensor (Empatica E4). The Empatica E4 wristband is a wearable research device that offers real-time physiological data acquisition (Empatica, 2019a). The technical specifications of the Empatica E4 wristband are provided in Figure 3.6. The Empatica E4 has four sensors: (1) Photoplethysmography sensor, (2) Electrodermal activity sensor, (3) 3-axis accelerometer and (4) Optical thermometer. These sensors produce the following data: (1) Blood volume pulse, at 64 Hz, (2) Inter beat interval: time, IBI (time) pair, (3) Electrodermal activity at 4 Hz, (4) XYZ raw acceleration at 32 Hz and (5) Skin temperature at 4 Hz (Empatica, 2019b).

This device was chosen for the study because it is comfortable, lightweight, reliable, has many sensors, easy to install and use for older adults in outdoor conditions without interfering with their daily living activities. To the best of my knowledge, the E4 wristband is the only certified device to offer such characteristics at present time. The E4 wristband has been recently used to measure heart-related parameters (Birenboim et al., 2019; Kim et al., 2019) and EDA (Ojha et al., 2019; Birenboim et al., 2019) in urban and rural environment settings. The Empatica E4 wristband was worn on the participant's non-dominant hand (i.e., a right-handed participant

would wear it on their left wrist) to minimise motion artifacts and allowed to adjust for 10 min (Empatica, 2019c; Picard et al., 2016).

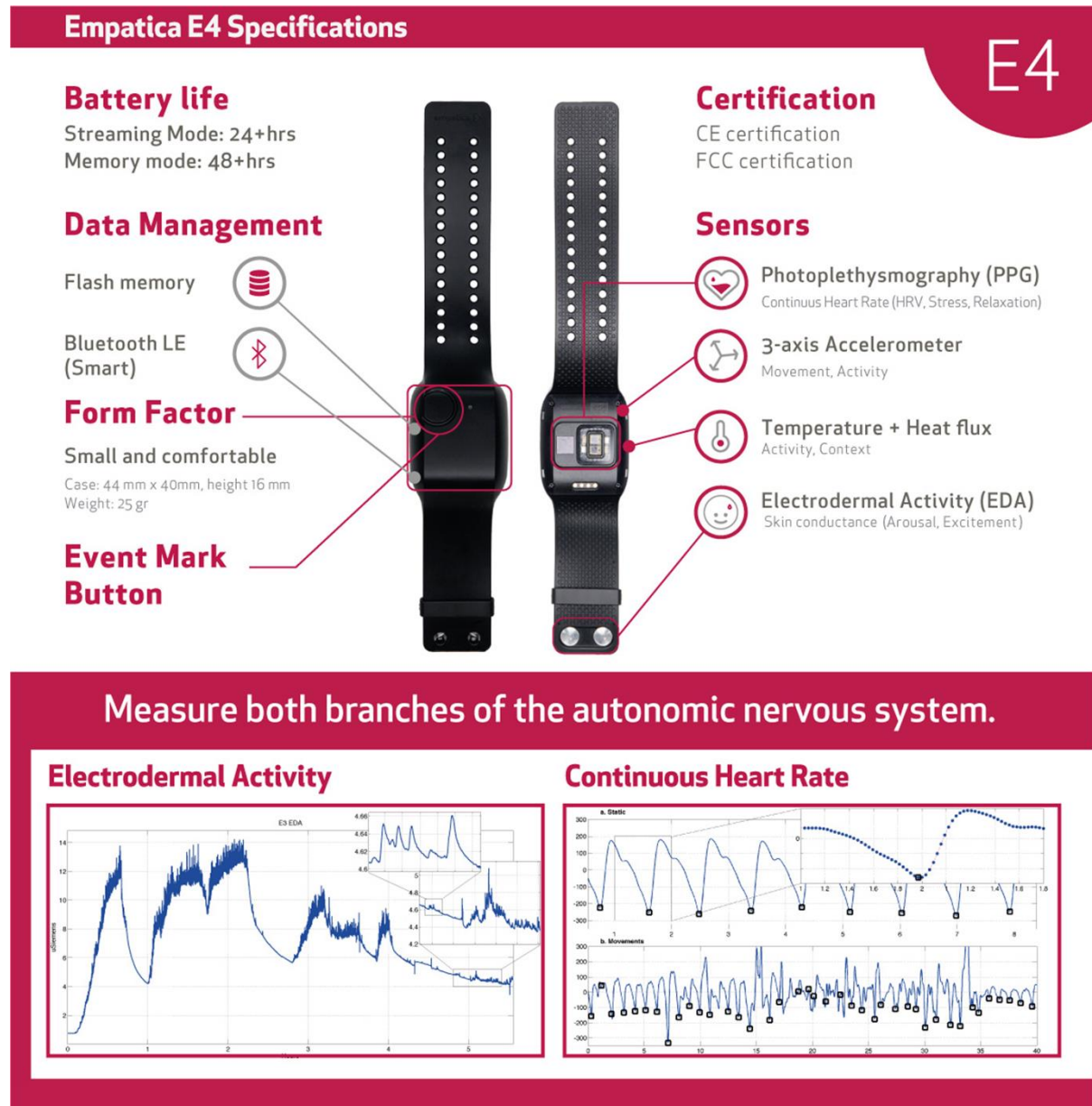


Figure 3.6: The physiological sensor used in the experiment.
Note. Image source: Empatica (2019b).

3.5.2 Cognitive Response Sensors

The brain electrical activity was recorded non-invasively from the scalp using a wearable EMOTIV EPOC+ 14 channel mobile EEG headset (Emotiv, 2019). The 14 channels

correspond to the international 10-20 position system (AF3, AF4, F3, F4, F7, F8, FC5, FC6, T7, T8, P7, P8, O1 and O2); P3 and P4 are the reference electrodes as shown in Figure 3.7. The EMOTIV EPOC+ headset records EEG at 128 Hz.

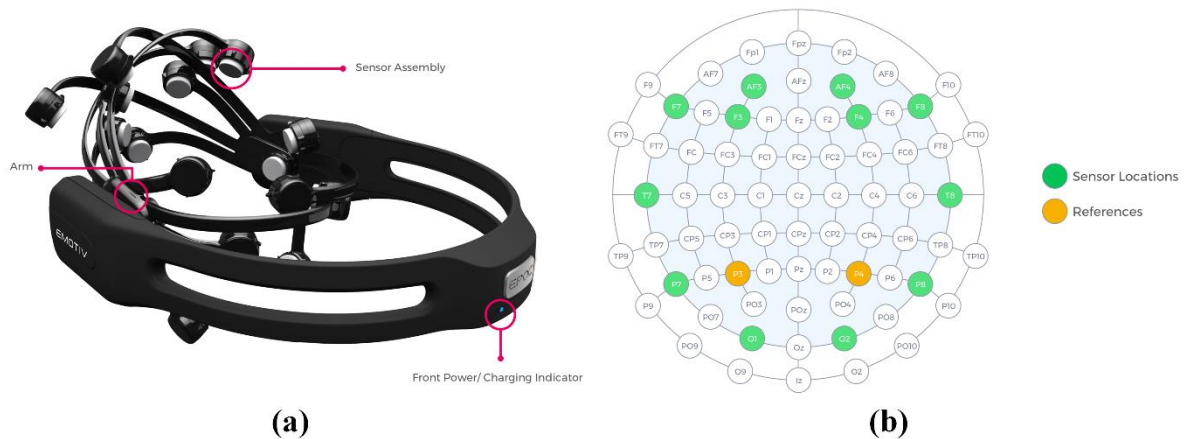


Figure 3.7: The cognitive sensor used in the experiment. (a) 14 channel mobile EEG headset. (b) The position of the 14 channels corresponds to the international 10-20 position system. *Note.* Image source: Emotiv (2019).

3.5.3 Behavioural (Gait and Motion) Response Sensors

Gait and motion data were captured in real-time during the walking course using a commercial wearable Moticon SCIENCE insole sensor (Moticon, 2019) as shown in Figure 3.8. Each left and right insole contains 16 pressure sensors and 6-axis IMU. The position of the IMU sensor is the origin of the coordinate system; three dimensions in space for acceleration and angular rate. The insole sensor records data at 50 Hz.

The Moticon SCIENCE insole sensor was chosen because it weighs no more than 80 grams, looks, and feels like a regular insole, reliable, easy to install and use for older adults in outdoor condition without interfering their gait. The validity and reliability of the Moticon SCIENCE insole sensor is verified in previous studies (Oerbekke et al., 2017; Stöggel and Martinier, 2017; Braun et al., 2015). The participants wore an approximately sized standardised neutral shoe

with the Moticon SCIENCE insole sensor sandwiched between the foot and the inside of the shoe. The original insole of the shoe was replaced with the Moticon SCIENCE insole sensor. The insole sensor was placed in both left and right shoes.

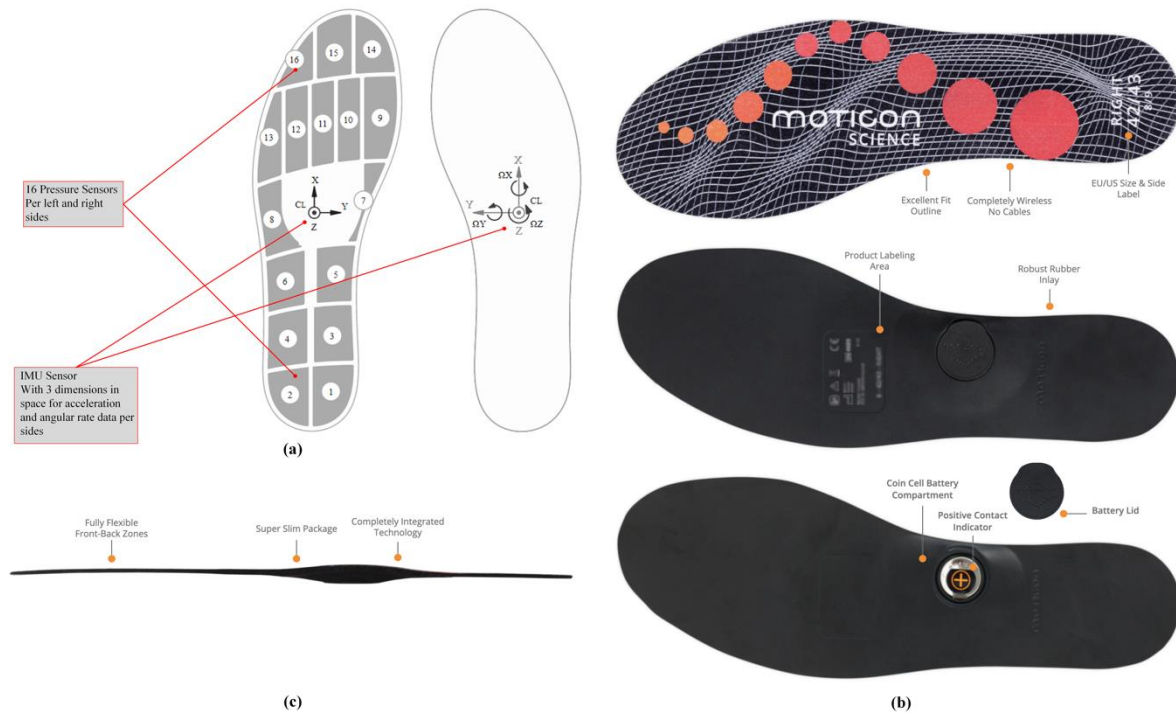


Figure 3.8: The behavioural (gait and motion) sensor used in the experiment. (a) Positions of pressure sensors and inertial measurement unit (IMU) in the insole sensor. (b) Top view and bottom view of insole sensor. (c) Thickness of insole sensor. *Note.* Image source: Moticon (2019).

3.5.4 Environmental Data Sensors

Generally, the infrastructure of the urban environment and season where the path is located is uniform. However, the experiment was conducted on different days and different time-of-day, which may affect the participants' bodily responses. Therefore, the environment temperature ($^{\circ}\text{C}$) and humidity (%) for each experiment day and time-of-day were recorded from the Hong Kong Observatory. The environment temperature ranges from 24°C - 29°C and the humidity ranges from 41% -55%. A belt-clip-type GPS sensor (Qstarz, 2019) as shown in Figure 3.9 was used to record GPS coordinates in latitude and longitude.



Figure 3.9: The GPS sensor used in the experiment.
Note. Image source: Qstarz (2019).

3.6 Ethics Statement

Ethical approval was obtained from the Human Subjects Ethics Sub-committee (HSESC) of The Hong Kong Polytechnic University (Reference Number: HSEARS20190826002). All the participants signed a written informed consent. Prior to signing the consent form, the project information was presented to the participants.

3.7 Data Analysis

3.7.1 Pre-Processing of Bodily Response Data

HRV Detection and Signal Pre-processing

Artefacts including missing, extra, or misaligned beats and ectopic beats such as premature ventricular contractions or other arrhythmias were corrected, and HRV analysis was conducted,

respectively, from the instantaneous heart rate using a proprietary algorithm (Tarvainen et al., 2014; Tarvainen et al., 2002).

EDA Signal Pre-processing

The raw EDA data was low pass filtered using a Butterworth filter with a cut-off frequency of 0.28 Hz and smoothed with a moving average filter to remove non-EDA related sensor readings. A low cut-off frequency of 0.28 Hz is recommended when data is recorded during a low-intensity activity such as walking (Posada-Quintero et al., 2018). Each participant's EDA data were first normalised against the baseline period to reduce inter-individual variance.

EEG Signal Pre-processing

A bandpass filter with a lower cut-off frequency of 0.5 Hz and a higher cut-off frequency of 60 Hz was used to remove external interference from the EEG signal. A discrete wavelet transformation—Daubechies wavelet with eight vanishing moments—with decomposition level 8 was adopted to remove ocular artefacts and extract relevant frequency bands. The following relevant frequency bands were extracted from each of the 14 EEG channels: delta (δ) (0.5–4 Hz), theta (θ) (4–7 Hz), alpha (α) (7–13 Hz), beta (β) (13–30 Hz) and gamma (γ) (30–60 Hz) frequency bands.

Plantar Pressure and Acceleration Signal Pre-processing

Human gait signals energy are low-frequency components; thus, the pressure and acceleration signals are easily corrupted by instrumentation noise, random noise, electric and magnetic noise (Wang et al., 2011). The presence of noise in the pressure and acceleration signals may result in an inaccurate estimation of gait. The raw data from the pressure and IMU sensors were denoised using a discrete wavelet transformation—Symlet wavelet with two vanishing

moments—with decomposition level four. A sure shrink with a soft thresholding technique was adopted to decompose and reconstruct the signals.

3.7.2 Baseline Normalisation

To reduce individual variability, the bodily responses were baseline normalised by subtracting the minimum value and dividing by the range from their baseline measurement values, in accordance with previous research (Healey and Picard, 2005).

3.7.3 Methods

The methods adopted or adapted in this study includes information entropy symmetric uncertainty, correlation analysis, and Random Forest algorithm (for Research Objective 1); statistically analysis (Wilcoxon signed-rank test), spatial clustering analysis (Getis-Ord General G statistic and Getis-Ord G_i^* statistics) and space-time pattern mining (for Research Objective 2); supervised machine learning, deep machine learning, kernel density estimation, simulation-based statistical power estimation of spatial relative risk (for Research Objective 3); and isovist analysis, self-organising maps, supervised machine learning and evolutionary fuzzy rule-based system (for Research Objective 4). A detailed explanation of these methods, model developments, and validations are presented in their respective chapters.

3.8 Chapter Summary

This chapter provided a comprehensive overview of the experiment design, data collection and data analysis. Ten eligible older adults aged 65 and above participated in an environmental walk while equipped with non-intrusive wearable sensors. The participants' perceived stress was also recorded. Two trained observers provided an assessment of the conditions of the path. Heart rate and EDA were recorded using E4 wristband from Empatica. The brain electrical

activity was recorded non-invasively from the scalp using a wearable EMOTIV EPOC+ 14 channel mobile EEG headset. The gait and motion data were captured in real-time during the walking course using a commercial wearable Moticon SCIENCE insole sensor. GPS coordinates were logged using a belt-clip-type GPS sensor. The raw data were pre-processed to remove artefacts and baseline normalised to compensate for inter-individual variance. The data analysis methods were also presented.

**PART III: DETECTING STRESSFUL OLDER ADULTS-
ENVIRONMENT INTERACTIONS**

CHAPTER 4

ASSESSMENT OF THE INFORMATIVENESS OF OLDER ADULTS' BODILY RESPONSE⁴

4.1 Introduction

This chapter aims to achieve research objective one: to assess the informativeness of people's bodily responses (i.e., physiological, behavioural, and cognitive responses) to different environmental conditions. The most informative bodily responses can be used to detect subtle and hidden changes in physiological, behavioural, and cognitive states between different environment settings and situations. Such knowledge about people's physiological, behavioural, or cognitive responses can be linked to different outdoor environmental conditions. The links will enable municipal officers, policymakers, and engineers to continuously assess and understand environmental conditions that trigger people's state of being and will be essential in determining what and when environmental interventions are needed to promote walkability.

⁴ This chapter is based a study that is currently under consideration for publication.

Torku, A., Chan, A.P.C., Yung, E.H.K., Seo, J. (2021). Wearable sensing and mining of the informativeness of older adults' bodily responses to detect demanding environmental conditions, *Environment and Behavior*. (Under Review). E&B-20-0532.R2

4.2 Methodological Framework: Assessing Informativeness of Bodily Response

This section presents a methodological framework for assessing the relevance and informativeness of people’s bodily responses. The framework, as shown in Figure 4.1, includes data collection, data pre-processing, AI-based information mining, and validation. The bodily response collection and pre-processing to remove noise is discussed in Chapter 3.

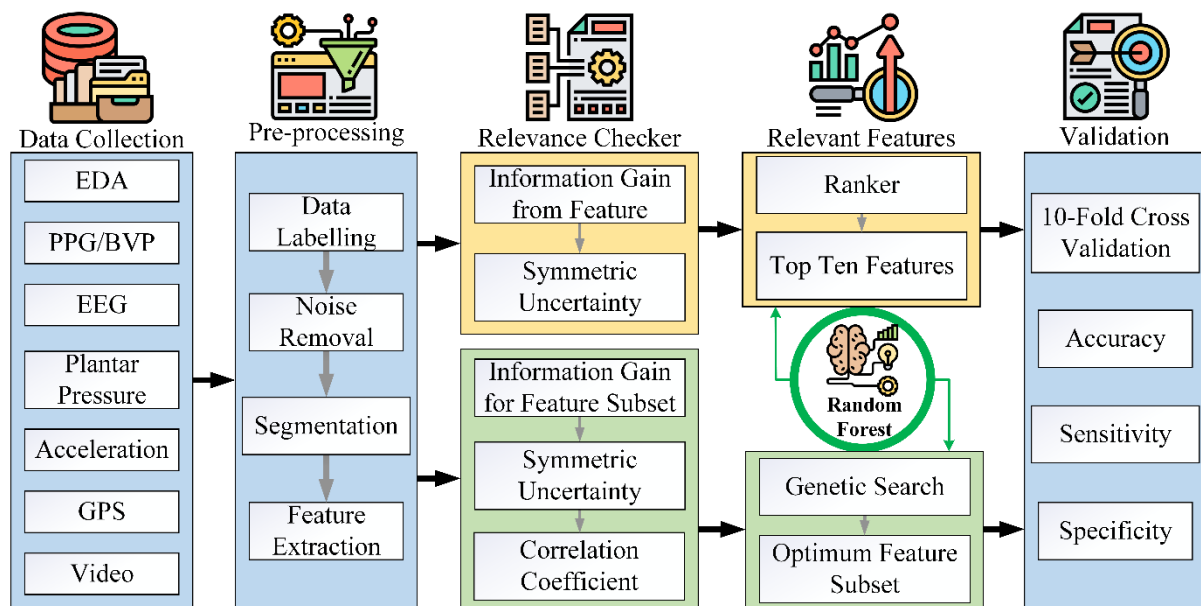


Figure 4.1: Methodological framework for assessing informativeness of bodily responses.

4.2.1 Feature Extraction

Feature extraction builds valuable information from the raw data by reformatting, combining, and transforming the raw data—the primary feature—into new features. The sensors deployed in human-centric sensing represent people’s interaction and experience in the environment as a series of data points ordered in time. The temporal changes and fluctuations in the signal data are reflected in the time-domain, frequency-domain, and nonlinear domain features (Antwi-Afari et al., 2018). Based on a literature review, several time-domain, frequency-domain, and nonlinear domain features commonly used in human-centric sensing were extracted from the physiological (Birenboim et al., 2019; Walford et al., 2017; Triguero-Mas et al., 2017),

behavioural (Twardzik et al., 2019; Duchowny et al., 2019; Kim et al., 2016), and cognitive signals (Bailey et al., 2018; Tilley et al., 2017; Neale et al., 2017). Because the data points for the recorded signals are large (i.e., 4 data points per second for EDA signal; 128 data points per second for EEG signal; and 50 data points per second for the plantar pressure sensor and accelerometer signal), extracting the features from one single signal reading is not informative (Jebelli et al., 2018). To address this problem, features were extracted from blocks of continuous readings referred to as windows. Selecting an appropriate window size impacts the informativeness of the features (Antwi-Afari et al., 2018).

The possible features that reflect the conditions of the environment would be a physiological, behaviour, or cognitive feature that continuously fluctuated, proportional to the older adult's experience throughout the environmental walk. To extract features with such attribute, continuous calculations were conducted using the optimal window size of the respective bodily response and advanced by 1 s for each second of the entire duration of each participant's walk on the path.

Features Extracted from HRV Signal

A continuous time series of HRV features were extracted from a window size of 60 s using Welch's periodograms (Tarvainen et al., 2014). Based on previous studies, a short-term window of 60 s can produce informative HRV features (Shaffer and Ginsberg, 2017). The frequently used features for human-centric sensing in the time-domain, frequency-domain, and nonlinear domain were computed, as presented in Table 4.1. A total of 31 HRV features were extracted for each participant.

Table 4.1: Features extracted from HRV signal

Feature	Description (Unit)
Time domain	
HR	Instantaneous heart rate values (1/min)
Mean RR	The mean of RR intervals (ms)
STD RR (SDNN)	Standard deviation of RR interval (ms)
Mean HR	The mean heart rate (1/min)
STD HR	Standard deviation of instantaneous heart rate values (1/min)
Min HR	Minimum heart rate (1/min)
Max HR	Maximum heart rate (1/min)
RMSSD	Square root of the mean squared differences between successive RR intervals (ms)
NN50	Number of successive RR interval pairs that differ more than 50 ms (beats)
pNN50	NN50 divided by the total number of RR intervals (%)
HRV triangular index	The integral of the RR interval histogram divided by the height of the histogram
TINN	Baseline width of the RR interval histogram (ms)
Frequency domain	
Absolute power	Absolute powers of very low frequency (VLF), low frequency (LF), and high frequency (HF) bands (ms^2)
Absolute power	Natural logarithm transformed values of absolute powers of VLF, LF, and HF bands (log)
Total power	Total spectral power (ms^2)
LF/HF	Ratio between LF and HF band powers
Nonlinear	
SD1	In Poincaré plot, the standard deviation perpendicular to the line-of-identity (ms)
SD2	In Poincaré plot, the standard deviation along the line-of-identity (ms)
SD2/SD1	Ratio between SD2 and SD1

Features Extracted from EDA Signal

Continuous decomposition analysis was conducted to decompose the processed EDA signal into two components: skin conductance level (SCL) (tonic component) and the skin conductance response (SCR) (phasic component) (Benedek and Kaernbach, 2010). The SCL reflects the baseline level of skin conductivity (tonic stimulus) and changes slowly over time, while the SCR increases in the amplitude of skin conductivity due to sympathetic stimulation. SCL and SCR features (Table 4.2) were extracted from a window size of 10 sec, with a minimum amplitude threshold of $0.05 \mu\text{S}$ to eliminate external interferences due to the experimental conditions and movement artefacts (Posada-Quintero and Chon, 2020; Benedek

and Kaernbach, 2010). Because a 10 s latency is sufficient for EDA reaction to extinguish after a stimulus (Posada-Quintero and Chon, 2020), it is expected that the informative EDA features will be produced within a window size of 10 s. A total of nine features were extracted from the EDA signal for each participant (Table 4.2).

Table 4.2: Features extracted from EDA signal

Feature	Description (unit)
nSCR	Number of significant (= above-threshold) SCRs within response window
Latency	Response latency of first significant SCR within response window (s)
AmpSum	Sum of SCR-amplitudes of significant SCRs within response window (reconvolved from corresponding phasic driver-peaks) (μS)
SCR	Average phasic driver within response window. Equals ISCR divided by size of response window; units are μS . This score represents phasic activity within response window most accurately but does not fall back on classic SCR amplitudes (μS)
ISCR	Area (i.e., time integral) of phasic driver within response window. It equals SCR multiplied by size of response window ($\mu\text{S}^*\text{s}$)
PhasicMax	Maximum value of phasic activity within response window (μS)
Tonic	Mean tonic activity within response window of decomposed tonic component
Global mean	Mean skin conductance (SC) value within response window
Global max deflection	Maximum positive deflection within response window

Features Extracted from EEG Signal

Based on previous studies, a suitable window size for EEG feature extraction might be within a window size less than 12 s (Candra et al., 2015). To find the optimal window size, features were extracted from different window sizes ranging from 1 to 12 sec. The window size of 2 s produced the most informative feature; hence 2 s was selected as the optimum window size for this EEG dataset. Time-domain features were computed from each of the 14 EEG channels. Frequency domain features were computed from each of the 14 EEG channels in the delta (δ) (0.5–4 Hz), theta (θ) (4–7 Hz), alpha (α) (7–13 Hz), beta (β) (13–30 Hz) and gamma (γ) (30–60 Hz) frequency bands. A total of 339 features were extracted from the EEG signal for each participant. The extracted features are listed in Table 4.3.

Table 4.3: Features extracted from EEG signal

Feature	Equation	Description
Time domain		
Mean value	$Mean_j = \frac{\sum_{i=1}^N EEG_{ij}}{N}$	Average value of EEG signal within window for EEG channel j .
Variance	$VAR_j = \frac{1}{N-1} \sum_{i=1}^N EEG_{ij}^2$	Variance of the EEG signal within window for EEG channel j .
Minimum window elements	$Min_j = \min EEG_{ij}$	Minimum EEG signal within window for EEG channel j .
Maximum window elements	$Max_j = \max EEG_{ij}$	Maximum EEG signal within window for EEG channel j .
Range	$Range_j = \max EEG_{ij} - \min EEG_{ij}$	Difference between maximum and minimum of EEG signals within window for EEG channel j .
Standard deviation (STD)	$STD_j = \sqrt{\frac{1}{N-1} \sum_{i=1}^N EEG_{ij}^2}$	Deviation of EEG signals within window for EEG channel j .
Root-mean-square level (RMS)	$RMS_j = \sqrt{\frac{\sum_{i=1}^N EEG_{ij}^2}{N}}$	Norm 2 of the EEG signals divided by the square root of the number of samples within window for EEG channel j .
Root-sum-of-squares level (RSSQ)	$RSSQ_j = \sqrt{\sum_{i=1}^N EEG_{ij} ^2}$	Norm of the EEG signals within window for EEG channel j .
Kurtosis (K)	$K_j = \frac{\frac{1}{N} \sum_i (EEG_{ij} - MAV_j)^4}{(\frac{1}{N} \sum_i (EEG_{ij} - MAV_j)^2)^2}$	Shows the sharpness of EEG signals peak within window for EEG channel j .
Frequency domain		
Normalised power $P_j(i)$	$P_j(w_i) = \frac{1}{N} X(w_i) ^2$	The mean normalised power [$P_j(i)$] of the power spectrum density [$P_j(w_i)$] of signal spectrum [$X(w_i)$] within a window for channel j .
Spectral entropy (SE)	$SE_j = - \sum_{i=1}^N P_j(i) \log_2 P_j(i)$	Entropy of the normalised power spectrum within window across frequency bands of EEG channel j .
Energy	$Energy_j = \frac{\sum_{i=1}^N FFT_{ji}^2}{N - Mean_j}$	Energy of the power spectrum within window across frequency bands EEG channel j .
Valence	$V = \frac{\alpha(F4)}{\beta(F4)} - \frac{\alpha(F3)}{\beta(F3)}$	Level of happiness.
Arousal	$A = \frac{\alpha(AF3 + AF4 + F3 + F4)}{\beta(AF3 + AF4 + F3 + F4)}$	Level of excitement.
Dominance	$D = \frac{\beta(FC6)}{\alpha(FC6)} + \frac{\beta(F8)}{\alpha(F8)} + \frac{\beta(P8)}{\alpha(P8)}$	Level of control over emotion.

Features Extracted from Plantar Pressure and Acceleration Signal

The window size of 5.12 s for pressure data and 10.24 s for acceleration data were the optimum window size for these datasets upon testing different window sizes. Time-domain and frequency-domain features for the foot plantar pressure sensor (Table 4.4) and acceleration signals (Table 4.5) were extracted from the segmented data. A total of 326 features from 32 pressure sensors and 70 features from 3-axes acceleration sensor were extracted.

4.2.2 AI-based Information Mining

A feature contains informative and measurable property of a detected signal (Jebelli et al., 2018). In this study, the relevance of a feature was determined by measuring the symmetrical uncertainty of information gain from people's interaction with the outdoor environment. First, the impurities in the features are measured using entropy. Entropy is a measure of uncertainty or lack of information of a random variable in a system (Hall, 1999; Wehrl, 1978). The entropy is computed as follows (Hall, 1999)

$$H(Y) = - \sum_{y \in Y} p(y) \log_2 p(y). \quad (4.1)$$

The entropy of Y after observing values of another variable X is computed using

$$H(Y | X) = - \sum_{x \in X} p(x) \sum_{y \in Y} p(y | x) \log_2 p(y | x), \quad (4.2)$$

where X and Y are discrete random variables. $p(y)$ is the prior probabilities for all values of Y and $p(y | x)$ is the posterior probabilities of Y when the values of X are given. Information gain is the amount by which the entropy of Y decreases reflect the additional information about Y provided by X (Doshi and Chaturvedi, 2014). Information gain is computed using (Hall, 1999; Muzammal et al., 2020; Mursalin et al., 2017)

$$Gain = H(Y) - H(Y | X) = H(X) - H(X | Y) \quad (4.3)$$

$$Gain = H(Y) + H(X) - H(X, Y). \quad (4.4)$$

Table 4.4: Features extracted from plantar pressure signal

Feature	Equation	Description
Time domain		
Mean	$Mean_j = \frac{\sum_{i=1}^N P_{ij}}{N}$	Average foot plantar pressure within window for pressure sensor j .
Variance	$VAR_j = \frac{i}{N-1} \sum_{i=1}^N P_{ij}$	Variance of the foot plantar pressure within window for pressure sensor j .
Maximum	$Max_{ij} = \max(P_{ij})$	Maximum foot plantar pressure within window for pressure sensor j .
Minimum	$Min_{ij} = \min(P_{ij})$	Minimum foot plantar pressure within window for pressure sensor j .
Range	$Range_j = \max_i P_{ij} - \min_i P_{ij}$	Difference between maximum and minimum of the foot plantar pressure within window for pressure sensor j .
Standard deviation (STD)	$STD_j = \sqrt{\frac{1}{N-1} \sum_{i=1}^N (P_{ij} - Mean_j)^2}$	Deviation of foot plantar pressure within window for pressure sensor j .
Kurtosis (K)	$K_j = \frac{\frac{1}{N} \sum_i (P_{ij} - Mean_j)^4}{\left(\frac{1}{N} \sum_i (P_{ij} - Mean_j)^2\right)^2}$	Shows the sharpness of the pressure signal peaks within window for pressure sensor j .
Pressure time integral (PTI)	$PTI_j = \sum_{t=1}^N P_{ij}(t) \times \Delta t$	PTI indicates the cumulative foot loading over time. N is the total number of pressure data samples in a window, P_{ij} is pressure value of sensor j at time t , and Δt is the duration of the window.
Centre of pressure (CoP) mean	$Mean_j = \frac{\sum_{i=1}^N CoP_{ij}}{N}$	Average centre of foot plantar pressure within window for axis j . X and Y axes
Total force (TF) mean	$Mean_j = \frac{\sum_{i=1}^N TF_{ij}}{N}$	Average total force within window for foot plantar j . Left and right foot plantar
Frequency domain		
Energy	$Energy_j = \frac{\sum_{i=1}^N FFT_{ji}^2}{N} - Mean_j$	N is the total number of pressure data within window, FFT_{ji} is the transformed i th foot pressure from time to frequency domain of the pressure sensor j .
Spectral entropy (SE)	$SE_j = - \sum_{i=1}^N P(i) \log_2 P(i)$	N is the total amount of foot pressure data within window, $P(i)$

Feature	Equation	Description
		is the normalised power spectrum of signal i of the pressure sensor j .

However, information gain is biased toward features with more values. Thus, symmetrical uncertainty (SU) is used to compensate for information gain's bias, and the resulting value is normalised to the range of [0, 1] using (Hall, 1999)

$$SU = 2.0 \times \left[\frac{Gain}{H(Y) + H(X)} \right]. \quad (4.5)$$

The Ranker algorithm in Java (Witten et al., 2017) was used to sort the features into rank order of the evaluation based on the SU. The Ranker algorithm returns an array of sorted (highest evaluation to lowest evaluation) features. The top ten ranked features are reported in this study. To determine the optimum number of features that gained the most information without overfitting, the merit of a subset of features were computed using (Hall, 1999; Muzammal et al., 2020; Mursalin et al., 2017)

$$Merit_S = \frac{k\overline{r_{cf}}}{\sqrt{k + k(k-1)\overline{r_{ff}}}}. \quad (4.6)$$

where $Merit_S$ is the heuristic merit of a feature subset S containing k features, $\overline{r_{cf}}$ is the average correlation value between feature and class labels, and $\overline{r_{ff}}$ represents the average correlation value between two features (feature-feature intercorrelation). The feature-feature intercorrelation was computed using symmetrical uncertainty. The heuristic merit discards irrelevant and redundant features because these features could decrease the information gained from human-environment interaction. A genetic algorithm was employed to search for each subset of features based on the $Merit_S$ in order to determine the optimum number of features.

Table 4.5: Features extracted from acceleration signal

Feature	Equation	Description
Time domain		
Mean	$Mean_j = \frac{\sum_{i=1}^N IMU_{ij}}{N}$	Average IMU data within window for acceleration axis j .
Variance	$VAR_j = \frac{1}{N-1} \sum_{i=1}^N (IMU_{ij} - Mean_j)^2$	N is the total amount of IMU data within window. IMU_i is the i th acceleration for axis j . Variance of the IMU data within window for each axis.
Maximum	$Max_{ij} = \max (IMU_{ij})$	Maximum IMU data within window for acceleration axis j .
Minimum	$Min_{ij} = \min (IMU_{ij})$	Minimum IMU data within window for acceleration axis j .
Range	$Range_j = \max_i IMU_{ij} - \min_i IMU_{ij}$	Difference between maximum and minimum of the IMU data within window for acceleration axis j .
Standard deviation (STD)	$STD_j = \sqrt{\frac{1}{N-1} \sum_{i=1}^N (IMU_{ij} - Mean_j)^2}$	Deviation of IMU data within window for acceleration axis j .
Root-mean-square (RMS)	$RMS_j = \sqrt{\frac{\sum_{i=1}^N IMU_{ij}^2}{N}}$	Norm 2 of the IMU data within window divided by the square root of the number of samples for acceleration axis j .
Root-sum-of-squares level (RSSQ)	$RSSQ_j = \sqrt{\frac{\sum_{i=1}^N IMU_{ij} ^2}{N}}$	Norm of the IMU data within window for acceleration axis j .
Kurtosis (K)	$K_j = \frac{\frac{1}{N} \sum_i (IMU_{ij} - Mean_j)^4}{\left(\frac{1}{N} \sum_i (IMU_{ij} - Mean_j)^2\right)^2}$	Shows the sharpness of the IMU signal peaks within window for acceleration axis j .
Signal vector magnitude (SVM)	$SVM = \frac{\sum_{i=1}^N \sqrt{x_i^2 + y_i^2 + z_i^2}}{N}$	SVM of the IMU signal within window. N is the total amount of IMU data, x_i is the i th acceleration of the x-axis, y_i is the i th acceleration of the y-axis, and z_i is the i th acceleration of the z-axis.
Signal magnitude area (SMA)	$SMA = \frac{\sum_{i=1}^N (x_i + y_i + z_i)}{N}$	SMA of the IMU signal within window. N is the total amount of IMU data, x_i is the i th acceleration of the x-axis, y_i is the i th acceleration of the y-axis, and z_i is the i th acceleration of the z-axis.
Frequency domain		

Feature	Equation	Description
Energy	$Energy_j = \frac{\sum_{i=1}^N FFT_{ji}^2}{N} - Mean_j$	N is the total amount of IMU data within window, FFT_{ji} is the transformed i th acceleration from time to frequency domain of the acceleration axis j .
Spectral entropy (SE)	$SE_j = - \sum_{i=1}^N P(i) \log_2 P(i)$	N is the total amount of IMU data within window, $P(i)$ is the normalised power spectrum of signal i of the acceleration axis j .

4.2.3 Validation

The walking path was divided into 24 sections grouped in eight distinct environment scenarios—segment A to segment H—as shown in Figure 3.2, Chapter 3. The length of each section is about 23.75 m. The segments were defined to cluster sections with a similar environmental condition expected to stimulate similar human experiences. The human experience in the environment is the human state of being affected by the surrounding conditions (Kaplan, 1988). It is expected that each segment of the path (the path was divided into 24 sections grouped in eight distinct environment scenarios—segment A to segment H—as shown in Figure 3.2) presents a unique experience to the older adults, and this unique experience can be captured through their bodily responses while interacting with the path segment. This means that the most informative bodily responses should capture a distinctive representation of the older adults’ experience in each path segment. A more informative bodily response should achieve a higher prediction performance of people’s interaction in each segment. Therefore, a supervised classification was performed using the path segments A to H as class labels. Each time point of the corresponding bodily response was signalled using a binary schema per second, where “1” signalled the presence of the participant in a segment at a specific time and “0” otherwise. A Random Forest (RF) classifier was used; RF is an ensemble of different trees. Each decision tree in the forest gives a classification, and the forest

chooses the final classification with the most votes (Lou et al., 2014). The RF classifier is chosen because it can accommodate models with imbalanced class labels, and it can provide an assessment of the variable importance (Saitis and Kalimeri, 2018). 10-fold cross-validation was conducted to validate the performance of the classification model over the selected features.

Accuracy represents the percentage of path segments that are correctly classified based on the selected features. Sensitivity is the true positive (TP) rate based on the selected features. That is the proportion of path segments that are actually positive and were predicted positive. Specificity is the true negative (TN) rate based on the selected features. That is the proportion of path segments that are actually negative and were predicted negative. Accuracy, sensitivity, and specificity are benefit criteria meaning the highest value is the most preferred. The performance measures are computed using the following equations

$$Accuracy = \frac{TP + TN}{TP + TN + FP + FN} , \quad (4.7)$$

$$Sensitivity = \frac{TP}{TP + FN} , \quad (4.8)$$

$$Specificity = \frac{TN}{TN + FP} , \quad (4.9)$$

where FN is the false negative, and FP is the false positive.

4.3 Results and Discussion

4.3.1 Physiological Response

The physiological signals are involuntary actions or response that are almost impossible to notice by external observation because it relates to how a living organism or bodily part functions (Alberdi et al., 2016). In this experiment, two main physiological responses were

collected and analysed—HRV and EDA. The HRV and EDA features that gained the most information are presented in Table 4.6 and Table 4.7, respectively.

For HRV features, minimum HR (with an accuracy of 75.96%, sensitivity of 76% and specificity of 95.7%) and maximum HR (with an accuracy of 71.77%, sensitivity of 71.8% and specificity of 95.4%) gained the most information about older adults' experience in the environment. It is important to mention the inconsistency reported in previous studies considering the use of HR and HRV to represent people's interaction with the environment. For example, some studies reported that HR and HRV contain relevant information, and other studies reported otherwise (Triguero-Mas et al., 2017; Birenboim et al., 2019). In this study, HR was ranked third but did not gain sufficient information about older adults' experience in the environment (accuracy of 23.59%, sensitivity of 23.6%, and specificity of 87.4%). Similarly, all HRV features (Table 4.6) gained very little information about older adults' experience in the environment. For example, the highest-ranked HRV feature is HF(Hz) achieved an accuracy of 29.43%, sensitivity of 29.4%, and specificity of 84.3%. A plausible explanation for this is that the physiological cardiovascular bodily responses are more susceptible to physical activity, and the influence of the walking activity in the experiment might dominate subtle environmental effects.

The findings from this study clarify the inconsistency in the reliability of HR and HRV features in measuring physiological responses by taking into account the information gained by several features. The AI-based information mining model further provided a subset of five HR and HRV features that can collectively gain more information than any single feature. This feature subset (Table 4.6) attained an accuracy of 92.31%, sensitivity of 98.7%, and specificity of 98.7%. The performance of this feature subset can be attributed to the fact that each feature

Table 4.6: Most informative HRV features

Top ten	PPG feature	Rank	Single feature performance	Cumulative performance
1	Min HR	0.36225	Acc. 75.96 Sen. 76.00 Spec. 95.70	Acc. 71.94 Sen. 71.90 Spec. 95.40
2	Max HR	0.35472	Acc. 71.77 Sen. 71.80 Spec. 95.40	Acc. 86.22 Sen. 86.20 Spec. 97.80
3	HR	0.15806	Acc. 23.59 Sen. 23.60 Spec. 87.40	Acc. 90.09 Sen. 90.10 Spec. 98.40
4	HF (Hz)	0.09242	Acc. 29.43 Sen. 29.40 Spec. 84.30	Acc. 92.28 Sen. 92.30 Spec. 98.70
5	SD1	0.08184	Acc. 52.14 Sen. 52.10 Spec. 92.00	Acc. 93.34 Sen. 93.30 Spec. 98.90
6	RMSSD	0.07823	Acc. 50.94 Sen. 50.90 Spec. 91.70	Acc. 93.53 Sen. 93.50 Spec. 98.90
7	pNN50	0.07481	Acc. 32.01 Sen. 32.00 Spec. 86.60	Acc. 94.05 Sen. 94.10 Spec. 99.00
8	STD HR	0.07281	Acc. 49.36 Sen. 49.40 Spec. 91.50	Acc. 94.54 Sen. 94.50 Spec. 99.10
9	NN50	0.0721	Acc. 27.91 Sen. 27.90 Spec. 83.60	Acc. 94.75 Sen. 94.70 Spec. 99.20
10	LF (Hz)	0.06962	Acc. 27.20 Sen. 27.20 Spec. 84.80	Acc. 94.97 Sen. 95.00 Spec. 99.20
Optimum subset of PPG features (5 selected features)				Acc. 92.31 Sen. 92.30 Spec. 98.70
HR	Max HR	Min HR	VLF (ms ²)	SD2/SD1

Note. Min HR = minimum heart rate; Max HR = maximum heart rate; HR = instantaneous heart rate; HF = absolute power of high frequency band; LF = absolute power of low frequency band; VLF = absolute power of very low frequency band; SD1 = standard deviation perpendicular to the line-of-identity in Poincaré plot; SD2 = standard deviation along the line-of-identity in Poincaré plot; STD HR = standard deviation of instantaneous heart rate values; RMSSD = square root of the mean squared differences between successive RR intervals; NN50 = Number of successive RR interval pairs that differ more than 50 ms; Acc. = accuracy; Sen. = sensitivity; Spec. = specificity.

gained specific information about older adults' experience in the environment. For example, minimum HR and maximum HR captures environmental conditions that stimulate a state of serenity and stress, respectively (Kreibig, 2010). HR, VLF, and SD2/SD1 reflect the parasympathetic-sympathetic balance (Triguero-Mas et al., 2017). The implication drawn from the results is that future studies should consider a subset of features instead of a specific feature in interpreting physiological cardiovascular bodily responses in the outdoor environment.

Considering the EDA features (Table 4.7), PhasicMax gained the most information about older adults' experience in the outdoor environment with an accuracy of 99.07%, sensitivity of 99.1%, and specificity of 99.9%. Although several features gained sufficient information (except nSCR and Latency), only PhasicMax was subsequently selected as the optimum feature. This signifies that the AI-based information mining model was able to avoid overfitting by discarding redundant EDA features in order to reduce computational cost and time while achieving high performance. Furthermore, the result from the study is in support of the growing consensus that the phasic component of the EDA signal represents an individual's response to discrete environmental stimuli (Birenboim et al., 2019; Chen et al., 2018). In comparison to the cognitive and behavioural responses, the physiological signal performed better in gaining information about older adults' interaction. The result proves that physiological signals can be monitored from wristband type sensors in an ambulatory, real-world setting and can be extended to capture older adult's response to subtle environmental stimuli.

Table 4.7: Most informative EDA features

Top ten	EDA feature	Rank	Single feature performance	Cumulative performance
1	PhasicMax	0.425	Acc. 99.07 Sen. 99.10 Spec. 99.90	Acc. 99.07 Sen. 99.10 Spec. 99.90
2	AmpSum	0.33725	Acc. 82.00 Sen. 82.00 Spec. 97.40	Acc. 99.58 Sen. 99.60 Spec. 99.90
3	Tonic	0.3062	Acc. 99.78 Sen. 99.80 Spec. 100.00	Acc. 99.91 Sen. 99.90 Spec. 100.00
4	Global mean	0.28601	Acc. 99.77 Sen. 99.80 Spec. 100.00	Acc. 99.91 Sen. 99.90 Spec. 100.00
5	Global max deflection	0.25437	Acc. 92.56 Sen. 92.60 Spec. 98.90	Acc. 99.91 Sen. 99.90 Spec. 100.00
6	ISCR	0.11883	Acc. 95.98 Sen. 96.00 Spec. 98.90	Acc. 99.91 Sen. 99.90 Spec. 100.00
7	SCR	0.11883	Acc. 95.98 Sen. 96.00 Spec. 98.90	Acc. 99.91 Sen. 99.90 Spec. 100.00
8	nSCR	0.02122	Acc. 24.34 Sen. 24.30 Spec. 81.00	Acc. 99.91 Sen. 99.90 Spec. 100.00
9	Latency	0.00135	Acc. 22.56 Sen. 22.60 Spec. 77.40	Acc. 99.91 Sen. 99.90 Spec. 100.00
Optimum EDA feature (1 selected feature)				Acc. 99.15 Sen. 99.10 Spec. 99.90
PhasicMax				

Note. PhasicMax = maximum value of phasic activity; SCR = average phasic driver; nSCR = number of significant (= above-threshold) SCRs; AmpSum = Sum of SCR-amplitudes of significant SCRs; ISCR = Area (i.e., time integral) of phasic driver; Acc. = accuracy; Sen. = sensitivity; Spec. = specificity.

4.3.2 Cognitive Response

The cognitive signals relate to the activities of the brain or mental state. All the EEG features gained insufficient information about older adults' experience in the environment. The highest-ranked EEG feature is variance in the F3 channel, achieving an accuracy of 22.46%, sensitivity

Table 4.8: Most informative EEG features

Top ten	EEG feature	Rank	Single feature performance	Cumulative performance
1	Variance (F3)	0.10626	Acc. 22.46 Sen. 22.50 Spec. 86.60	Acc. 21.64 Sen. 21.60 Spec. 86.60
2	RMS (F3)	0.10469	Acc. 21.57 Sen. 21.60 Spec. 86.50	Acc. 21.64 Sen. 21.60 Spec. 86.50
3	RSSQ (F3)	0.10469	Acc. 21.57 Sen. 21.60 Spec. 86.50	Acc. 22.28 Sen. 22.30 Spec. 86.50
4	RMS (AF3)	0.09472	Acc. 18.53 Sen. 18.50 Spec. 86.10	Acc. 32.94 Sen. 32.90 Spec. 88.10
5	RSSQ (AF3)	0.09472	Acc. 18.53 Sen. 18.50 Spec. 86.10	Acc. 34.94 Sen. 34.90 Spec. 88.20
6	Variance (AF3)	0.09208	Acc. 20.74 Sen. 20.70 Spec. 86.50	Acc. 36.66 Sen. 36.70 Spec. 88.50
7	STD (AF3)	0.09208	Acc. 20.78 Sen. 20.80 Spec. 86.50	Acc. 36.23 Sen. 36.20 Spec. 88.40
8	Range (AF3)	0.09066	Acc. 37.94 Sen. 37.90 Spec. 89.40	Acc. 38.63 Sen. 38.60 Spec. 88.70
9	STD (FC6)	0.08716	Acc. 19.92 Sen. 19.90 Spec. 86.30	Acc. 47.50 Sen. 47.50 Spec. 90.30
10	Variance (FC6)	0.08716	Acc. 20.03 Sen. 0.20 Spec. 86.40	Acc. 49.14 Sen. 49.10 Spec. 90.70
Optimum EEG features (96 selected features)				Acc. 80.69 Sen. 80.70 Spec. 96.20
Mean (AF3)	Minimum (F7)	STD (T7)	RSSQ (FC5)	Entropy_beta (T8)
Mean (F7)	Minimum (T7)	STD (O1)	RSSQ (T7)	Energy_alpha (T8)
Mean (F3)	Minimum (O1)	STD (O2)	RSSQ (P7)	Energy_alpha (FC6)
Mean (P7)	Minimum (O2)	STD (T8)	RSSQ (T8)	Energy_beta (FC6)
Mean (O2)	Minimum (P8)	STD (FC6)	Kurtosis (P7)	Entropy_theta (F4)
Mean (FC6)	Minimum (T8)	RMS (AF3)	Energy_delta (AF3)	Energy_theta (F4)
Mean (AF4)	Minimum (F8)	RMS (F7)	Energy_gamma (AF3)	Energy_gamma (F4)
Variance (T7)	Minimum (AF4)	RMS (F3)	Entropy_gamma (F7)	Energy_beta (F8)
Variance (O1)	Range (AF3)	RMS (FC5)	Entropy_theta (F3)	Energy_alpha (AF4)
Variance (FC6)	Range (F7)	RMS (P7)	Energy_delta (F3)	Energy_beta (AF4)
Variance (AF4)	Range (FC5)	RMS (O1)	Energy_alpha (FC5)	Power_gamma (F7)
Maximum (AF3)	Range (P7)	RMS (O2)	Entropy_theta (P7)	Power_delta (FC5)

Maximum (F7)	Range (O2)	RMS (P8)	Energy_delta (P7)	Power_gamma (T7)
Maximum (FC5)	Range (T8)	RMS (FC6)	Energy_theta (P7)	Power_beta (P7)
Maximum (P7)	Range (F4)	RMS (F4)	Energy_gamma (P7)	Power_gamma (O1)
Maximum (O1)	Range (F8)	RMS (F8)	Entropy_gamma (O1)	Power_beta (O2)
Maximum (T8)	STD (AF3)	RMS (AF4)	Energy_delta (O1)	Power_gamma (O2)
Maximum (F4)	STD (F7)	RSSQ (AF3)	Energy_alpha (O1)	Power_beta (FC6)
Minimum (AF3)	STD (FC5)	RSSQ (F3)	Entropy_theta (T8)	Power_theta (FC6)
				Power_theta (AF4)

Note. RMS = root-mean-square level; RSSQ = root-sum-of-squares level; STD = standard deviation; Acc. = accuracy; Sen. = sensitivity; Spec. = specificity.

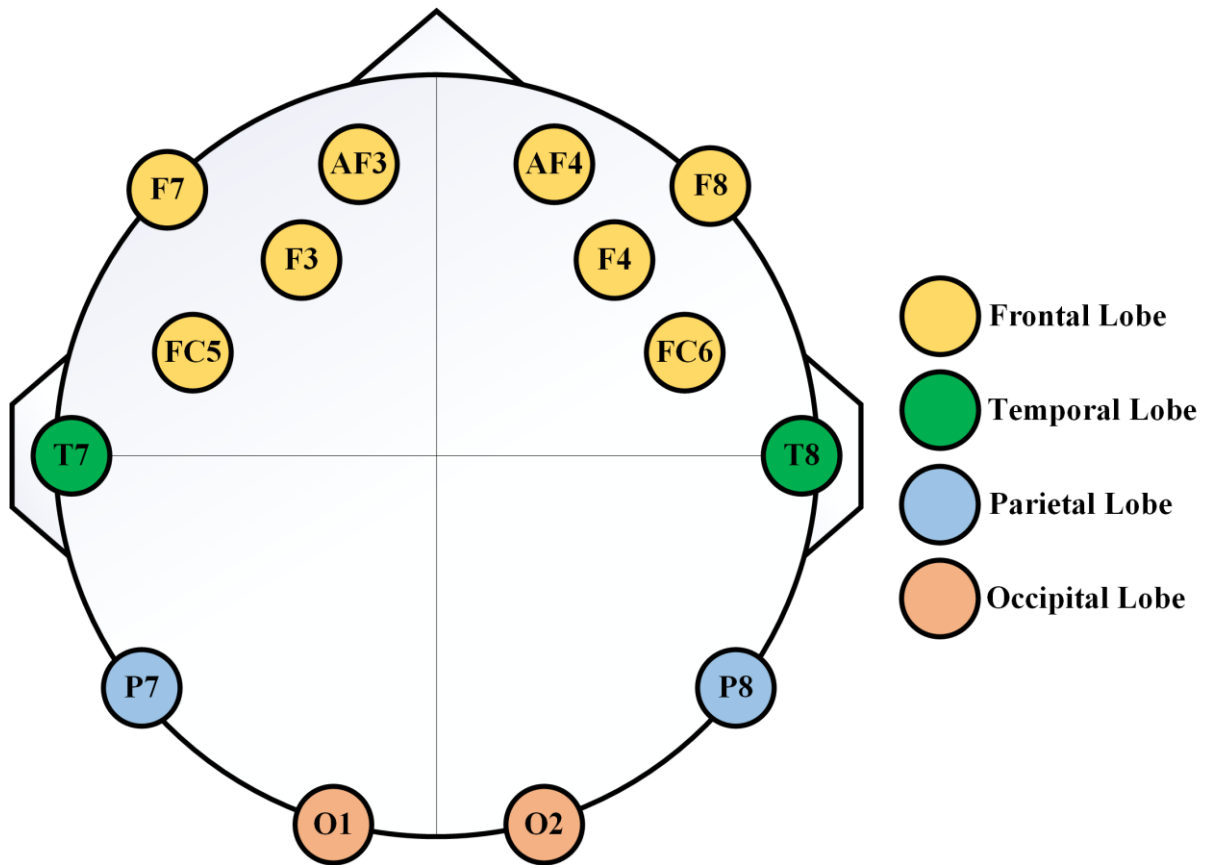


Figure 4.2: Distribution of the EEG channels across the scalp.

of 22.5%, and specificity of 86.6% (Table 4.8). All the top 10 ranked EEG features only capture the activity of the cortical neurons in the frontal lobe (Figure 4.2). The low performance of the EEG features proves that the urban environment is becoming more complex and cognitively demanding to older adults. Therefore, the brain will require more cognitive resources to gain sufficient information. As a result, the proposed AI-based information mining model identified a subset of 96 features (Table 4.8) that gained more information than any single EEG feature.

The feature subset achieved an accuracy of 80.69%, sensitivity of 80.7%, and specificity of 96.2%. The optimum subset of EEG features is dominated by features extracted from the frontal lobe, followed by the occipital lobe, temporal lobe, and parietal lobe.

Considering the frequency bands, the optimum EEG feature subset is dominated by the gamma band, followed by theta band, beta band, alpha, and delta band. The higher frequency band (gamma and beta) correlates with heavy mental loads such as concentration, anxiousness, and stress; the alpha band correlates with a relaxed state of mind; the lower frequency bands (delta and theta) correlate with less intense brain function (Bailey et al., 2018). The results confirmed that walking in different environmental conditions activates millions of cortical neurons and produces an electrical field that can be measured from the human scalp using wearable EEG. The information gained by the cortical neurons is encoded in EEG signal amplitudes, specific frequency bands, and different brain regions; this explains why today's urban environment is more cognitively demanding. Furthermore, different environmental conditions are associated with distinctive brain activity patterns, which means that humans interact differently with varying environmental conditions.

Although the EEG signal is somewhat informative, monitoring people's brain activity using current EEG sensors in an ambulatory, real-world setting is still a major challenge. It can lead to the loss of informative data. Current wearable and mobile EEG sensors are not stable in the wild. For instance, the walking activity during the environmental walk affected the stability and functioning of the EEG sensor for five participants. Therefore, developers should focus on improving the stability of wearable and mobile EEG sensors.

4.3.3 Behavioural Response

Behavioural signals are somewhat voluntary actions that can be externally observed (Alberdi et al., 2016). The foot plantar pressure distribution and acceleration of both left and right feet were observed while older adults interact with the environment. The foot plantar pressure and acceleration features that gain the most information are presented in Table 4.9 and Table 4.10, respectively.

For the foot plantar pressure features (Table 4.9), pressure-time integral (PTI) gained the most information about older adults' experience in the environment with an accuracy of 41.1%, sensitivity of 41.1%, and specificity of 88.7%. All the top 10 ranked features are the PTI in different sensor locations and mostly from the right foot. Although the PTI features were not very informative, the AI-based information mining model identified a feature subset (comprised of 91 plantar pressure features) that was able to gain more information about older adults' experience in the environment. The feature subset achieved an accuracy of 82.05%, sensitivity of 82.1%, and specificity of 96.6%.

For the acceleration features (Table 4.10), signal magnitude area (SMA) (17.16%, sensitivity of 17.2%, and specificity of 85.6%) and signal vector magnitude (SVM) (17.16%, sensitivity of 17.2%, and specificity of 85.6%) were the most informative features. The AI-based information mining model identified a subset of 15 acceleration features that gained more information than any single acceleration feature with an accuracy of 35.84%, sensitivity of 35.8%, and specificity of 86.5%. Generally, the acceleration signal and the foot plantar pressure features performed poorly in gaining information about older adults' experience in the environment.

Table 4.9: Most informative plantar pressure features

Top ten	Pressure sensor feature	Rank	Single feature performance	Cumulative performance
1	PTI_Sensor4 (R)	0.2603	Acc. 41.10 Sen. 41.10 Spec. 88.70	Acc. 41.10 Sen. 41.10 Spec. 88.70
2	PTI_Sensor11 (R)	0.2375	Acc. 43.61 Sen. 43.60 Spec. 87.00	Acc. 53.31 Sen. 53.30 Spec. 91.00
3	PTI_Sensor10 (L)	0.2233	Acc. 40.58 Sen. 40.60 Spec. 86.50	Acc. 58.14 Sen. 58.10 Spec. 91.80
4	PTI_Sensor11 (L)	0.1996	Acc. 37.83 Sen. 37.80 Spec. 86.30	Acc. 59.71 Sen. 59.70 Spec. 92.40
5	PTI_Sensor9 (R)	0.1950	Acc. 36.60 Sen. 36.60 Spec. 85.80	Acc. 62.17 Sen. 62.20 Spec. 93.20
6	PTI_Sensor10 (R)	0.1940	Acc. 35.22 Sen. 35.20 Spec. 84.70	Acc. 64.96 Sen. 65.00 Spec. 93.70
7	PTI_Sensor15 (R)	0.1844	Acc. 36.74 Sen. 36.70 Spec. 84.60	Acc. 67.57 Sen. 67.60 Spec. 94.20
8	PTI_Sensor3 (R)	0.1830	Acc. 35.51 Sen. 35.50 Spec. 85.80	Acc. 68.80 Sen. 68.80 Spec. 94.40
9	PTI_Sensor4 (L)	0.1721	Acc. 34.09 Sen. 34.10 Spec. 84.90	Acc. 69.46 Sen. 69.50 Spec. 94.60
10	PTI_Sensor1 (R)	0.1632	Acc. 33.62 Sen. 33.60 Spec. 87.70	Acc. 73.48 Sen. 73.50 Spec. 95.20
Optimum pressure sensor features (91 selected features)				Acc. 82.05 Sen. 82.10 Spec. 96.60
Mean_Sensor5 (L)	Variance_Sensor14 (L)	Minimum_Sensor7 (L)	STD_Sensor11 (R)	PTI_Sensor7 (R)
Mean_Sensor6 (L)	Variance_Sensor15 (L)	Minimum_Sensor10 (L)	Kurtosis_Sensor1 (L)	PTI_Sensor9 (R)
Mean_Sensor9 (L)	Variance_Sensor1 (R)	Minimum_Sensor11 (L)	Kurtosis_Sensor2 (L)	PTI_Sensor11 (R)
Mean_Sensor11 (L)	Variance_Sensor6 (R)	Minimum_Sensor12 (L)	Kurtosis_Sensor5 (L)	PTI_Sensor14 (R)
Mean_Sensor12 (L)	Variance_Sensor7 (R)	Minimum_Sensor13 (L)	Kurtosis_Sensor2 (R)	PTI_Sensor15 (R)
Mean_Sensor16 (L)	Variance_Sensor10 (R)	Minimum_Sensor16 (L)	Kurtosis_Sensor10 (R)	PTI_Sensor16 (R)

Mean_Sensor1 (R)	Variance_Sensor11 (R)	Minimum_Sensor3 (R)	PTI_Sensor1 (L)	Energy_Sensor7 (L)
Mean_Sensor19 (R)	Variance_Sensor13 (R)	Minimum_Sensor11 (R)	PTI_Sensor3 (L)	Energy_Sensor9 (L)
Mean_Sensor3 (R)	Variance_Sensor15 (R)	Range_Sensor3 (L)	PTI_Sensor4 (L)	Energy_Sensor1 (R)
Mean_Sensor6 (R)	Maximum_Sensor1 (L)	Range_Sensor5 (L)	PTI_Sensor7 (L)	Energy_Sensor2 (R)
Mean_Sensor8 (R)	Maximum_Sensor8 (L)	Range_Sensor8 (L)	PTI_Sensor9 (L)	Energy_Sensor9 (R)
Mean_Sensor9 (R)	Maximum_Sensor10 (L)	Range_Sensor11 (L)	PTI_Sensor10 (L)	Entropy_Sensor1 (L)
Mean_Sensor14 (R)	Maximum_Sensor11 (L)	Range_Sensor10 (R)	PTI_Sensor11 (L)	Entropy_Sensor6 (L)
Mean_Sensor15 (R)	Maximum_Sensor13 (L)	STD_Sensor7 (L)	PTI_Sensor13 (L)	Entropy_Sensor9 (L)
Variance_Sensor1 (L)	Maximum_Sensor15 (L)	STD_Sensor9 (L)	PTI_Sensor16 (L)	Entropy_Sensor10 (L)
Variance_Sensor3 (L)	Maximum_Sensor14 (R)	STD_Sensor12 (L)	PTI_Sensor1 (R)	Entropy_Sensor11 (L)
Variance_Sensor7 (L)	Minimum_Sensor1 (L)	STD_Sensor14 (L)	PTI_Sensor3 (R)	Entropy_Sensor16 (R)
Variance_Sensor13 (L)	Minimum_Sensor6 (L)	STD_Sensor7 (R)	PTI_Sensor6 (R)	CoP_X axis (L)
				CoP_X axis (R)

Note. PTI = pressure time integral; CoP = centre of pressure; STD = standard deviation; (R) = right foot; (L) = left foot; X-axis = anterior-posterior; Acc. = accuracy; Sen. = sensitivity; Spec. = specificity.

The poor performance can be attributed to the characteristics of the population being studied older adults aged 65 or above. Gait usually changes with ageing (Salzman, 2010); as a result, older adults tend to have a diverse abnormal gait, which affected the informativeness of the foot plantar and acceleration features. The gait abnormality among older adults affected the acceleration signal more than the foot plantar pressure signal. This is because the IMU used to extract acceleration features track movement in 3-axes. The X-axis (anterior-posterior) and Y-axis (medial-lateral), as shown in Figure 4.3, are directed towards space and are more susceptible to gait abnormality among older adults. In contrast, all the foot plantar pressure sensors are directed toward the ground surface and were able to gain distinct information from the ground surface. For example, the plantar pressure distributions between a person's foot and

Table 4.10: Most informative acceleration features

Top ten	Acceleration signal feature	Rank	Single feature performance	Cumulative performance
1	SMA (L)	0.0722	Acc. 17.16 Sen. 17.20 Spec. 85.60	Acc. 15.54 Sen. 15.50 Spec. 85.60
2	SVM (L)	0.0674	Acc. 19.54 Sen. 19.50 Spec. 86.00	Acc. 19.16 Sen. 19.20 Spec. 85.40
3	SVM (R)	0.0633	Acc. 18.97 Sen. 19.00 Spec. 86.50	Acc. 20.78 Sen. 20.80 Spec. 85.60
4	Mean_Z axis (R)	0.0629	Acc. 16.30 Sen. 16.30 Spec. 85.60	Acc. 21.35 Sen. 21.40 Spec. 85.80
5	RSSQ_X axis (L)	0.0604	Acc. 17.73 Sen. 17.70 Spec. 86.00	Acc. 22.59 Sen. 22.60 Spec. 85.50
6	RMS_X axis (L)	0.0604	Acc. 17.73 Sen. 17.70 Spec. 86.00	Acc. 22.31 Sen. 22.30 Spec. 85.60
7	RMS_Z axis (R)	0.0597	Acc. 18.50 Sen. 18.50 Spec. 86.1	Acc. 22.88 Sen. 22.90 Spec. 85.60
8	RSSQ_Z axis (R)	0.0597	Acc. 18.50 Sen. 18.50 Spec. 86.10	Acc. 25.55 Sen. 25.50 Spec. 85.80
9	SMA (R)	0.0565	Acc. 16.78 Sen. 16.80 Spec. 85.70	Acc. 26.12 Sen. 26.10 Spec. 85.80
10	Entropy_Z axis (R)	0.0548	Acc. 15.54 Sen. 15.50 Spec. 85.60	Acc. 25.93 Sen. 25.90 Spec. 85.70
Optimum acceleration signal features (15 selected features)				Acc. 35.84 Sen. 35.80 Spec. 86.50
Mean_Z axis (R)	Minimum_Z axis (R)	RMS_X axis (L)	RSSQ_Y axis (L)	SMA (L)
Variance_Z axis (R)	Range_Z axis (R)	RMS_Z axis (R)	SVM (L)	Energy_Z axis (L)
Minimum_Z axis (L)	STD_X axis (L)	RSSQ_X axis (L)	SVM (R)	Entropy_Z axis (R)

Note. SMA = signal magnitude area; SVM = signal vector magnitude; RSSQ = root-sum-of-squares level; RMS = root-mean-square; (R) = right foot; (L) = left foot; X-axis = anterior-posterior; Y-axis = medial-lateral; Z-axis = vertical axis; Acc. = accuracy; Sen. = sensitivity; Spec. = specificity.

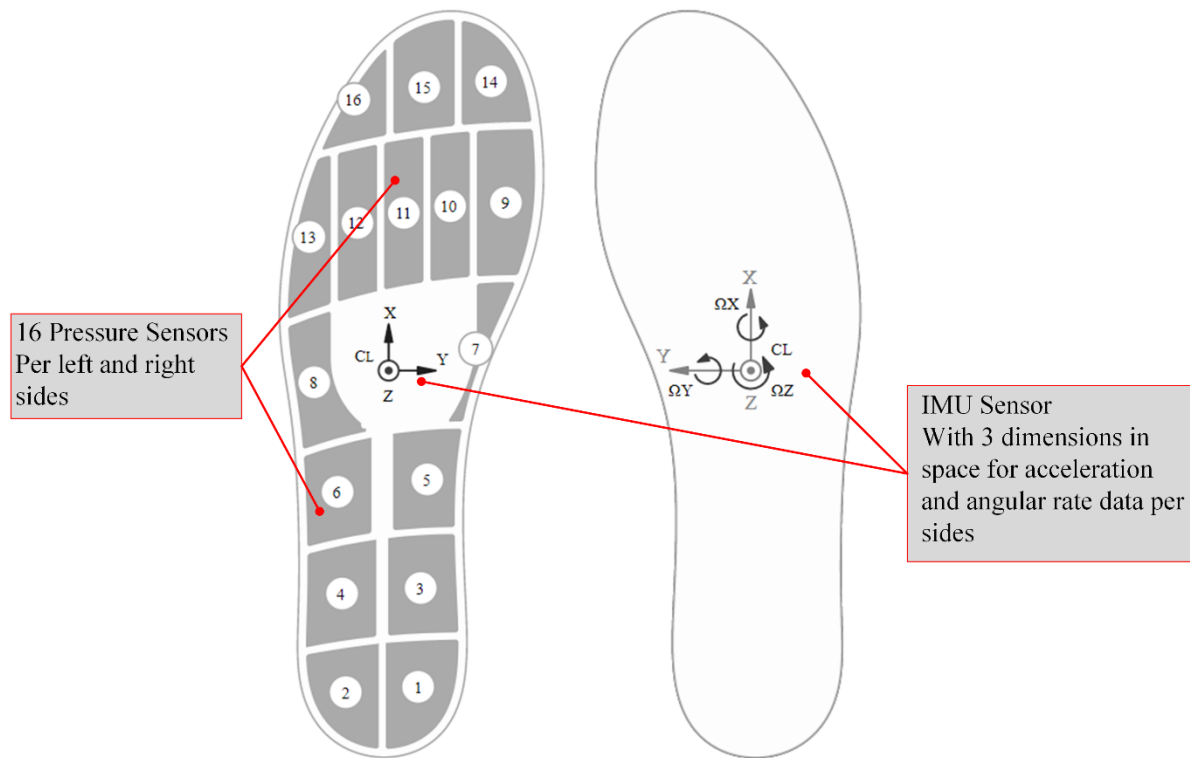


Figure 4.3: Plantar pressure sensors and IMU sensor positions.

footpaths with tarmac, paving slab, or gravel surfacing material are different. This distinctive information from the ground surfacing reflected in the Z-axis (vertical axis) of the acceleration signal which is directed towards the ground surface. As a result, the top 10 most informative acceleration features and the optimum subset of informative acceleration features were dominated by features extracted from the Z-axis. Nevertheless, researchers should be cautious when using older adults' gait to represent their interaction with the environment because older adults' gait abnormality can overwhelm the result.

4.4 Chapter Summary

This chapter aimed to achieve research objective one: to assess the informativeness of the bodily response collected in the ambulatory, real-world environment. This objective was achieved using information entropy, symmetric uncertainty, correlation analysis, RF algorithm. In summary, older adults' physiological response is more informative than the cognitive and

behavioural responses. The informativeness of the EEG sensor was affected by the walking activity, and the gait abnormality among older adults affected their behavioural response. Researchers should be cautious when using older adults' gait to represent their interaction with the environment because older adults' gait abnormality can overwhelm the result. With more advances in wearable technologies, it is hoped that future EEG sensors will be more stable in the wild. The result proves that physiological signals can be monitored from wristband type sensors in an ambulatory, real-world setting and can be extended to capture older adults' response to subtle environmental stimuli. The analysis in the subsequent chapters will be based on only the older adults' physiological response. A computational approach for representing people's interaction with the environment using the optimum feature set will be introduced. However, before this can be achieved, it is crucial to examine the statistical, spatial, and temporal associations in older adults' physiological response. The next chapter will focus on understanding the statistical, spatial, and temporal associations in older adults' physiological response.

CHAPTER 5

Interaction of Older Adults' Physiological Response with the Built Environment: Statistical, Spatial and Temporal Relationships⁵

5.1 Introduction

This chapter aims to achieve research objective two: to examine the relationships in older adult's bodily responses resulting from their interaction with the environment. Because older adults' behavioural and cognitive responses are not very informative, this chapter only focuses on the physiological response. Figure 5.1 is an overview of the study presented in this chapter. The methods adopted in this chapter are illustrated in Figure 5.2.

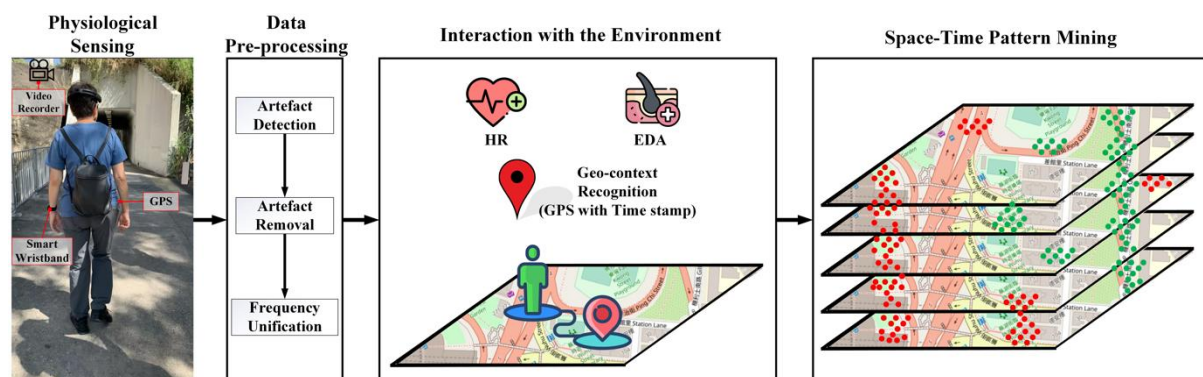


Figure 5.1: Overview of the study.

⁵ Parts of this chapter has been published in a journal.

Torku, A., Chan, A.P.C., Yung, E.H.K., Seo, J. (2021). The influence of urban visuospatial configuration on older adults' stress: A wearable physiological-perceived stress sensing and data mining based-approach, *Building and Environment*, 108298. <https://doi.org/10.1016/j.buildenv.2021.108298>

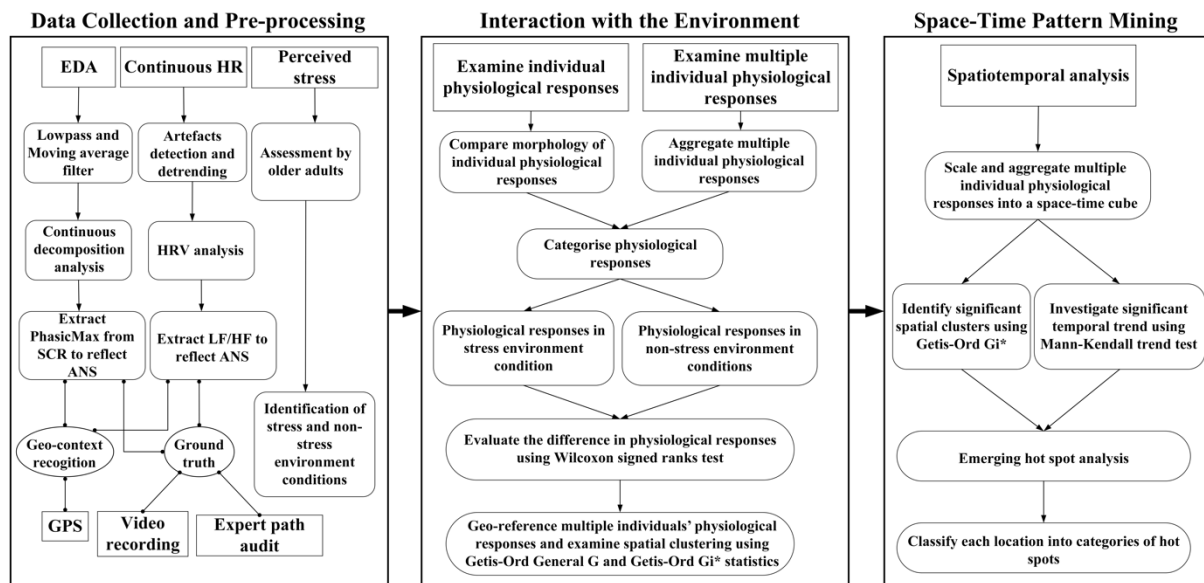


Figure 5.2: Methodological flow chart.

Note. EDA = electrodermal activity; HRV = heart rate variability; ANS = autonomic nervous system; *LF/HF* = The ratio of absolute spectral power of the low frequency (LF) band (0.04-0.15) and high frequency (HF) band (0.15-0.4); SCR = skin conductance response; PhasicMax = The maximum value of phasic activity within 10 s response window; GPS = Global Positioning System.

5.2 Methods

5.2.1 Physiological Reflectors of Human-Environment Stressful Interactions

The path for the environmental walk was classified into two categories using the older adults' perceived stress as presented in Chapter 3. The first category represents environmental conditions that older adults perceive as non-stress, and the second category represents environmental conditions perceived as stress. Older adults' physiological responses to these environment conditions were analysed by assessing the dynamics of their autonomic nervous system (ANS). The ANS is one of the major neural pathways activated by stress (Won et al., 2016; Boucsein, 2012). Heart rate variability (HRV) and electrodermal activity (EDA) are reliable indicators of the sympathetic and parasympathetic nervous system (Acharya et al., 2006; Boucsein, 2012). The parasympathetic nervous system modulates heart rate at all frequencies between 0.15 and 0.4 Hz. The sympathetic nervous system modulates heart rate (with significant gain) at frequencies between 0.04 to 0.15 Hz (Healey and Picard, 2005;

Acharya et al., 2006). To precisely model the effect of environmental stressors, the ratio of the low-frequency heart rate absolute spectral power to high-frequency heart rate absolute spectral power was computed to represent the ratio of the sympathetic to parasympathetic (sympathovagal balance) influence on the heart. The absolute spectral power of the low frequency (LF) band (0.04-0.15) and high frequency (HF) band (0.15-0.4) were calculated, and the ratio LF/HF was derived.

An increase in the eccrine sweat gland activity is observed when the sympathetic nervous system is stimulated, thus changing the conductivity of the skin (Zhang et al., 2018; Kleckner et al., 2018). EDA measures the conductivity of the skin and is one of the most frequently employed signals for detecting physiological arousal levels and stress (Kleckner et al., 2018; Boucsein, 2012; Posada-Quintero and Chon, 2020). To precisely model the effect of environmental stressors, the EDA is first decomposed into two components—phasic component and tonic component—using a continuous decomposition analysis method as shown in Figure 5.3 (Benedek and Kaernbach, 2010). The phasic component results from an underlying sympathetic reaction to a stimulus while the tonic component are responses to tonic stimulus and changes slowly over time (Posada-Quintero and Chon, 2020; Benedek and Kaernbach, 2010). Because the tonic EDA component cannot be linked to a specific stimulus, this study used only the phasic EDA component to represent older adults' physiological response. The maximum value of phasic activity within 10 s response window (PhasicMax) extracted from the phasic component (skin conductance response [SCR]) of the EDA signal was used as an indicator of older adults' physiological response. The collection of these data and pre-processing methods are presented in Chapter 3, and the informativeness of the features was assessed in Chapter 4.

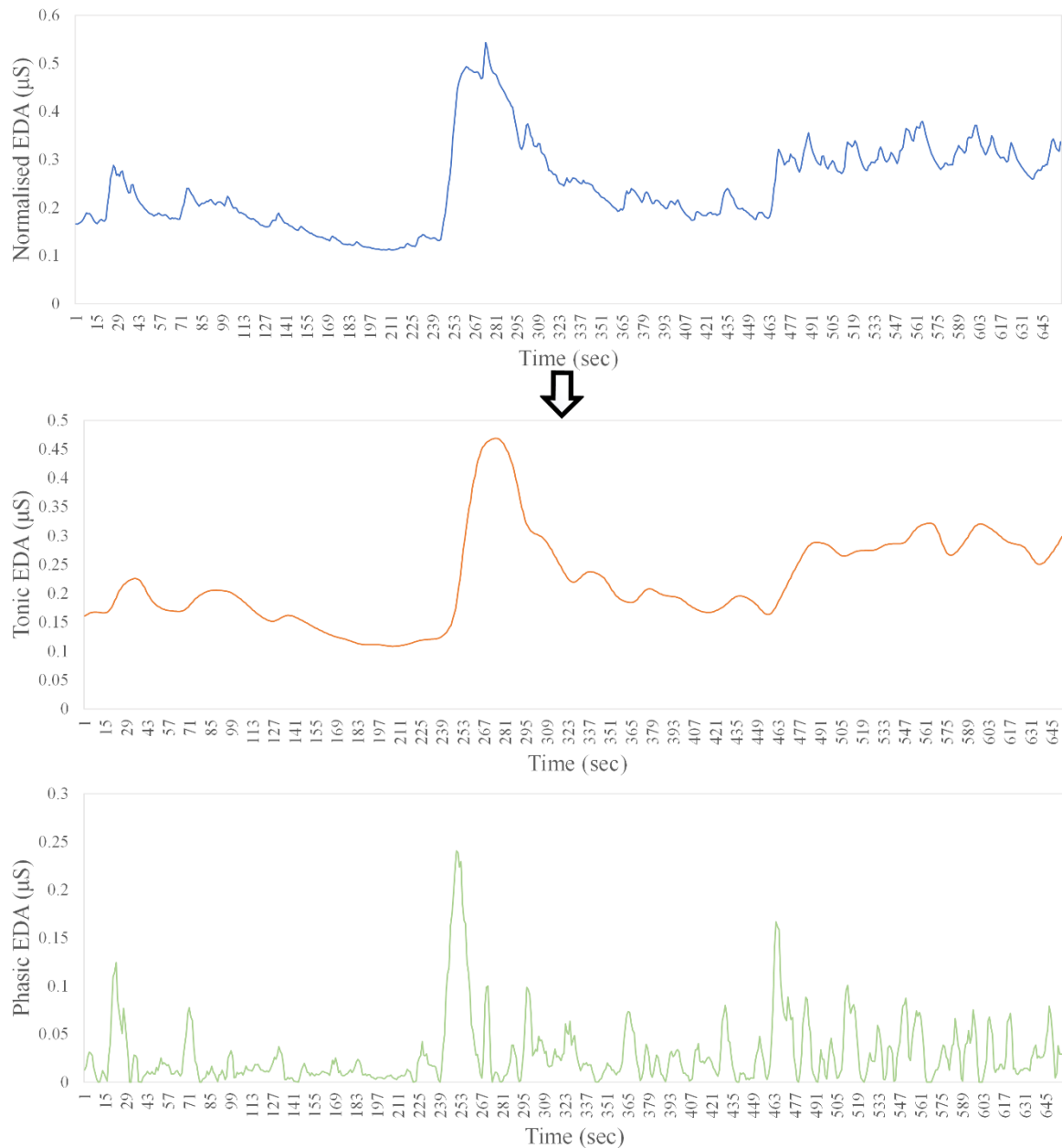


Figure 5.3: A continuous decomposition of EDA into tonic component and phasic component.

5.2.2 Statistical Analysis

A Wilcoxon signed-rank test was conducted to understand whether the physiological responses to environmental conditions perceived as non-stress was statistically and significantly different from environmental conditions perceived as stress. A Wilcoxon signed-rank test is a nonparametric statistical hypothesis test that compares two related samples or repeated

measurements on a single sample to assess whether their population mean ranks differ (Woolson, 2007).

5.2.3 Spatial Analysis

A participant experiencing a high or low physiological response at a location could result from random factors or spatial factors. However, if multiple participants tend to experience a common physiological response at a location, this could indicate that the physiological response was due to spatial factors. Spatial clustering analysis was conducted using Getis-Ord General G to confirm whether there is any spatial association in participants' physiological response. Getis-Ord General G statistic is an inferential statistic that assesses the degree of spatial association in an entire sample or relation to a single observation for a given study area (Getis and Ord, 2010). The Getis-Ord General G statistic is computed as follows (Getis and Ord, 2010)

$$G = \frac{\sum_{i=1}^n \sum_{j=1}^n w_{i,j} x_i x_j}{\sum_{i=1}^n \sum_{j=1}^n x_i x_j}, \forall_j \neq i, \quad (5.1)$$

where x_i and x_j are attribute values for physiological responses i and j , and $w_{i,j}$ is the spatial weight between physiological response i and j . n is the number of physiological response in the study area.

To determine locations on the path that stimulated a common physiological response among multiple participants, a hot spot analysis was conducted using Getis-Ord G_i^* statistics. The Getis-Ord G_i^* statistics returns a z-score and a p-value for each physiological response experienced on the path by each participant. The resultant z-scores and p-values show the statistically significant spatial clusters of all participants' high or low physiological responses. A location is determined as a hot spot if the physiological response at that location is high and

the physiological responses at the neighbouring locations are also high. The Getis-Ord G_i^* statistics (Ord and Getis, 1995) is given as

$$G_i^* = \frac{\sum_{j=1}^n w_{i,j} x_j - \bar{X} \sum_{j=1}^n w_{i,j}}{S \sqrt{\frac{[n \sum_{j=1}^n w_{i,j}^2 - (\sum_{j=1}^n w_{i,j})^2]}{n-1}}}, \quad (5.2)$$

where x_j is the attribute value for physiological response j , $w_{i,j}$ is the spatial weight between physiological response i and j , n is equal to the total number of physiological responses and

$$\bar{X} = \frac{\sum_{j=1}^n x_j}{n}, \quad (5.3)$$

$$S = \sqrt{\frac{\sum_{j=1}^n x_j^2}{n} - (\bar{X})^2}. \quad (5.4)$$

5.2.4 Spatiotemporal Analysis

Despite researchers' considerable efforts to advance human-centric sensing, their studies were unable to account for how environmental conditions change over time. Time-dependent environment conditions such as illuminance, temperature, and humidity impact human-environment interaction, thus their physiological response (Huang et al., 2016; Huisman et al., 2012). For instance, a path without street lighting can only be perceived as an environmental barrier during the night. A path may be considered as an environmental barrier during the rainy season when it is flooded or during the winter when it is covered with snow, but this same path may not be a barrier during the summer. This study introduces a space-time pattern mining approach to spatiotemporally aggregate older adults' physiological responses. Discovering such spatiotemporal pattern can be useful to municipal decision-makers and urban planners to monitor, detect, prioritise, and allocate resources to improve neighbourhood walkability and designing of age-friendly cities and communities.

Space-time pattern mining is based on a series of statistical computations for analysing data distributions and identifying patterns within the spatial and temporal context of the data (Zhu and Newsam, 2016). All participants' physiological responses were scaled and aggregated into a space-time cube (STC), as depicted in Figure 5.3. A STC can be pictured as a three-dimensional cube consisting of space-time bins with x and y dimensions (representing the locations of the physiological responses in space) and the t dimension (representing the respective time the physiological response was collected). Each bin in the STC contains a participant's physiological responses at a specific location (x, y) and time (t). A hexagon grid (here, set as 3 m along the path) was used to construct the bins because the circularity of the hexagon makes it more representative of the curves in the path. More importantly, the significance of physiological response at every location will be analysed based on a fixed neighbourhood distance, and the hexagon grid allows more neighbouring physiological responses to be included in the analysis (Birch et al., 2007). The participants' physiological responses were temporally bin at a daily interval for a total of ten days (only ten days of data was collected). Because each bin could span across more than one GPS points and contain multiple physiological responses, the median physiological response was computed to measure the central tendency of the multiple physiological responses in each bin. The median was used because it is less influenced by skewed values; hence a bin with a few extremely high physiological responses will not dominate the aggregated value of that bin.

The emerging hot spot analysis tool in ArcGIS (Esri, 2020a) was used to identify and understand the trends in the STC. First, the spatial clusters (locations with statistically significant high and low physiological responses) are computed using the Getis-Ord G_i^* statistic as already described in equation 5.2. Secondly, the trends in the STC are analysed based on Mann-Kendall trend test. The Mann-Kendall trend test is a nonparametric test used

to analyse data collected over time for consistently increasing or decreasing trends (Hamed, 2009; McLeod, 2005). The Mann-Kendall trend test is conducted on every location as an independent bin time-series test. The test returns a z-score and p-value for each bin time series. The trend analysis examines whether participants' physiological responses are increasing (positive z-score) or decreasing (negative z-score) over time and confirms whether the changes are statistically significant. Finally, the emerging hot spot analysis uses the Mann-Kendall trend test's z-score and p-value for each location and the Getis-Ord G_i^* 's z-score and p-value for each bin to classify each location on the path into several categories of hot spot (Esri, 2020a).

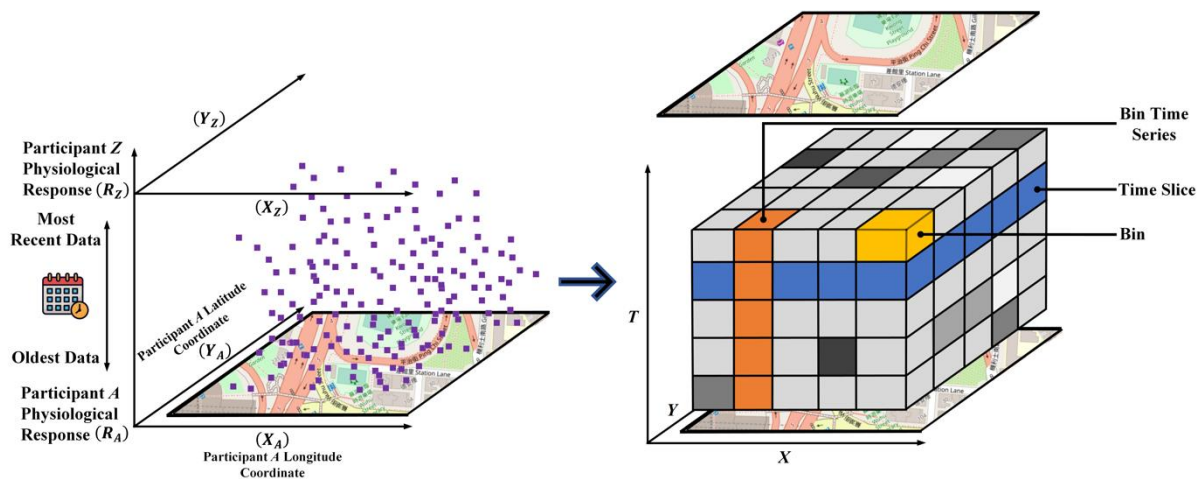


Figure 5.4: Aggregating participants' physiological responses into space-time bins with GPS coordinates (adapted from Esri, 2020a).

5.3 Results

5.3.1 Physiological Reflectors of Human-Environment Stressful Interactions

The data from this study indicate that older adult interaction with the environment results in changes in their physiological responses. Figure 5.4 and Figure 5.5 shows noticeable changes in two participants' HRV measure (i.e., LF/HF) and SCR (i.e., PhasicMax) during the environmental walk on the entire path. Although each participant walked through the same segment along the path, it can be observed that their interaction with path is somewhat different.

For example, participant 3 in Figure 5.4 spent more time in most of the segments than participants 2. Similarly, participant 8 in Figure 5.5 spent less time in each segment compared to participant 5. This is an indication that, the differences in pace, walking behaviour and level of observation influenced how the participants' interacted with the path hence their physiological responses.

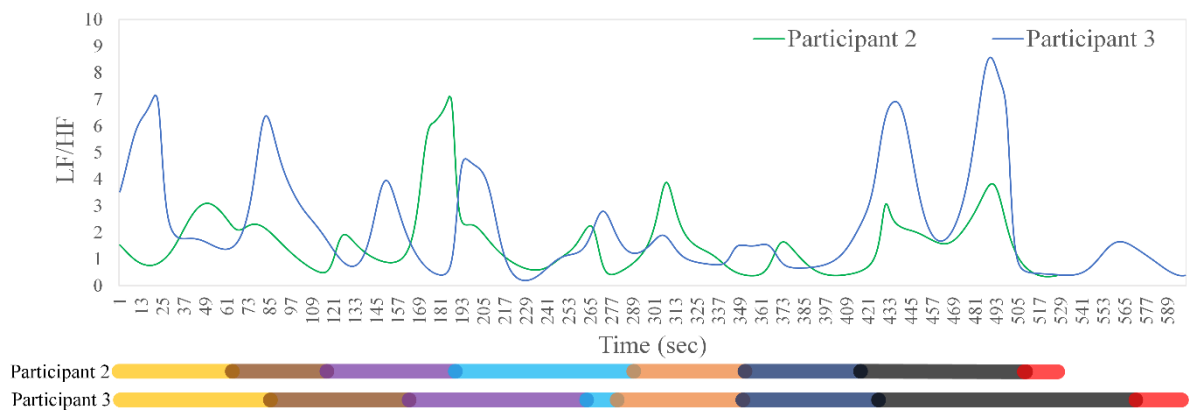


Figure 5.5: The *LF/HF* measure of two participants during the environmental walk on the path.

Note. The coloured stacked bar represents each participant's time to complete each path segment—starting from segment A (yellow bar) to segment H (red bar).

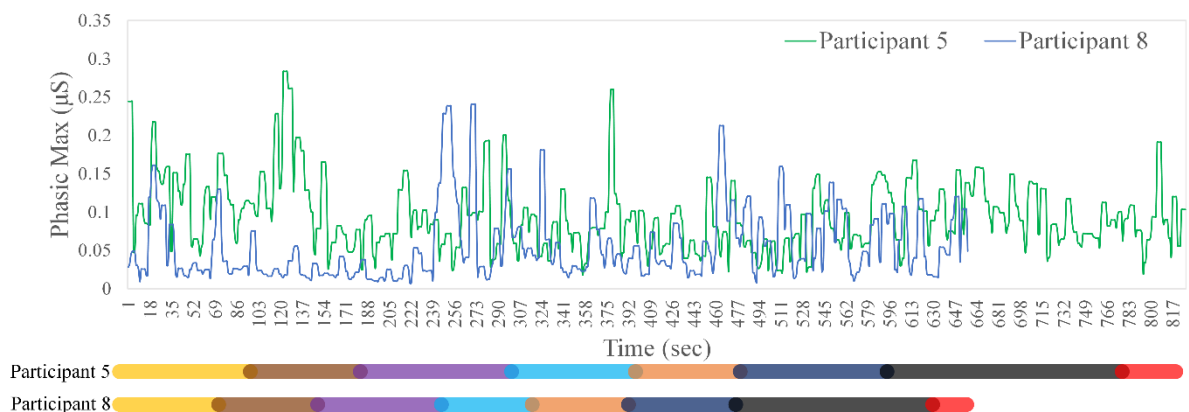


Figure 5.6: The *PhasicMax* measure of two participants during the environmental walk on the path.

Note. The coloured stacked bar represents each participant's time to complete each path segment—starting from segment A (yellow bar) to segment H (red bar).

5.3.2 Statistical Analysis

The results of the Wilcoxon signed-rank test (Table 5.1 and Table 5.2) indicate a statistically significant difference in some of the older adults' physiological responses to environmental conditions perceived as non-stress and environmental conditions perceived as stress. However, there are variations among some of the participants' physiological responses. For instance, participant 3 experienced a statistically significantly higher *LF/HF* response to environmental conditions perceived as stress than environmental conditions perceived as non-stress, whereas participant 6 experienced a statistically significantly lower *LF/HF* response to environmental conditions perceived as stress than environmental conditions perceived as non-stress. Participant 2 experienced a statistically significantly higher PhasicMax response to environmental conditions perceived as stress than environment conditions perceived as non-stress, while Participant 1 experienced a statistically significantly lower PhasicMax response to environmental conditions perceived as stress than environmental conditions perceived as non-stress.

The differences in individual participant's physiological responses to the environmental conditions indicate that there is no specific physiological response that represents an environment's condition; a high or low (*LF/HF* and PhasicMax) response can indicate either stress and/or non-stress environmental condition. Further analyses show that the differences in individual participant's physiological responses can be due to their physical characteristics and gender. Physical characteristics were measured using participant's body mass index [$weight/(height^2)$]. Body mass index (BMI) is a surrogate measure of body fatness and an approximate indicator of health, physical fitness, and activity level (Ding and Jiang, 2020; Prentice and Jebb, 2001; Luppino, 2010; Han et al., 1998). Studies have indicated an inverse relationship between physical activity and body mass index (Hemmingsson and Ekelund, 2007;

Table 5.1: A comparison of *LF/HF* measure in environmental conditions perceived as non-stress and environmental conditions perceived as stress

Participant	Environmental condition	Descriptive statistics		Wilcoxon signed ranks test	
		Mean (SD)	Median	Z	p
1	Non-stress	1.924 (1.301)	1.564	-1.399	.162
	Stress	2.787 (3.164)	1.432		
2	Non-stress	1.938 (0.799)	1.979	-1.248	.212
	Stress	1.537 (1.331)	1.117		
3	Non-stress	2.708 (2.209)	3.870	-2.341	.019*
	Stress	1.964 (1.683)	1.429		
4	Non-stress	2.211 (2.616)	1.132	-2.498	.013*
	Stress	2.479 (1.765)	1.987		
5	Non-stress	1.753 (1.951)	1.027	-2.016	.044*
	Stress	1.990 (2.838)	1.015		
6	Non-stress	2.335 (2.505)	1.254	-2.957	.003*
	Stress	1.984 (2.548)	1.172		
8	Non-stress	6.764 (13.119)	2.027	-0.155	.877
	Stress	4.366 (6.606)	2.212		
9	Non-stress	2.473 (1.600)	2.079	-0.508	.611
	Stress	3.671 (3.920)	2.413		
10	Non-stress	4.768 (6.313)	1.929	-2.326	.020*
	Stress	2.462 (2.562)	1.487		
Collective response	Non-stress	2.997 (5.475)	1.621	-3.862	.000**
	Stress	2.541 (3.370)	1.428		
BMI above 24.9	Non-stress	2.719 (3.475)	1.538	-2.940	.003*
BMI below 24.9		3.386 (7.400)	1.683		
BMI above 24.9	Stress	2.436 (2.730)	1.497	-0.201	.841
BMI below 24.9		2.669 (4.012)	1.340		
Female	Non-stress	3.041 (6.194)	1.673	-3.218	.001*
Male		2.925 (4.006)	1.389		
Female	Stress	2.784 (3.760)	1.544	-1.381	.167
Male		2.108 (2.476)	1.251		

Note. * $p < .05$. ** $p < .001$. SD = standard deviation.

Bassett et al., 2004). According to the Centres for Disease Control and Prevention, an adult with BMI below 18.5 is underweight, BMI between 18.5 and 24.9 is a healthy weight, BMI between 25.0 and 29.9 is overweight, and a BMI of 30.0 and above is obese (CDC, 2021). In a non-stress environmental condition, only the data source from the heart rate (LF/HF) was statistically significant. Participants with a normal or healthy weight (BMI below 24.9) experienced higher LF/HF than overweight participants (BMI above 24.9). In a stress environmental condition, only the data source from the SCR (PhasicMax) was statistically significant. Overweight participants (BMI above 24.9) experienced higher PhasicMax than

Table 5.2: A comparison of PhasicMax measure in environmental conditions perceived as non-stress and environmental conditions perceived as stress

Participant	Environmental condition	Descriptive statistics		Wilcoxon signed ranks test	
		Mean (SD)	Median	Z	p
1	Non-stress	0.990 (0.692)	1.082	-12.035	.000**
	Stress	0.360 (0.420)	0.136		
2	Non-stress	0.277 (0.150)	0.256	-2.694	.007*
	Stress	0.315 (0.204)	0.284		
3	Non-stress	0.547 (0.403)	0.490	-9.712	.000**
	Stress	0.365 (0.258)	0.324		
4	Non-stress	0.130 (0.789)	0.126	-1.376	.169
	Stress	0.117 (0.085)	0.100		
5	Non-stress	0.108 (0.492)	0.997	-2.242	.025*
	Stress	0.091 (0.044)	0.083		
6	Non-stress	0.281 (0.298)	0.166	-1.882	.060
	Stress	0.237 (0.187)	0.177		
8	Non-stress	0.053 (0.036)	0.039	-0.751	.453
	Stress	0.059 (0.052)	0.040		
9	Non-stress	13.316 (7.435)	15.532	-11.035	.000**
	Stress	8.476 (5.741)	6.724		
10	Non-stress	0.335 (0.169)	0.300	-3.588	.000**
	Stress	0.388 (0.175)	0.355		
Collective response	Non-stress	1.730 (4.714)	0.201	-5.665	.000**
	Stress	0.996 (2.966)	0.157		
BMI above 24.9	Non-stress	2.723 (6.031)	0.226	-1.608	.108
BMI below 24.9		0.406 (0.538)	0.158		
BMI above 24.9	Stress	1.635 (0.184)	0.131	-4.958	.000**
BMI below 24.9		0.244 (0.288)			
Female	Non-stress	2.549 (5.759)	0.208	-7.217	.000**
Male		0.312 (0.307)	0.180		
Female	Stress	1.399 (3.617)	0.160	-0.479	.632
Male		0.252 (0.221)	0.153		

Note. * $p < .05$. ** $p < .001$. SD = standard deviation.

participants with a normal or healthy weight (BMI below 24.9). This result could be an indication that a stress environmental condition poses high demand to overweight older adults. The female participants experienced a statistically significantly higher physiological response (both *LF/HF* and PhasicMax) to non-stress environmental conditions than the male participants.

The source of the physiological response (i.e., the related organ) influenced some of the participants' physiological responses. For example, when the data source is from the heart rate

(*LF/HF*) participant 5 experienced a statistically significantly higher physiological response to environmental conditions perceived as stress than environmental conditions perceived as non-stress. Whereas, when the data source is from the SCR (PhasicMax), the same participant (participant 5) experienced a statistically significantly lower physiological response to environmental conditions perceived as stress than environment conditions perceived as non-stress.

Aggregating all participants' physiological responses (collective response) produced a consistent result across the HR and SCR data sources. The result from the collective physiological responses shows that, on average, participants experienced a statistically significant higher physiological response at environmental conditions perceived as non-stress than environmental conditions perceived as stress. A recent study on relatively younger adults reported similar physiological responses from EDA data (skin conductive) (Chrisinger and King, 2018). Chrisinger and King (2018) reported that EDA was higher in environmental conditions with favourable features and lower in environmental conditions with less favourable features.

5.3.3 Spatial Analysis

All participants physiological responses were georeferenced to the corresponding GPS positions (Latitude and Longitude) for the entire path. The null hypothesis of the Getis-Ord General G statistic stipulates that there is no spatial clustering of participants' physiological response. An incremental spatial autocorrelation was conducted to determine the optimum scale of the analysis (Mitchel, 2005). The threshold distance of 11 m was obtained for the *LF/HF* measure. However, no optimal distance could be found for participants' PhasicMax measure; therefore, the scale of analysis was determined based on the average distance to the

K nearest neighbours. K was approximated based on the average nearest neighbours determine for the (*LF/HF*) measure. Using 220 (K) nearest neighbours, a threshold distance of 12.37 m was obtained for the PhasicMax measure. The resulting z-scores of the Getis-Ord General G statistic for the *LF/HF* and PhasicMax measures were 2.595 and 7.890, respectively. There was a less than 1% likelihood that the spatial clustering of participants' physiological responses (both *LF/HF* and PhasicMax measures) could be the result of random chance. The spatial clustering analysis confirms that multiple participants' physiological responses are spatially associated and possess some common characteristics. The result implies that aggregating participants' physiological responses could act as a reliable indicator of an environmental condition.

A hot spot analysis was conducted on the *LF/HF* and PhasicMax measures using a threshold distance of 11 m and 12.37 m to determine the environmental conditions that triggered a common physiological response among multiple participants. The hot spot analysis result for *LF/HF* and PhasicMax measures are presented in Figure 5.6 and Figure 5.7, respectively. The hot spots are locations on the path with statistically significant high physiological response value clusters. The cold spots are locations on the path with statistically significant low physiological response value clusters. Note that the result from the Wilcoxon signed-rank test indicated that participant experienced high physiological responses (corresponding to hot spots) in environmental conditions perceived as non-stress and low physiological responses (corresponding to cold spots) in environmental conditions perceived as stress. A total of 1105 and 2178 samples from the *LF/HF* measure were determined as a hot spot and cold spot, respectively, at a 95% confidence level. A total of 1529 and 2184 samples from the PhasicMax measure were determined as a hot spot and cold spot, respectively, at a 95% confidence level.

In other words, these hot and cold spots were the results of older adults' physiological responses to the environmental conditions (spatial factors) at a 95% confidence level.

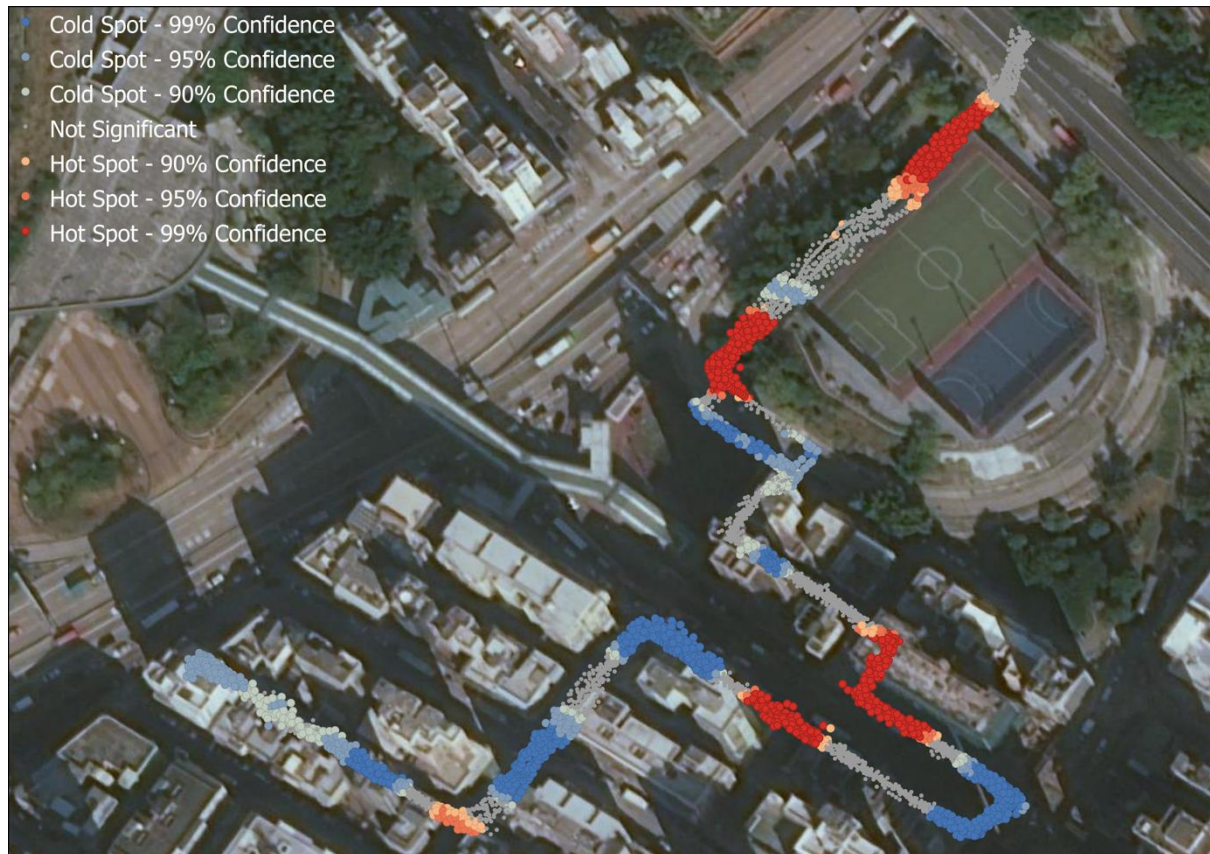


Figure 5.7: Spatial clusters of collective physiological responses based on LF/HF measure. *Note.* The hot spots are locations on the path where multiple participants experienced statistically significant high values of LF/HF . The cold spots are locations on the path where multiple participants experienced statistically significant low values of LF/HF . Note that high values of LF/HF correspond to environmental conditions perceived as non-stress and low values of LF/HF correspond to environmental conditions perceived as stress. Basemap data copyrighted Esri, Maxar, GeoEye, Earthstar Geographics, CNES/Airbus DS, USDA, USGS, AeroGRID, IGN, and the GIS User Community.

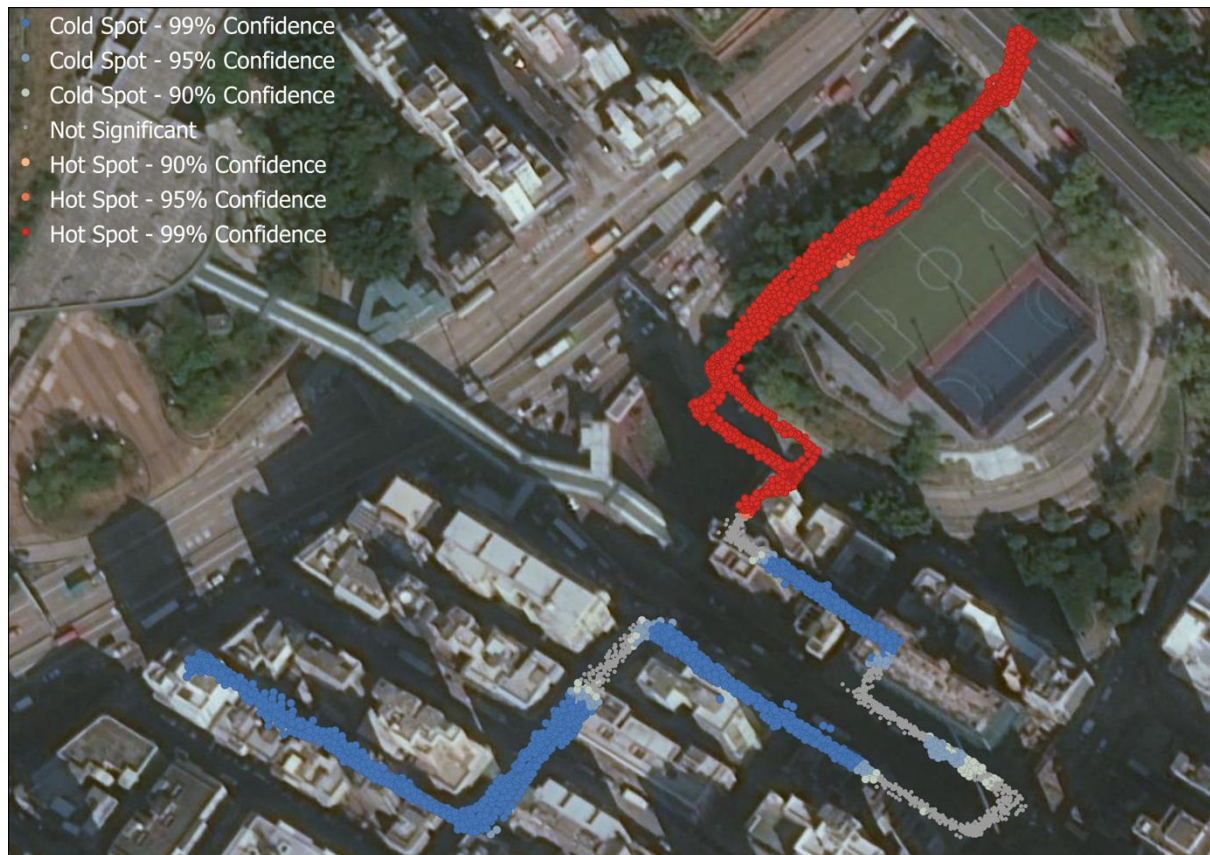


Figure 5.8: Spatial clusters of collective physiological responses based on PhasicMax measure.

Note. The hot spots are locations on the path where multiple participants experienced statistically significant high values of PhasicMax. The cold spots are locations on the path where multiple participants experienced statistically significant low values of PhasicMax. Note that high values of PhasicMax correspond to environmental conditions perceived as non-stress and low values of PhasicMax correspond to environmental conditions perceived as stress. Basemap data copyrighted Esri, Maxar, GeoEye, Earthstar Geographics, CNES/Airbus DS, USDA, USGS, AeroGRID, IGN, and the GIS User Community.

5.3.4 Spatiotemporal Analysis

Because the field data collection was conducted for only ten days and some of the participant's physiological responses were corrupted or abnormal, this study only demonstrated the effectiveness of the space-time pattern mining using the *LF/HF* measure. The result of the space-time pattern mining based on *LF/HF* measure with a threshold distance of 11 m and a time interval of one day is presented in Figure 5.8. Several clusters of high physiological responses (hot spot) and low physiological responses (cold spot) were detected on the path. These hot and cold spot locations on the path are furthered categorised based on their

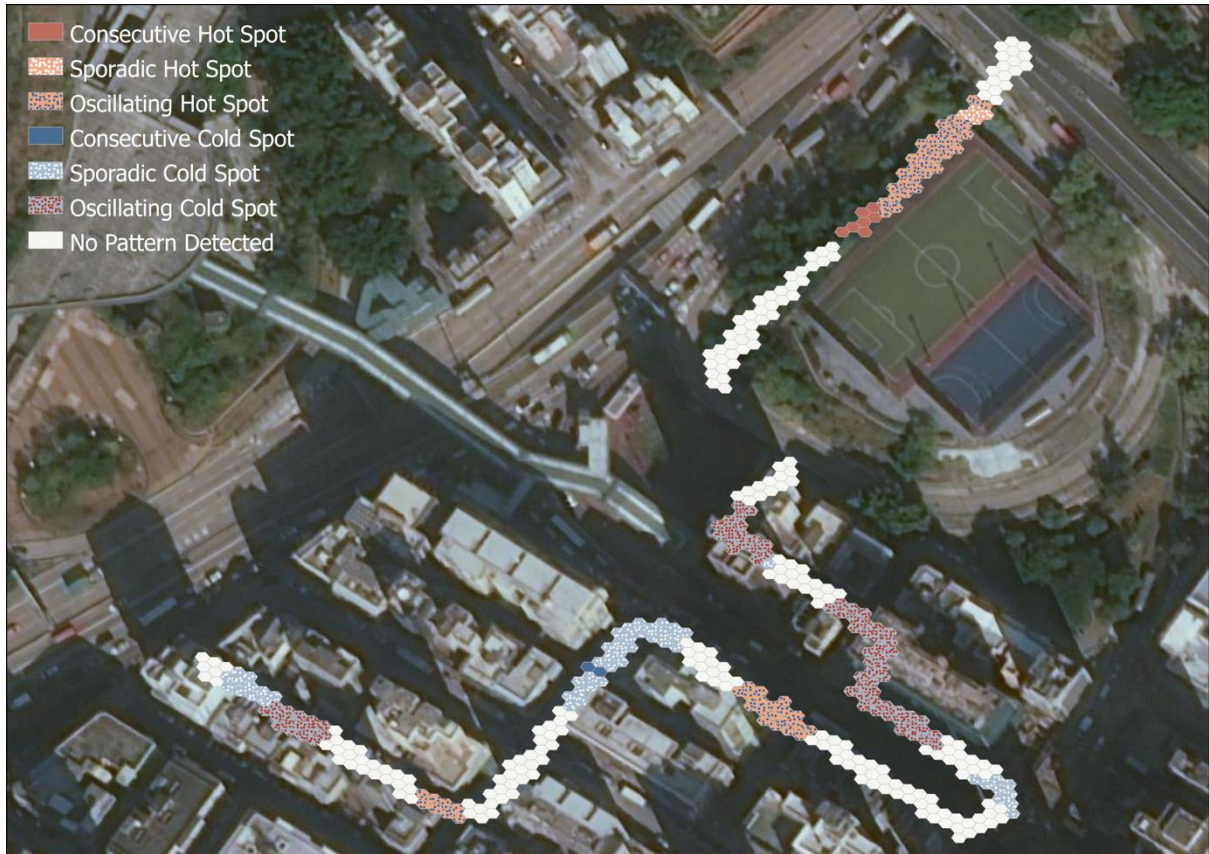


Figure 5.9: Spatiotemporal clusters of collective physiological responses based on LF/HF measure.

Note. The hot and cold spot locations on the path are furthered categorised based on their occurrence over time. Note that high values of LF/HF correspond to environmental conditions perceived as non-stress and low values of LF/HF correspond to environmental conditions perceived as stress. Basemap data copyrighted Esri, Maxar, GeoEye, Earthstar Geographics, CNES/Airbus DS, USDA, USGS, AeroGRID, IGN, and the GIS User Community.

occurrence over time. A consecutive hot (or cold) spot is a location with a single uninterrupted run of statistically significant hot (or cold) spot bins in the final time-step intervals. A sporadic hot (or cold) spot is a location that is an on-again then off-again hot (or cold) spot. An oscillating hot (or cold) spot is a statistically significant hot (or cold) spot for the final time-step interval that has a history of also being a statistically significant cold (or hot) spot during a prior time step. A consecutive hot (or cold) spot is a location with a single uninterrupted run of statistically significant hot (or cold) spot bins in the final time-step intervals. There were seven consecutive hot spots, four sporadic hot spots, 59 oscillating hot spots, two consecutive

cold spots, 51 sporadic cold spots, 75 oscillating cold spot, and 217 spots with no pattern detected on the path.

5.4 Discussion

5.4.1 A Comparison of Older Adults' Physiological-Environmental Interactions, Older Adults' Perceived Stress Assessments, and Observers' Path Audit

The older adults' physiological-environmental interactions were compared with the older adults' perceived stress assessments and the observers' audits of the path condition to confirm how well the elderly-centric sensing can represent the older adults' interaction with the built environment. A comparison of perceived stress, observers' path audit, and detected hot and cold spots on the path is presented in Figure 5.9.

Segment A (an alley with several path obstructions) was perceived as stress by the participants. Segment A's environmental condition was rated as poor by the observers, and segment A was detected as a statistically significant cold spot, corresponding to physiological stress. The results across the three different assessment approaches confirm one another. The PhasicMax measure provided a more accurate representation of this segment with a higher confidence level than the *LF/HF* measure. The participants perceived segment B (a wide street) as non-stress. The observers rated it as moderate, and half of segment B was detected as a statistically significant cold spot, corresponding to physiological stress. Participants had to cross a street road in segment B; this street road has vehicles parked along its shoulders. The anticipation of an approaching vehicle while crossing the road and having their field of view limited by the parked vehicles could have resulted in physiological stress. Because this occurrence is time-dependent, it could easily be missed during the path audit or while the participant reported their perceived stress. A review of the spatiotemporal analysis indicates a sporadic cold spot for

parts of segment B immediately after the crossing, implying that the older adults experienced physiological stress on some days and were not stress on other days.

Segment C was perceived as stress, the environmental condition at segment C was rated as moderate, and parts of segment C was detected as a statistically significant cold spot (physiological stress) and hot spot (non-physiological stress) based on the *LF/HF* measure and cold spot (physiological stress) based on PhasicMax measure. Segment D was perceived as stress by the participants, rated as good by the observers and was only detected as a significant cold spot (physiological stress) based on the *LF/HF* measure. Segment D is a crosswalk with traffic signals. Although the crosswalk was rated as good, it was perceived as stress and experienced as physiological stress. A plausible explanation for such responses could be the waiting time at the traffic light, which was about 68 seconds. The spatiotemporal analysis further indicates a sporadic cold spot on the crosswalk, suggesting that the participants were stressed on the days with longer waiting time for the traffic signal to turn green and non-stressed on the days the waiting time is shorter. This is another time-dependent occurrence that was not captured in the observers' path audit.

The participants perceived segment E (an on-going construction site) and segment F (an alley with path obstructions) as stress, and the observers' rated it as poor. Segment E and F were detected as a statistically significant (95% confidence level) physiological stress spot by the PhasicMax measure. It was observed that all the segments that were perceived as stress and rated as poor only resulted in physiological stress when the data source is from the SCR (PhasicMax) with a 95% confidence level. Physiological data sourced from the heart rate (*LF/HF*) mostly misclassify such segments or detected them with a 90% confidence level.

This indicates that segments rated as poor conditions have more pronounced effects on older adults' SCR than heart rate measures.

Physiological data sourced from the heart rate (*LF/HF*) is more indicative of the path conditions perceived as high stress or low stress than the data source is from the SCR (PhasicMax). For instance, segment G (a green space) was perceived as non-stress by the participants, the environmental condition of segment A was rated as good by the observers. Segment H (subway with graffiti) was perceived as high-stress and rated as moderate. Both heart rate and SCR data sources detected segment G as non-stress, consistent with the perceived and path audit assessments. However, only the heart rate (*LF/HF*) measure was able to detect segment H as stress at a 90% confidence level.

Overall, the older adults' perceived assessment of the path, the observers' path audit and the assessment based on physiological responses confirm one another more than they contradict. These contradictions are expected because all of these assessment methods have inherent limitations. For instance, the older adults' perceived assessment is subjective; they could rate the mere presence of a gas station as stressful with a high-intensity rating, although the gas station may not distress the older adult. Although the observers' path audit is objective, they cannot adequately distinguish between an environmental condition that is stressful for a person and not stress for another person. Therefore, it is expected that the perceived, objective, and physiological response based assessments should have some contradictions. Despite the contradictions, these methods can complement one another and improve the assessment of the built environment for older adults.

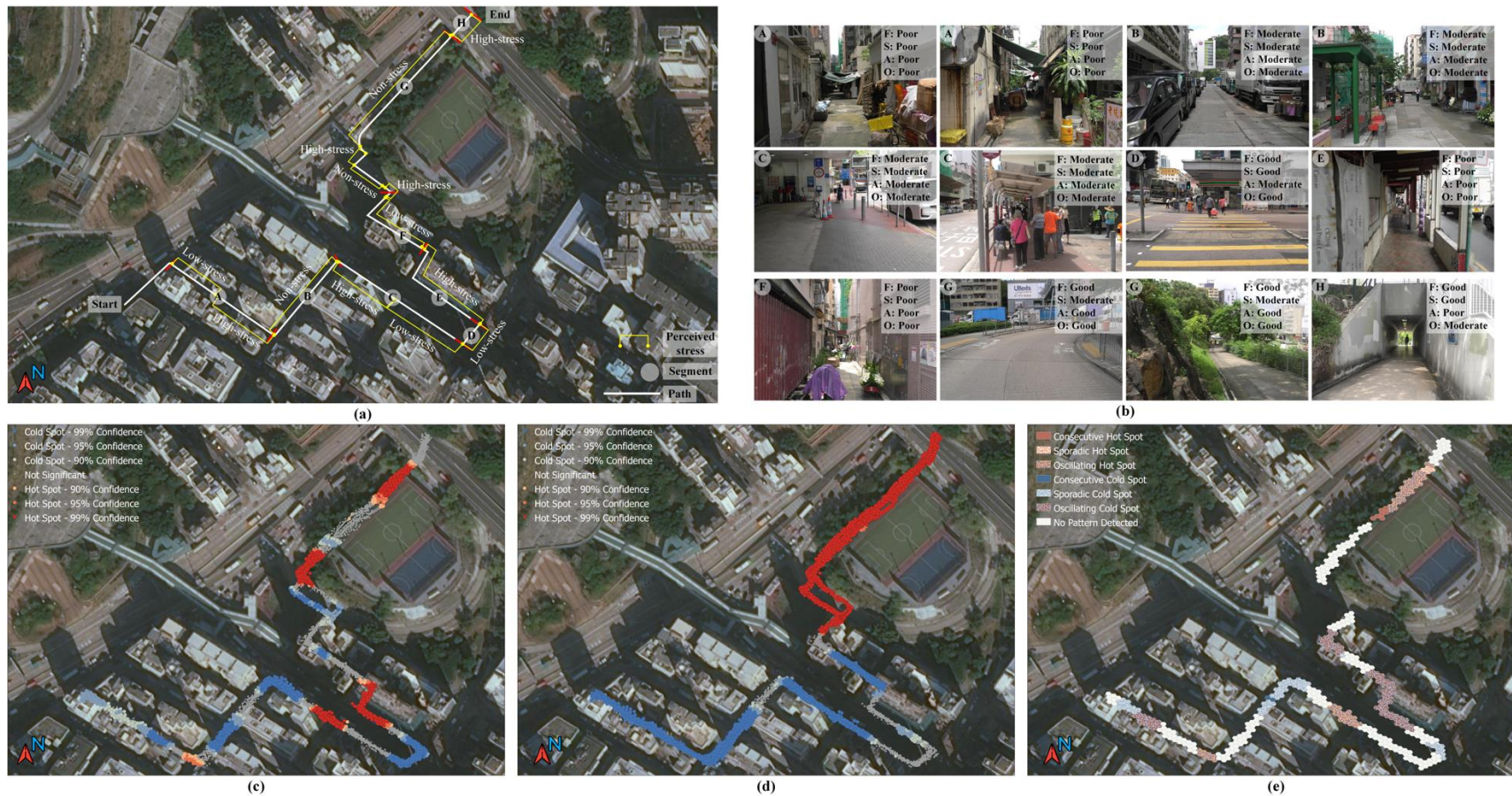


Figure 5.10: Comparison of perceived stress, observers' path audit, and detected hot and cold spots on the path.

Note. (a) Perceived stress and non-stress locations reported by participants. (b) Path audit by observers. The environmental condition was rated as poor, moderate or good. F = Rating for functionality; S = Rating for safety; A = Rating for aesthetics; O = Overall rating of path segment. (c) Spatial clusters of physiological responses based on LF/HF measure. (d) Spatial clusters of physiological responses based on PhasicMax measure. (e) Spatiotemporal clusters of physiological responses based on LF/HF measure. Basemap data copyrighted Esri, Maxar, GeoEye, Earthstar Geographics, CNES/Airbus DS, USDA, USGS, AeroGRID, IGN, and the GIS User Community. Photographs by author.

5.4.2 Collective Sensing can Address Individual Variability

This study shows that the relationships between older adults' physiological response and the environmental condition are less apparent at the individual level. An individual's pace, walking behaviour, level of observation, physical characteristics and gender influenced their physiological responses to stress and non-stress environmental conditions. The physiological response data source (i.e., the related organ) and time-dependent environmental factors also contributed to the variability in older adults physiological responses. The variability in older adults' physiological response is what motivated this study. Assuming there was no individual variability (which will be the case when sensors are attached to mobility aids), an environment's condition can be determined by using the intensity of older adults' physiological response. Using the intensity of older adults' physiological responses to represent older adult's environment interaction would be misleading in this study. This study shows that using collective sensing (aggregating multiple participants' physiological responses) can accommodate the individual variability and capture any normality in the data, which is indicative of an environment's condition.

5.5 Chapter Summary

This chapter aimed to achieve research objective two: to examine the relationships in older adult's bodily responses resulting from their interaction with the environment. This objective was achieved using statistical analysis (Wilcoxon signed-rank test), spatial clustering analysis (Getis-Ord General G statistic and Getis-Ord G_i^* statistics), and space-time pattern mining. The results show that the relationships between older adults' physiological response and the environmental condition are less apparent at the individual level. An individual's pace, walking behaviour, level of observation, physical characteristics, gender, data source (i.e., the related organ) and time-dependent environmental factors influenced their physiological responses to

stress and non-stress environmental conditions. However, using collective sensing (aggregating multiple participants' physiological responses) can accommodate the individual variability and capture any normality in the data, which is indicative of an environment's condition. The collective physiological responses are consistent with the older adults' perceived assessment and the observers' audit of the environment's condition. Current advances in machine learning intelligence will be harness in the next chapter to develop and test a more efficient approach to detecting older adults' stressful interaction with the built environment.

CHAPTER 6

AN OPTIMISED ENVIRONMENTAL STRESS DETECTION FRAMEWORK BASED ON MACHINE LEARNING INTELLIGENCE⁶

6.1 Introduction

It is clear from Chapter 5 that older adults' collective physiological responses to the environment are spatially and temporally associated and possess some common characteristics indicative of stress and non-stress environmental conditions. Now this chapter turns to the task of optimising the current stress detection approach. This will lead to achieving research objective three: to detect older adults' stressful environmental interactions in near-real time.

The Geographic Information System (GIS)-based hot and cold spot analysis presented in Chapter 5 has shown the potential to distinguish between stress and non-stress environmental conditions. Despite such potential, the GIS-based approach cannot maximise the full potential of representing peoples' interaction with the environment using their physiological responses. For instance, the GIS-based approach presented in Chapter 5 could only represent human-

⁶ This chapter is based on a study that is currently under consideration for publication.

Torku, A., Chan, A.P.C., Yung, E.H.K., Seo, J. (2021). Learning to detect older adults' environmental stress hotspots to improve neighbourhood mobility: A multimodal physiological sensing, machine learning and risk hotspot analysis-based approach, *Cities* (Under Review). JCIT-D-21-01443

environment interaction with one physiological feature. As established in Chapter 4, relying on only one physiological feature or modality might not be informative enough when it comes to understanding stressful human-environment interactions in ambulatory, real-world setting. Therefore, there is a need to develop a computational approach for representing human-environment interaction using an optimum set of informative physiological features.

In this chapter, several machine learning algorithms were trained on an optimum set of informative physiological features, environmental data, and user-perceived stress response. The algorithms were trained and tested to detect (1) stress and non-stress human-environment interactions and (2) low-stress and high-stress human-environment interactions. The detected stressful interactions were visualised using kernel density estimation. A simulation-based statistical power estimation was used to examine areas within the study area that are sufficiently powered to detect stress hot spot that pose more higher risk to the older adults. An overview of the optimised environmental stress detection framework is depicted in Figure 6.1.

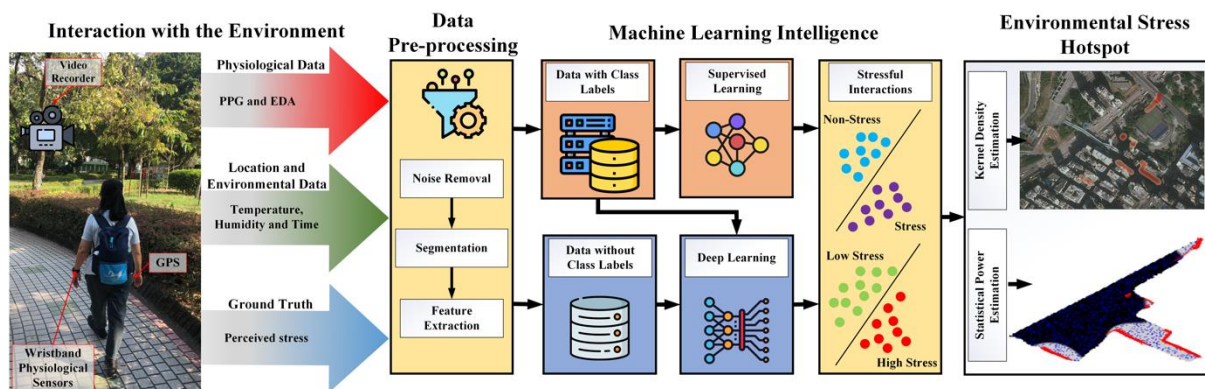


Figure 6.1: Optimised environmental stress detection framework.

6.2 Optimised Stress Detection Framework

6.2.1 The Optimum Set of Informative Features

The data collection, pre-processing, and feature extraction are explained in Chapter 3 and Chapter 4. The following features were extracted in addition to the physiological features that were extracted in Chapter 4: (1) the time a participant was present at a location on the path, (2) the environment temperature, and (3) the environment humidity for consideration in the selection of the optimum set of informative features. These environmental and location features were added because previous studies have confirmed that environment weather affects mood (Taylor et al., 2017; Li et al., 2014). The optimum set of informative features were identified using the information mining model developed in Chapter 4. However, because the focus here is on a specific type of human-environment interaction (i.e., human interaction with stress and non-stress environmental conditions), older adults' perceived stress assessment of the environmental conditions was used as class labels. The optimum feature set was constrained to include at least one feature from each data source (i.e., HRV data, EDA data, location, and environmental data). This approach was adopted to improve the diversity and generalisation of the stress detection framework. The next section provides more details about how data from different sources was harnessed to improve diversity and generalisation.

6.2.2 Multimodal Sensing and Fusion

Information about stressful human-environment interaction can be acquired among others from different types of sensors, at different conditions, in multiple participants or experiments. Each acquisition framework is termed a modality and is associated with one data set. A complete setup of the framework making use of multiple modalities for each data set to interact and inform each other is termed multimodal (Lahat et al., 2015; Alberdi et al., 2016). Multimodal fusion is a well-established technique. Its effectiveness is demonstrated by minimising the

effects of incorrect data acquisition and providing complementary data (collective knowledge) that enhance the diversity of the system. Diversity helps improve the reliability, accuracy, robustness, uniqueness and generalisation of the system (Lahat et al., 2015).

Multimodal information can be fused at three main hierarchical levels: signal level (raw) data fusion, feature level fusion and decision level fusion (King et al., 2017; Hall and Llinas, 1997). Signal level fusion is applied to data measuring the same signal property (commensurate data) directly. Feature level fusion is applied to combine data measuring separate signal properties (non-commensurate data). Decision level fusion is implemented at the highest level of abstraction from sensor data, and it is more appropriate when modalities have differences in time scale (King et al., 2017; Nweke et al., 2019). In this study, three different modalities (i.e., HRV data, EDA data, location, and environmental data) are measured to represent stressful human-environment interaction. Feature level fusion strategy is the most appropriate for this study because the HRV data, EDA data, location, and environmental data measure different signal properties. In this case, features extracted from sensor data are used to form a feature vector and combined using parametric or non-parametric machine learning algorithms to discriminate and represent the data into higher abstractions (King et al., 2017; Nweke et al., 2019).

6.2.3 Machine Learning Algorithms

Different supervised learning algorithms, including Decision Tree, Gaussian Support Vector Machine (SVM), k-Nearest Neighbour (kNN), and Ensemble bagged tree were employed in this study. Other supervised learning algorithms with different similarity functions were explored in this study, but their performance was poor and was not pursued further. Additionally, a deep learning algorithm using a deep belief network was trained and tested.

Supervised Learning

Decision Tree is a non-parametric supervised learning method used for classification and regression. It is a tree-like classification process that classifies a data set into a subdivision based on the decision framework defined by the tree (Friedl and Brodley, 1997).

SVM is a machine learning technique that performs classification by constructing a hyperplane that best split the data into two classes (Guenther and Schonlau, 2016). Aside from linear classification, SVM efficiently performs non-linear classification using kernel functions to map inputs into high-dimensional feature spaces.

kNN is a non-parametric learning algorithm that classifies an unseen pattern based on its nearest neighbours in a database. It involves assigning an unclassified dataset or unknown pattern to the class represented by most of its k nearest neighbours (Denoeux, 1995).

Ensemble methods combine multiple decision trees (but not exclusively) to improve generalisation and predictive performance (Myles et al., 2004). Bagging or bootstrap aggregating is a popular ensemble technique; it is generally appropriate for unstable classifiers such as decision trees (Dietterich, 2000). In bagging, a series of decision trees are trained, each based on a different bootstrap sampling of the training sample. Each bootstrap sample is chosen randomly with replacement from the training sample. The individual prediction of the decision tree models is combined by voting; the class with the most vote is selected (Myles et al., 2004; Dietterich, 2000).

Deep Learning: Deep Belief Network

Recently, automatic discovery of representative features through deep learning methods has been successfully used to analyse physiological signals in multiple modalities for several detection and prediction tasks (Hassan et al., 2019). A deep belief network (DBN) was trained to detect stress and high-stress samples in this study. Deep belief networks are probabilistic generative neural network models with multiple layers of hidden explanatory factor with a greedy layer-wise unsupervised learning algorithm. DBN only needs small, labelled data which is important for real-world applications (Le Roux and Bengio, 2008; Långkvist et al., 2014).

6.2.4 Validation

In this study, both supervised and unsupervised machine learning classification algorithms were trained and tested to detect: (1) stress and non-stress samples from the collected data; and (2) low-stress and high-stress samples from the stress samples. Three performance indicators were computed for each classification algorithms: accuracy, precision, and recall. The definitions of the indicators are given below:

$$Accuracy = \frac{TP + TN}{TP + FP + FN + TN} \quad (6.1)$$

$$Precision = \frac{TP}{TP + FP} \quad (6.2)$$

$$Recall = \frac{TP}{TP + FN} \quad (6.3)$$

where TP represent true positive, FP represent false positive, FN represent false negative and TN represent true negative. The trained algorithm with the highest accuracy, precision and recall was used for stress detection.

6.2.5 Visualisation of Detected Stress Samples

The detected stress samples for each participant were associated with the corresponding GPS positions (Latitude and Longitude) for the entire path. A weighted kernel density estimation (KDE) was computed to visualise locations with clusters of stress samples. KDE is a non-parametric means of computing the probability density function of a random variable in feature space (Scott, 2015; Gisbert, 2003). KDE is appropriate for the study because the detected stress samples do not follow any formal or theoretically known probability distribution. The KDE was computed based on the Esri proposed formula (Esri, 2020b). The kernel density for a (x, y) location was predicted using

$$Density = \frac{1}{(radius)^2} \sum_{i=1}^n \left[\frac{3}{\pi} \cdot pop_i \left(1 - \left(\frac{dist_i}{radius} \right)^2 \right)^2 \right] \quad (6.4)$$

For $dist_i < radius$

where $i = 1, \dots, n$ are the inputs points within the radius distance of the (x, y) location, pop_i is the population field value of point i , $dist_i$ is the distance between point i and the (x, y) location. The calculated density is then multiplied by the sum of the population field. The search radius was determined as (Esri, 2020b)

$$Search\ Radius = 0.9 \times \min \left(SD_w, \sqrt{\frac{1}{\ln(2)}} \times D_m \right) \times n^{-0.2} \quad (6.5)$$

where D_m is the weighted median distance from the weighted mean centre, n is the sum of the population field values, SD_w is the weighted standard distance.

6.2.6 Identifying Spatial Clusters of Risk Stress Hot spot

A neighbourhood with significant built environment infrastructure approaching their design life is more likely to have several environmental stress hot spots for older adults. Given the limited resources available to most cities and communities, it will be more beneficial to identify

the stress hot spot that pose higher risk to the older adults. Such stress hot spot can be prioritised and alleviated to improve neighbourhood mobility for older adults.

Spatial relative risk (SRR) is a well-understood concept and has been applied in spatial epidemiology to determine where spatial clustering is likely occurring (Buller et al., 2021; Waller and Gotway, 2004; Lawson, 2013). The essential attribute of the SRR is its ability to estimate ratios of risks from two sample groups (e.g., case and control groups) without having access to their population denominators (Bithell, 1991). The estimator of SRR is a ratio of two kernel-estimated density functions of two distinct samples of point locations defined on a common spatial window (Bithell, 1991; Davies et al., 2018). Based on the definition of SRR, this study defined SRR stress hot spot as the ratio of kernel density estimates of stress samples and non-stress samples of point locations in a common study area (e.g., a neighbourhood). The statistical power (Buller et al., 2021) of the SRR stress hot spot was computed to assess the probability of a stress hot spot occurring within a study area. This study applied Buller et al.'s (2021) procedure to estimate the statistical power of the SRR stress hot spot as follows.

The focus here is the locations where clusters of SRR high-stress hot spot is likely occurring. The detected high-stress samples (i.e., the case) and control samples (i.e., non-stress and low-stress samples) for each participant were associated with the corresponding GPS positions (Latitude and Longitude) for the entire path. Based on the case and control samples of point locations within the study window, simulated point locations were randomly generated (assuming complete spatial randomness) to reflect the expected study design at a resolution of (128 × 128 grid). The simulation-based approach was adopted to ensure realistic study power analyses (Buller et al., 2021; Ensor et al., 2018). The bandwidth calculation was based on the maximal smoothing principle (Terrell, 1990). The SRR function (Davies et al., 2018)—

originally developed to study the spatial variation of larynx and lung cancer in the UK (Kelsall and Diggle, 1995; Bithell, 1990)—has been successfully employed to detect local clustering in many spatial analyses (Buller et al., 2021; Wheeler, 2007; Fernando and Hazelton, 2014). The SRR function was used to estimate the SRR high-stress hot spot for each grid cell within the simulated data area. The statistical significance of the spatial clustering of each grid cell was tested—the alpha level was set to 0.05. These steps were repeated for 10,000 iterations (recommended for power calculation [Buller et al., 2021]). The statistical power (power threshold of 0.8) of the SRR high-stress hot spot at each grid cell was calculated as the proportion of rejected null hypotheses from the simulated 10,000 iterations.

6.3 Results

6.3.1 The Optimum Set of Informative Features

The optimum set of informative feature contains 12 features, which are listed in Table 6.1. The optimum set of the informative feature includes eight features sourced from the heart rate, three features sourced from EDA and one feature sourced from the location and environment data.

6.3.2 Performance of the Machine Learning Algorithms

The distribution of the collected data across the class samples were unequal [(3691 samples were labelled as stress while 1827 samples were labelled as non-stress), (1938 samples were labelled as low-stress while 1753 samples were labelled as high-stress)]. To avoid an imbalance classification, the majority class was randomly under-sampled to make the classes have equal distribution. The under-sampling was repeated 20 times, resulting in 20 random train/test splits of the equally distributed data. 10-fold cross-validation was conducted to evaluate the performance of the machine learning algorithms. The average performance indicators of each machine learning algorithm over the 20 random train/test split data were computed.

Table 6.1: Optimum set of informative features for stress detection

Modality	Feature	Description [unit]
HRV data	HR	Instantaneous heart rate values [1/min]
	Mean RR	The mean of RR intervals [ms]
	Min HR	Minimum heart rate computed using five beat moving average [1/min]
	Max HR	Maximum heart rate computed using five beat moving average [1/min]
	Peak frequency HF	High frequency (HF) (0.15 – 0.4 Hz) band peak frequency [Hz]
	Absolute power LF (log)	Natural logarithm transformed value of absolute power of low frequency (LF) (0.04 – 0.15 Hz) band [log]
	Normalised power HF (n.u.)	Power of high frequency (HF) (0.15 – 0.4 Hz) band in normalised unit [n.u.]
	Total power	Total spectral power [ms ²]
	EDA data	PhasicMax
Tonic		Mean tonic activity within response window of decomposed tonic component
Global Mean		Mean skin conductance (SC) value within response window
Location and environmental data	Time	Time of day [Unix time]

Table 6.2: Performance of the machine learning algorithms

Task	Algorithm	20 trains average score		
		Accuracy (%)	Precision (%)	Recall (%)
Detecting non-stress and stress samples	Decision tree	92.16	93.36	90.77
	Gaussian SVM	95.47	94.31	96.79
	kNN	95.96	96.00	95.90
	Ensemble bagged tree	98.13	98.59	97.65
	DBN	83.38	82.58	84.61
Detecting low and high-stress samples	Decision tree	89.45	90.61	88.56
	Gaussian SVM	95.94	96.83	95.14
	kNN	96.54	97.26	95.87
	Ensemble bagged tree	98.25	98.30	98.20
	DBN	73.76	75.01	74.08

The stress detection performance of the algorithms deployed in this study is summarised in Table 6.2. The result indicates that the Ensemble bagged tree algorithm outperformed the other algorithms, achieving a classification accuracy of 98.13% (for detecting stress and non-stress

samples) and 98.25% (for detecting low and high-stress samples). The confusion matrix of the best performance Ensemble bagged tree algorithm among the 20 random train/test splits data is depicted in Figure 6.2.

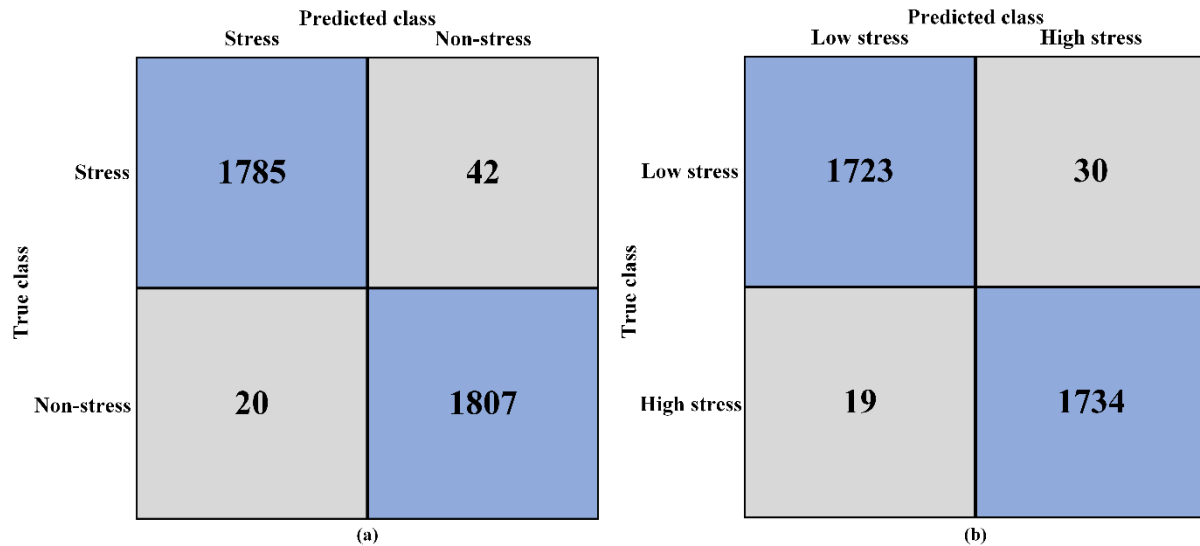


Figure 6.2: Confusion matrix of the best performance Ensemble bagged tree algorithm for (a) detecting non-stress and stress samples; (b) detecting low and high-stress samples.

6.3.3 Visualisation of Detected Stress Samples

Given the impressive performance of the Ensemble bagged tree algorithm, the best performance Ensemble bagged tree algorithm (the confusion matrix is depicted in Figure 6.2) was deployed to classify each of the participant’s collected data into (1) non-stress and stress; and (2) low-stress and high-stress. The deployed algorithm detected 66.35% of stress samples and 26.73% of high-stress samples from all participants data. The detection result for each participant is shown in Table 6.3. The detected stress samples and high-stress samples for all participants were geographically referenced with their corresponding GPS coordinates. The resulting density distribution of the stress hot spot and high-stress hot spot locations along the path is shown in Figure 6.3 alongside the perceived stress assessment provided by older adults’

and observers' path audit. Overall, the detected stress and high-stress samples matched older adults perceived stress assessment of the path.

Table 6.3: Classification of participant's interaction with the environment into (1) non-stress and stress; and (2) low-stress and high-stress samples based on Ensemble bagged tree algorithm

Participant	Total sample	Detected stress and non-stress samples		Detected low and high-stress samples	
		Non-stress samples	Stress samples	Low-stress samples	High-stress samples
1	700	210	490	270	220
2	527	142	385	241	144
3	599	208	391	187	204
4	535	198	337	170	167
5	827	264	563	563	0
6	596	220	376	199	177
8	657	211	446	220	226
9	537	206	331	164	167
10	540	198	342	172	170

6.3.4 Spatial Relative Risk Stress Hot spot

The detected high-stress samples (i.e., the case) and control samples (i.e., non-stress and low-stress samples) for all participants were geographically referenced with their corresponding GPS coordinates. The first iteration of the simulated randomly generated point-level physiological data is shown in Figure 6.4. The proportion of simulation significant SRR high-stress hot spot clusters for the 10,000 iterations is presented in Figure 6.5(a). The areas within the study area that are sufficiently powered to detect spatial clustering of a high-stress hot spot are shown in Figure 6.5(b). These results demonstrate that the path for the environmental walk has some real spatial clusters of high-stress hot spots.



Figure 6.3: (a) Detected stress hot spot locations. (b) Detected high-stress hot spot locations. (c) Perceived stress and non-stress assessment by participants. (d) Path audit by observers. The environmental condition was rated as poor, moderate or good. F = Rating for functionality; S = Rating for safety; A = Rating for aesthetics; O = Overall rating of path segment.

Note. Basemap data copyrighted Esri, DigitalGlobe, GeoEye, Earthstar Geographics, CNES/Air bus DS, USDA, USGS, AeroGRID, IGN, and the GIS User Community. Photographs by author.

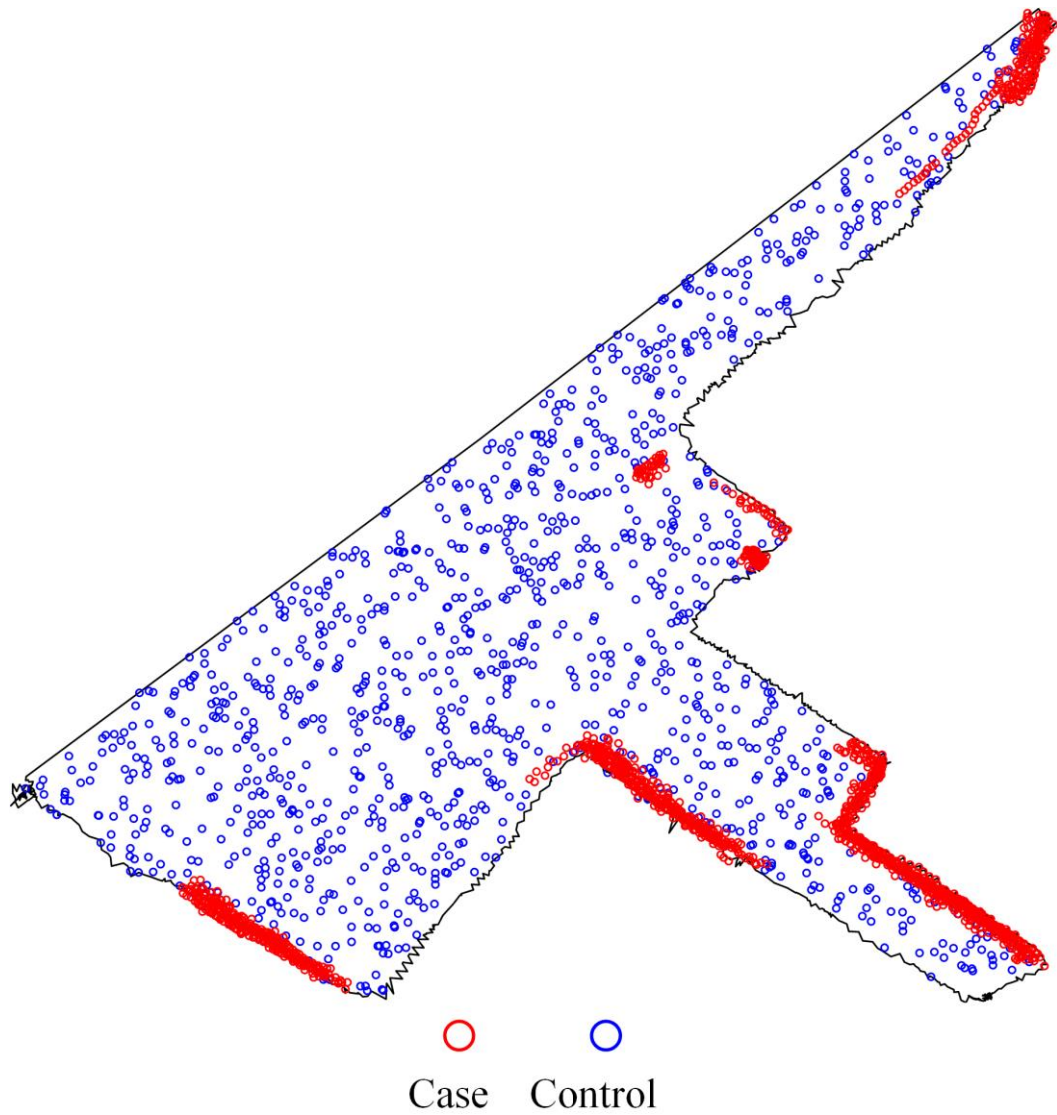


Figure 6.4: First iteration of simulated randomly generated point-level physiological data assuming complete spatial randomness.
Note. Simulated case (i.e., high-stress samples) locations are red-coloured circles and simulated control (i.e., non-stress and low-stress samples) locations are blue-coloured circles.

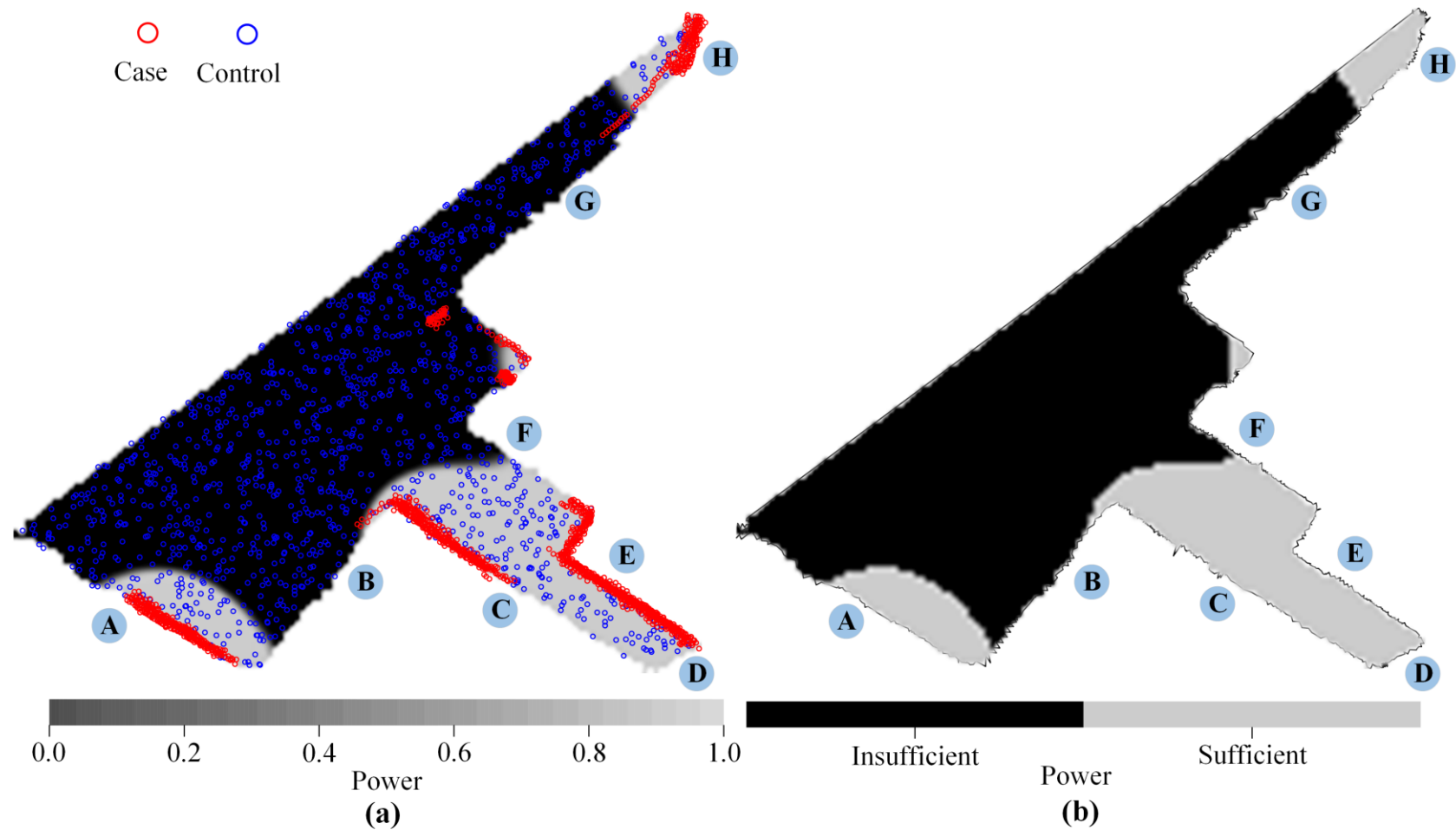


Figure 6.5: Clusters of SRR high-stress hot spot within study area (i.e., path segment A to H). (a) Proportion of simulation significant SRR high-stress hot spot clusters for the simulated 10,000 iterations. (b) Areas within the study area that are sufficiently powered to detect spatial clustering of a high-stress hot spot.

Note. Simulated case (i.e., high-stress samples) locations are red-coloured circles and simulated control (i.e., non-stress and low-stress samples) locations are blue-coloured circles.

6.3.5 Examination of Spatial Clusters of Risk Stress Hot spot

Upon examining the risk stress hot spot locations, the authors identified some environmental barriers relating to the functionality, safety, and aesthetics of the path conditions (Figure 6.6 and Figure 6.7). Environmental barriers A1, S1, and F1, were identified in risk stress hot spot 1. The authors found that the risk stress hot spot 1 was mainly caused by a restaurant. Old gas cylinders, broken furniture, and several old or broken restaurant equipment were found outside the restaurant and on the path (barrier A1 and F1). The path surface was wet (barrier F1). Some of the participants were observed taking precautionary measures by slowing their pace. About three dogs were spotted in this location during the environmental walk (S1). All the participants reported that they felt stressed while walking through this spot. For instance, one of the participants commented that she would not have been able to walk this segment of the path alone. “Why would someone eat here?” one of the participants asked rhetorically.

Risk stress hot spot 2 consists of environmental barriers A2-A5, S2-S4, and F2-F6, extending from segment C to F as shown in Figure 6.6 and Figure 6.7. This spot has a gas station and a bus stop beside path segment C. The authors noticed that some of the participants interacted with vehicles entering or exiting the gas station; this interaction could be stressful, especially if not perceived in advance (barrier S2). Another group of participants mentioned that they realised it was a gas station from a distance, and they were hoping they would not encounter any car entering or exiting the gas station. This anticipation about what will happen in the near distance could have resulted in stress (barrier S2). Path obstructions such as traffic cones and bollard barricades were identified on the sidewalk beside the gas station (barrier F2). The participants that engaged in the environmental walk in the midmorning remarked that the bus stop was too crowded and was stressful to navigate (barrier F3). The view from this spot is a bamboo scaffolding with screen nets on a high-rise building, which at first glance, seems a

little frightening (barrier A2). Although the pedestrian crosswalk (segment D) has traffic calming devices (traffic signal and traffic island), it was still detected in the risk stress hot spot 2. Some of the participants mentioned that the waiting time (which was about 68 seconds) at the traffic signal was stressful (barrier S3). Segment E—an ongoing construction—was surrounded by unattractive views (barrier A3 and barrier A4) with heavy trucks entering or exiting the construction site (S4). Most of the participants reported feeling stressed at this spot. There were inconsistent path surface materials (F4), a dumpster and barricades (barrier F5) that obstructed the participants during the walk. There was a flower shop in segment F. The authors identified that several flower wreaths and wooden stands were obstructing the path (barrier F6 and barrier A5). The path surface was also wet (barrier F6). One participant described her interaction with this spot as: “I felt uncomfortable when I saw the funeral flower wreath on the street—It made me picture death and burial”.

Risk stress hot spot 3 is located at the end of segment F. This hot spot was caused by a stair with about 11 steps (barrier F7). While some participants reported this stair to be good for their fitness, others reported feeling stressed. An increase in participants’ physiological responses was observed at this spot. Lastly, risk stress hot spot 4 is located in a subway (segment H). The subway has dominant graffiti features (barrier A6), resulting in stress among the participants.



Figure 6.6: Environmental barriers at locations of risk stress hot spot. Base map and data copyrighted 2020 Esri, OpenStreetMap contributors and the GIS user community.



Figure 6.7: Pictures of environmental barriers at locations of risk stress hot spot.
Note. Photographs by author.

6.4 Discussion

Several machine learning algorithms were trained using supervised and unsupervised learning methods. The results showed that the Ensemble bagged tree algorithm achieved the highest performance among the tested algorithms. Accuracy on the held-out test data (i.e., the proportion of collected samples in which the algorithm prediction matches the true label) provides an estimation of the stress detection result to be expected on new data. Therefore, the Ensemble bagged tree algorithm would be able to detect older adults' stressful interactions with an accuracy of 98.13% (for detecting stress and non-stress samples) and 98.25% (for detecting low and high-stress samples). The high performance of the Ensemble bagged tree algorithm is possible because it combines several decision trees (bootstrap aggregation) to produce better predictive performance; this approach helps to reduce the variance of a model (Rokach, 2010).

The high performance of the ensemble method means that it can be used for data collected in an ambulatory, real-world setting. Ambulatory, real-world sensing of human physiology pose several methodological challenges such as missing and noisy data. For instance, if a modality is missing data for a given pedestrian or on a sample day, the ensemble method is able to abstain that classifier in order to achieve better performance. Although the Ensemble bagged tree algorithm performed better than the deep learning algorithm, the Ensemble bagged tree algorithm required sufficient labelled data for training while the deep learning required little or no labelled data. Collecting sufficient labelled data from pedestrians in cities and communities is somewhat impractical and may hinder a large-scale deployment of the stress detection algorithm in smart age-friendly cities. Furthermore, supervised learning required careful engineering and considerable domain expertise to extract and select handcrafted features that are important for discrimination. This implies that failure to extract and select the informative features may affect the performance of the supervised learning algorithm. However, the deep

learning algorithm automatically learns good features and produces representations that are selective to the relevant aspect of signal pattern important for discrimination.

Going forward, using an unsupervised deep learning approach is imperative for the efficient deployment of the stress detection algorithm in cities and communities. This study hypothesises that developing a deep learning algorithm that accounts for interindividual variability can improve the detection of stressful interactions for pedestrians. An environmental condition that results in stressful interaction for one person may not result in stressful interaction for another person. For example, participant 5 (Table 6.3) did not experience any high-stress interaction with the environment, although other participants experienced high-stress interaction. A plausible explanation for this is because of individual difference. Future studies should deploy a multi-task learning technique to train a personalised machine learning model tailored specifically for each pedestrian but still learns from all available data.

Given that the built environment infrastructure in many cities and communities is approaching their design life, sampling peoples' physiological interactions for the entire built environment is currently impossible. The simulation-based approach adopted in this study shows promising result in generating reproducible physiological point-level data to reflect an entire study area. Detecting locations with high statistical power will be useful for researchers and urban planners during the design stage of a study to detect real urban stress hot spot and understand the association between built environment and stress.

6.5 Chapter Summary

This chapter aimed to achieve research objective three: to detect older adults' stressful environmental interactions in near-real time. An optimised environmental stress detection

framework was developed to achieve the objective. Several machine learning algorithms were trained on an optimum set of informative physiological features, environmental data, and user-perceived stress response. Machine learning algorithms including Gaussian SVM, Ensemble bagged tree and DBN were trained to detect older adult's stressful interactions from their physiological signals. Based on three statistical performance evaluation indicators, the results produced by the machine learning intelligence models were evaluated. The obtained results show that the machine learning models can achieve a satisfactory performance of detecting older adult's stressful interaction (over 70% accuracy), with Ensemble bagged tree achieving the best performance (98.25% accuracy). The detected stressful interactions were visualised using kernel density estimation. Overall, the detected stress and high-stress samples matched older adults perceived stress assessment of the path. A simulation-based approach was used to examine areas within the study area that are sufficiently powered to detect stress hot spots that pose high risk to older adults. The results demonstrate that urban planners and municipal decision-makers can use this approach to detect and alleviate stressful environmental conditions more efficiently; as a result, improving older adult's mobility in the built environment. In the next chapter, the optimised environmental stress detection framework will be integrated with evolutionary computing to understand the influence of urban visuospatial configuration on older adults' physiological stress.

**PART IV: THE INFLUENCE OF URBAN ENVIRONMENT
CONFIGURATIONS ON OLDER ADULTS' STRESS
RESPONSE**

CHAPTER 7

INFLUENCE OF VISUOSPATIAL CONFIGURATION OF THE URBAN ENVIRONMENT ON OLDER ADULTS' PHYSIOLOGICAL STRESS⁷

7.1 Introduction

This chapter aims to further our understanding of the relationship between the visuospatial configuration of urban space and older adults' physiological stress response using current advances in machine learning and evolutionary computing. Older adults' perceived visual elements of the urban environment were extracted using isovist analysis. A machine learning-based approach was developed to identify isovist indicator levels that are responsible for stress and non-stress physiological responses and their hierarchy of influence. An evolutionary rule-based system that generates visuospatial configurations that produce a specific physiological effect was also developed. This chapter concludes with a comparison between older adults' visuospatial preference and younger adults' visuospatial preference. An overview of this chapter and the methods adopted is presented in Figure 7.1.

⁷ Parts of this chapter has been published in a journal.

Torku, A., Chan, A.P.C., Yung, E.H.K., Seo, J. (2021). The influence of urban visuospatial configuration on older adults' stress: A wearable physiological-perceived stress sensing and data mining based-approach, *Building and Environment*, 108298. <https://doi.org/10.1016/j.buildenv.2021.108298>

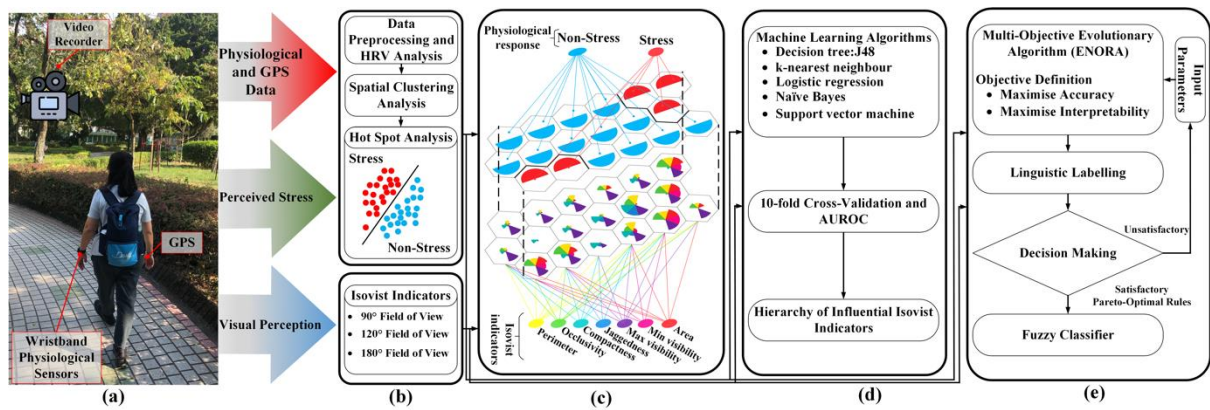


Figure 7.1: Research overview and methodological framework.

Note. (a) Data collection during an environmental walk. (b) Data processing, heart rate variability (HRV) analysis, hot spot analysis, and computing isovist indicators from different fields of view. (c) Self-organising Maps depicting the influence of visual perception on physiological response. (d) Adopting machine learning algorithms to identify the most influential isovist indicators of physiological response. The performance of the algorithms was examined using the Area under the Receiver Operating Characteristic (AUROC) based on 10-fold cross-validation. (e) Adopting an evolutionary rule-based system to generate visuospatial configurations that produce a specific physiological effect.

7.2 Visuospatial Perception

For sighted individuals, spatial information acquisition occurs in large part through their sense of vision (Kiefer et al., 2017). The spatial properties of the environment as perceived through the eyes are referred to as the visuospatial properties of the environment. The visuospatial properties of the environment are influenced by two main elements: the surface characteristic and appearance (e.g., material, texture, and colour) and the configuration (e.g., arrangement and size) of the spatial forms (Schneider and Koenig, 2012). This study considers only the visuospatial configurations of the environment.

In the broader environmental psychology literature, several theories have emphasised that human behaviour and experience are determined by the properties of the spatial form of the environment. For example, the prospect-refuge theory discovered by Appleton (1975) postulates that humans prefer a spatial configuration that affords both the ability to see (prospect) without being seen (refuge). “Where these conditions are present their perception is

attended with pleasure; anxiety is set aside, and relaxation is possible. Where they are absent anxiety continues and there is no relaxation” (Appleton, 1975, p. 71). Akin to the prospect-refuge theory is the defensible space theory that suggests that the environment can be configured to influence its residents’ territoriality, image, milieu, and surveillance behaviours (Reynald and Elffers, 2009). The mystery theory propounded that humans behavioural and emotional responses are influenced by spatial configurations promising new information when proceeding further into the environment (Kaplan, 1988). The complexity concept suggests that human involvement (the concern to figure out, to learn, to be stimulated) in an environment is affected by the diversity or richness (how much there is to look at) in the environment (Kaplan, 1988; Scott, 1993). These theories have been evaluated on several architecture spaces (including Frank Lloyd Wright’s architecture) and urban space (Dawes and Ostwald, 2014; Wu et al., 2020; Franz and Wiener, 2005; Xiang et al., 2020). The theories collectively suggest that the human visuospatial perception of a space generated by or associated with a spatial configuration affects human behaviour and experience; this effect on humans is an important factor for creating and maintaining a liveable environment (Gehl, 2011).

The human visuospatial perception of a horizontal slice through space can be measured using isovist analysis. An isovist is a space in an environment visible to a person from an observation point from which various geometrical and mathematical measures are computed to define the person’s visuospatial perception (Benedikt, 1979; Batty, 2001). Isovist can be studied in both two and three dimensions. This study is limited to the two-dimensional isovist analysis. Isovist analysis is capable of describing a space “‘from inside’, from the point of view of individuals, as they perceive it, interact with it, and move through it” (Turner et al., 2001, p.103). Isovist analysis has been widely used in the fields of architecture and urban planning in the study of wayfinding (Meilinger et al., 2012), visibility (Wu et al., 2020), Prospect-Refuge Theory

(Dawes and Ostwald, 2014; Ostwald and Dawes, 2013) and urban stress (Li et al., 2016; Knöll et al., 2018; Xiang et al., 2020). Pertinent isovist research has shown that several geometrical and mathematical measures (referred to as isovist indicators): area, perimeter, compactness, occlusivity, jaggedness, maximum visibility, and minimum visibility (Benedikt, 1979; Batty, 2001; Schneider and Koenig, 2012) are to some extent associated with spatial perceptions including those relating to elements of prospect, refuge (in the prospect-refuge theory), mystery (in the mystery theory), and complexity (in the complexity theory). These isovist indicators and the experiential properties associated with them are presented in Table 7.1.

Table 7.1: Isovist indicators and corresponding experiential properties

Isovist indicator	Spatial experience	Spatial property	References
Isovist area	Prospect	Spaciousness	Chun et al. (2019), Ostwald and Dawes (2013), Dawes and Ostwald (2013), Franz and Wiener (2005), Xiang et al. (2020), Reynald and Elffers (2009), Dawes and Ostwald (2014), Wu et al. (2020)
Isovist perimeter	Prospect	Spaciousness	
Maximum visibility length	Prospect	Spaciousness	
Minimum visibility length	Refuge	Spaciousness	
Occlusivity	Refuge	Openness	
Occlusivity	Mystery	The promise of more information	Dawes and Ostwald (2013), Benedikt (1979), Kaplan (1988), Xiang et al. (2020), Dawes and Ostwald (2014)
Jaggedness	Complexity	Diversity or richness	Dawes and Ostwald (2013), Kaplan (1988), Scott (1993), Franz and Wiener (2005), Wiener and Franz (2004), Xiang et al. (2020), Ma et al., (2020)
Compactness	Complexity	Diversity or richness	

Isovist area represents the area of all spaces visible from a person’s observation point. Isovist perimeter measures the length of the edge of all space visible from an observation point. Compactness expresses the relationship between area and perimeter relative to a circle; it indicates the complexity or compactness of the field of view (Schneider and Koenig, 2012).

Occlusivity describes the length of open edges (i.e., edges without physical boundaries such as a wall) of the field of view (Dawes and Ostwald, 2014). Occlusivity is small in locations with few or no views into other parts of the spatial configuration of the environment. For instance, an observation point within a completely closed, convex space has an occlusivity of 0. Jaggedness describes the convexity (i.e., the number of vertices and vertex density) of the field of view (Wiener and Franz, 2004). The maximum visibility and minimum visibility refer to the length of the longest and shortest single view, respectively, available at an observation point.

7.3 Methods

7.3.1 Detecting Stress and Non-stress Responses

The data collection and pre-processing to remove noise is discussed in Chapter 3. To understand the influence of spatial factors on stress, it is important to distinguish stressful person-environment interactions due to spatial factors from stressful person-environment interactions due to other environmental or personal factors. This study harnesses the advantages of the perceived stress rating and the physiological responses stress detection (physiological-perceived stress). The aim is to (1) estimate stress and non-stress environmental conditions using perceived response (2) integrate physiological response with GPS data, conduct hot spot analysis to identify hot spots and cold spots (3) spatially match hot spots and cold spots to perceived response to detect stressful person-environment interactions due to spatial factors in order to enhance our understanding of the relationship between the visuospatial configuration of urban space and older adults stress response.

A participant experiencing a high or low physiological response at a location could result from spatial factors (e.g., spatial configuration), temporal factors (e.g., noise level and weather) or individual factors (e.g., health condition and previous experience). Because the participants'

responses to the environment were collected on different days and different time-of-day, there was no direct mutual interference between them; therefore, it is assumed that their responses were comparatively independent. As a result, spatial clustering analysis—specifically hot spot—was conducted to amplify the physiological responses induced by spatial factors while reducing the impact of temporal and random factors.

The *LF/HF* ratio was used to model older adults' physiological stress responses to urban environmental conditions. Hot spot analysis was performed using Getis-Ord G_i^* statistics to detect locations in the study area that elicited a common physiological response among multiple participants. Please refer to Chapter 5 for a more detailed explanation and analysis of the hot spot analysis using the *LF/HF* ratio. The detected hot spots and cold spots were spatially matched with the commonly perceived stress and non-stress path segments. The hot spots and cold spots within perceived stress path segments were detected as spatial significant stress locations, and hot spots and cold spots within the perceived non-stress path segments were detected as spatial significant non-stress locations.

Before the hot spot analysis, the recorded video of each participant's environmental walk was inspected by the authors and unintended person-environment interaction (e.g., older adults' interaction with vehicles, people, and losing stability due to encounters with path obstructions such as potholes, stairs, or curbs) that could affect stress were excluded to ensure that the physiological response was mainly influenced by spatial factors.

7.3.2 Measuring Visuospatial Perception: Isovist Analysis

The spatial layout of the experiment neighbourhood (Hung Hom, Kowloon, Hong Kong) was generated using OpenStreetMap (OpenStreetMap and Contributors, 2019), as shown in Figure

7.2(a). The isovist was generated using DepthmapX (SpaceGroupUCL, 2019). DepthmapX has the following field of view options: 90°, 120°, 180°, and 360°. The combined visual field for both human eyes is 130-135° vertically and 200-220° horizontally (Szinte and Cavanagh, 2012; Dagnelie, 2011). During the environmental walk, the participants walked the path in one direction (i.e., from start to end, as shown in Figure 7.3); therefore, the maximum horizontal visible urban space to the participants is about 220°. Due to the limited field of view options available in DepthmapX, only the 90°, 120°, and 180° fields of view were used for the isovist analysis. Hence, the far peripheral vision of the human eye beyond 180° was ignored in this study. An example of the generated 90°, 120°, and 180° fields of view from an observation point on the path is presented in Figure 7.2(b), Figure 7.2(c), and Figure 7.2(d), respectively. In order to capture a more realistic isovist, a view distance of 200 m was set, considering the visual acuity for an average 65-year-old. For instance, it would be unrealistic to assume that people have near infinite isovists in an open space. Figure 7.2(b) depicts a more realistic isovist with a visibility boundary from an observation point. The isovist within the visibility boundary represents a closed polygon from which isovist indicators: area, perimeter, compactness, occlusivity, jaggedness, maximum visibility, and minimum visibility were calculated. The isovist was generated for the entire path using the fields of view, the view distance, and the GPS locations as observation points. Isovist area is calculated as the total space bounded by the edges of the polygon, isovist perimeter is calculated as the total length of the edges of the polygon, isovist maximum and minimum visibility is calculated as the length of the longest and shortest line to the solid edge of the polygon from an observation point. The formulas for compactness, occlusivity, and jaggedness are

$$Compactness = 1 - \frac{2\sqrt{\pi S}}{P}, \quad (7.1)$$

$$Occlusivity = P - P_f, \quad (7.2)$$

$$Jaggedness = \frac{P^2}{S}, \quad (7.3)$$

where S is the isovist area, P is the isovist perimeter, and P_f is the total length of the solid edges within the isovist area (S).



Figure 7.2: Generated spatial layout with isovist from an observation point.

Note. (a) Spatial layout of the experiment neighbourhood with predefined path. (b) Isovist with 90° field of view from an observation point R with a defined boundary, M = visibility limit of 200 m (equivalent to the maximum visibility length), m = minimum visibility length. (c) Isovist with 120° field of view from an observation point R . (d) Isovist with 180° field of view from an observation point R . Basemap data copyrighted OpenStreetMap (and) contributors.



Figure 7.3: Path with perceiver’s view in the forward direction, starting from A to L.
Note. Basemap data copyrighted Esri, DigitalGlobe, GeoEye, Earthstar Geographics, CNES/Air bus DS, USDA, USGS, AeroGRID, IGN, and the GIS User Community. Photographs by author.

7.3.3 Influence of Visuospatial Perception on Physiological Response: Self-Organising

Map

A self-organising map (SOM) is a type of artificial neural network trained using unsupervised learning to visualise and explore different patterns and relationships in the data (Kohonen,

2013). SOM has a unique property of effectively projecting input space (high-dimensional space) into a low-dimensional (usually two-dimensional) regular grid such that the proximity relations are preserved (Vesanto and Alhoniemi, 2000). Maps that are generated using unsupervised SOM mainly capture the significant factors that influence the similarities in the data (e.g., clustering in the data). This study is interested in variations in factors resulting in a specific effect (i.e., the isovist indicators that influence physiological response). Supervised SOMs offer the opportunity to study the isovist indicators influencing physiological response by increasing their importance on the organisation of the maps (Platon et al., 2017; Wongravee et al., 2010; Kuzmanovski et al., 2007).

SOM Architecture

Note that three different fields of view were considered in this study. Therefore, a prototype SOM of two-dimensional grid size $M \times N = U$ nodes was generated for each field of view dataset. The input data \mathbf{X} , to be projected on the SOM of dimension $I \times J$ (which is 3283×7 for each field of view) and its label \mathbf{Y} has dimensions $I \times K$ (where $K = 2$, representing the two classes of the physiological response [stress and non-stress]).

The Learning Process

Given a set of samples $(\mathbf{x}_i, \mathbf{y}_i)$ from the dataset (\mathbf{X}, \mathbf{Y}) , $i = 1, \dots, n$, where \mathbf{x}_i is the input vector of the i th sample and \mathbf{y}_i is a vector corresponding to its label (recall that the dimension of \mathbf{y}_i is equal to the number of classes in the label, which is 2 in this study). If the class of \mathbf{x} is l , the l th component of \mathbf{y}_i is equal to 1 and the other component is equal to 0. The supervised SOM is able to learn a function $f: \mathbf{X} \rightarrow \mathbf{Y}$ by training on an augmented vector $\mathbf{x} = [x_v, x_l]$, which is a combination of label vector x_l with the input vectors x_v . Each node r , in the supervised SOM has a weight vector $\mathbf{w}_r = [w_r^v, w_r^l]$. During the competitive learning process, the distance

between \mathbf{x}_i and \mathbf{w}_r of each node is computed. The best matching unit (BMU) is determined by finding the node r , having the closest weight vector \mathbf{w}_r , to the input vector \mathbf{x}_i :

$$b = \arg \min_r d(\mathbf{x}_i, \mathbf{w}_r), \quad (7.4)$$

where b denotes the index of the BMU and $d(\mathbf{x}_i, \mathbf{w}_r)$ is the Tanimoto distance between \mathbf{x}_i and \mathbf{w}_r (note that the \mathbf{Y} is categorical, hence the reason for using Tanimoto distance measure). The BMU and its topological neighbours are updated as

$$\mathbf{w}_r(t + 1) = \mathbf{w}_r(t) + \alpha(t)h_{br}[\mathbf{x}_i - \mathbf{w}_r(t)], \quad (7.5)$$

where $\alpha(t)$ is the learning rate at time t [$\alpha(t)$ is a monotonically decreasing function], and h_{br} is the neighbourhood function between BMU and the r th node at time t . The two traditional neighbourhood functions are the bubble function and Gaussian function. Both neighbourhood functions were tested. The learning process adopted in this study is based on the classical sequential SOM algorithm (Kohonen, 2013). The learning process is repeated until there is convergence in \mathbf{X} and \mathbf{Y} . Several SOM were trained in parallel using different hyperparameters settings. The optimal SOM was selected using the Area under the Receiver Operating Characteristic (AUROC) based on 10-fold cross-validation. The AUROC and the validation of the SOM are explained in the validation section.

7.3.4 Identifying the Most Influential Iovist Indicators of Physiological Response

The SOM is able to provide the iovist indicator levels that are responsible for stress and non-stress physiological responses. However, it is also important to ascertain which of the iovist indicator (s) have the greatest influence on older adults' physiological responses. Hence, subsets of iovist indicator (s) based on their correlation and intercorrelation were generated. Subsets of iovist indicator (s) that are highly correlated with the physiological responses, while having low intercorrelation, have greater influence (Hall, 1999). A greedy forward search was performed through the space of the generated subsets to create a hierarchy of influential iovist

indicator (s) subsets. A greedy forward search is an efficient method to select a choice from multiple choices that achieve the largest possible improvement or fitness in the value of some measure (Resende and Ribeiro, 2010).

The hierarchy of influential subsets of isovist indicator (s) was subsequently confirmed by considering its ability to discriminate between stress and non-stress physiological responses when used to train several machine learning algorithms. Decision tree (J48), k-nearest neighbour (kNN), logistic regression, Naïve Bayes, and support vector machine were used because they have been successful used in previous studies to detect stress (Panicker and Gayathri, 2019). The performance of the algorithms was examined using the Area Under the Receiver Operating Characteristic (AUROC) based on 10-fold cross-validation.

7.3.5 Design by Evolutionary Algorithmic Rule: Generative Design

Urban planners, municipal officials, and developers often use predefined rules and guidelines such as pattern books and urban form-based codes to create spatial configurations that meet certain specific visual qualities (Talen, 2009; Borchers, 2008). An example is the Hong Kong Urban Design Guidelines (Hong Kong Planning Department, 2015), which contain several design considerations for streets, streetscapes, and building height. Although this approach effectively ensures that cities and communities are planned to meet a specific standard, it is somewhat limited and inflexible to adequately accommodate changing context and complexity (Batty and Marshall, 2012; Schneider and Koenig, 2012). Every planning and design problem is unique, and it is rather impossible for urban codes to offer solutions to all of these problems. For instance, the Hong Kong Urban Design Guidelines has no specific requirement on the influence of visual perception on physiological stress. The complexity and interactions of urban forms further limit the abilities of predefined standards to adequately respond to these problems

(Marshall, 2012). Pattern books usually contain a few of these spatial configurations and can only be of limited use in designing and planning a unique visuospatial effect.

Instead of having only a few spatial configurations that create a specific visuospatial effect, it would be more beneficial to have an approach that generates multiple spatial configurations that produce a specific visuospatial effect. Such an approach will be well-adaptable to many unique urban design problems, thereby enabling planners to explore design space. This study presents a method for implementing such an approach using a multi-objective evolutionary fuzzy rule system algorithm to generate visuospatial configurations (from different isovist indicator levels) that produce a specific physiological effect.

7.3.6 Multi-Objective Evolutionary Fuzzy Systems

People's bounded rationality has consequences, including decision making (Wheeler, 2018). In the psychology literature, how well a given claim is supported by evidence affects people's rationality (Stanovich et al., 2016). Specifically, urban planners, municipal officials and developers are more likely to agree to the visuospatial configurations generated by a system when it is supported by evidence. Thus, it is crucial to develop decision support systems that are capable of interpreting themselves. Interpretability is the ability of a system to explain its behaviour such that it is easily understandable by the users of that system (Jiménez et al., 2018). Rule-based systems have been recognised for their ability to achieve a high level of interpretability because they are based on a human-like logic. The rules are represented in an easily understandable schema:

IF (Condition 1) and (Condition 2) and ... (Condition N) THEN (Statement).

A fuzzy system is a rule-based system in which fuzzy logic (a way of describing and measuring nonstatistical uncertainty and approximate reasoning) is used to represent different forms of

knowledge about a problem and to model the interactions and relationships between its variables (Jimenez et al., 2014; Shi et al., 1999). This ability of fuzzy rule-based systems is important in this study because the if-then fuzzy rules can represent the conditions for a visuospatial configuration (isovist indicator levels) to be associated with a physiological response (stress or non-stress) in a computationally efficient manner that approximate human reasoning. In this way, the fuzzy rule-based system is implemented as a classification learning system.

Evolutionary algorithm is a commonly used approach to generate fuzzy rules automatically; it has been successfully used to search poorly understood, irregular space (Ishibuchi and Yamamoto, 2004; Kim et al., 2019). Evolutionary algorithm is an optimisation algorithm that reflects the process of natural evolution such as crossover, mutation, and natural selection to find an optimal solution to a problem within specific constraints (Deb et al., 2002; Shi et al., 1999). Evolutionary fuzzy systems combine the approximate reasoning ability of fuzzy systems with the adaptation abilities of evolutionary algorithm.

To ensure system transparency, the fuzzy rule-based system was defined with two objectives: interpretation and accuracy. Hence, a multi-objective evolutionary fuzzy rule-based system was implemented in this study using ENORA, a multi-objective evolutionary algorithm. ENORA is a state-of-the-art evolutionary algorithm; it is recognised for its ability to achieve high performance (Jiménez et al., 2018; Onan et al., 2017). A multi-objective evolutionary fuzzy rule-based system is capable of generating Pareto-optimal fuzzy rules (visuospatial configurations) that maximise accuracy in classifying physiological responses and minimise the number of rules for easy interpretation of the system.

The ENORA algorithm was run with 10-fold cross-validation using the parameters shown in Table 7.2. A population size of $N = 100$ is often used in evolutionary computing. A similarity constraint $g_s = 0.1$ is imposed to reach transparency by ensuring that no two fuzzy sets (sets of visuospatial configurations) overlapped more than 10%. A 10% maximum similarity is sufficient to achieve an interpretable system (Setnes et al., 1998). A set of linguistic labels: Very Low, Low, Moderately Low, Moderate, Moderate High, High, Very High (maximum set of linguistic labels) are assigned to each fuzzy set. The number of the linguistic label is equal to the maximum number of fuzzy sets. Maximum number of fuzzy sets $L_{max} = 7$ and maximum number of linguistic labels $L_i = 7$, are used to ensure interpretability. Minimum variance parameter $\gamma_1 = 30$ was established to ensure $g_s = 0.1$ and $L_{max} = 7$. Maximum variance parameter $\gamma_1 = 2$ ensures $\geq 47.72\%$ of any Gaussian fuzzy set is retained in the variable domain. The minimum number of rules M_{min} and maximum number of rules M_{max} will be decided by the designer based on the design problem. $M_{min} = 2$ and $M_{max} = 20$ were used in this study as an example to generate sets of visuospatial configurations from the 180° field of view dataset.

Table 7.2: Parameters used to run multi-objective evolutionary fuzzy rule-based system

Size of population $N = 100$
Minimum number of rules (visuospatial configurations) $M_{min} = 2$
Maximum number of rules (visuospatial configurations) $M_{max} = 20$
Minimum variance parameter $\gamma_1 = 30$
Maximum variance parameter $\gamma_1 = 2$
Maximum number of fuzzy sets $L_{max} = 7$
Maximum number of linguistic labels $L_i = 7, L_i \leftarrow \{VL, L, ML, M, MH, H, VH\}$
Maximum similarity threshold for fuzzy sets $g_s = 0.1$

7.3.7 Validation

k-fold cross-validation (k = 10) was used to evaluate the performance of the SOM and the machine learning algorithms. Cross-validation is a resampling procedure that has been widely

used in machine learning to estimate the skill of a model on unseen data (Bengio and Grandvalet, 2004). k-fold cross-validation involves randomly splitting the original sample data into k groups of approximately equal size. One group out of the k groups is held out to validate the model, and the remaining k-1 groups are used to train the model. The training and validation are repeated k times to calculate the performance of the model on the validation data set. The value of $k = 10$ was used for the cross-validation; this value has been proven to produce validation results that suffer neither from excessively high bias nor from very high variance (James et al., 2013).

The performance of the models was evaluated using the Area Under the Receiver Operating Characteristic (AUROC). The Receiver Operating Characteristic (ROC) curve is constructed by plotting the model's true positive rate (sensitivity) against the false positive rate (1-specificity) at various threshold settings. AUROC is a performance metric for discrimination; it indicates a model's ability to discriminate between positive and negative cases (Brown and Davis, 2006). An AUROC of 1.0 corresponds to a perfect performance; the lower the AUROC, the worse the performance. In general, AUROC above 0.5 indicates good performance, whereas AUROC below 0.5 indicates poor performance. The model with the highest AUROC value was selected as the optimal model.

7.4 Results

7.4.1 Detected Stress and Non-stress Responses

The path was labelled using the commonly perceived stress and non-stress reported by the participants, as shown in Figure 7.4(a). The hot spot analysis result is presented in Figure 7.4(b). The hot spots and cold spots were determined at a 95% confidence level. In other words, these hot and cold spots were the results of older adults' physiological responses to spatial

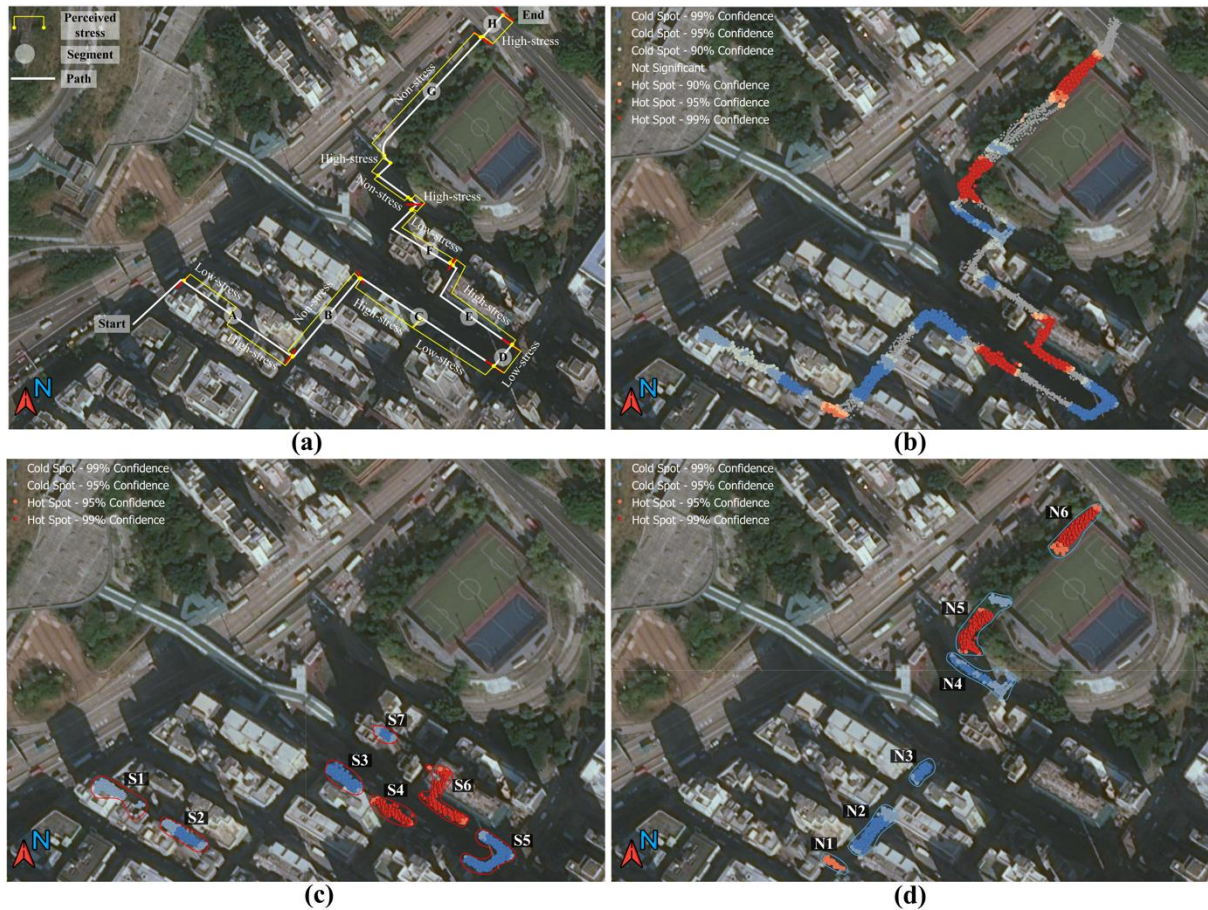


Figure 7.4: Detected spatial significant stress and non-stress locations.

Note. (a) The commonly perceived stress and non-stress response by the participants. (b) Spatial significant clusters of high (hot spot) and low (cold spot) physiological responses of the participants. (c) The distribution of spatial significant stress locations on the path. S1 to S7 correspond to spatial significant stress locations based on physiological-perceived responses. (d) The distribution of spatial significant non-stress locations on the path. N1 to N6 correspond to non-stress locations based on physiological-perceived responses.

factors at a 95% confidence level. The spatial significant sample points corresponding to the perceived responses were used to determine the stress and non-stress locations on the path in order to further analyse the spatial attributes—here, the visuospatial configurations—stimulating such stress and non-stress responses. The hot spots and cold spots within the perceived stress path segments (i.e., 2161 points of spatial significant stress samples) were distributed approximately across seven locations on the path (i.e., S1 to S7) as shown in Figure 7.4(c). The hot spots and cold spots within the perceived non-stress path segments (i.e., 1122

points of spatial significant stress samples) were distributed approximately across six locations on the path (i.e., N1 to N6) as shown in Figure 7.4(d).

7.4.2 Influence of Visuospatial Perception on Stress and Non-stress Response

Older adults' visuospatial perceptions (i.e., the values for all isovist indicators) were spatially matched with the spatial significant stress samples and non-stress samples. A Wilcoxon signed-rank test was conducted to determine whether there is a significant difference in their visuospatial perceptions during stress and non-stress physiological states. The results indicate that all isovist indicators were statistically and significantly different under the two different physiological states with a 95% significance level. This is an indication that the isovist indicators somewhat influenced the participants' stress and non-stress physiological states.

Principal component analysis (PCA) was conducted on the spatially significant matched samples of isovist indicators and physiological responses for each field of view to determine whether the variation retained in the first two principal components contains relevant information about the samples. Before PCA was conducted, the data for each isovist indicator was mean centred and then divided by the standard deviation of the isovist indicator (data normalisation). This way, each isovist indicator has zero mean and unit standard deviation to ensure that the PCA is based on how much variation the isovist indicators explain to improve numerical stability.

The biplots of the two largest principal components for 90° field of view, 120° field of view, and 180° field of view are shown in Figure 7.5(a), Figure 7.5(b), and Figure 7.5(c), respectively. From the biplots, it can be observed that the two largest principal components (i.e., PC1 on the x-axis and PC2 on the y-axis) for all the fields of view explain more than 80%

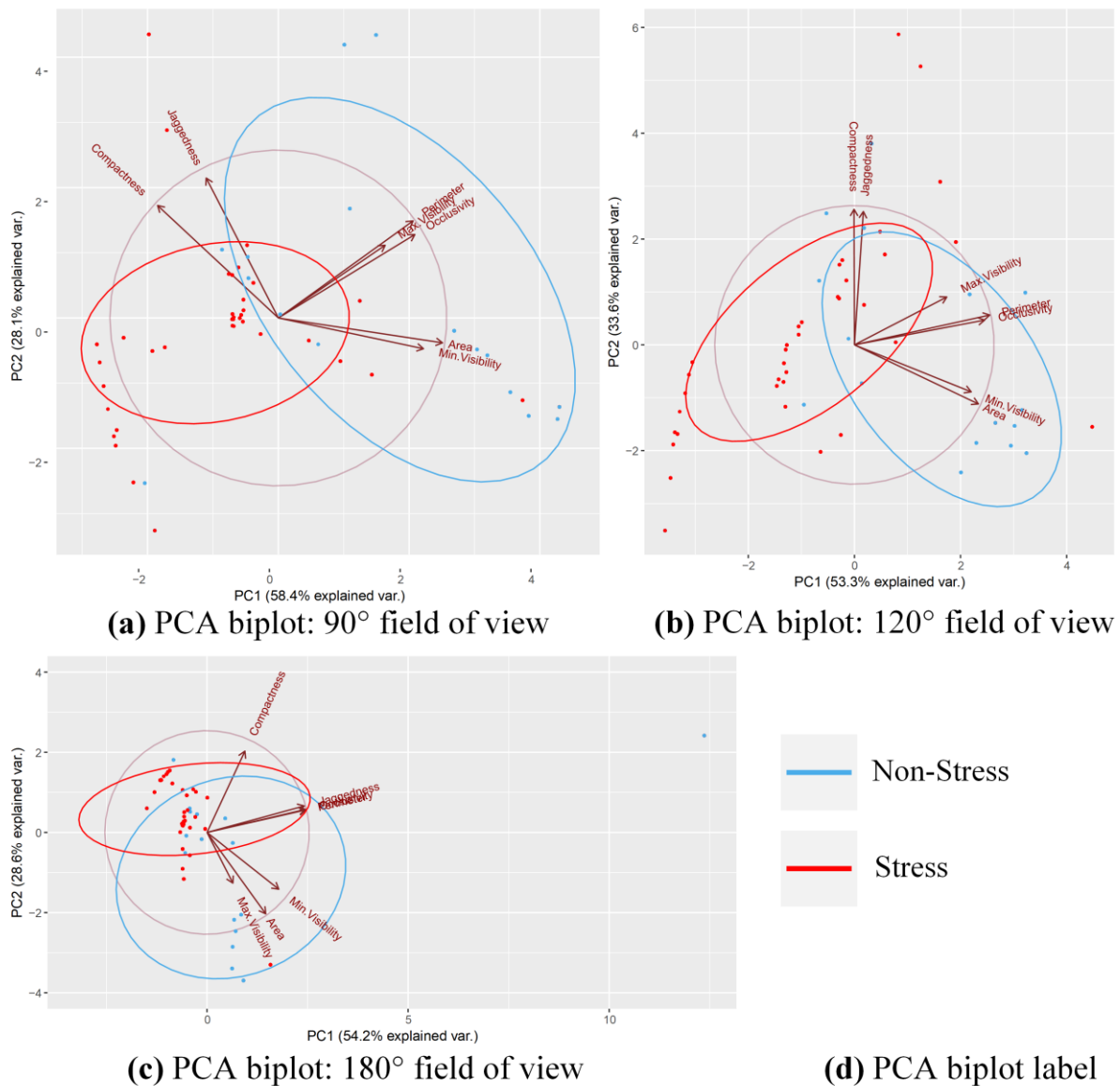


Figure 7.5: PCA biplot of spatially significant matched samples of isovist indicators and physiological responses.

Note. (a) 90° field of view. (b) 120° field of view. (c) 180° field of view. (d) PCA biplot label for stress and non-stress physiological responses. PC1 = principal component 1; PC2 = principal component 2.

(i.e., the sum of PC1 and PC2) of the variability in the data. The biplot reveals that non-stress responses are characterised by increasing values of area, perimeter, occlusivity, minimum and maximum visibility, while stress is somewhat characterised by increasing values of jaggedness and compactness. However, note that the PCA is only providing information on the global

structure of the data; therefore, further data exploration was conducted using SOM and machine learning to understand the local structure of the data.

7.4.3 The Learning Process

The optimal hyperparameter settings for the SOM are reported in Table 7.3. Note that the isovist indicators were normalised. The learning process for 90° field of view, 120° field of view, and 180° field of view dataset are shown in Figure 7.6(a), Figure 7.6(d), and Figure 7.6(g), respectively. Figure 7.6(a), Figure 7.6(d), and Figure 7.6(g) show the mean distance to the closest unit decreased during the learning process, stabilised at a very small value and reached a minimum plateau. A small value of mean distance is an indication that the weight vector of a node is similar to the input data x_i (isovist indicator) and corresponding label y_i (physiological response) represented by that node. The marginal improvement in the mean distance after the first 60 iterations prove the convergence of the SOM. Figure 7.6(b), Figure 7.6(e), and Figure 7.6(h) present the count plot for 90°, 120°, and 180° fields of view, respectively. The count plot shows the number of input data points in each node. The neighbourhood distance plots in Figure 7.6(c), Figure 7.6(f), and Figure 7.6(i) for 90°, 120°,

Table 7.3: Optimal hyperparameters settings for SOM and SOM validation result

Hyperparameters	Field of view		
	90°	120°	180°
Grid size	3×4	3×4	3×4
Topography	Hexagonal	Hexagonal	Hexagonal
User weights	0.8	0.2	0.8
Distance weights	2.444	2.444	2.444
Neighbourhood function	Bubble	Bubble	Bubble
Distance function	Tanimoto	Tanimoto	Tanimoto
Training length	100	100	100
Learning rate (initial, final)	0.05, 0.01	0.05, 0.01	0.05, 0.01
10-fold cross-validation			
AUROC	0.960	0.931	0.937
Sensitivity	0.843	0.767	0.790
Specificity	0.929	0.939	0.934

Note. AUROC = area under the receiver operating characteristic.

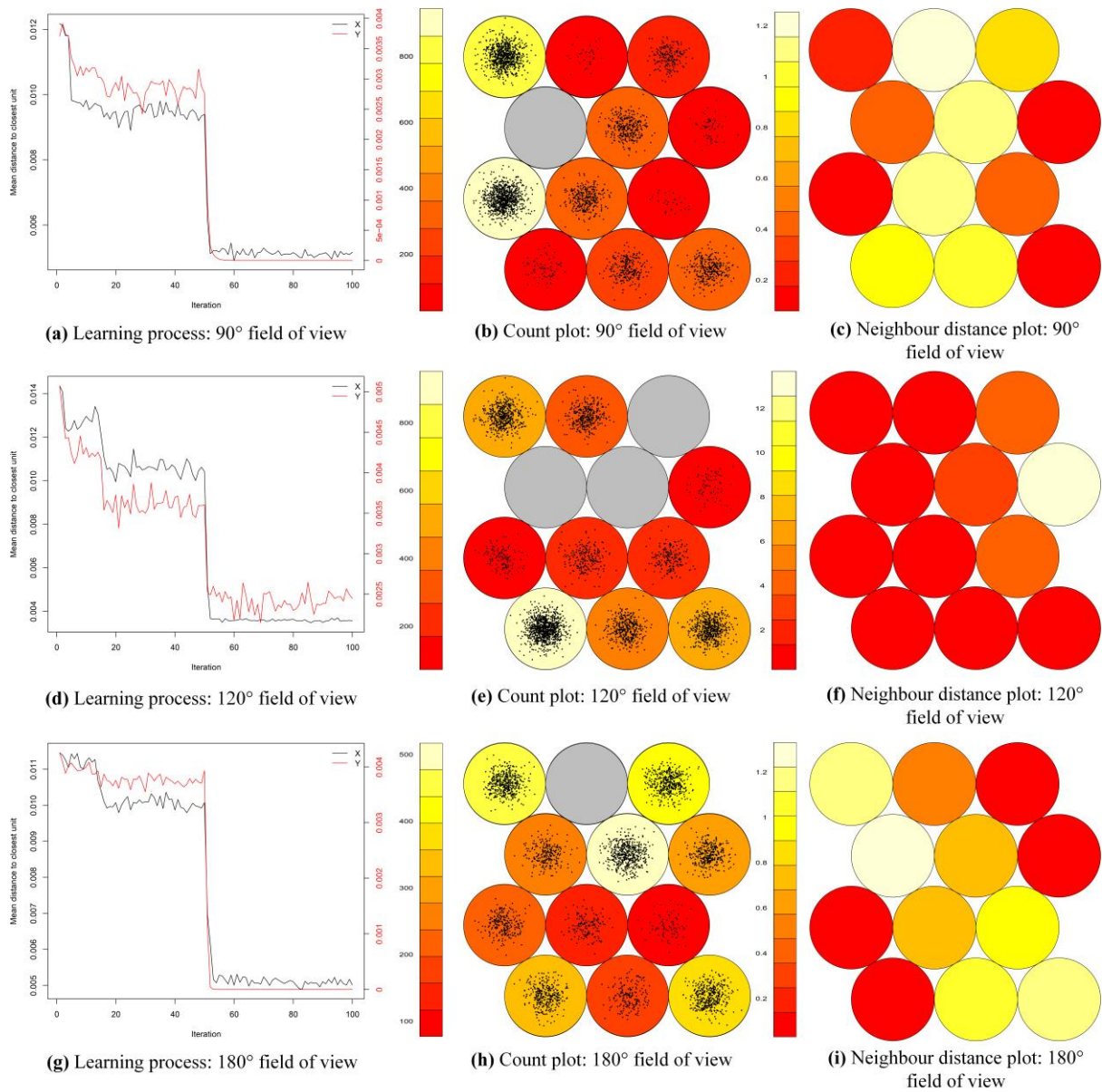


Figure 7.6: SOM architecture.

and 180° fields of view, respectively, shows further clustering in the data. Areas of low neighbour distance (dark regions) indicate the group of nodes with similar properties, and the further apart nodes (light regions) indicate natural borders in the map.

7.4.4 Visualisation of the SOM

Hierarchical clustering analysis was conducted to show the clustering information in the SOM. The clustering shows a clear boundary of isovist indicators resulting in non-stress and stress physiological responses. The SOM with cluster boundaries for 90° field of view, 120° field of view, and 180° field of view analyses are presented in Figure 7.7. The SOM shows the level of isovist indicators (Figure 7.7[a], Figure 7.7[d], and Figure 7.7[g]) that influence older adults' physiological response (Figure 7.7[b], Figure 7.7[e], and Figure 7.7[h]). The cluster of participants influence by a specific isovist indicator (s) is shown in Figure 7.7(c), Figure 7.7(f), and Figure 7.7(i) for 90°, 120°, and 180° fields of view, respectively. The SOM reveals the local structure of the data. For instance, participant 1's experience is best captured by node 5, node 6, and node 9 for 90°, 120°, and 180° fields of view, respectively. Participant 1 experienced stress when there is a high level of maximum visibility, a medium level of compactness and low levels of area, minimum visibility, perimeter, occlusivity, and jaggedness for 90° and 180° fields of view. However, a small increase in minimum visibility and area resulted in a non-stress physiological response when the field of view is 120°. None of participant 8's data was captured in nodes 9 and 6 (90° fields of view), implying that the levels of isovist indicators in these nodes have no influence on participant 8. The male participants (participants 3, 5 and 10) samples dominated the count in node 1 (90° fields of view), indicating that minimum visibility, maximum visibility, area, perimeter and occlusivity (in order of importance) influence their physiological response. A summary of the dominant patterns in the SOM is explained in Table 7.4.

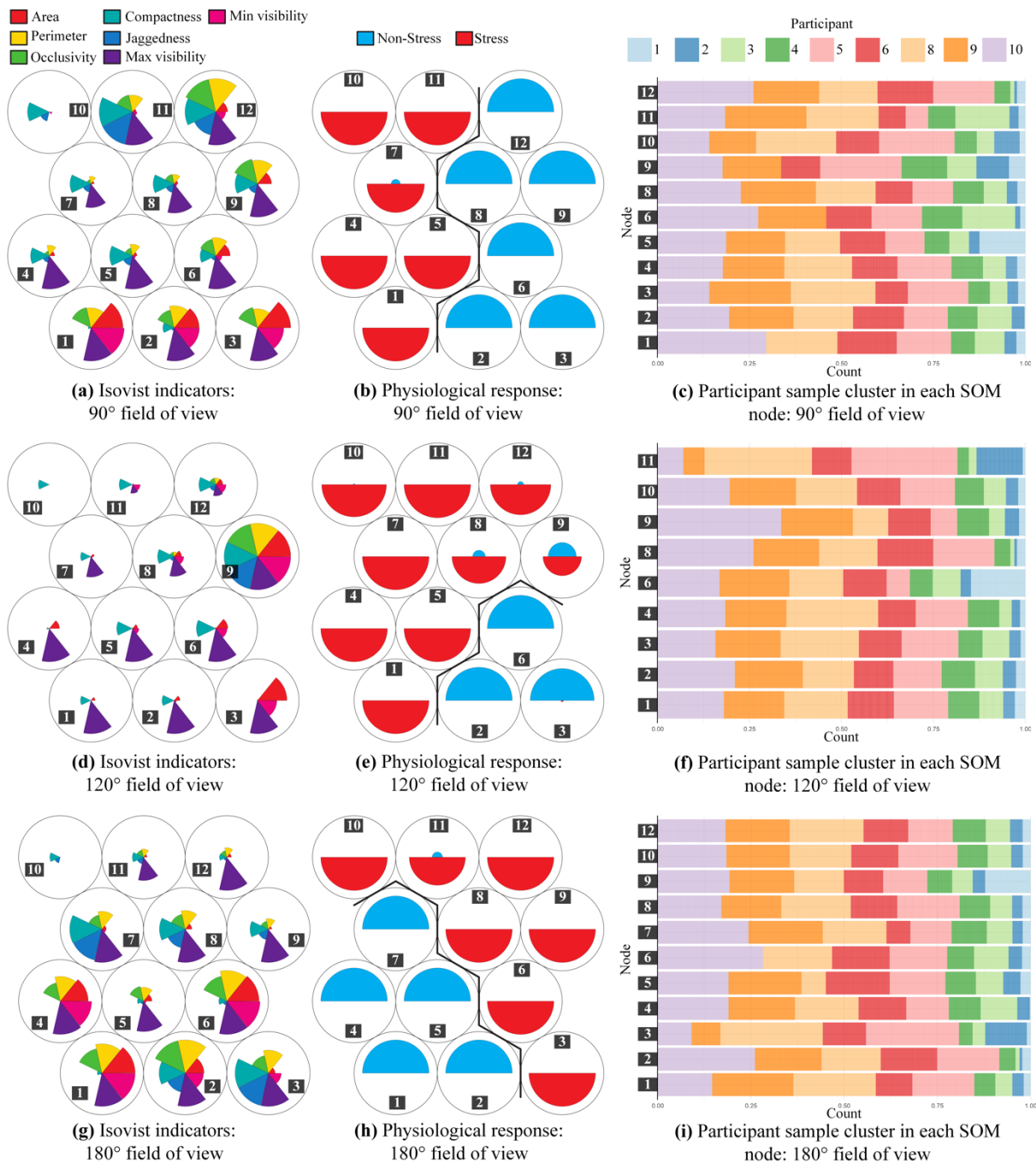


Figure 7.7: Influence of isovist indicators on participants' physiological stress.

Note. (a), (d), and (g) is a “fan diagram”, each node of the “fan diagram” consist of individual fans, which represents the magnitude of each input variable (i.e., the isovist indicator) in the weight vector. (b), (e), and (h) is read in conjunction with (a). It shows the isovist indicator levels eliciting a specific physiological response. (c), (f), and (i) show the participants sample data that were clustered into a specific self-organising map (SOM) node. The SOM consist of 12 nodes.

7.4.5 Most Influential Isovist Indicators of Physiological Response

The hierarchy of influential isovist indicator (s) subsets is provided in Figure 7.8. Minimum visibility was the most influential under 90°, 120° and 180° fields of view. Most of the machine learning models achieved higher performance when only the most influential isovist indicator is used to discriminate between stress and non-stress physiological responses. Minimum visibility, occlusivity, perimeter, and isovist area (for 90° field of view); minimum visibility, occlusivity, isovist area, and compactness (for 120° field of view); and minimum visibility, isovist area, and occlusivity (for 180° field of view) appeared in most of the influential isovist indicator (s) subsets. The level of influence is presented alongside the dominant pattern observed in the PCA and SOM in Table 7.4.

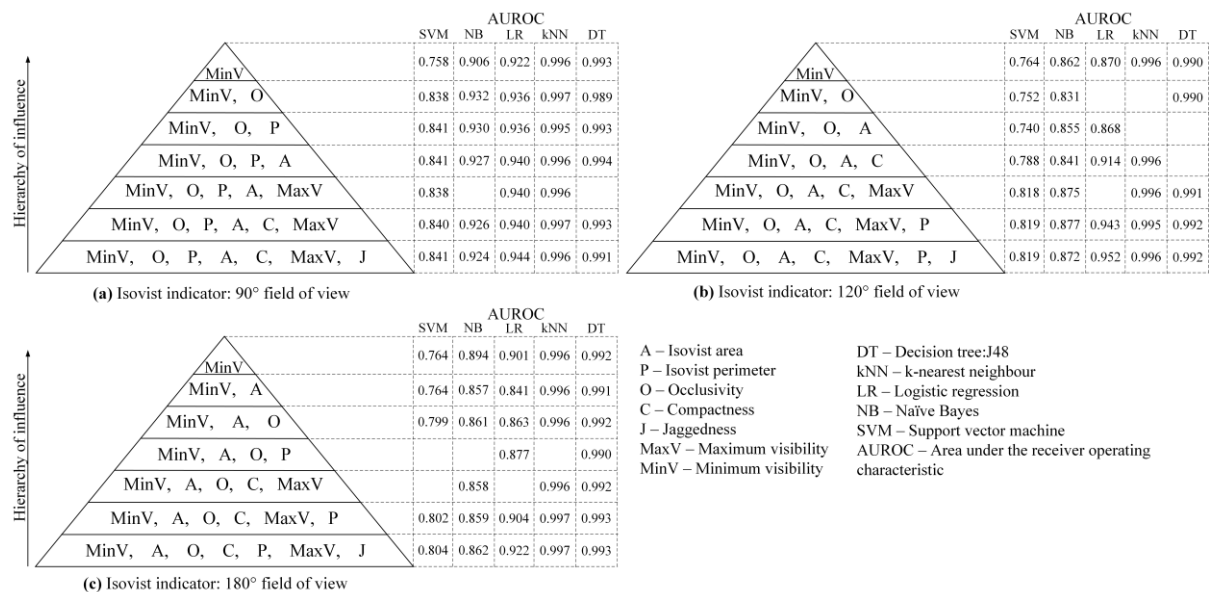


Figure 7.8: Hierarchy of influential isovist indicator (s) subsets with corresponding performance when tested on machine learning algorithms with 10-fold cross-validation.

Table 7.4: Dominant pattern in the SOM

Isovist indicator	90° field of view		120° field of view		180° field of view	
	Non-stress	Stress	Non-stress	Stress	Non-stress	Stress
Area	↑ ⁴	↓ ⁴	↑ ³	↓ ³	↑ ²	↓ ²
Perimeter	↑ ³	↓ ³	↑ ⁶	↓ ⁶	↑ ⁴	↓ ⁴
Occlusivity	↑ ²	↓ ²	↑ ²	↓ ²	↑ ³	↓ ³
Compactness	↓ ⁶	↑ ⁶	↓ ⁴	↑ ⁴	↓ ⁴	↑ ⁴
Jaggedness	↓ ⁷	↑ ⁷	↓ ⁷	↑ ⁷	↓ ⁷	↑ ⁷
Maximum visibility	↑ ⁵	↓ ⁵	↑ ⁵	↓ ⁵	↑ ⁴	↓ ⁴
Minimum visibility	↑ ¹	↓ ¹	↑ ¹	↓ ¹	↑ ¹	↓ ¹

Note. ↑ = increase in isovist indicator; ↓ = decrease in isovist indicator; ¹ = most influential; ⁷ = least influential.

7.4.6 Multi-objective Evolutionary Fuzzy Systems: Generated Visuospatial

Configurations with Physiological Effect

The multi-objective evolutionary fuzzy rule-based system was tested on the 180° field of view. The system generated 17 sets of visuospatial configurations with specific physiological effect with an accuracy of 86.8%, precision of 86.4%, recall of 86.9%, and AUROC of 0.826 over 10-fold cross-validation. The generated visuospatial configurations with physiological effect are presented in Table 7.5.

7.5 Discussion

The result from the PCA, SOM, and machine learning algorithms show that minimum visibility, occlusivity, and isovist area have the most significant influence on physiological responses among older adults at individual and group levels. In the prospect-refuge theory, minimum visibility is the visual indicator for “refuge”. This implies that older adults’ physiological responses are strongly influenced in an environment with refuge value. Occlusivity is another indicator of refuge; occlusivity is the second most influential predictor of physiological response. However, when this refuge element is present, older adults displayed a preference for a high minimum visibility length and high occlusivity, which results in a non-stress physiological response, while a low minimum visibility length and low occlusivity result

Table 7.5: Visuospatial configurations with physiological effect

	Visuospatial configuration		Linguistic label	Dimension (SD)
Rule 1:				
IF	Isovist area	IS	Low	4156.807 m ² (495.337)
	AND Isovist perimeter	IS	Medium	410.722 m (21.284)
	AND Occlusivity	IS	Moderately High	374.510 m (24.058)
	AND Compactness	IS	High	0.596 (0.020)
	AND Jaggedness	IS	Very High	179.208 (7.276)
	AND Maximum visibility	IS	Very High	94.574 m (7.913)
	AND Minimum visibility	IS	Medium	41.930 m (2.969)
THEN	the physiological effect IS Stress			
Rule 2:				
IF	Isovist area	IS	Low	4156.807 m ² (495.337)
	AND Isovist perimeter	IS	Medium	410.722 m (21.284)
	AND Occlusivity	IS	Moderately High	374.510 m (24.058)
	AND Compactness	IS	Very Low	0.198 (0.019)
	AND Jaggedness	IS	Very High	179.208 (7.276)
	AND Maximum visibility	IS	Low	34.622 m (4.158)
	AND Minimum visibility	IS	Moderately Low	29.207 m (2.969)
THEN	the physiological effect IS Stress			
Rule 3:				
IF	Isovist area	IS	Very Low	1616.546 m ² (699.152)
	AND Isovist perimeter	IS	Very High	696.734 m (22.145)
	AND Occlusivity	IS	Moderately High	374.510 m (24.058)
	AND Compactness	IS	High	0.596 (0.020)
	AND Jaggedness	IS	Very High	179.208 (7.276)
	AND Maximum visibility	IS	Medium	61.944 m (3.698)
	AND Minimum visibility	IS	Low	15.821 m (4.074)
THEN	the physiological effect IS Stress			
Rule 4:				
IF	Isovist area	IS	Medium	8044.802 m ² (495.337)
	AND Isovist perimeter	IS	Very Low	104.413 m (29.372)
	AND Occlusivity	IS	Medium	281.987 m (17.945)
	AND Compactness	IS	Moderately High	0.5147 (0.027)
	AND Jaggedness	IS	Moderately High	121.743 (7.264)
	AND Maximum visibility	IS	Very High	94.574 m (7.913)
	AND Minimum visibility	IS	Very Low	1.942 m (3.392)
THEN	the physiological effect IS Stress			
Rule 5:				
IF	Isovist area	IS	Very Low	1616.546 m ² (699.152)
	AND Isovist perimeter	IS	Medium	410.722 m (21.284)
	AND Occlusivity	IS	High	458.410 m (19.365)
	AND Compactness	IS	Very High	0.704 (0.032)
	AND Jaggedness	IS	Moderately Low	87.129 (5.447)
	AND Maximum visibility	IS	Very High	94.574 m (7.913)

	Visuospatial configuration		Linguistic label	Dimension (SD)
THEN	AND Minimum visibility the physiological effect IS Stress	IS	Medium	41.930 m (2.969)
Rule 6:				
IF	Isovist area	IS	Medium	8044.802 m ² (495.337)
	AND Isovist perimeter	IS	Low	198.233 m (26.860)
	AND Occlusivity	IS	High	458.410 m (19.365)
	AND Compactness	IS	High	0.596 (0.020)
	AND Jaggedness	IS	Low	60.693 (5.447)
	AND Maximum visibility	IS	Very High	94.574 m (7.913)
	AND Minimum visibility	IS	Moderately Low	29.207 m (2.969)
THEN	the physiological effect IS Stress			
Rule 7:				
IF	Isovist area	IS	Low	4156.807 m ² (495.337)
	AND Isovist perimeter	IS	High	605.518 m (23.312)
	AND Occlusivity	IS	Moderately Low	181.401 m (17.945)
	AND Compactness	IS	Low	0.3038 (0.019)
	AND Jaggedness	IS	Low	60.693 (5.447)
	AND Maximum visibility	IS	Very High	94.574 m (7.913)
	AND Minimum visibility	IS	Medium	41.930 m (2.969)
THEN	the physiological effect IS Stress			
Rule 8:				
IF	Isovist area	IS	Very Low	1616.546 m ² (699.152)
	AND Isovist perimeter	IS	Medium	410.722 m (21.284)
	AND Occlusivity	IS	Very Low	79.555 m (18.095)
	AND Compactness	IS	Moderately Low	0.413 (0.019)
	AND Jaggedness	IS	Very High	179.208 (7.276)
	AND Maximum visibility	IS	Moderately High	73.800 m (2.766)
	AND Minimum visibility	IS	Moderately Low	29.207 m (2.969)
THEN	the physiological effect IS Stress			
Rule 9:				
IF	Isovist area	IS	Moderately High	10321.695 m ² (650.645)
	AND Isovist perimeter	IS	Moderately High	502.173 m (21.284)
	AND Occlusivity	IS	Moderately High	374.510 m (24.058)
	AND Compactness	IS	Moderately Low	0.413 (0.019)
	AND Jaggedness	IS	Moderately High	121.743 (7.264)
	AND Maximum visibility	IS	Very High	94.574 m (7.913)
	AND Minimum visibility	IS	Medium	41.930 m (2.969)
THEN	the physiological effect IS Non-Stress			
Rule 10:				
IF	Isovist area	IS	Medium	8044.802 m ² (495.337)
	AND Isovist perimeter	IS	Very Low	104.413 m (29.372)
	AND Occlusivity	IS	Very High	535.316 m (23.791)
	AND Compactness	IS	Moderately Low	0.413 (0.019)
	AND Jaggedness	IS	Low	60.693 (5.447)

	Visuospatial configuration		Linguistic label	Dimension (SD)
	AND Maximum visibility	IS	Very High	94.574 m (7.913)
	AND Minimum visibility	IS	High	64.747 m (2.969)
THEN	the physiological effect IS Non-Stress			
Rule 11:				
IF	Isovist area	IS	Low	4156.807 m ² (495.337)
	AND Isovist perimeter	IS	Moderately Low	289.448 m (21.284)
	AND Occlusivity	IS	Moderately High	374.510 m (24.058)
	AND Compactness	IS	Low	0.304 (0.019)
	AND Jaggedness	IS	Moderately Low	87.129 (5.447)
	AND Maximum visibility	IS	Moderately High	73.800 m (2.766)
	AND Minimum visibility	IS	Very High	83.398 m (3.559)
THEN	the physiological effect IS Non-Stress			
Rule 12:				
IF	Isovist area	IS	Very High	13700.860 m ² (801.068)
	AND Isovist perimeter	IS	Moderately Low	289.448 m (21.284)
	AND Occlusivity	IS	Moderately High	374.510 m (24.058)
	AND Compactness	IS	Moderately Low	0.413 (0.019)
	AND Jaggedness	IS	Very Low	31.832 (5.447)
	AND Maximum visibility	IS	Very High	94.574 m (7.913)
	AND Minimum visibility	IS	Medium	41.930 m (2.969)
THEN	the physiological effect IS Non-Stress			
Rule 13:				
IF	Isovist area	IS	Moderately High	10321.695 m ² (650.645)
	AND Isovist perimeter	IS	High	605.518 m (23.312)
	AND Occlusivity	IS	Medium	281.987 m (17.945)
	AND Compactness	IS	Very High	0.704 (0.032)
	AND Jaggedness	IS	Very High	179.208 (7.276)
	AND Maximum visibility	IS	Very High	94.574 m (7.913)
	AND Minimum visibility	IS	Low	15.821 m (4.074)
THEN	the physiological effect IS Non-Stress			
Rule 14:				
IF	Isovist area	IS	Very Low	1616.546 m ² (699.152)
	AND Isovist perimeter	IS	Moderately Low	289.448 m (21.284)
	AND Occlusivity	IS	Moderately Low	181.401 m (17.945)
	AND Compactness	IS	Very High	0.704 (0.032)
	AND Jaggedness	IS	Very High	179.208 (7.276)
	AND Maximum visibility	IS	Moderately Low	46.745 m (2.766)
	AND Minimum visibility	IS	Medium	41.930 m (2.969)
THEN	the physiological effect IS Non-Stress			
Rule 15:				
IF	Isovist area	IS	Moderately High	10321.695 m ² (650.645)
	AND Isovist perimeter	IS	Low	198.233 m (26.860)
	AND Occlusivity	IS	Moderately High	374.510 m (24.059)
	AND Compactness	IS	Low	0.304 (0.019)

	Visuospatial configuration		Linguistic label	Dimension (SD)
	AND Jaggedness	IS	Low	60.693 (5.447)
	AND Maximum visibility	IS	Low	34.622 m (4.159)
	AND Minimum visibility	IS	Very High	83.398 m (3.559)
THEN	the physiological effect IS Non-Stress			
Rule 16:				
IF	Isovist area	IS	Very High	13700.860 m ² (801.068)
	AND Isovist perimeter	IS	Moderately High	502.173 m (21.284)
	AND Occlusivity	IS	Moderately High	374.510 m (24.058)
	AND Compactness	IS	Low	0.304 (0.019)
	AND Jaggedness	IS	High	145.087 (5.447)
	AND Maximum visibility	IS	Very High	94.574 m (7.913)
	AND Minimum visibility	IS	Low	15.821 m (4.074)
THEN	the physiological effect IS Non-Stress			
Rule 17:				
IF	Isovist area	IS	Moderately High	10321.695 m ² (650.645)
	AND Isovist perimeter	IS	Moderately Low	289.448 m (21.284)
	AND Occlusivity	IS	High	458.410 m (19.365)
	AND Compactness	IS	Very High	0.704 (0.032)
	AND Jaggedness	IS	Moderately High	121.743 (7.264)
	AND Maximum visibility	IS	Very High	94.574 m (7.913)
	AND Minimum visibility	IS	Very Low	1.942 m (3.392)
THEN	the physiological effect IS Non-Stress			

Note. SD = standard deviation; Compactness and Jaggedness are unitless. Compactness is within the range [0,1].

in a stress physiological response. Hong Kong has a high refuge value because its spatial configuration is enclosed by high-density and high-rise buildings. This explains why ‘refuge’ emerged as the most significant element in a visuospatial configuration. For older adults to experience a non-stress physiological response in a high refuge value environment such as Hong Kong, the spatial configuration should have more open edges (increased occlusivity) and a longer minimum nearest distance to physical boundaries (increased minimum visibility). This finding is quite interesting because it does not conform to the theory of refuge (enclosure evokes a sense of safety) because having more open edges and visibility increases the chances of being seen by other people. It is plausible that these isovist indicators (i.e., minimum visibility and occlusivity) captured the claustrophobic element in older adults’ reaction, where

a visuospatial configuration that is too enclosed triggers claustrophobic tendencies, causing an increase in physiological stress.

While the claustrophobic tendency explains the reason for such physiological response, there might actually be more to it than that. A spatial configuration with more open edges (high occlusivity) tends to promise more information (mystery). Older adults are even more likely to experience non-stress physiological response due to an increase in mystery when the field of view is between 90° and 180° . Therefore, creating a visuospatial configuration with high mystery might as well reduce the tendency of feeling claustrophobic among older adults.

Isovist area is another influential determinant of physiological response; its influence increases with an increasing field of view. The behavioural and experience relevance of the isovist area corresponds to “prospect” in the prospect-refuge theory. The perimeter and maximum visibility length also quantify the prospect theory. Older adults experienced a non-stress physiological response when the environment offers a configuration conducive to attaining a larger view, while a stress physiological response is experienced when the view is small. According to the prospect theory, being able to “fetch” information from all spaces at an observation point in a large space induces a sense of security. This explains why older adults experienced non-stress physiological response when prospect elements (isovist area, perimeter, and maximum visibility length) increase.

Isovist area, compactness and maximum visibility became increasingly influential when the field of view increases. This could be because the distribution of visuospatial information increases with an increasing field of view. The complexity and mystery in the environment become more relevant when the field of view increases which can either cause humans to

display preference or aversion depending on the varying proportions of the elements in the spatial configuration. Specifically, older adults experienced physiological stress when spatial complexity increases (i.e., increased compactness); this physiological stress due to complexity is even more likely when the field of view increases.

This study demonstrates that the multi-objective evolutionary rule-based system has the potential to generate visuospatial configurations that produce a specific visuospatial effect. A more critical look into the generated rules shows that weakness in any specific quality (e.g., lack of prospect elements due to layout restrictions) can be compensated for with the strength in others (e.g., increasing the value of mystery).

7.5.1 Comparison with Similar Studies

Previous researchers (as shown in Table 7.6) that have studied this topic mainly focused on younger adults with an average age of about 25 years. These studies were conducted in Switzerland, Germany, and Hong Kong. Interestingly, there are some differences and commonalities between the impact of visuospatial configurations on younger adults and older adults.

Study 1 and Study 5 finds that younger adults prefer urban spaces that are enclosed in order for them to feel safe. These findings on younger adults are contrary to the current finding on older adults; older adults feel claustrophobic (leading to physiological stress) when the urban spaces are too enclosed or when they are too close to a physical boundary (e.g., a wall). Older adults show a preference for spaces that are not too enclosed with more open edges in order for them to be seen by other pedestrians. Study 3 and Study 4 reports that younger adults perceived spaces with high visibility and perimeter to be stressful because they can be seen from a larger

Table 7.6: Summary of previous studies

Study	Background	Visuospatial element	Influence
Study 1: Li et al. (2016)	Participants' mean age: 25 (2.5 standard deviation) Experiment location: Zürich, Switzerland Data: Skin conductivity	Compactness	Higher compactness causes positive emotion
		Maximum visibility	Higher visibility causes positive emotion
		Refuge value (minimum visibility or occlusivity)	Enclosed urban spaces are very important in fostering a sense of security in pedestrians
Study 2: Hijazi et al. (2016)	Participants: Students and lecturers Experiment location: Zürich, Switzerland Data: Skin conductivity	Occlusivity (60°)	Significant for predicting negative emotional arousal
		Perimeter (360°)	Significant for predicting negative emotional arousal
		Compactness (360°)	Significant for predicting positive emotional arousal
		Perimeter (60°)	Significant for predicting positive emotional arousal
Study 3: Knöll et al. (2018)	Participants' median age: 25 years (range 22 to 35, 2.2 standard deviation) Experiment location: Darmstadt, Germany Data: Questionnaire to collect perceived urban stress	Visibility	Visibility is positively related to perceived urban stress
		Perimeter	Perimeter is positively related to perceived urban stress
		Isovist vertices numbers (indicates the complexity)	Isovist vertices numbers relate negatively to perceived urban stress
		Visibility and perimeter Vertices number	Outdoor spaces visibility and perimeter, which describe the shape of a space and vertices number, which indicates the complexity of a shape, are more important isovist characteristics to explain perceived urban stress.
Study 4: Ojha et al. (2019)	Participants' mean age: Not provided Experiment location: Zürich, Switzerland Data: Skin conductivity	Isovist area	High value of isovist area resulted in an aroused physiological state
		Perimeter	Data was collected but result not reported
		Compactness	Data was collected but result not reported
		Occlusivity	Data was collected but result not reported
Study 5: Xiang et al. (2020)	Participants' mean age: 24.77 years (0.718 standard deviation) Experiment location: Hong Kong	Isovist area (90°)	Negatively related to negative emotion
		Compactness	Insignificant
		Isovist drift angle (90°)	Negatively related to negative emotion

Study	Background	Visuospatial element	Influence
	Data: Skin conductivity	Isovist drift magnitude (90°, 120°, 180°)	Negatively related to negative emotion
		Max-radial (90°, 120°)	Negatively related to negative emotion
		Occlusivity	Insignificant
		Perimeter (90°, 120°)	Negatively related to negative emotion
		Jaggedness (90°, 120°, 180°)	Positively related to negative emotion
		Enclosure (refuge value)	To avoid negative emotions, a space must be enclosed to guarantee a sense of security

area. In contrast, older adults experienced a non-stress physiological response when urban spaces have a larger view and perimeter because they are able to see all their surroundings which heighten the feeling of security. In summary, older adults prefer urban spaces where they can be seen, while younger adults prefer spaces where they cannot be seen.

While Study 1 and Study 2 conclude that higher compactness causes positive emotions for younger adults, this current study indicates that higher compactness causes physiological stress for older adults. The results from Study 3 shows that younger adults are more likely to perceive an urban space with low complexity (measured using isovist vertices numbers) as stressful. However, Study 5 presented that high complexity (measured using jaggedness) is related to younger adults' negative emotions. In this current study, older adults felt stressed when complexity (measured using jaggedness) increases.

While these differences are worth sharing, theoretically, it should be noted that the spatial layout, living arrangement, and cultural background in these countries are different, which can influence an individual's response. Methodologically, all these studies, including the presented study, were limited to two dimensional isovist which omits other relevant spatial factors. Study

1, 2, 4 and 5 used only physiological responses for their analysis and Study 3 used only perceived responses for their analysis. This study combined both perceived and physiological responses.

7.6 Chapter Summary

This chapter aimed to understand the influence of visuospatial configurations of urban space on older adults' physiological stress. The study further presented an integrated methodology based on machine learning and an evolutionary rule-based system to achieve this aim. The following conclusions were made. (1) Isovist minimum visibility, occlusivity, and isovist area are the most influential determinants of older adults' physiological response. (2) Older adults experienced non-stress physiological response when prospect elements (isovist area, perimeter, and maximum visibility length) increase. (3) Older adults feel stressed when the environment is too enclosed. (4) Isovist indicators can complement one another to achieve a specific physiological effect. (5) In comparing older adults and younger adults, older adults prefer urban configurations where they can be seen, while the younger adults prefer spaces where they cannot be seen. Overall, the findings from this study can be used to inform urban design and planning.

PART V: RESEARCH CONCLUSION

CHAPTER 8

CONCLUSIONS AND RECOMMENDATIONS⁸

8.1 Summary of Research

With the current rate of population ageing and the ageing of built environment infrastructure—double ageing—urban planners and municipal decision-makers need a more efficient approach to continuously assess and detect excessively demanding environmental conditions to promote active ageing. The overall goal of this research is (1) to enable practitioners to detect stressful older adults-environment interactions in near real-time and (2) to bring to the limelight the influence of urban environment configurations on older adults' stress response. Four specific

⁸ This chapter is based on studies that are published or currently under consideration for publication.

Torku, A., Chan, A.P.C., Yung, E.H.K., Seo, J. (2021). The influence of urban visuospatial configuration on older adults' stress: A wearable physiological-perceived stress sensing and data mining based-approach, *Building and Environment*, 108298. <https://doi.org/10.1016/j.buildenv.2021.108298>

Torku, A., Chan, A.P.C., and Yung, E.H.K. (2021). Implementation of age-friendly initiatives in smart cities: Probing the barriers through a systematic review, *Built Environment Project and Asset Management*, 11(3), 412-426. <https://doi.org/10.1108/BEPAM-01-2020-0008>

Torku, A., Chan, A.P.C., and Yung, E.H.K. (2021). Age-friendly cities and communities: A critical review and future directions, *Ageing & Society*, 41(1), 2242-2279. <https://doi.org/10.1017/S0144686X20000239>

Torku, A., Chan, A.P.C., Yung, E.H.K., Seo, J. (2021). Wearable sensing and mining of the informativeness of older adults' bodily responses to detect demanding environmental conditions, *Environment and Behavior*. (Under Review). E&B-20-0532.R2

Torku, A., Chan, A.P.C., Yung, E.H.K., Seo, J. (2021). Learning to detect older adults' environmental stress hotspots to improve neighbourhood mobility: A multimodal physiological sensing, machine learning and risk hotspot analysis-based approach, *Cities* (Under Review). JCIT-D-21-01443

objectives were identified to achieve this goal. The specific objectives are (1) to assess the informativeness of people's bodily responses (i.e., physiological, behavioural, and cognitive responses) to different environmental conditions, (2) to examine the relationships in older adults' bodily responses resulting from their interaction with the environment, (3) to detect older adults' stressful environmental interactions in near-real time, and (4) to examine the influence of visuospatial configuration of urban space on older adults' stress response. To achieve these objectives, this research harnessed the current advances in wearable sensing technologies to collect older adults' bodily responses to their interaction with the environment as a means of assessing and detecting environmental barriers. A summary of how the four specific objectives were achieved is presented in the following.

8.1.1 Objective 1: To Assess the Informativeness of People's Bodily Responses

This objective was achieved by extracting several features from sensed physiological (heart rate, heart rate variability, and electrodermal activity), cognitive (electroencephalography), and behavioural (foot plantar pressure distribution and contact forces, and 3-axis acceleration data) responses to different environmental conditions. A framework based on information entropy, symmetric uncertainty, correlation analysis, and Random Forest algorithm was developed to assess the informativeness of people's bodily response. The framework provides individual informative features and an optimum set of informative features with their respective performance.

The extracted features from the sensed physiological (heart rate, heart rate variability, and electrodermal activity), cognitive (electroencephalography), and behavioural (foot plantar pressure distribution and contact forces, and 3-axis acceleration data) responses were analysed using the developed framework to understand how much information a feature gained about

older adults' interaction and experience in the outdoor environment. The results show that older adults' physiological response is more informative than the cognitive and behavioural responses. The informativeness of the cognitive response was affected by the walking activity, and the gait abnormality among older adults affected their behavioural responses. The rest of the objectives only considered older adults' physiological responses.

8.1.2 Objective 2: To Examine the Relationships in Older Adult's Bodily Responses Resulting from their Interaction with the Environment

A Wilcoxon signed-rank test was conducted to understand whether the physiological responses to environmental conditions perceived as non-stress was statistically and significantly different from environmental conditions perceived as stress. Spatial clustering analysis was performed using Getis-Ord General G to confirm whether there is any spatial association in participants' physiological responses. A hot spot analysis using Getis-Ord G_i^* statistics was conducted to determine locations on the path that stimulated a common physiological response among multiple participants. The study introduced a space-time pattern mining approach to spatiotemporally aggregate older adults' physiological responses.

The result indicated that, on average, participants experienced a statistically significant higher physiological response at environment conditions perceived as non-stress than environment conditions perceived as stress. The spatial clustering analysis and the space-time pattern mining confirmed that multiple participants' physiological responses are spatially associated and possess some common characteristics. The results further demonstrate that the relationships between older adults' physiological response and the environmental condition are less apparent at the individual level. An individual's pace, walking behaviour, level of observation, physical characteristics, gender, data source (i.e., the related organ) and time-dependent environmental

factors influenced their physiological responses to stress and non-stress environmental conditions. However, using collective sensing (aggregating multiple participants' physiological responses) can accommodate the individual variability and capture any normality in the data, which is indicative of an environment's condition. The collective physiological responses are consistent with the older adults' perceived assessment and the observers' audit of the environment's condition.

8.1.3 Objective 3: To Detect Older Adults' Stressful Environmental Interactions in Near-Real Time

Several machine learning algorithms, including Gaussian Support Vector Machine, Ensemble bagged tree, and deep belief network were trained and tested to detect (1) stress and non-stress human-environment interactions and (2) low-stress and high-stress human-environment interactions using an optimum set of informative features. The optimum set of informative features included older adults' physiological responses, environmental and location data; it was determined using the framework developed in Objective 1. Older adults' perceived stress assessment was used as labels. The Ensemble bagged tree algorithm achieved the best performance among the tested algorithms. The Ensemble bagged tree algorithm detected older adults' stressful interactions with an accuracy of 98.13% (for detecting stress and non-stress samples) and 98.25% (for detecting low and high-stress samples). The detected stressful interactions were visualised using kernel density estimation. Overall, the detected stress and high-stress samples matched older adults perceived stress assessment of the path. A simulation-based approach was used to detect areas within the study area that are sufficiently powered to detect stress hot spot that pose higher risk to older adults.

8.1.4 Objective 4: To Examine the Influence of Visuospatial Configuration of Urban Space on Older Adults' Stress Response

An integrated methodology based on machine learning and an evolutionary rule-based system was developed to further our understanding of the influence of visuospatial configurations of urban space on older adults' physiological stress. Isovist analysis was conducted to represent older adults' perceived visual elements in the urban environment from 90°, 120°, and 180° fields of view. Older adults' stress responses due to spatial factors were detected using their physiological-perceived stress and spatial clustering analysis.

The result revealed that isovist minimum visibility, occlusivity, and isovist area are the most influential determinants of older adults' physiological response. Older adults experienced a non-stress physiological response when prospect elements (isovist area, perimeter, and maximum visibility length) increase and older adults feel stressed when the environment is too enclosed. Isovist indicators can complement each other to achieve a specific physiological effect. In comparing older adults and younger adults, older adults prefer urban configurations where they can be seen, while younger adults prefer spaces where they cannot be seen.

8.2 Contribution to Knowledge, Practice and Impact

8.2.1 Contributions to Academia

The following models and frameworks were developed and tested in this study:

- An information mining-based methodological framework was developed to assess the relevance and informativeness of people's bodily responses
- A space-time pattern mining approach is introduced to spatiotemporally aggregate older adults' physiological responses
- An optimised environmental risk stress hot spot detection framework

- A machine learning and evolutionary rule-based system to examine the influence and generate visuospatial configurations that produce a specific physiological effect

The models and frameworks provide a computational foundation for future studies to develop applications and new computational approaches to improve neighbourhood walkability in smart and age-friendly cities. With increasing urban ageing, cities need to evolve and adapt; new computational approaches to urban system design and management have the opportunity to make cities the best environment to accommodate older adults.

8.2.2 Incorporating the Elderly-centric Wearable Sensing-based Approach into Urban Planning

This study shows that assessing the walkability or quality of the built environment features using either a site audit (i.e., EAST-HK, SWEAT-R, or other audit tools) or the elderly-centric wearable sensing-based approach alone does not provide a holistic perspective of the built environment for older adults. It is of paramount importance to measure both the exposure environment and the outcomes of the exposure to the environment in order to understand the potential effect of the built environment on people (Cerin et al., 2011). These findings indicate that the site audit is more accurate at assessing the exposure environment, but it is limited in assessing the outcome of the exposure. However, the elderly-centric wearable sensing-based approach is more accurate at assessing the outcome of the exposure but limited in assessing the exposure environment. For instance, the site auditors can identify demanding environmental conditions (i.e., environmental barriers), but they cannot differentiate between an environmental feature that is demanding for one person and non-demanding for another person. The elderly-centric wearable sensing-based approach can determine a person's reaction to

different environmental conditions or how different people react to the same environmental condition but cannot provide a detailed assessment of the underlying environmental conditions.

It is recommended that the elderly-centric wearable sensing-based approach should be used as an early warning system. If a location is detected as a high-risk stress hot spot, a system could notify urban planners or municipal decision-makers. Then, trained observers can use predefined protocols or tools (e.g., EAST-HK and SWEAT-R) to identify environmental barriers within these high-risk stress hot spots. While identifying these high-risk stress hot spots is essential, it is only the first step to creating an AFCC. How the identified environmental barriers are addressed is critical to improving the well-being and participation of older adults in outdoor activities. Table 8.1 presents a few recommendations based on the WHO AFCC guide (WHO, 2007) to address the identified environmental barriers in this study. Although these recommendations can be adapted and adopted in other cities and communities, it not a gold standard.

It is important to mention that the stress hot spots were identified through older adults-centred approach; this is motivated by the fact that involving older adults is very important in evaluating the age-friendliness of the environment (WHO, 2007; Torquato et al., 2021). Therefore, urban planners should adopt a bottom-up approach—with a supportive top-down back-up—throughout the process of addressing these stress hot spots; in this way, older adults become place-makers.

Table 8.1: Age-friendly recommendations to address environmental barriers

Domain	Environmental barrier	WHO (2007) Age-friendly guide
Functionality	<ul style="list-style-type: none"> ▪ Path condition (wet and slippery streets) ▪ Path slope ▪ Path obstruction ▪ Major barriers (roadwork, steep staircases) ▪ Minor barriers (cracks, holes, bumps, parking meters) ▪ Street crowd ▪ Motor vehicles parked on footpath ▪ Hawkers and shops on streets ▪ Path width ▪ Path material ▪ Curb cut features ▪ Permeability 	<ul style="list-style-type: none"> ▪ Well-maintained paths with smooth, level, and non-slip surface ▪ The path width should be sufficient to accommodate wheelchairs ▪ The path should have dropped curbs that taper off to be level with the road ▪ The path should be free from obstructions such as street vendors, parked cars, trees, dog droppings, snow ▪ Pedestrians have priority of use
Safety	<ul style="list-style-type: none"> ▪ Pedestrian crossing ▪ Traffic load ▪ Traffic calming devices ▪ Streetlight ▪ Directional sign ▪ Presence of people ▪ Signs of crime/disorder ▪ Stray dogs /other animals 	<ul style="list-style-type: none"> ▪ Roads should have a non-slip, regularly spaced pedestrian crossing ▪ Roads should have well-designed and appropriately placed physical structures, such as traffic islands, overpasses, or underpasses, to assist pedestrians in crossing busy roads ▪ Pedestrian crossing lights should allow sufficient time for older adults to cross the road ▪ Pedestrian crossing lights should have visual and audio signals ▪ Strict enforcement of traffic rules and regulations ▪ Drivers should give way to pedestrians ▪ Good street lighting and visible directional sign ▪ Police patrols to ensure safety ▪ Enforcement of by-laws, support for community and personal safety initiatives
Aesthetics	<ul style="list-style-type: none"> ▪ Views ▪ Building attractiveness ▪ Attractive natural sights 	<ul style="list-style-type: none"> ▪ Regular cleaning of city and community ▪ Enforce regulations to limit noise levels and unpleasant odours

Destination	<ul style="list-style-type: none"> ▪ Streetscape ▪ Litter ▪ Graffiti ▪ Pollution (noise and air) ▪ Greenery ▪ Transport-related ▪ Public open space ▪ Recreational ▪ Government/public services ▪ Public facilities ▪ Commercial destinations 	<ul style="list-style-type: none"> ▪ Well-maintained and safe green spaces with easily accessed seating, shelter, and toilet ▪ Graffiti removal ▪ Available and well-maintained outdoor seating spaced at regular intervals and patrolled to ensure safe access by all ▪ Services are easily accessed and located near older adults ▪ Special customer service arrangement for older adults
-------------	--	--

8.2.3 Research Impact

In addition to the academic and practical significance, this study will have a sustained impact on (1) Older adults, (2) Society and community, (3) Urban planners and policymakers, (4) the economy.

Older Adults

The elderly-centric wearable sensing-based approach is centred on the older adults—it considers older adults as place-makers—therefore, they are engaged and directly involved in creating age-friendly interventions. Relying on these wearable sensors (especially the smart wristband) will cause less interference with their daily routines. Over the long term, this study will contribute to creating environments that are inclusive and accessible to promote active ageing.

Society and Community

As with many inclusive features, identifying older adults' stress hot spots and adopting age-friendly initiatives to address these stress hot spots could be advantageous for all generations. If a street is 'friendly' to older adults, it is likely to be 'friendly' to everyone. For example, a street that older adults find easy to use might be more walkable for someone carrying luggage or a parent with a toddler in a stroller.

Urban Planners and Policymakers

Currently, built environment assessments are conducted by trained observers (for neighbourhood inspection) from governmental departments. The intervals between assessments are generally long due to limited staff, budget and other resources. The combined use of the observational assessment approach and the elderly-centric wearable sensing-based

approach has the potential to improve neighbourhood assessment in cities and communities. The elderly-centric wearable sensing-based approach will enable urban planners and policymakers to identify stress risk hot spots; they can prioritise, plan, monitor, and allocate resources to these high-risk hot spots.

The Economy

In the long term, this study will provide a cost-effective approach to tackling double ageing. Ageing built environment infrastructure with high risk will be detected, and appropriate interventions can be taken to rectify their design or renovation. At the same time, more older adults—the fastest growing population—will age actively. An active ageing population will reduce the massive pressure on the already gridlocked medical, social welfare and elderly support services system in Hong Kong and worldwide.

8.3 Limitations and Future Research

Although the experiment findings are very promising, several limitations need to be mentioned. The number of participants is relatively small, and future studies should include larger and more diverse participants. The unequal number of male and female participants in the study may affect the results because gender can significantly impact human perception and physiological, behavioural, and cognitive responses to environmental conditions. The field experiment was conducted on a predefined path, and the environmental walk lasted for only a few days. In the urban environment, people decide whether to use a path or not; therefore, restricting older adults to a particular path may affect how they interact with the environment. For the purpose of this study, it was necessary to have older adults interact with the same path to facilitate a more direct comparison of their bodily response, their perceived assessments and

the observers' audit of the path. Future studies should consider collecting data in a free-form environment where participants are not be restricted to any particular path.

Although the wearable sensors deployed in this study were demonstrated to the participants to increase their familiarity and acceptance of the sensors, there is a possibility that wearing some of the sensors, particularly the EEG headset in public, may have negatively influenced the data collection. Unlike the wristband and insole sensor, the EEG headset is not a subtle device. The public's reactions towards the participants wearing this sensor may have caused discomfort and stress to the participants. This shows that the wider public's perception and acceptance of wearable sensors are critical for effective elderly-centric sensing in outdoor environments. The EEG headset used in this had wet electrodes, which means that a conductive gel must be applied between the electrode and the scalp for a reliable measurement. Because this study was conducted in a naturalistic environment, the conductive gel might have dehydrated, which might have affected the stability of the EEG sensor of some participants. Future studies should explore the possibility of using other types of electrodes.

Further research should be conducted to understand the influence of surface characteristic and appearance (e.g., material, texture, and colour) on older adults' physiological stress. The generative potential of the multi-objective evolutionary algorithm should be exploited to generate geometrical designs with specific physiological effects that can fit into new or existing space in the urban environment. Conducting this research in a real-world setting makes it impossible to ensure that all participants experienced the same environmental conditions. However, conducting this research in a real-world setting was necessary to achieve ecological validity. Future researchers should explore a hybrid environmental condition, i.e., a combination of real-world and virtual environment settings.

APPENDIX A

TINETTI ASSESSMENT TOOL

Tinetti Assessment Tool: Balance

PARTICIPANT NAME: _____

Initial Instructions: Subject is seated on a hard, armless chair. The following maneuvers are tested.

TASK	DESCRIPTION OF BALANCE	Possible	Score	Date
1. SITTING BALANCE	Leans or slides in chair	0		
	Steady, safe	1		
2. RISES FROM CHAIR	Unable without help	0		
	Able, uses arms to help up	1		
	Able without using arms	2		
3. ATTEMPTS TO RISE FROM CHAIR	Unable without help	0		
	Able, requires > 1 attempt	1		
	Able to rise in 1 attempt	2		
4. IMMEDIATE STANDING BALANCE (first 5 seconds)	Unsteady (swaggers, moves feet, trunk sways)	0		
	Steady but uses walker or other support	1		
	Steady without walker or other support	2		
5. STANDING BALANCE	Unsteady	0		
	Steady but wide stance (heels 4 inches apart) and uses cane or other support	1		
	Narrows stance without support	2		
6. NUDGED (subject at max position with feet as close together as possible, examiner pushes lightly on subject's sternum with palm of hand 3 times)	Begins to fall	0		
	Staggers, grabs, catches self	1		
	Steady	2		
7. EYES CLOSED (at max position – see #6 above)	Unsteady	0		
	Steady	1		
8. TURNING 360 DEGREES	Discontinuous steps	0		
	Continuous steps	1		
	Unsteady (grabs, swaggers)	0		
	Steady	1		
9. SITTING DOWN	Unsafe (misjudged distance, falls into Chair)	0		
	Uses arms or not a smooth motion	1		
	Safe, smooth motion	2		
BALANCE SCORES:				

DATE OF ASSESSMENT	ASSESSOR SIGNATURE AND TITLE	LOCATION DURING ASSESSMENT

Tinetti Assessment Tool: Gait

PARTICIPANT NAME: _____

Initial Instructions: Subject stands with examiner, walks down the hallway or across the room, first at “usual” pace, then back at “rapid but safe” pace. Use usual walking aid.

TASK	DESCRIPTION OF BALANCE	Possible	Score	Date
10. INITIATION OF GAIT (immediately after told to “go)	Any hesitancy or multiple attempts to start	0		
	No hesitancy	1		
11. STEP LENGTH AND HEIGHT	RIGHT swing foot does not pass left stance foot with step	0		
	RIGHT foot passes left stance foot	1		
	RIGHT foot does not clear floor completely with step	0		
	RIGHT foot completely clears floor	1		
	LEFT swing foot does not pass right Stance foot with step	0		
	LEFT foot passes right stance foot	1		
	LEFT foot does not clear floor Completely with step	0		
	LEFT foot completely clears floor	1		
12. STEP SYMMETRY	RIGHT AND LEFT step length not equal (estimate)	0		
	RIGHT AND LEFT step appear equal	1		
13. STEP CONTINUITY	Stopping or discontinuity between steps	0		
	Steps appear to continue	1		
14. PATH (estimated in relation to floor tiles, 12-inch diameter. Observe excursion of 1 foot over about 10 feet of the course)	Marked deviation	0		
	Mild/moderate deviation or uses walking aid	1		
	Straight without walking aid	2		
15. TRUNK	Marked sway or uses walking aid	0		
	No sway – but flexion of knees or back, or spreads arms out while walking	1		
	No sway, no flexion, no use of arms, and no use of walking aid	2		
16. WALKING STANCE	Heels apart	0		
	Heels almost touching while walking	1		
		Score – GAIT:		
		Score – BALANCE:		
		Total Score: BALANCE & GAIT:		

DATE OF ASSESSMENT	ASSESSOR SIGNATURE AND TITLE	LOCATION DURING ASSESSMENT

APPENDIX B

THE MINI-MENTAL STATE EXAMINATION

The Original Version of the Mini-Mental State Examination

		“MINI-MENTAL STATE”
Maximum Score	Achieved Score	
ORIENTATION		
5		What is the (year) (season) (date) (day) (month)?
5		Where are we: (state) (county) (town) (hospital) (floor).
REGISTRATION		
3		Name 3 objects: 1 second to say each. Then ask the patient all 3 after you have said them. Give 1 point for each correct answer. Then repeat them until he learns all 3. Count trials and record.
ATTENTION AND CALCULATION		
5		Serial 7’s. 1 point for each correct. Stop after 5 answers. Alternatively spell “world” backwards.
RECALL		
3		Ask for the 3 objects repeated above. Give 1 point for each correct.
LANGUAGE		
9		Name a pencil, and watch (2 points) Repeat the following “No ifs, ands or buts.” (1 point) Follow a 3-stage command: “Take a paper in your right hand, fold it in half, and put it on the floor” (3 points) Read and obey the following: CLOSE YOUR EYES (1 point) Write a sentence (1 point) Copy design (1 point)
30		Total score

The Cantonese Version of the Mini-Mental State Examination

簡短智能測驗

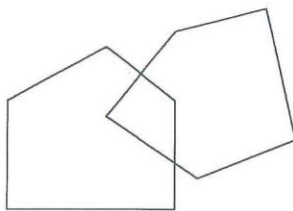
最高

分數 分數

- 5 () 依家係乜野日子(年份)(季節)(月份)(幾號)(星期幾)?
- 5 () 我地依家係邊嘅?
(九龍/新界/香港)(九龍/新界/香港既邊度)(醫院)(邊層樓)(病房)
或:(九龍/新界/香港)(九龍/新界/香港既邊度)(邊一科診所)(診所名字)
(邊層樓)
或:(九龍/新界/香港)(九龍/新界/香港既邊度)(邊條街)(邊一座)(邊層樓)
或:(九龍/新界/香港)(九龍/新界/香港既邊度)(邊個屋村)(中心名字)
(邊層樓)
- 3 () 依家我會講三樣野既名, 講完之後, 請你重複一次。
請記住佢地, 因為幾分鐘後, 我會叫你再講番俾我聽。
[蘋果]、[報紙]、[火車]。依家請你講番哩三樣野俾我聽。
(以第一次講的計分, 一個一分; 然後重複物件, 直至全部三樣都記住。)
- 5 () 請你用一百減七, 然後再減七, 一路減落去, 直至我叫你停為止。
(減五次後便停) ()
或: 依家我讀幾個數目俾你聽, 請你倒轉頭講番出黎。
[4 2 7 3 1] ()
- 3 () 我頭先叫你記住既三樣野係乜野呀?
- 9 () 哩樣係乜野? (鉛筆)(手錶)。(2)
請你跟我講句說話 [姨丈買魚腸](1)
依家檯上面有一張紙。用你既右手拿起張紙, 用兩隻手一齊將紙摺成一半, 然後放番張紙係檯上面。(3)
請讀出哩張紙上面既字, 然後照住去做。(1)
請你講任何一句完整既句子俾我聽。例如: [我係一個人]、
[今日天氣好好]。(1)
哩處有幅圖, 請你照住黎畫啦。(1)

總分: _____

拍手



APPENDIX C

INTEGRATED VERSION OF THE EAST-HK WITH SWEAT-R ASSESSMENT TOOL

Observer ID			
Date (mm/dd/yy)			
Segment ID			
Start time			
Temperature (°C)			
Humidity (%)			
Is it raining?			
Weather (eg. Grey & misty; Sunny & warm; Sunny & cold; Very sunny & warm; Cloudy & cold)			
FUNCTIONALITY			
Buildings		Response (Mark as appropriate)	Notes
<i>Building type</i>			
Single-family home			
Multi-family home			
4–6 floors apartment blocks			
7–12 floors apartment blocks			

13–20 floors apartment blocks			
Over 20 floors apartment blocks			
Walking surface			
<i>Type of path</i>			
Bike lanes			
Footpaths			
Covered footpaths			
Indoor air-conditioned places for walking			
Bridge/overpass or tunnel			
<i>Path condition</i>			
Footpaths well-maintained			
Wet and slippery streets			
<i>Path slope</i>			
Hilly streets	Flat/Gently		
	Moderate		
	Steep		
<i>Path obstructions</i>			
Major barriers (roadwork, steep staircases)			
Minor barriers (cracks, holes, bumps, parking meters)			
Street crowded	(Give an estimate of number of people/moving objects per minutes if possible)		
Motor vehicles parked on footpath			
Hawkers and shops on streets			

<i>Path width (in meters)</i>			
<i>Path material</i>			
Concrete/Asphalt			
Brick/Tile			
Dirt/Gravel/Grass/Lawn			
Other			
<i>Curb cut features</i>			
Presence of a curb cut			
Groove or bumps			
Colour contrast with ground surface			
Material contrast with ground surface			
Measured maximum curb height at this segment (in inches)			
<i>Permeability</i>			
<i>Street connectivity</i>			
Cul-de-sacs			
More than 3 intersections in segment			
<i>Other points of access</i>			
Need to cross bridge/overpass to access services			
Overall Rating for Functionality	Poor		
	Moderate		
	Good		
SAFETY			
Personal			
<i>Street lighting</i>	(count street light if present)		

<i>Stray dogs /other animals</i>			
<i>Presence of people</i>	(Give an estimate of number of people if possible)		
Adults or teenagers			
Older people			
Children			
People talking and greeting each other			
<i>Signs of crime/disorder</i>			
People fighting			
Prostitutes			
Homeless people			
Needles/syringes			
Traffic			
<i>Road type</i>			
Freeway	(Passing vehicles per minute)		
<i>Traffic load</i>			
Dirt/grass strip			
Crossing aids			
Parked vehicles make it difficult to see incoming traffic			
Aggressive drivers			
<i>Pedestrian safety</i>			
Traffic calming devices (stop light; traffic island; crosswalk)			
Fence or dirt/grass strip			
Crossing aids			

Parked vehicles make it difficult to see incoming traffic			
Aggressive drivers			
Overall Rating for Safety	Poor		
	Moderate		
	Good		
AESTHETICS			
Views			
<i>Building attractiveness</i>			
Attractive buildings	None		
	Few		
	Some		
	All/Almost		
Abandoned/vacant buildings	None		
	Few		
	Some		
	All/Almost		
<i>Attractive natural sights</i>	None		
	Few		
	Some		
	All/Almost		
Streetscape			
<i>Litter</i>			
Litter	Yes, dominant feature		
	Yes, but not dominant feature		
	None or almost none		

Broken bottles and cans	Yes, dominant feature		
	Yes, but not dominant feature		
	None or almost none		
Dog/animal fouling	Yes, dominant feature		
	Yes, but not dominant feature		
	None or almost none		
<i>Graffiti</i>	Yes, dominant feature		
	Yes, but not dominant feature		
	None or almost none		
<i>Pollution</i>			
Noise pollution	None		
	Low		
	Moderate		
	High		
Air pollution	None		
	Low		
	Moderate		
	High		
<i>Presence of trees</i>	(Count mature trees if present)		
Overall Rating for Aesthetics	Poor		
	Moderate		
	Good		

DESTINATIONS

<i>Transport-related</i>			
Parking lot			
Public transit/bus stop			
<i>Public open space</i>			
Parks			
Beach			
Playground			
<i>Recreational</i>			
Outdoor sport fields			
Swimming pool			
Gym/fitness facility			
<i>Government/public services</i>			
Museum			
Community/elderly centre			
Police department			
Health services			
Primary school			
Other schools			
Religious places			
Library			
Post-office			
<i>Public facilities</i>			
Benches/places for sitting			
Public toilets			
<i>Commercial destinations</i>			
Convenience store			
Supermarket			
Fresh food			

Hardware store			
Clothing			
Pharmacy			
Book/stationary			
Chained fast food			
Chinese coffee/tea			
Chinese non-fast food			
Western/international non-fast food			
Western/international coffee shop			
Bakery			
Hotel			
Warehouse			
Betting branches			
Movies/theatre			
Office buildings			
Banks			
DVD/video hire			
Laundry			
Salon/barber			
Overall Rating for Segment	Poor		
	Moderate		
	Good		

REFERENCES

- Acharya, U. R., Joseph, K. P., Kannathal, N., Lim, C. M., & Suri, J. S. (2006). Heart rate variability: A review. *Medical and Biological Engineering and Computing*, *44*(12), 1031-1051.
- Adolph, K. (2020). 48 ecological validity: mistaking the lab for real life. In Sternberg, R. (Ed.), *My biggest research mistake: Adventures and misadventures in psychological research* (pp. 187-190). US: SAGE Publications, Inc.
- Aghaabbasi, M., Moeinaddini, M., Shah, M. Z., Asadi-Shekari, Z., & Kermani, M. A. (2018). Evaluating the capability of walkability audit tools for assessing sidewalks. *Sustainable Cities and Society*, *37*, 475-484.
- Agmon, M., & Armon, G. (2016). A cross-sectional study of the association between mobility test performance and personality among older adults. *BMC Geriatrics*, *16*(1), 105.
- Alberdi, A., Aztiria, A., & Basarab, A. (2016). Towards an automatic early stress recognition system for office environments based on multimodal measurements: A review. *Journal of Biomedical Informatics*, *59*, 49-75.
- Alley, D., Liebig, P., Pynoos, J., Banerjee, T., & Choi, I. H. (2007). Creating elder-friendly communities: Preparations for an aging society. *Journal of Gerontological Social Work*, *49*(1-2), 1-18.
- Alvarsson, J. J., Wiens, S., & Nilsson, M. E. (2010). Stress recovery during exposure to nature sound and environmental noise. *International Journal of Environmental Research and Public Health*, *7*(3), 1036-1046.
- Antwi-Afari, M. F., Li, H., Seo, J., & Wong, A. Y. L. (2018). Automated detection and classification of construction workers' loss of balance events using wearable insole pressure sensors. *Automation in Construction*, *96*, 189-199.
- Appleton, J. (1975). *The experience of landscape*. London: John Wiley & Sons.
- Aspinall, P. A., Borooah, S., Al Alouch, C., Roe, J., Laude, A., Gupta, R., Gupta, M., Montarzino, A., & Dhillon, B. (2014). Gaze and pupil changes during navigation in age-related macular degeneration. *British Journal of Ophthalmology*, *98*(10), 1393-1397.

- Austin, C., McClelland, R., Sieppert, J., Holinda, D., Hartley, D., & Flux, D. (2001). *A Place to Call Home: The Final Report of the Elder Friendly Communities Project*. Calgary, Canada: Faculty of Social Work, The University of Calgary.
- Bailey, A. W., Allen, G., Herndon, J., & Demastus, C. (2018). Cognitive benefits of walking in natural versus built environments. *World Leisure Journal*, 60(4), 293-305.
- Barbosa, J., Tavares, J., Cardoso, I., Alves, B., & Martini, B. (2018). TrailCare: An indoor and outdoor Context-aware system to assist wheelchair users. *International Journal of Human-Computer Studies*, 116, 1-14.
- Barnett, A., Cerin, E., Ching, C. S., Johnston, J. M., & Lee, R. S. (2015). Neighbourhood environment, sitting time and motorised transport in older adults: A cross-sectional study in Hong Kong. *BMJ Open*, 5(4).
- Bassett, D. R., Schneider, P. L., & Huntington, G. E. (2004). Physical activity in an Old Order Amish community. *Medicine & Science in Sports & Exercise*, 36(1), 79-85.
- Batty, M. (2001). Exploring isovist fields: Space and shape in architectural and urban morphology. *Environment and Planning B: Planning and Design*, 28(1), 123-150.
- Batty, M., & Marshall, S. (2012). The origins of complexity theory in cities and planning. In *Portugali J., Meyer H., Stolk E., Tan E. (eds) Complexity Theories of Cities have come of Age* (pp. 21-45). Berlin, Heidelberg: Springer.
- Beil, K., & Hanes, D. (2013). The influence of urban natural and built environments on physiological and psychological measures of stress—A pilot study. *International Journal of Environmental Research and Public Health*, 10(4), 1250-1267.
- Benedek, M., & Kaernbach, C. (2010). A continuous measure of phasic electrodermal activity. *Journal of Neuroscience Methods*, 190(1), 80-91.
- Benedikt, M. L. (1979). To take hold of space: Isovists and isovist fields. *Environment and Planning B: Planning and Design*, 6(1), 47-65.
- Berto, R., Massaccesi, S., & Pasini, M. (2008). Do eye movements measured across high and low fascination photographs differ? Addressing Kaplan's fascination hypothesis. *Journal of Environmental Psychology*, 28(2), 185-191.
- Bilgel, M., Jedynek, B. M., & Alzheimer's Disease Neuroimaging Initiative (2019). Predicting time to dementia using a quantitative template of disease progression. *Alzheimer's & Dementia: Diagnosis, Assessment & Disease Monitoring*, 11, 205-215.
- Birch, C. P., Oom, S. P., & Beecham, J. A. (2007). Rectangular and hexagonal grids used for observation, experiment and simulation in ecology. *Ecological Modelling*, 206(3-4), 347-359.
- Birenboim, A., Dijst, M., Scheepers, F. E., Poelman, M. P., & Helbich, M. (2019). Wearables and location tracking technologies for mental-state sensing in outdoor environments. *The Professional Geographer*, 1-13.

- Birenboim, A., Helbich, M., & Kwan, M. P. (2021). Advances in portable sensing for urban environments: Understanding cities from a mobility perspective. *Computers, Environment and Urban Systems*, 88, 101650.
- Bithell, J. F. (1990). An application of density estimation to geographical epidemiology. *Statistics in Medicine*, 9(6), 691-701.
- Bithell, J. F. (1991). Estimation of relative risk functions. *Statistics in Medicine*, 10(11), 1745-1751.
- Borchers, J. O. (2008). A pattern approach to interaction design. In Gill S. (eds) *Cognition, Communication and Interaction* (pp. 114-131). London: Springer.
- Boucsein, W. (2012). *Electrodermal activity*. New York: Springer.
- Braun, B. J., Veith, N. T., Hell, R., Döbele, S., Roland, M., Rollmann, M., Holstein, J., & Pohlemann, T. (2015). Validation and reliability testing of a new, fully integrated gait analysis insole. *Journal of Foot and Ankle Research*, 8(1), 54.
- Bronfenbrenner, U. (1977). Toward an experimental ecology of human development. *American Psychologist*, 32(7), 513-531.
- Brown, C. D., & Davis, H. T. (2006). Receiver operating characteristics curves and related decision measures: A tutorial. *Chemometrics and Intelligent Laboratory Systems*, 80(1), 24-38.
- Brownson, R. C., Hoehner, C. M., Day, K., Forsyth, A., & Sallis, J. F. (2009). Measuring the built environment for physical activity: state of the science. *American Journal of Preventive Medicine*, 36(4), S99-S123.
- Brownson, R. C., Kelly, C. M., Eyler, A. A., Carnoske, C., Grost, L., Handy, S. L., Maddock, J. E., Pluto, D., Ritacco, B. A., Sallis, J. F., & Schmid, T. L. (2008). Environmental and policy approaches for promoting physical activity in the United States: A research agenda. *Journal of Physical Activity and Health*, 5(4), 488-503.
- Buller, I. D., Brown, D. W., Myers, T. A., Jones, R. R., & Machiela, M. J. (2021). sparrpowR: A flexible R package to estimate statistical power to identify spatial clustering of two groups and its application. *International Journal of Health Geographics*, 20(1), 1-7.
- Candra, H., Yuwono, M., Chai, R., Handojoseno, A., Elamvazuthi, I., Nguyen, H. T., & Su, S. (2015). Investigation of window size in classification of EEG-emotion signal with wavelet entropy and support vector machine. In *2015 37th Annual international conference of the IEEE Engineering in Medicine and Biology Society (EMBC)* (pp. 7250-7253). IEEE.
- Castro-Toledo, F. J., Perea-García, J. O., Bautista-Ortuño, R., & Mitkidis, P. (2017). Influence of environmental variables on fear of crime: Comparing self-report data with physiological measures in an experimental design. *Journal of Experimental Criminology*, 13(4), 537-545.

- CDC (Centres for Disease Control and Prevention) (2019). *Subjective cognitive decline — A public health issue*. Available at: <https://www.cdc.gov/aging/data/subjective-cognitive-decline-brief.html> (accessed 16 September 2021).
- CDC (Centres for Disease Control and Prevention) (2021). *About adult BMI*. https://www.cdc.gov/healthyweight/assessing/bmi/adult_bmi/index.html#InterpretedAdults (accessed 16 September 2021).
- Cerin, E., Chan, K. W., Macfarlane, D. J., Lee, K. Y., & Lai, P. C. (2011). Objective assessment of walking environments in ultra-dense cities: development and reliability of the Environment in Asia Scan Tool—Hong Kong version (EAST-HK). *Health & Place, 17*(4), 937-945.
- Chang, C. Y., Hammitt, W. E., Chen, P. K., Machnik, L., & Su, W. C. (2008). Psychophysiological responses and restorative values of natural environments in Taiwan. *Landscape and Urban Planning, 85*(2), 79-84.
- Chen, Z., He, Y., & Yu, Y. (2016). Enhanced functional connectivity properties of human brains during in-situ nature experience. *PeerJ, 4*, e2210.
- Chen, Z., Schulz, S., Qiu, M., Yang, W., He, X., Wang, Z., & Yang, L. (2018). Assessing affective experience of in-situ environmental walk via wearable biosensors for evidence-based design. *Cognitive Systems Research, 52*, 970-977.
- Chiang, Y. C., Sullivan, W., & Larsen, L. (2017). Measuring neighborhood walkable environments: A comparison of three approaches. *International Journal of Environmental Research and Public Health, 14*(6), 593.
- Chittaro, L., & Sioni, R. (2014). Affective computing vs. affective placebo: Study of a biofeedback-controlled game for relaxation training. *International Journal of Human-Computer Studies, 72*(8-9), 663-673.
- Chiu, H. F. K., Lam, L. C. W., Chi, I., Leung, T., Li, S. W., Law, W. T., Chung, D. W. S., Fung, H. H. L., Kan, P. S., Lum, C. M., Ng, J., & Lau, J. (1998). Prevalence of dementia in Chinese elderly in Hong Kong. *Neurology, 50*(4), 1002-1009.
- Chiu, H. F., Lee, H. C., Chung, W. S., & Kwong, P. K. (1994). Reliability and validity of the Cantonese version of mini-mental state examination—a preliminary study. *Hong Kong Journal of Psychiatry, 4*(2), 25.
- Chrisinger, B. W., & King, A. C. (2018). Stress experiences in neighborhood and social environments (SENSE): A pilot study to integrate the quantified self with citizen science to improve the built environment and health. *International Journal of Health Geographics, 17*(1), 17.
- Chun, J. A., Psarras, S., & Koutsolampros, P. (2019). Agent based simulation for ‘Choice of Seats’: A Study on the Human Space Usage Pattern. In *Proceedings of the 12th International Space Syntax Symposium*. International Space Syntax Symposium. Beijing, China.
- Cottet, M., Vaudor, L., Tronchère, H., Roux-Michollet, D., Augendre, M., & Brault, V. (2018). Using gaze behavior to gain insights into the impacts of naturalness on city dwellers'

- perceptions and valuation of a landscape. *Journal of Environmental Psychology*, 60, 9-20.
- Crosby, F., & Hermens, F. (2018). Does it look safe? An eye tracking study into the visual aspects of fear of crime. *Quarterly Journal of Experimental Psychology*, 1747021818769203.
- Cunningham, G. O., Michael, Y. L., Farquhar, S. A., & Lapidus, J. (2005). Developing a reliable senior walking environmental assessment tool. *American Journal of Preventive Medicine*, 29(3), 215-217.
- Dagnelie, G. (2011). *Visual prosthetics: Physiology, bioengineering, rehabilitation*. US: Springer Science & Business Media.
- Dai, C., & Lian, Z. (2018). The effects of sound loudness on subjective feeling, sympathovagal balance and brain activity. *Indoor and Built Environment*, 27(9), 1287-1300.
- Davies, T. M., Marshall, J. C., & Hazelton, M. L. (2018). Tutorial on kernel estimation of continuous spatial and spatiotemporal relative risk. *Statistics in Medicine*, 37(7), 1191-1221.
- Dawes, M. J., & Ostwald, M. J. (2013). Using isovists to analyse Prospect-Refuge Theory: Measuring Spatio-Visual Relations in Wright's Heurtley House. *The International Journal of the Constructed Environment*, 1(3), 25-40.
- Dawes, M. J., & Ostwald, M. J. (2014). Prospect-Refuge theory and the textile-block houses of Frank Lloyd Wright: An analysis of spatio-visual characteristics using isovists. *Building and Environment*, 80, 228-240.
- Deb, K., Anand, A., & Joshi, D. (2002). A computationally efficient evolutionary algorithm for real-parameter optimization. *Evolutionary Computation*, 10(4), 371-395.
- Denoeux, T. (1995). A k-nearest neighbor classification rule based on Dempster-Shafer theory. *IEEE Transactions on Systems, Man, and Cybernetics*, 25(5), 804-813.
- Dietterich, T. G. (2000). An experimental comparison of three methods for constructing ensembles of decision trees: Bagging, boosting, and randomization. *Machine Learning*, 40(2), 139-157.
- Ding, C., & Jiang, Y. (2020). The relationship between body mass index and physical fitness among Chinese University students: Results of a longitudinal study. *Healthcare (Basel)* 8(4), 570.
- Dixon, P. C., Jacobs, J. V., Dennerlein, J. T., & Schiffman, J. M. (2018). Late-cueing of gait tasks on an uneven brick surface impacts coordination and center of mass control in older adults. *Gait & Posture*, 65, 143-148.
- Doshi, M., & Chaturvedi, S. K. (2014). Correlation based feature selection (CFS) technique to predict student Performance. *International Journal of Computer Networks & Communications*, 6(3), 197.

- Duchowny, K., Clarke, P., Gallagher, N. A., Adams, R., Rosso, A. L., & Alexander, N. B. (2019). Using mobile, wearable, technology to understand the role of built environment demand for outdoor mobility. *Environment and Behavior*, *51*(6), 671-688.
- Dupont, L., Ooms, K., Duchowski, A. T., Antrop, M., & Van Eetvelde, V. (2017). Investigating the visual exploration of the rural-urban gradient using eye-tracking. *Spatial Cognition & Computation*, *17*(1-2), 65-88.
- Elderly Commission (2020). *Report on healthy ageing executive summary*. Available at: <https://www.elderlycommission.gov.hk/en/library/Ex-sum.ht> (accessed 16 September 2021).
- Elderly Health Service (2016). *Elderly health service-activity and elder, dementia, Department of Health, Hong Kong*. Available at: https://www.elderly.gov.hk/english/common_health_problems/dementia/dementia.html (accessed 16 September 2021).
- Elsadek, M., Sun, M., Sugiyama, R., & Fujii, E. (2019). Cross-cultural comparison of physiological and psychological responses to different garden styles. *Urban Forestry & Urban Greening*, *38*, 74-83.
- Emotiv (2019). *EPOC+ headset details*. Available at: https://emotiv.gitbook.io/epoc-user-manual/using-headset/epoc+_headset_details (accessed 5 July 2019).
- Empatica (2019a). *Real-time physiological signals, E4 EDA/GSR sensor*. Available at: <https://www.empatica.com/research/e4/> (accessed 2 July 2019).
- Empatica (2019b). *E4 wristband technical specifications—Empatica Support*. Available at: <https://support.empatica.com/hc/en-us/articles/202581999-E4-wristband-technical-specifications> (accessed 2 July 2019).
- Empatica (2019c). *Wear your E4 wristband—Empatica support*. Available at: <https://support.empatica.com/hc/en-us/articles/206374015-Wear-your-E4-wristband-> (accessed 2 July 2019).
- Enzor, J., Burke, D. L., Snell, K. I., Hemming, K., & Riley, R. D. (2018). Simulation-based power calculations for planning a two-stage individual participant data meta-analysis. *BMC Medical Research Methodology*, *18*(1), 1-16.
- Esri (2020a). *Emerging hot spot analysis (space time pattern mining)-ArcGIS Pro, Documentation*. Available at: <https://pro.arcgis.com/en/pro-app/tool-reference/space-time-pattern-mining/emerginghotspots.htm> (accessed 10 September 2020).
- Esri (2020b). *How kernel density works—ArcMap, Documentation*. Available at: <https://desktop.arcgis.com/en/arcmap/latest/tools/spatial-analyst-toolbox/how-kernel-density-works.htm> (accessed 10 November 2020).
- Feldman, P. H., & Oberlink, M. R. (2003). The AdvantAge initiative: Developing community indicators to promote the health and well-being of older people. *Family & Community Health*, *26*(4), 268-274.

- Fernando, W. S., & Hazelton, M. L. (2014). Generalizing the spatial relative risk function. *Spatial and Spatio-Temporal Epidemiology*, 8, 1-10.
- Folstein, M. F., Folstein, S. E., & McHugh, P. R. (1975). "Mini-mental state": A practical method for grading the cognitive state of patients for the clinician. *Journal of Psychiatric Research*, 12(3), 189-198.
- Forsyth, A. 2015. "What is a walkable place? The walkability debate in urban design." *Urban Design International* 20(4): 274-292.
- Franěk, M., & Režný, L. (2017). The effect of priming with photographs of environmental settings on walking speed in an outdoor environment. *Frontiers in Psychology*, 8, 73.
- Franěk, M., Režný, L., Šefara, D., & Cabal, J. (2018b). Effect of traffic noise and relaxations sounds on pedestrian walking speed. *International Journal of Environmental Research and Public Health*, 15(4), 752.
- Franěk, M., Šefara, D., Petružálek, J., Cabal, J., & Myška, K. (2018a). Differences in eye movements while viewing images with various levels of restorativeness. *Journal of Environmental Psychology*, 57, 10-16.
- Franz, G., & Wiener, J. M. (2005). Exploring isovist-based correlates of spatial behavior and experience. In van Nes, A. (Ed.) *5th International Space Syntax Symposium* (pp. 503-517). Techne Press, Amsterdam, The Netherlands.
- Friedl, M. A., & Brodley, C. E. (1997). Decision tree classification of land cover from remotely sensed data. *Remote Sensing of Environment*, 61(3), 399-409.
- Fujiyama, T., & Tyler, N. (2010). Predicting the walking speed of pedestrians on stairs. *Transportation Planning and Technology*, 33(2), 177-202.
- Gaire, N., Sharifi, M. S., Christensen, K. M., Chen, A., & Song, Z. (2017). Walking behavior of individuals with and without disabilities at right-angle turning facility. *Journal of Accessibility and Design for All*, 7(1), 56-75.
- Gehl, J. (2011). *Life between buildings: Using public space*. Island press.
- Getis, A., & Ord, J. K. (2010). The analysis of spatial association by use of distance statistics. In L. Anselin, S. Rey (Eds.), *Perspectives on spatial data analysis* (pp. 127-145). Springer, Berlin, Heidelberg.
- Gibson, J. J. (1977). The theory of affordances. *Hilldale, USA*, 1(2), 67-82.
- Gidlow, C. J., Jones, M. V., Hurst, G., Masterson, D., Clark-Carter, D., Tarvainen, M. P., Smith, G., & Nieuwenhuijsen, M. (2016b). Where to put your best foot forward: Psychophysiological responses to walking in natural and urban environments. *Journal of Environmental Psychology*, 45, 22-29.
- Gidlow, C. J., Randall, J., Gillman, J., Smith, G. R., & Jones, M. V. (2016a). Natural environments and chronic stress measured by hair cortisol. *Landscape and Urban Planning*, 148, 61-67.

- Gisbert, F. J. G. (2003). Weighted samples, kernel density estimators and convergence. *Empirical Economics*, 28(2), 335-351.
- Gladwell, V. F., Brown, D. K., Barton, J. L., Tarvainen, M. P., Kuoppa, P., Pretty, J., Suddaby, J. M., & Sandercock, G. R. H. (2012). The effects of views of nature on autonomic control. *European Journal of Applied Physiology*, 112(9), 3379-3386.
- Gladwell, V., Kuoppa, P., Tarvainen, M., & Rogerson, M. (2016). A lunchtime walk in nature enhances restoration of autonomic control during night-time sleep: Results from a preliminary study. *International Journal of Environmental Research and Public Health*, 13(3), 280.
- Grassini, S., Revonsuo, A., Castellotti, S., Petrizzo, I., Benedetti, V., & Koivisto, M. (2019). Processing of natural scenery is associated with lower attentional and cognitive load compared with urban ones. *Journal of Environmental Psychology*, 62, 1-11.
- Greenwood, A., & Gatersleben, B. (2016). Let's go outside! Environmental restoration amongst adolescents and the impact of friends and phones. *Journal of Environmental Psychology*, 48, 131-139.
- Grimmer, M., Riener, R., Walsh, C. J., & Seyfarth, A. (2019). Mobility related physical and functional losses due to aging and disease—a motivation for lower limb exoskeletons. *Journal of Neuroengineering and Rehabilitation*, 16(1), 1-21.
- Guenther, N., & Schonlau, M. (2016). Support vector machines. *The Stata Journal*, 16(4), 917-937.
- Gullón, P., Badland, H. M., Alfayate, S., Bilal, U., Escobar, F., Cebrecos, A., Diez, J., & Franco, M. (2015). Assessing walking and cycling environments in the streets of Madrid: Comparing on-field and virtual audits. *Journal of Urban Health*, 92(5), 923-939.
- Hagedorn, R. (2001). *Foundations for practice in occupational therapy*. Edinburgh, UK: Elsevier.
- Hall, D. L., & Llinas, J. (1997). An introduction to multisensor data fusion. *Proceedings of the IEEE*, 85(1), 6-23.
- Hall, M. A. (1999). *Correlation-based feature selection for machine learning* [Doctoral dissertation, Department of Computer Science, Waikato University, New Zealand].
- Hamed, K. H. (2009). Exact distribution of the Mann–Kendall trend test statistic for persistent data. *Journal of Hydrology*, 365(1-2), 86-94.
- Han, T. S., Tijhuis, M. A., Lean, M. E., & Seidell, J. C. (1998). Quality of life in relation to overweight and body fat distribution. *American Journal of Public Health*, 88(12), 1814-1820.
- Handy, S. L., Boarnet, M. G., Ewing, R., & Killingsworth, R. E. (2002). How the built environment affects physical activity: views from urban planning. *American Journal of Preventive Medicine*, 23(2), 64-73.
- Hanson, D., & Emlet, C. A. (2006). Assessing a community's elder friendliness: a case example of The AdvantAge Initiative. *Family & Community Health*, 29(4), 266-278.

- Harding E. D. (2007). *Towards Lifetime Neighbourhoods: Designing Sustainable Communities for All*. London: Department for Communities and Local Government.
- Hassan, M. M., Alam, M. G. R., Uddin, M. Z., Huda, S., Almogren, A., & Fortino, G. (2019). Human emotion recognition using deep belief network architecture. *Information Fusion, 51*, 10-18.
- Havard, C., & Willis, A. (2012). Effects of installing a marked crosswalk on road crossing behaviour and perceptions of the environment. *Transportation Research Part F: Traffic Psychology and Behaviour, 15*(3), 249-260.
- Healey, J. A., & Picard, R. W. (2005). Detecting stress during real-world driving tasks using physiological sensors. *IEEE Transactions on Intelligent Transportation Systems, 6*(2), 156-166.
- Hedblom, M., Gunnarsson, B., Schaefer, M., Knez, I., Thorsson, P., & Lundström, J. N. (2019). Sounds of Nature in the City: No Evidence of Bird Song Improving Stress Recovery. *International Journal of Environmental Research and Public Health, 16*(8), 1390.
- Hemmingsson, E., & Ekelund, U. (2007). Is the association between physical activity and body mass index obesity dependent?. *International Journal of Obesity, 31*(4), 663-668.
- Hietanen, J. K., Klemetilä, T., Kettunen, J. E., & Korpela, K. M. (2007). What is a nice smile like that doing in a place like this? Automatic affective responses to environments influence the recognition of facial expressions. *Psychological Research, 71*(5), 539-552.
- Hijazi, I. H., Koenig, R., Schneider, S., Li, X., Bielik, M., Schmit, G. N. J., & Donath, D. (2016). Geostatistical analysis for the study of relationships between the emotional responses of urban walkers to urban spaces. *International Journal of E-Planning Research (IJEPR), 5*(1), 1-19.
- Hoehner, C. M., Ramirez, L. K. B., Elliott, M. B., Handy, S. L., & Brownson, R. C. (2005). Perceived and objective environmental measures and physical activity among urban adults. *American Journal of Preventive Medicine, 28*(2), 105-116.
- Hollander, J. B., Purdy, A., Wiley, A., Foster, V., Jacob, R. J., Taylor, H. A., & Brunyé, T. T. (2019). Seeing the city: using eye-tracking technology to explore cognitive responses to the built environment. *Journal of Urbanism: International Research on Placemaking and Urban Sustainability, 12*(2), 156-171.
- Hollander, J., & Foster, V. (2016). Brain responses to architecture and planning: A preliminary neuro-assessment of the pedestrian experience in Boston, Massachusetts. *Architectural Science Review, 59*(6), 474-481.
- Holleman, G. A., Hooge, I. T., Kemner, C., & Hessels, R. S. (2020). The 'real-world approach' and its problems: A critique of the term ecological validity. *Frontiers in Psychology, 11*, 721.
- Holliday, K. M., Lin, D. Y., Chakladar, S., Castañeda, S. F., Daviglus, M. L., Evenson, K. R., Marqueze, D. X., Qi, Q., Shay, C. M., Sotres-Alvarez, D., Vidot, D. C., Zeng, D., & Avery, C. L. (2017). Targeting physical activity interventions for adults: When should intervention occur?. *Preventive Medicine, 97*, 13-18.

- Hong Kong Planning Department (2015, November). Hong Kong urban design guidelines. In *Hong Kong Planning Standards and Guidelines*.
- Huang, J., Zhou, C., Zhuo, Y., Xu, L., & Jiang, Y. (2016). Outdoor thermal environments and activities in open space: An experiment study in humid subtropical climates. *Building and Environment*, 103, 238-249.
- Huisman, E. R., Morales, E., van Hoof, J., & Kort, H. S. (2012). Healing environment: A review of the impact of physical environmental factors on users. *Building and Environment*, 58, 70-80.
- Hunter, M. R. (2019). Urban nature experiences reduce stress in the context of daily life based on salivary biomarkers. *Frontiers in Psychology*, 10, 722.
- Inclusive Design for Getting Outdoors (2010). Researching how the design of streets and neighbourhoods can make a difference to older people's wellbeing and quality of life. Available at http://www.idgo.ac.uk/useful_resources/Publications/OPENspace_MTP_brochure_FIN_AL.pdf (accessed 11 March 2019).
- Inclusive Design for Getting Outdoors (2013). The design of streets with older people in mind. Available at: http://www.idgo.ac.uk/design_guidance/streets.htm (accessed 11 March 2019).
- Irwin, A., Hall, D. A., Peters, A., & Plack, C. J. (2011). Listening to urban soundscapes: Physiological validity of perceptual dimensions. *Psychophysiology*, 48(2), 258-268.
- Ishibuchi, H., & Yamamoto, T. (2004). Fuzzy rule selection by multi-objective genetic local search algorithms and rule evaluation measures in data mining. *Fuzzy Sets and Systems*, 141(1), 59-88.
- James, G., Witten, D., Hastie, T., & Tibshirani, R. (2013). *An introduction to statistical learning* (Vol. 112, p. 18). New York: Springer.
- James, R., & O'Boyle, M. (2019). Graffiti and perceived neighborhood safety: A neuroimaging study. *Property Management*, 37(1), 69-81.
- Jebelli, H., Hwang, S., & Lee, S. (2018). EEG-based workers' stress recognition at construction sites. *Automation in Construction*, 93, 315-324.
- Jiang, B., Chang, C. Y., & Sullivan, W. C. (2014). A dose of nature: Tree cover, stress reduction, and gender differences. *Landscape and Urban Planning*, 132, 26-36.
- Jiménez, F., Martínez, C., Miralles-Pechuán, L., Sánchez, G., & Sciavicco, G. (2018). Multi-objective evolutionary rule-based classification with categorical data. *Entropy*, 20(9), 684.
- Jimenez, F., Sanchez, G., & Juarez, J. M. (2014). Multi-objective evolutionary algorithms for fuzzy classification in survival prediction. *Artificial Intelligence in Medicine*, 60(3), 197-219.
- Jo, H., Rodiek, S., Fujii, E., Miyazaki, Y., Park, B. J., & Ann, S. W. (2013). Physiological and psychological response to floral scent. *HortScience*, 48(1), 82-88.

- Kadali, B. R., & Vedagiri, P. (2016). Proactive pedestrian safety evaluation at unprotected mid-block crosswalk locations under mixed traffic conditions. *Safety Science*, 89, 94-105.
- Kalache, A., & Kickbusch, I. (1997). A global strategy for healthy ageing. *World Health*, 50(4), 4-5.
- Kaplan, S. (1988). Perception and landscape: Conceptions and misconceptions. In (Ed. Nasar, J.) *Environmental Aesthetics: Theory, research, and application*.
- Kelly, C. M., Wilson, J. S., Baker, E. A., Miller, D. K., & Schootman, M. (2013). Using Google Street View to audit the built environment: inter-rater reliability results. *Annals of Behavioral Medicine*, 45(suppl_1), S108-S112.
- Kelsall, J. E., & Diggle, P. J. (1995). Kernel estimation of relative risk. *Bernoulli*, 1(1-2), 3-16.
- Kiefer, P., Giannopoulos, I., Raubal, M., & Duchowski, A. (2017). Eye tracking for spatial research: Cognition, computation, challenges. *Spatial Cognition & Computation*, 17(1-2), 1-19.
- Kihl, M., Breenan, D., Gabhawala, N., List, J., & Mittal, P. (2005). *Livable communities: An evaluation guide*. AARP Public Policy Institute, Washington DC.
- Kihl, M., Breenan, D., Gabhawala, N., List, J., & Mittal, P. (2005). *Livable communities: An evaluation guide*. Washington DC: AARP Public Policy Institute.
- Kim, G. W., & Jeong, G. W. (2014). Brain activation patterns associated with the human comfortability of residential environments: 3.0-T functional MRI. *Neuroreport*, 25(12), 915-920.
- Kim, G. W., Jeong, G. W., Kim, T. H., Baek, H. S., Oh, S. K., Kang, H. K., Lee, S. G., Kim, Y. S. & Song, J. K. (2010b). Functional neuroanatomy associated with natural and urban scenic views in the human brain: 3.0 T functional MR imaging. *Korean Journal of Radiology*, 11(5), 507-513.
- Kim, H., & Yi, Y. K. (2019). QuVue implementation for decisions related to high-rise residential building layouts. *Building and Environment*, 148, 116-127.
- Kim, H., Ahn, C. R., & Yang, K. (2016). A people-centric sensing approach to detecting sidewalk defects. *Advanced Engineering Informatics*, 30(4), 660-671.
- Kim, J., Ahn, C. R., & Nam, Y. (2019). The influence of built environment features on crowdsourced physiological responses of pedestrians in neighborhoods. *Computers, Environment and Urban Systems*, 75, 161-169.
- Kim, J., Ahn, C. R., & Nam, Y. (2019). The influence of built environment features on crowdsourced physiological responses of pedestrians in neighborhoods. *Computers, Environment and Urban Systems*, 75, 161-169.
- Kim, J., Yadav, M., Chaspari, T., & Ahn, C. R. (2020). Saliency detection analysis of collective physiological responses of pedestrians to evaluate neighborhood built environments. *Advanced Engineering Informatics*, 43, 101035.

- Kim, M., Cheon, S., & Kang, Y. (2019b). Use of Electroencephalography (EEG) for the Analysis of Emotional Perception and Fear to Nightscapes. *Sustainability*, *11*(1), 233.
- Kim, T. H., Jeong, G. W., Baek, H. S., Kim, G. W., Sundaram, T., Kang, H. K., Lee, S. W., Kim, H. J., & Song, J. K. (2010a). Human brain activation in response to visual stimulation with rural and urban scenery pictures: A functional magnetic resonance imaging study. *Science of the Total Environment*, *408*(12), 2600-2607.
- King, R. C., Villeneuve, E., White, R. J., Sherratt, R. S., Holderbaum, W., & Harwin, W. S. (2017). Application of data fusion techniques and technologies for wearable health monitoring. *Medical Engineering & Physics*, *42*, 1-12.
- Kleckner, I. R., Jones, R. M., Wilder-Smith, O., Wormwood, J. B., Akcakaya, M., Quigley, K. S., Lord, C., & Goodwin, M. S. (2018). Simple, transparent, and flexible automated quality assessment procedures for ambulatory electrodermal activity data. *IEEE Transactions on Biomedical Engineering*, *65*(7), 1460-1467.
- Knöll, M., Neuheuser, K., Cleff, T., & Rudolph-Cleff, A. (2018). A tool to predict perceived urban stress in open public spaces. *Environment and Planning B: Urban Analytics and City Science*, *45*(4), 797-813.
- Kobayashi, H., Song, C., Ikei, H., Kagawa, T., & Miyazaki, Y. (2015). Analysis of individual variations in autonomic responses to urban and forest environments. *Evidence-Based Complementary and Alternative Medicine*, *2015*.
- Kobayashi, H., Song, C., Ikei, H., Park, B. J., Lee, J., Kagawa, T., & Miyazaki, Y. (2017). Population-based study on the effect of a forest environment on salivary cortisol concentration. *International Journal of Environmental Research and Public Health*, *14*(8), 931.
- Kohonen, T. (2012). *Self-organizing maps* (Vol. 30). Springer Science & Business Media.
- Kohonen, T. (2013). Essentials of the self-organizing map. *Neural Networks*, *37*, 52-65.
- Korpela, K. M., Klemetilä, T., & Hietanen, J. K. (2002). Evidence for rapid affective evaluation of environmental scenes. *Environment and Behavior*, *34*(5), 634-650.
- Kreibig, S. D. (2010). Autonomic nervous system activity in emotion: A review. *Biological Psychology*, *84*(3), 394-421.
- Kuzmanovski, I., Dimitrovska-Lazova, S., & Aleksovska, S. (2007). Classification of perovskites with supervised self-organizing maps. *Analytica Chimica Acta*, *595*(1-2), 182-189.
- Kyriakou, K., Resch, B., Sagl, G., Petutschnig, A., Werner, C., Niederseer, D., Liedlgruber, M., Wilhelm, F.H., Osborne, T., & Pykett, J. (2019). Detecting moments of stress from measurements of wearable physiological sensors. *Sensors*, *19*(17), 3805.
- Lacuesta, R., Garcia, L., García-Magariño, I., & Lloret, J. (2017). System to recommend the best place to live based on wellness state of the user employing the heart rate variability. *IEEE Access*, *5*, 10594-10604.

- Lahat, D., Adali, T., & Jutten, C. (2015). Multimodal data fusion: an overview of methods, challenges, and prospects. *Proceedings of the IEEE*, 103(9), 1449-1477.
- Långkvist, M., Karlsson, L., & Loutfi, A. (2014). A review of unsupervised feature learning and deep learning for time-series modeling. *Pattern Recognition Letters*, 42, 11-24.
- Lao, S. S. W., Low, L. P. L., & Wong, K. K. Y. (2019). Older residents' perceptions of family involvement in residential care. *International Journal of Qualitative Studies on Health and Well-Being*, 14(1), 1611298.
- Laumann, K., Gärling, T., & Stormark, K. M. (2003). Selective attention and heart rate responses to natural and urban environments. *Journal of Environmental Psychology*, 23(2), 125-134.
- Lawson, A. B. (2013). *Statistical methods in spatial epidemiology*. West Sussex, England: John Wiley & Sons.
- Lawton, M. P. (1982). Competence, environmental press, and the adaptation of older people. *Aging and the Environment: Theoretical Approaches*, 33-59.
- Lazarus, R. S. (1990). Theory-based stress measurement. *Psychological Inquiry*, 1(1), 3-13.
- Le Roux, N., & Bengio, Y. (2008). Representational power of restricted Boltzmann machines and deep belief networks. *Neural Computation*, 20(6), 1631-1649.
- Lee, G., Choi, B., Ahn, C. R., & Lee, S. (2020). Wearable biosensor and hotspot analysis-based framework to detect stress hotspots for advancing elderly's mobility. *Journal of Management in Engineering*, 36(3), 04020010.
- Lee, J., Park, B. J., Ohira, T., Kagawa, T., & Miyazaki, Y. (2015). Acute effects of exposure to a traditional rural environment on urban dwellers: A crossover field study in terraced farmland. *International Journal of Environmental Research and Public Health*, 12(2), 1874-1893.
- Lee, J., Park, B. J., Tsunetsugu, Y., Kagawa, T., & Miyazaki, Y. (2009). Restorative effects of viewing real forest landscapes, based on a comparison with urban landscapes. *Scandinavian Journal of Forest Research*, 24(3), 227-234.
- Lewis, C. (1993). Balance, gait test proves simple yet useful. *P.T. Bulletin*, 2/10:9 & 40.
- Li, D., & Sullivan, W. C. (2016). Impact of views to school landscapes on recovery from stress and mental fatigue. *Landscape and Urban Planning*, 148, 149-158.
- Li, J., Wang, X., & Hovy, E. (2014). What a nasty day: Exploring mood-weather relationship from twitter. In *proceedings of the 23rd ACM International Conference on Conference on Information and Knowledge Management* (pp. 1309-1318).
- Li, W., Winter, P. L., Milburn, L. A., & Padgett, P. E. (2021). A dual-method approach toward measuring the built environment-sampling optimization, validity, and efficiency of using GIS and virtual auditing. *Health & Place*, 67, 102482.

- Li, X., Hijazi, I., Koenig, R., Lv, Z., Zhong, C., & Schmitt, G. (2016). Assessing essential qualities of urban space with emotional and visual data based on GIS technique. *ISPRS International Journal of Geo-Information*, 5(11), 218.
- Ling, K. K., & Lee, K. (2019). Tackling double-ageing with double-smart. *Journal of the Hong Kong Institute of Planners*, 33, 4-20.
- Liu, Y., Hu, M., & Zhao, B. (2019). Audio-visual interactive evaluation of the forest landscape based on eye-tracking experiments. *Urban Forestry & Urban Greening*, 46, 126476.
- Lou, W., Wang, X., Chen, F., Chen, Y., Jiang, B., & Zhang, H. (2014). Sequence based prediction of DNA-binding proteins based on hybrid feature selection using random forest and Gaussian naive Bayes. *PloS One*, 9(1), e86703.
- Lu, S. Y., Lee, C. L., Lin, K. Y., & Lin, Y. H. (2018). The acute effect of exposure to noise on cardiovascular parameters in young adults. *Journal of Occupational Health*, 2017-0225.
- Lui, C. W., Everingham, J. A., Warburton, J., Cuthill, M., & Bartlett, H. (2009). What makes a community age-friendly: A review of international literature. *Australasian Journal on Ageing*, 28(3), 116-121.
- Luppino, F. S., de Wit, L. M., Bouvy, P. F., Stijnen, T., Cuijpers, P., Penninx, B. W., & Zitman, F. G. (2010). Overweight, obesity, and depression: A systematic review and meta-analysis of longitudinal studies. *Archives of General Psychiatry*, 67(3), 220-229.
- Mair, C. A., Cutchin, M. P., & Peek, M. K. (2011). Allostatic load in an environmental riskscape: The role of stressors and gender. *Health & Place*, 17(4), 978-987.
- Markevych, I., Thiering, E., Fuertes, E., Sugiri, D., Berdel, D., Koletzko, S., von Berg, A., Bauer, C. P., & Heinrich, J. (2014). A cross-sectional analysis of the effects of residential greenness on blood pressure in 10-year old children: results from the GINIplus and LISAplus studies. *BMC Public Health*, 14(1), 477.
- Marshall, S. (2012). Planning, design and the complexity of cities. In *Portugali J., Meyer H., Stolk E., Tan E. (eds) Complexity Theories of Cities have Come of Age* (pp. 191-205). Springer, Berlin, Heidelberg.
- Martínez-Soto, J., Gonzales-Santos, L., Pasaye, E., & Barrios, F. A. (2013). Exploration of neural correlates of restorative environment exposure through functional magnetic resonance. *Intelligent Buildings International*, 5(sup1), 10-28.
- Mascetti, S., Civitarese, G., El Malak, O., & Bettini, C. (2020). SmartWheels: Detecting urban features for wheelchair users' navigation. *Pervasive and Mobile Computing*, 62, 101115.
- Matsuda, Y., Fedotov, D., Takahashi, Y., Arakawa, Y., Yasumoto, K., & Minker, W. (2018). EmoTour: Estimating emotion and satisfaction of users based on behavioral cues and audiovisual data. *Sensors (Basel)*, 18(11).
- McLeod, A. I. (2005). Kendall rank correlation and Mann-Kendall trend test. *R Package Kendall*.

- Meilinger, T., Franz, G., & Bülthoff, H. H. (2012). From isovists via mental representations to behaviour: first steps toward closing the causal chain. *Environment and Planning B: Planning and Design*, 39(1), 48-62.
- Melander, C. A., Kikhia, B., Olsson, M., Walivaara, B. M., & Savenstedt, S. (2018). The impact of using measurements of electrodermal activity in the assessment of problematic behaviour in dementia. *Dementia and Geriatric Cognitive Disorders Extra*, 8(3), 333-347.
- Menec, V. H., Means, R., Keating, N., Parkhurst, G., & Eales, J. (2011). Conceptualizing age-friendly communities. *Canadian Journal on Aging/La Revue Canadienne du Vieillissement*, 30(3), 479-493.
- Michael, Y. L., Keast, E. M., Chaudhury, H., Day, K., Mahmood, A., & Sarte, A. F. (2009). Revising the senior walking environmental assessment tool. *Preventive Medicine*, 48(3), 247-249.
- Mitchel, A. (2005). *The ESRI Guide to GIS analysis, Volume 2: Spatial measurements and statistics*. ESRI Press.
- Mitschke, V., Goller, J., & Leder, H. (2017). Exploring everyday encounters with street art using a multimethod design. *Psychology of Aesthetics, Creativity, and the Arts*, 11(3), 276.
- Miyasike-daSilva, V., Allard, F., & McIlroy, W. E. (2011). Where do we look when we walk on stairs? Gaze behaviour on stairs, transitions, and handrails. *Experimental Brain Research*, 209(1), 73-83.
- Moniruzzaman, M., & Páez, A. (2016). An investigation of the attributes of walkable environments from the perspective of seniors in Montreal. *Journal of Transport Geography*, 51, 85-96.
- Moticon (2019). *Moticon support*. Available at: <https://www.moticon.de/support#resources> (accessed 5 July 2019).
- Moura, F., Cambra, P., & Gonçalves, A. B. (2017). Measuring walkability for distinct pedestrian groups with a participatory assessment method: A case study in Lisbon. *Landscape and Urban Planning*, 157, 282-296.
- Mourcou, Q., Fleury, A., Dupuy, P., Diot, B., Franco, C., & Vuillerme, N. (2013). Wegoto: A smartphone-based approach to assess and improve accessibility for wheelchair users. In *2013 35th Annual International Conference of the IEEE Engineering in Medicine and Biology Society (EMBC)* (pp. 1194-1197). IEEE.
- Mursalin, M., Zhang, Y., Chen, Y., & Chawla, N. V. (2017). Automated epileptic seizure detection using improved correlation-based feature selection with random forest classifier. *Neurocomputing*, 241, 204-214.
- Muzammal, M., Talat, R., Sodhro, A. H., & Pirbhulal, S. (2020). A multi-sensor data fusion enabled ensemble approach for medical data from body sensor networks. *Information Fusion*, 53, 155-164.

- Myles, A. J., Feudale, R. N., Liu, Y., Woody, N. A., & Brown, S. D. (2004). An introduction to decision tree modeling. *Journal of Chemometrics: A Journal of the Chemometrics Society*, *18*(6), 275-285.
- Neale, C., Aspinall, P., Roe, J., Tilley, S., Mavros, P., Cinderby, S., Coyne, R., Thin, N., Bennett, G., & Thompson, C. W. (2017). The aging urban brain: Analyzing outdoor physical activity using the Emotiv Affectiv suite in older people. *Journal of Urban Health*, *94*(6), 869-880.
- Neisser, U. (1976). *Cognition and reality*. San Francisco: Freeman.
- New Zealand Ministry of Social Development (2007). *Positive ageing indicators 2007*. Wellington: Ministry of Social Development.
- Nweke, H. F., Teh, Y. W., Mujtaba, G., & Al-Garadi, M. A. (2019). Data fusion and multiple classifier systems for human activity detection and health monitoring: Review and open research directions. *Information Fusion*, *46*, 147-170.
- Oerbekke, M. S., Stukstette, M. J., Schütte, K., de Bie, R. A., Pisters, M. F., & Vanwanseele, B. (2017). Concurrent validity and reliability of wireless instrumented insoles measuring postural balance and temporal gait parameters. *Gait & Posture*, *51*, 116-124.
- Oh, Y. A., Kim, S. O., & Park, S. (2019). Real Foliage Plants as Visual Stimuli to Improve Concentration and Attention in Elementary Students. *International Journal of Environmental Research and Public Health*, *16*(5), 796.
- Ojha, V. K., Griego, D., Kuliga, S., Bielik, M., Buš, P., Schaeben, C., Treyer, L., Standfest, M., Schneider, S., König, R., & Donath, D. (2019). Machine learning approaches to understand the influence of urban environments on human's physiological response. *Information Sciences*, *474*, 154-169.
- Onan, A., Korukoğlu, S., & Bulut, H. (2017). A hybrid ensemble pruning approach based on consensus clustering and multi-objective evolutionary algorithm for sentiment classification. *Information Processing & Management*, *53*(4), 814-833.
- OpenStreetMap and Contributors (2019). Planet dump retrieved from <https://planet.osm.org>, Available at: <https://www.openstreetmap.org> (accessed 11 November 2019).
- Ord, J. K., & Getis, A. (1995). Local spatial autocorrelation statistics: distributional issues and an application. *Geographical Analysis*, *27*(4), 286-306.
- Osborne, T., & Jones, P. I. (2017). Biosensing and geography: A mixed methods approach. *Applied Geography*, *87*, 160-169.
- Ostwald, M. J., & Dawes, M. (2013). Prospect-refuge patterns in Frank Lloyd Wright's Prairie houses: Using isovist fields to examine the evidence. *The Journal of Space Syntax*, *4*(1), 136-159.
- Ottosson, J., Lavesson, L., Pinzke, S., & Grahn, P. (2015). The significance of experiences of nature for people with parkinson's disease, with special focus on freezing of gait—The necessity for a biophilic environment. A multi-method single subject study. *International Journal of Environmental Research and Public Health*, *12*(7), 7274-7299.

- Pagliai, G., Sofi, F., Dinu, M., Sticchi, E., Vannetti, F., Lova, R. M., Ordovàs, J. M., Gori, A. M., Marcucci, R., Giusti, B., & Macchi, C. (2019). CLOCK gene polymorphisms and quality of aging in a cohort of nonagenarians—The MUGELLO Study. *Scientific Reports*, 9(1), 1472.
- Panicker, S. S., & Gayathri, P. (2019). A survey of machine learning techniques in physiology based mental stress detection systems. *Biocybernetics and Biomedical Engineering*, 39(2), 444-469.
- Papas, M. A., Alberg, A. J., Ewing, R., Helzlsouer, K. J., Gary, T. L., & Klassen, A. C. (2007). The built environment and obesity. *Epidemiologic Reviews*, 29(1), 129-143.
- Pedersen, E., & Johansson, M. (2018). Dynamic pedestrian lighting: Effects on walking speed, legibility and environmental perception. *Lighting Research & Technology*, 50(4), 522-536.
- Peper, E., Harvey, R., Lin, I.M., Tylova, H., & Moss, D. (2007). Is there more to blood volume pulse than heart rate variability, respiratory sinus arrhythmia, and cardiorespiratory synchrony?. *Biofeedback*, 35(2).
- Picard, R. W., Fedor, S., & Ayzenberg, Y. (2016). Multiple arousal theory and daily-life electrodermal activity asymmetry. *Emotion Review*, 8(1), 62-75.
- Pikora, T., Giles-Corti, B., Bull, F., Jamrozik, K., & Donovan, R. (2003). Developing a framework for assessment of the environmental determinants of walking and cycling. *Social Science & Medicine*, 56(8), 1693-1703.
- Platon, L., Zehraoui, F., & Tahi, F. (2017). Self-organizing maps with supervised layer. In *2017 12th International Workshop on Self-Organizing Maps and Learning Vector Quantization, Clustering and Data Visualization (WSOM)* (pp. 1-8). IEEE.
- Portegijs, E., Rantakokko, M., Viljanen, A., Rantanen, T., & Iwarsson, S. (2017). Perceived and objective entrance-related environmental barriers and daily out-of-home mobility in community-dwelling older people. *Archives of Gerontology and Geriatrics*, 69, 69-76.
- Posada-Quintero, H. F., & Chon, K. H. (2020). Innovations in electrodermal activity data collection and signal processing: A systematic review. *Sensors*, 20(2), 479.
- Posada-Quintero, H. F., Reljin, N., Mills, C., Mills, I., Florian, J. P., VanHeest, J. L., & Chon, K. H. (2018). Time-varying analysis of electrodermal activity during exercise. *PloS One*, 13(6), e0198328.
- Prentice, A. M., & Jebb, S. A. (2001). Beyond body mass index. *Obesity Reviews*, 2(3), 141-147.
- Pujol, J., Martínez-Vilavella, G., Macià, D., Fenoll, R., Alvarez-Pedrerol, M., Rivas, I., Forns, L., Blanco-HinojoJaume, J., Capellades, X., Querol, J., Deus, J., & Sunyer, M. (2016). Traffic pollution exposure is associated with altered brain connectivity in school children. *Neuroimage*, 129, 175-184.

- Qin, J., Zhou, X., Sun, C., Leng, H., & Lian, Z. (2013). Influence of green spaces on environmental satisfaction and physiological status of urban residents. *Urban Forestry & Urban Greening*, *12*(4), 490-497.
- Qstarz (2019). *Qstarz International Co., Ltd.* Available at: <http://www.qstarz.com/Qstarz-index.html> (accessed 8 July 2019).
- Rahm, J., & Johansson, M. (2018). Assessing the pedestrian response to urban outdoor lighting: A full-scale laboratory study. *PLoS One*, *13*(10), e0204638.
- Ramirez, L. K. B., Hoehner, C. M., Brownson, R. C., Cook, R., Orleans, C. T., Hollander, M., Barker, D. C., Bors, P., Ewing, R., Killingsworth, R., Petersmarck, K., Schmid, T., & Wilkinson, W. (2006). Indicators of activity-friendly communities: An evidence-based consensus process. *American Journal of Preventive Medicine*, *31*(6), 515-524.
- Rantanen, T. (2013). Promoting mobility in older people. *Journal of Preventive Medicine and Public Health*, *46*(Suppl 1), S50.
- Rebecchi, A., Buffoli, M., Dettori, M., Appolloni, L., Azara, A., Castiglia, P., D'Alessandro, D., & Capolongo, S. (2019). Walkable environments and healthy urban moves: Urban context features assessment framework experienced in Milan. *Sustainability*, *11*(10), 2778.
- Resende, M. G., & Ribeiro, C. C. (2010). Greedy randomized adaptive search procedures: Advances, hybridizations, and applications. In *Gendreau M., Potvin J. Y. (eds) Handbook of Metaheuristics* (pp. 283-319). Springer, Boston, MA.
- Reynald, D. M., & Elffers, H. (2009). The future of Newman's Defensible Space Theory: Linking Defensible Space and the routine activities of place. *European Journal of Criminology*, *6*(1), 25-46.
- Roe, J. J., Aspinall, P. A., Mavros, P., & Coyne, R. (2013). Engaging the brain: The impact of natural versus urban scenes using novel EEG methods in an experimental setting. *Journal of Environmental Sciences*, *1*(2), 93-104.
- Rokach, L. (2010). *Pattern classification using ensemble methods* (Vol. 75). World Scientific.
- Sadek, M., Sayaka, S., Fujii, E., Koriesh, E., Moghazy, E., & El Fatah, Y. (2013). Human emotional and psycho-physiological responses to plant color stimuli. *Journal of Food, Agriculture & Environment*, *11*(3&4), 1584-1591.
- Sahlin, E., Lindegård, A., Hadzibajramovic, E., Grahn, P., Vega Matuszczyk, J., & Ahlborg Jr, G. (2016). The influence of the environment on directed attention, blood pressure and heart rate—An experimental study using a relaxation intervention. *Landscape Research*, *41*(1), 7-25.
- Saitis, C., & Kalimeri, K. (2018). Multimodal Classification of stressful environments in visually impaired mobility using EEG and peripheral biosignals. *IEEE Transactions on Affective Computing*.
- Sallis, J. F. (2009). Measuring physical activity environments: A brief history. *American Journal of Preventive Medicine*, *36*(4), S86-S92.

- Sallis, J. F., & Saelens, B. E. (2000). Assessment of physical activity by self-report: status, limitations, and future directions. *Research Quarterly for Exercise and Sport*, 71(sup2), 1-14.
- Sallis, J., Bauman, A., & Pratt, M. (1998). Environmental and policy interventions to promote physical activity. *American Journal of Preventive Medicine*, 15(4), 379-397.
- Salzman, B. (2010). Gait and balance disorders in older adults. *American Family Physician*, 82(1), 61-68.
- Schmuckler, M. A. (2001). What is ecological validity? A dimensional analysis. *Infancy*, 2(4), 419-436.
- Schneider, S., & Koenig, R. (2012). Exploring the generative potential of isovist fields: The evolutionary generation of urban layouts based on isovist field properties. In *30th International Conference on Education Research in Computer Aided Architectural Design in Europe, Prague* (pp. 355–363).
- Scott, D. W. (2015). *Multivariate density estimation: Theory, practice, and visualization*. New York: John Wiley & Sons.
- Scott, S. C. (1993). Complexity and mystery as predictors of interior preferences. *Journal of Interior Design*, 19(1), 25-33.
- Seo, J., Laine, T. H., & Sohn, K. A. (2019). Machine learning approaches for boredom classification using EEG. *Journal of Ambient Intelligence and Humanized Computing*, 1-16.
- Setnes, M., Babuska, R., Kaymak, U., & van Nauta Lemke, H. R. (1998). Similarity measures in fuzzy rule base simplification. *IEEE Transactions on Systems, Man, and Cybernetics, Part B (Cybernetics)*, 28(3), 376-386.
- Shaffer, F., & Ginsberg, J. P. (2017). An overview of heart rate variability metrics and norms. *Frontiers in Public Health*, 5, 258.
- Shi, Y., Eberhart, R., & Chen, Y. (1999). Implementation of evolutionary fuzzy systems. *IEEE Transactions on Fuzzy Systems*, 7(2), 109-119.
- Shields, K. N., Cavallari, J. M., Hunt, M. J. O., Lazo, M., Molina, M., Molina, L., & Holguin, F. (2013). Traffic-related air pollution exposures and changes in heart rate variability in Mexico City: a panel study. *Environmental Health*, 12(1), 7.
- Shumway-Cook, A., Patla, A., Stewart, A., Ferrucci, L., Ciol, M. A., & Guralnik, J. M. (2003). Environmental components of mobility disability in community-living older persons. *Journal of the American Geriatrics Society*, 51(3), 393-398.
- Slone, E., Burles, F., & Iaria, G. (2016). Environmental layout complexity affects neural activity during navigation in humans. *European Journal of Neuroscience*, 43(9), 1146-1155.
- Song, C., Ikei, H., & Miyazaki, Y. (2018). Physiological effects of visual stimulation with forest imagery. *International Journal of Environmental Research and Public Health*, 15(2), 213.

- Song, C., Ikei, H., Igarashi, M., Miwa, M., Takagaki, M., & Miyazaki, Y. (2014). Physiological and psychological responses of young males during spring-time walks in urban parks. *Journal of Physiological Anthropology*, 33(1), 8.
- Song, C., Ikei, H., Igarashi, M., Takagaki, M., & Miyazaki, Y. (2015c). Physiological and psychological effects of a walk in urban parks in fall. *International Journal of Environmental Research and Public Health*, 12(11), 14216-14228.
- Song, C., Ikei, H., Kobayashi, M., Miura, T., Li, Q., Kagawa, T., Kumeda, S., Imai, M., & Miyazaki, Y. (2017). Effects of viewing forest landscape on middle-aged hypertensive men. *Urban Forestry & Urban Greening*, 21, 247-252.
- Song, C., Ikei, H., Kobayashi, M., Miura, T., Taue, M., Kagawa, T., Li, Q., Kumeda, S., & Miyazaki, Y. (2015a). Effect of forest walking on autonomic nervous system activity in middle-aged hypertensive individuals: A pilot study. *International Journal of Environmental Research and Public Health*, 12(3), 2687-2699.
- Song, C., Joung, D., Ikei, H., Igarashi, M., Aga, M., Park, B. J., Miwa, M., Takagaki, M., & Miyazaki, Y. (2013). Physiological and psychological effects of walking on young males in urban parks in winter. *Journal of Physiological Anthropology*, 32(1), 18.
- South, E. C., Kondo, M. C., Cheney, R. A., & Branas, C. C. (2015). Neighborhood blight, stress, and health: A walking trial of urban greening and ambulatory heart rate. *American Journal of Public Health*, 105(5), 909-913.
- SpaceGroupUCL (2019). DepthmapX Multi-Platform Spatial Network Analysis Software. Version 0.7.0 Open Source. Available at: <https://github.com/SpaceGroupUCL/depthmapX/releases/tag/v0.7.0> (accessed 3 July 2020).
- Stanovich, K. E., West, R. F., & Toplak, M. E. (2016). *The rationality quotient: Toward a test of rational thinking*. MIT press.
- Stevenson, M. P., Dewhurst, R., Schilhab, T., & Bentsen, P. (2019). Cognitive restoration in children following exposure to nature: Evidence from the Attention Network Task and mobile eye tracking. *Frontiers in Psychology*, 10.
- Stigsdotter, U. K., Corazon, S. S., Sidenius, U., Kristiansen, J., & Grahn, P. (2017). It is not all bad for the grey city—A crossover study on physiological and psychological restoration in a forest and an urban environment. *Health & Place*, 46, 145-154.
- Stöggl, T., & Martiner, A. (2017). Validation of Moticon's OpenGo sensor insoles during gait, jumps, balance and cross-country skiing specific imitation movements. *Journal of Sports Sciences*, 35(2), 196-206.
- Subramanian, R., Wache, J., Abadi, M. K., Vieriu, R. L., Winkler, S., & Sebe, N. (2018). Ascertain: Emotion and personality recognition using commercial sensors. *IEEE Transactions on Affective Computing*, 9(2), 147-160.
- Sun, B., Zhang, Z., Liu, X., Hu, B., & Zhu, T. (2017). Self-esteem recognition based on gait pattern using Kinect. *Gait Posture*, 58, 428-432.

- Svoray, T., Dorman, M., Shahar, G., & Kloog, I. (2018). Demonstrating the effect of exposure to nature on happy facial expressions via Flickr data: Advantages of non-intrusive social network data analyses and geoinformatics methodologies. *Journal of Environmental Psychology*, 58, 93-100.
- Szinte, M., & Cavanagh, P. (2012). Apparent motion from outside the visual field, retinotopic cortices may register extra-retinal positions. *PLoS One*, 7(10), e47386.
- Tageldin, A., & Sayed, T. (2019). Models to evaluate the severity of pedestrian-vehicle conflicts in five cities. *Transportmetrica A: Transport Science*, 15(2), 354-375.
- Talen, E. (2009). Design by the rules: The historical underpinnings of form-based codes. *Journal of the American Planning Association*, 75(2), 144-160.
- Tang, I. C., Tsai, Y. P., Lin, Y. J., Chen, J. H., Hsieh, C. H., Hung, S. H., ... & Chang, C. Y. (2017). Using functional Magnetic Resonance Imaging (fMRI) to analyze brain region activity when viewing landscapes. *Landscape and Urban Planning*, 162, 137-144.
- Tarvainen, M. P., Niskanen, J. P., Lipponen, J. A., Ranta-Aho, P. O., & Karjalainen, P. A. (2014). Kubios HRV—heart rate variability analysis software. *Computer Methods and Programs in Biomedicine*, 113(1), 210-220.
- Tarvainen, M. P., Ranta-Aho, P. O., & Karjalainen, P. A. (2002). An advanced detrending method with application to HRV analysis. *IEEE Transactions on Biomedical Engineering*, 49(2), 172-175.
- Taylor, S. A., Jaques, N., Nosakhare, E., Sano, A., & Picard, R. (2017). Personalized multitask learning for predicting tomorrow's mood, stress, and health. *IEEE Transactions on Affective Computing*, 11(2), 200-213.
- Terrell, G. R. (1990). The maximal smoothing principle in density estimation. *Journal of the American Statistical Association*, 85(410), 470-477.
- Thompson, C. W., Roe, J., Aspinall, P., Mitchell, R., Clow, A., & Miller, D. (2012). More green space is linked to less stress in deprived communities: Evidence from salivary cortisol patterns. *Landscape and Urban Planning*, 105(3), 221-229.
- Tilley, S., Neale, C., Patuano, A., & Cinderby, S. (2017). Older people's experiences of mobility and mood in an urban environment: A mixed methods approach using electroencephalography (EEG) and interviews. *International Journal of Environmental Research and Public Health*, 14(2), 151.
- Timmermans, E. J., Schaap, L. A., Visser, M., van der Ploeg, H. P., Wagtenonk, A. J., van der Pas, S., & Deeg, D. J. (2016). The association of the neighbourhood built environment with objectively measured physical activity in older adults with and without lower limb osteoarthritis. *BMC Public Health*, 16(1), 710.
- Tinetti, M. E. (1986). Performance-oriented assessment of mobility problems in elderly patients. *Journal of the American Geriatrics Society*, 34(2), 119-126.
- Torku, A., Chan, A. P. C., & Yung, E. H. K. (2020/2021). Age-friendly cities and communities: A review and future directions. *Ageing & Society*, 41(10), 2242-2279-38.

- Triguero-Mas, M., Gidlow, C. J., Martínez, D., De Bont, J., Carrasco-Turigas, G., Martínez-Íñiguez, T., Hurst, G., Masterson, D., Donaire-Gonzalez, D., Seto, E., Jones, M. V., & Nieuwenhuijsen, M. J. (2017). The effect of randomised exposure to different types of natural outdoor environments compared to exposure to an urban environment on people with indications of psychological distress in Catalonia. *PLoS One*, *12*(3), e0172200.
- Tsunetsugu, Y., Lee, J., Park, B. J., Tyrväinen, L., Kagawa, T., & Miyazaki, Y. (2013). Physiological and psychological effects of viewing urban forest landscapes assessed by multiple measurements. *Landscape and Urban Planning*, *113*, 90-93.
- Turner, A., Doxa, M., O'sullivan, D., & Penn, A. (2001). From isovists to visibility graphs: A methodology for the analysis of architectural space. *Environment and Planning B: Planning and Design*, *28*(1), 103-121.
- Twardzik, E., Duchowny, K., Gallagher, A., Alexander, N., Strasburg, D., Colabianchi, N., & Clarke, P. (2019). What features of the built environment matter most for mobility? Using wearable sensors to capture real-time outdoor environment demand on gait performance. *Gait & Posture*, *68*, 437-442.
- Tyrväinen, L., Ojala, A., Korpela, K., Lanki, T., Tsunetsugu, Y., & Kagawa, T. (2014). The influence of urban green environments on stress relief measures: A field experiment. *Journal of Environmental Psychology*, *38*, 1-9.
- Ulrich, R. S. (1981). Natural versus urban scenes: Some psychophysiological effects. *Environment and Behavior*, *13*(5), 523-556.
- Ulrich, R. S., Simons, R. F., Losito, B. D., Fiorito, E., Miles, M. A., & Zelson, M. (1991). Stress recovery during exposure to natural and urban environments. *Journal of Environmental Psychology*, *11*(3), 201-230.
- United Nations (2020). *World Population Ageing 2020 Highlights: Living arrangements of older persons*. New York: United Nations. ST/ESA/SER.A/451
- US Department of Health and Human Services (2008). *2008 Physical activity guidelines for Americans*. U.S. Department of Health and Human Services, Washington.
- Valtchanov, D., & Ellard, C. G. (2015). Cognitive and affective responses to natural scenes: effects of low level visual properties on preference, cognitive load and eye-movements. *Journal of Environmental Psychology*, *43*, 184-195.
- Valtchanov, D., Barton, K. R., & Ellard, C. (2010). Restorative effects of virtual nature settings. *Cyberpsychology, Behavior, and Social Networking*, *13*(5), 503-512.
- Van Cauwenberg, J., De Bourdeaudhuij, I., De Meester, F., Van Dyck, D., Salmon, J., Clarys, P., & Deforche, B. (2011). Relationship between the physical environment and physical activity in older adults: A systematic review. *Health & Place*, *17*(2), 458-469.
- Van den Berg, M. M., Maas, J., Muller, R., Braun, A., Kaandorp, W., Van Lien, R., Van Poppel, M. N., Van Mechelen, W., & Van den Berg, A. E. (2015). Autonomic nervous system responses to viewing green and built settings: differentiating between sympathetic and parasympathetic activity. *International Journal of Environmental Research and Public Health*, *12*(12), 15860-15874.

- van Heezik, Y., Freeman, C., Buttery, Y., & Waters, D. L. (2020). Factors affecting the extent and quality of nature engagement of older adults living in a range of home types. *Environment and Behavior*, 52(8), 799-829.
- Van Hoof, J., Kazak, J. K., Perek-Białas, J. M., & Peek, S. (2018). The challenges of urban ageing: Making cities age-friendly in Europe. *International Journal of Environmental Research and Public Health*, 15(11), 2473.
- Verbrugge, L. M. (2020). Revisiting the disablement process. In Jagger C., Crimmins E., Saito Y., De Carvalho Yokota R., Van Oyen H., & Robine J. M. (eds) *International Handbook of Health Expectancies* (pp. 275-285). Cham: Springer.
- Verbrugge, L. M., & Jette, A. M. (1994). The disablement process. *Social Science & Medicine*, 38(1), 1-14.
- Vesanto, J., & Alhoniemi, E. (2000). Clustering of the self-organizing map. *IEEE Transactions on Neural Networks*, 11(3), 586-600.
- Walford, N., Phillips, J., Hockey, A., & Pratt, S. (2017). Assessing the needs of older people in urban settings: integration of emotive, physiological and built environment data. *Geo: Geography and Environment*, 4(1), e00037.
- Waller, L. A., & Gotway, C. A. (2004). *Applied spatial statistics for public health data* (Vol. 368). New Jersey: John Wiley & Sons.
- Wan, L., Gao, S., Wu, C., Jin, Y., Mao, M., & Yang, L. (2018). Big data and urban system model-substitutes or complements? A case study of modelling commuting patterns in beijing. *Computers, Environment and Urban Systems*, 68, 64-77.
- Wang, W. Z., Guo, Y. W., Huang, B. Y., Zhao, G. R., Liu, B. Q., & Wang, L. (2011). Analysis of filtering methods for 3D acceleration signals in body sensor network. In *International Symposium on Bioelectronics and Bioinformatics*, (pp. 263-266). IEEE.
- Webber, S. C., Porter, M. M., & Menec, V. H. (2010). Mobility in older adults: A comprehensive framework. *The Gerontologist*, 50(4), 443-450.
- Wehrl, A. (1978). General properties of entropy. *Reviews of Modern Physics*, 50(2), 221.
- Wenczel, F., Hepperle, L., & von Stülpnagel, R. (2017). Gaze behavior during incidental and intentional navigation in an outdoor environment. *Spatial Cognition & Computation*, 17(1-2), 121-142.
- Wheeler, D. C. (2007). A comparison of spatial clustering and cluster detection techniques for childhood leukemia incidence in Ohio, 1996–2003. *International Journal of Health Geographics*, 6(1), 1-16.
- Wheeler, G. (2018). “Bounded Rationality”, *The Stanford Encyclopedia of Philosophy* (Winter 2018 Edition), Edward N. Zalta (ed.).
- WHO (World Health Organisation) (2001). *International Classification of Functioning, Disability, and Health*. Geneva, Switzerland: WHO Press.

- WHO (World Health Organisation) (2002). *Active aging: A policy framework*. Geneva, Switzerland: WHO Press.
- WHO (World Health Organisation) (2007). *Global age-friendly cities: A guide*. Geneva, Switzerland: WHO Press.
- WHO (World Health Organisation) (2009). *Global health risks, mortality, and burden of disease attributable to selected major risks*. World Health Organization, Geneva, Switzerland: WHO Press.
- WHO (World Health Organisation) (2018). *The Global Network for Age-friendly Cities and Communities: Looking back over the last decade, looking forward to the next*. Geneva, Switzerland: WHO Press.
- WHO (World Health Organisation) (2020). *About the Global Network for Age-friendly Cities and Communities*. Available at: <https://extranet.who.int/agefriendlyworld/who-network/> (accessed 2 December 2020).
- Wiener, J. M., & Franz, G. (2004). Isovists as a means to predict spatial experience and behavior. In *International Conference on Spatial Cognition* (pp. 42-57). Springer, Berlin, Heidelberg.
- Willis, A., Gjersoe, N., Havard, C., Kerridge, J., & Kukla, R. (2004). Human movement behaviour in urban spaces: Implications for the design and modelling of effective pedestrian environments. *Environment and Planning B: Planning and Design*, 31(6), 805-828.
- Witten, I. H., Frank, E., Hall, M. A., Pal, C. J. Witten, I. H., & Frank, E. (2017). *Data mining: Practical machine learning tools and techniques with Java implementations*. (4th ed.). United States: Morgan Kaufmann Publishers, *Acm Sigmod Record*, 31(1), 76-77.
- Won, E., & Kim, Y. K. (2016). Stress, the autonomic nervous system, and the immunokynurenine pathway in the etiology of depression. *Current Neuropharmacology*, 14(7), 665-673.
- Wong, T. W. (2019). Examining conscious motor processing and the effect of single-task, dual-task and analogy training on walking during rehabilitation by older adults at risk of falling in Hong Kong: Design and methodology of a randomized controlled trial. *Contemporary Clinical Trials Communications*, 100398.
- Wongravee, K., Lloyd, G. R., Silwood, C. J., Grootveld, M., & Brereton, R. G. (2010). Supervised self organizing maps for classification and determination of potentially discriminatory variables: Illustrated by application to nuclear magnetic resonance metabolomic profiling. *Analytical Chemistry*, 82(2), 628-638.
- Woolson, R. F. (2007). Wilcoxon signed-rank test. *Wiley Encyclopedia of Clinical Trials*, 1-3.
- Wu, X., Oldfield, P., & Heath, T. (2020). Spatial openness and student activities in an atrium: A parametric evaluation of a social informal learning environment. *Building and Environment*, 182, 107141.

- Xiang, L., Papastefanou, G., & Ng, E. (2020). Isovist indicators as a means to relieve pedestrian psycho-physiological stress in Hong Kong. *Environment and Planning B: Urban Analytics and City Science*.
- Yameqani, A. S., & Alesheikh, A. A. (2019). Predicting subjective measures of walkability index from objective measures using artificial neural networks. *Sustainable Cities and Society*, 48, 101560.
- Yang, B. Y., Markevych, I., Bloom, M. S., Heinrich, J., Guo, Y., Morawska, L., Dharmage, S. C., Knibbs, L. D., Jalaludin, B., Jalava, P., Zeng, X., W., Hu, L. W., Liu, K. K., & Dong, G. H. (2019). Community greenness, blood pressure, and hypertension in urban dwellers: The 33 Communities Chinese Health Study. *Environment International*, 126, 727-734.
- Yang, F., Bao, Z. Y., & Zhu, Z. J. (2011). An assessment of psychological noise reduction by landscape plants. *International Journal of Environmental Research and Public Health*, 8(4), 1032-1048.
- Yang, T. C., & Matthews, S. A. (2010). The role of social and built environments in predicting self-rated stress: A multilevel analysis in Philadelphia. *Health & Place*, 16(5), 803-810.
- Yin, L. (2017). Street level urban design qualities for walkability: Combining 2D and 3D GIS measures. *Computers, Environment and Urban Systems*, 64, 288-296.
- Yu, C. P., Lee, H. Y., & Luo, X. Y. (2018). The effect of virtual reality forest and urban environments on physiological and psychological responses. *Urban Forestry & Urban Greening*, 35, 106-114.
- Zhang, C. J., Barnett, A., Johnston, J. M., Lai, P. C., Lee, R. S., Sit, C. H., & Cerin, E. (2019). Objectively-measured neighbourhood attributes as correlates and moderators of quality of life in older adults with different living arrangements: the ALECS cross-sectional study. *International Journal of Environmental Research and Public Health*, 16(5), 876.
- Zhang, X., Xu, C., Xue, W., Hu, J., He, Y., & Gao, M. (2018). Emotion recognition based on multichannel physiological signals with comprehensive nonlinear processing. *Sensors*, 18(11), 3886.
- Zhou, H., He, S., Cai, Y., Wang, M., & Su, S. (2019). Social inequalities in neighborhood visual walkability: Using Street View imagery and deep learning technologies to facilitate healthy city planning. *Sustainable Cities and Society*, 50, 101605.
- Zhu, Y., & Newsam, S. (2016). Spatio-temporal sentiment hotspot detection using geotagged photos. In *Proceedings of the 24th ACM SIGSPATIAL International Conference on Advances in Geographic Information Systems* (pp. 1-4).
- Zietz, D., & Hollands, M. (2009). Gaze behavior of young and older adults during stair walking. *Journal of Motor Behavior*, 41(4), 357-366.